EGG-EA-5460

May 1981

PDR

KUOSHENG MECHANICAL IMPEDANCE TESTING

NRC Research and Technical Assistance Report

V. W. Gorman

U.S. Department of Energy
Idaho Operations Office • Idaho National Engineering Laboratory

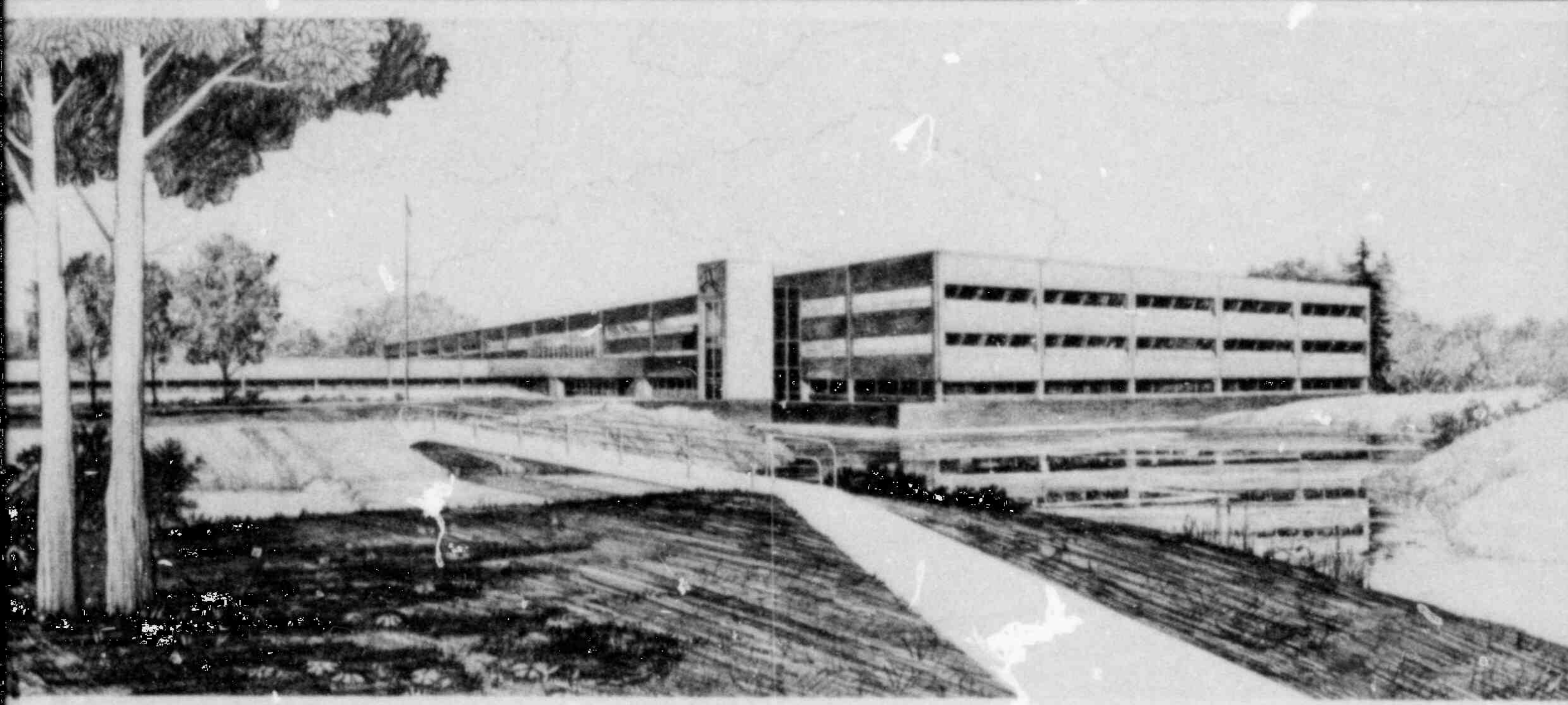

This is an informal report intended for use as a preliminary or working document

Prepared for the
U.S. Nuclear Regulatory Commission
Under DOE Contract No. DE-AC07-76ID01570
FIN No. A6353

EG&G Idaho

EG&G Idaho, Inc

FORM EG&G-398
(Rev. 11-79)

INTERIM REPORT

Accession No. ______________

Report No. EGG-EA-5460

Contract Program or Project Title:

Kuosheng SRV Discharge and Piping Vibration Tests

Subject of this Document:

Kuosheng Mechanical Impedance Testing

Type of Document

Informal Report

Author(s):

V. W. Gorman

NRC Research and Technical Assistance Report

Date of Document:

May 1981

Responsible NRC Individual and NRC Office or Division:

J. A. O'Brien - GRSR: MERB

This document was prepared primarily for preliminary or internal use. It has not received full review and approval. Since there may be substantive changes, this document should not be considered final.

EG&G Idaho, Inc.
Idaho Falls, Idaho 83415

Prepared for the
U.S. Nuclear Regulatory Commission
Washington, D.C.
Under DOE Contract No. DE-AC07-76ID01570
NRC FIN No. A6353

INTERIM REPORT

ABSTRACT

This report documents the results of mechanical impedance tests conducted on five USNRC selected plant components at the Kuosheng Nuclear Power Station (Unit 1) located in Taiwan which is operated by Taiwan Power Company (Taipower). The plant will be the world's first operational boiling water reactor (BWR) using the General Electric designed BWR-6 Mark III containment system. The specific purpose of the tests was to measure resonant frequencies, damping ratios and structural mode shapes of the test items over a frequency range of 1 to 100 hertz (Hz) using input acceleration levels up to 0.4 g. Three different methods of testing (impulse hammer, electromagnetic shaker and hydraulic shaker) were utilized to excite the components with an impulse or pseudo random noise. Output response from accelerometers placed on the components were processed by a minicomputer based spectrum analyzer to obtain the required data. The results of these tests were found to be consistent with tests on similar components.

ACKNOWLEDGEMENTS

This work was performed by TRANSITEK, Inc. for EG&G Idaho, Inc. under EG&G subcontract K-7685.

The following TRANSITEK personnel participated in the project:

M. C. Plummer ---- Principal Engineer
G. P. Coleman ---- Manager
A. Nothelfer ----- Senior Engineer
P. Barney -------- Technician

I. K. Hall of EG&G Idaho assisted TRANSITEK and acted as technical monitor and control over the testing aspects of the project.

We are particularly indebted to Taipower personnel for granting permission to run the tests, providing assistance for customs clearance, moving the test equipment, providing test fixtures and, in general, aiding the test staff. We are also indebted to Drs. Tim Lee and John O'Brien of the USNRC for assistance in coordination of the effort, securing export licensing and international communications.

CONTENTS

TABLES

APPENDICES

KUOSHENG MECHANICAL IMPEDANCE TESTING

INTRODUCTION

The Kuosheng Nuclear Power Station, located on the northern tip of Taiwan close to the port city of Keelung, will be the world's first operational boiling water reactor (BWR) using the General Electric (GE) designed BWR-6 Mark III pressure suppression containment system. The plant was constructed by the Bechtel Power Corporation under contract with the plant owner, the Taiwan Power Company (Taipower). Fuel loading was completed in January 1981 and preoperational testing, including an extensive safety relief valve (SRV) test program is planned for mid-year of 1981. Information obtained from the Kuosheng tests will provide data useful to the United States Nuclear Regulatory Commission (USNRC) licensing determinations for safety evaluations of the U.S. systems.

Late in 1980 EG&G Idaho was requested by USNRC to conduct mechanical impedance tests on selected components at the Kuosheng Nuclear Power Station in Taiwan in cooperation with Taipower's startup test program. Since EG&G Idaho did not have on hand the proper equipment to provide this service nor sufficient time to purchase it before required testing in January 1981, the task was subcontracted. TRANSITEK, Inc. was retained for the task because of their expertise and previous experience in performing tests on similar components at La Salle and Zimmer nuclear power plants.

TRANSITEK, with EG&G Idaho assisting and acting as technical monitor and in cooperation with Taipower, performed on-site tests from January 18 to January 27, 1981. The components tested are listed in Table 1.

Appendix A describes the impedance test procedures utilized for each component tested along with test equipment used; analysis methods used for data reduction to obtain resonant frequencies, damping ratios and structural mode shapes; and, finally, results and conclusions concerning the test

TABLE 1. COMPONENTS TESTED

Item	Equipment No.	Model No.	Manufacturer	Date of Mfg
Jet Pump Instrument Panel B	R-53-H22-P009	282-R2C31*	GE	7-27-78
Recirculation Control Valve B	R-57-B33-D003	205-AH740*	GE	11-22-77
RHR Pump A-3	IP-48C	5K6336XC295A	Byron Jackson	7-12-79
480V Motor Control Center 1C1D (located in auxiliary building)		Series No. 5600	Gould/ITE	10-19-77
3-Inch Motor Operated Valve (located near SRV-V8 discharge)		SMB-000-2	Anchor Darling	3-10-17

* GE Purchase Order No.

program which include figures depicting mode shapes and tables defining resonant frequencies and damping ratios. Table 2 presents a summary of the first four frequencies and damping ratios for each component tested. Appendix B contains figures of personnel involved in the testing, equipment tested and some of the test equipment. Appendix C contains supplementary information regarding data obtained during the tests. Appendix D contains microfiche with mode shapes listed.

TABLE 2. SUMMARY OF FREQUENCIES AND DAMPING RATIOS

		Mode			
		1	2	3	4
Jet Pump Instrumentation Panel B	Hz[a]	19.87	21.32	22.70	31.45
	ζ[b]	2.1	0.9	3.7	2.4
Recirculation Control Valve B	Hz	16.21	18.97	22.57	27.07
	ζ	9.0	3.8	8.5	3.3
RHR Pump A-3	Hz	17.34	18.30	87.00	92.12
	ζ	2.3	2.4	1.7	3.1
480V Motor Control Center	Hz	7.40	29.19	33.93	39.72
	ζ	2.4	2.6	4.4	1.4
3-Inch Motor Operated Valve	Hz	18.20	20.60	21.1	21.4
	ζ	1.1	4.1	1.0	1.0

a -- Frequency in hertz (Hz)

b -- Percent of critical damping

APPENDIX A

TEST RESULTS

Transitek, Inc.

2328 J Walsh Avenue
Santa Clara, CA 95050
Telephone 408-246-1616

FINAL REPORT

TEST RESULTS

MECHANICAL IMPEDANCE TESTS

ON

SELECTED COMPONENTS

KUOSHENG NUCLEAR POWER STATION

for

EG&G Idaho, Inc.
P.O. Box 1625
Idaho Falls, Idaho 83415

Subcontract No. K-7685
to
Contract No. DE-AC07-76ID01570
TRANSITEK Job No. [illegible]

May 15, 1981

Written by: Mitty C. Plummer, PhD., P.E., President — May 15, 1981 (Date)

Reviewed by: Gerald P. Coleman, Manager, Data Services — 5-15-81 (Date)

Transactions in Technology

TABLE OF CONTENTS

EXECUTIVE SUMMARY

TRANSITEK, Inc. was retained by EG&G under Subcontract No. K-7685 of Contract No. DE-AC07-761 D01570 to provide mechanical impedance measurements on five items of plant equipment of the Kuosheng Nuclear Power Station - Unit 1. The tests were performed on-site from January 18 to January 27, 1981. Analysis of the test data proceeded from February 6 to March 13, 1981 at the TRANSITEK offices in Santa Clara, California. Analysis was performed concurrently with analysis of supporting data from other power plants.

The equipment tested and included in this report consists of the following items:

Jet Pump Instrumentation Panel B, Equipment No. R-53-H22-P009

Recirculation Control Valve B, Equipment No. R-57-B33-D003

RHR Pump A-3, Equipment No. IP-48C

480 V Motor Control Center 1C1D (located in auxiliary building)

3" Motor Operated Valve near V-8 SRV discharge

Resonances were found on each piece of equipment in the 33 to 100 Hz frequency range. These resonances are in the frequency range above the original seismic qualification (1 to 33 Hz) and in the frequency range where LOCA loads contribute to dynamic loads. The measured resonant frequencies, dampings and mode shapes are believed to be generally accurate and entirely usable in confirmation of subsequent computer modeling for equipment qualification. The one item of equipment on which the data quality is degraded, due to restrictions imposed by Taipower of .2 g maximum acceleration and 33 Hz maximum frequency is motor control center 1C1D. The resulting low input force levels, coupled with ambient vibrations of .01 to .03 g, had the end result of poor quality mode shapes and probably reduced estimates of damping.

1.0 PURPOSE

Background Information: The dynamic qualification of Kuosheng Nuclear Power Station safety related equipment has been achieved for seismic loads. Later determination from test data developed by G.E. and others showed the hydrodynamic loads from the pressure suppression pool contained frequency components greater than 33 Hz, the cut-off frequency for the original seismic qualification. In some cases, it is difficult to determine the sensitivity of the equipment to the high frequency loads.

The purpose of this project is to measure the dynamic characteristics of five representative items of equipment. The equipment tested includes the following:

Jet Pump Instrumentation Panel B, Equipment No. R-53-H22-P009

Recirculation Control Valve B, Equipment No. R-57-B33-D003

RHR Pump A-3, Equipment No. IP-48C

480 V Motor Control Center 1C1D (located in auxiliary building)

3" Motor Operated Valve near V-8 SRV discharge

The characteristics measured include resonant frequency, damping, and mode shape. On each item of equipment in the containment vibration was induced to a sufficiently high level (.4 g) to excite all modes between 1 and 100 Hz. This procedure allowed us to measure dynamic properties in both the seismic and higher frequency ranges of interest.

For the RHR pump and the 480 V MCC we used decreasing force amplitudes between 30 and 100 Hz. This procedure was successful in giving us all modes on the RHR pump. An additional restriction (.2 g max.) on the MCC panel caused reduced quality of the higher frequency data and distorted mode shapes of the lower frequency data.

2.0 TEST METHODS

In the performance of this program, three different methods of testing were used to excite resonances of the equipment. Each are discussed separately in the following sections. The theory behind the data collection procedures are discussed in Section 2.1.

The instrument systems used in this testing program were based on the GenRad 2508 four-channel data acquisition system. The theoretical background information of Section 2.1 is of general application to any mini-computer based analyzer. The specific comments for hammer and shaker tests are unique to this system and to the MPLUS[1] computer program which was used exclusively in this project.

An overview of modal testing activities is shown in Figure 2.1.

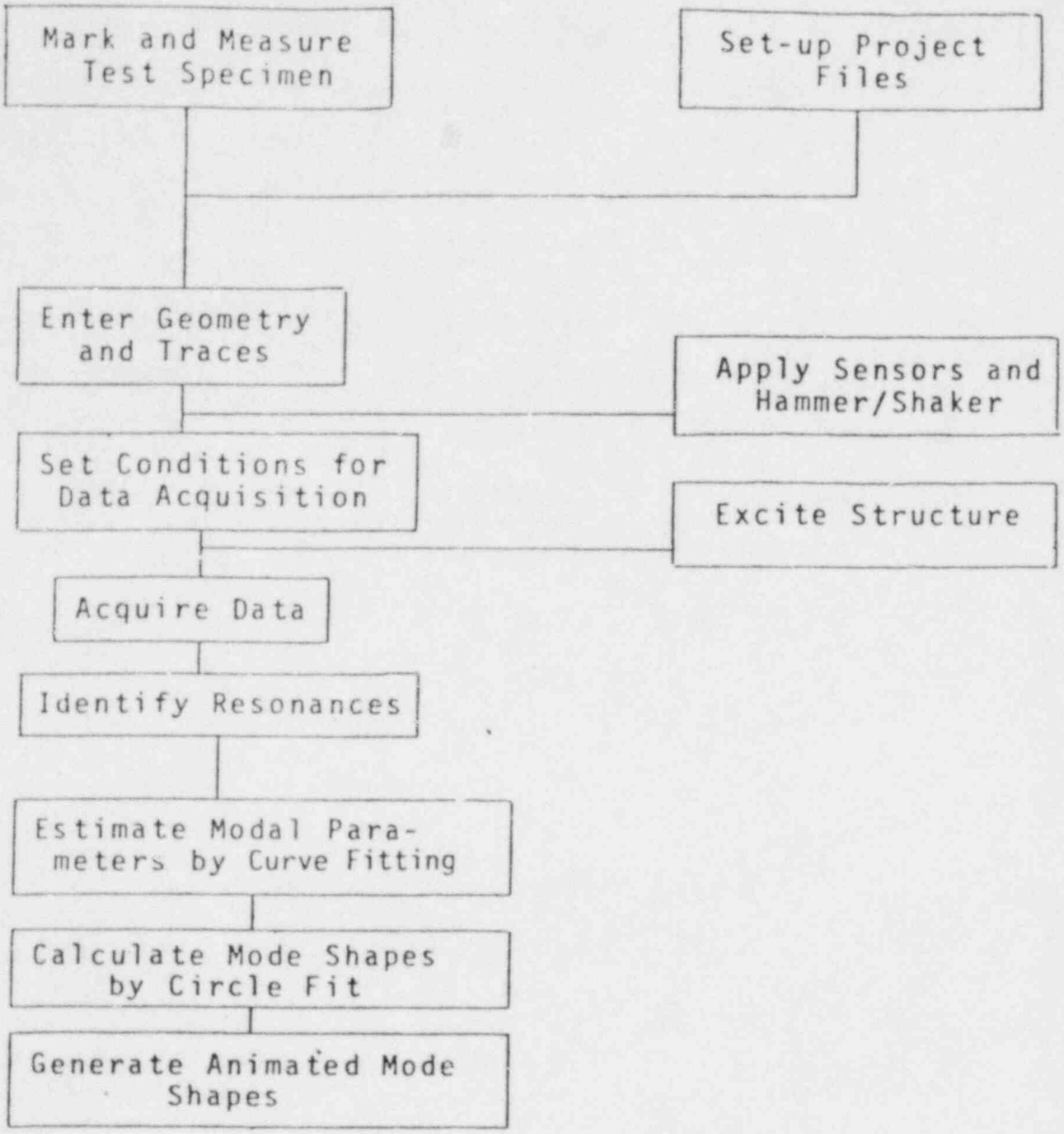

FIGURE 2.1

A FLOW DIAGRAM SHOWING THE OVERVIEW OF MODAL TEST ACTIVITIES

2.1 Theoretical Background:

2.1.1 Overview

With the evolution of the dual channel minicomputer based frequency analyzers in the early 1970's, engineers were making the first applications of these instruments to perform modal tests in a few hours on structures that had previously taken weeks to perform with swept sine techniques and analog analyzers. In the following section, we will detail the considerations that made these advances possible.

2.1.2 FFT Processes in Modal Analysis

The first operation performed on the analog signal entering the Gen Rad system is low pass filtering. The filtered signal is then digitized and undergoes a Fast Fourier Transform (FFT) in a dedicated microprocessor.

The filters are included to prevent "aliasing" of higher frequency signals which appear as low frequency signals in the range of interest. Figure 2.1.2.1 shows how a high frequency signal can be misinterpreted as a low frequency by the digitization process.

Generally, the filters cut off frequencies (F_c) are set to at least one-half of the sampling frequency (F_{max}) and generally less (.45 to .25). Aliasing then occurs only in the upper half of the channels in the frequency data block. These frequency channels (the hatched areas of Figure 2.1.2.2) contain invalid data and are disregarded (set to zero) and only the valid frequencies are displayed or stored.

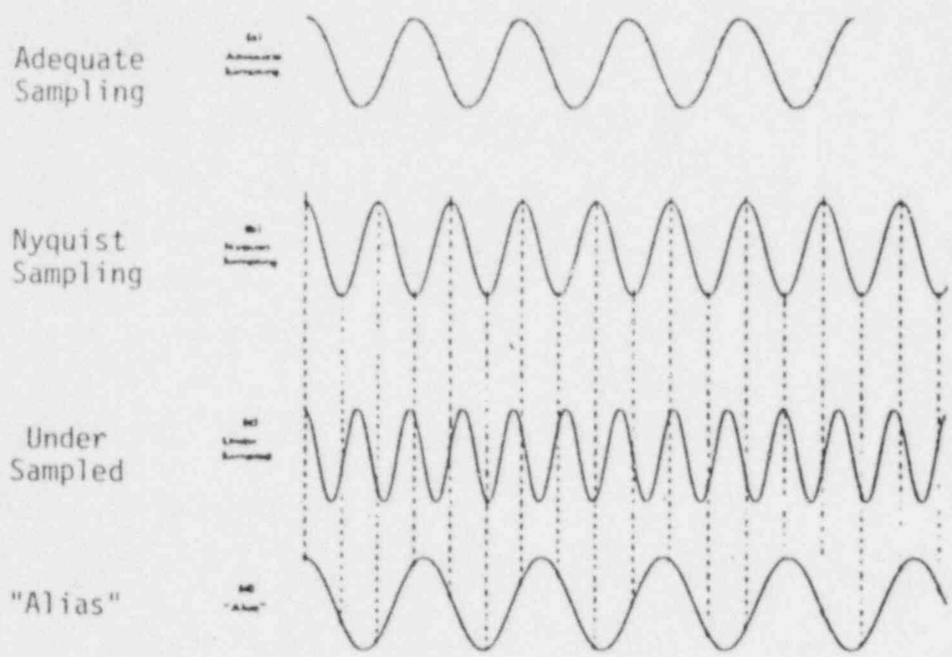

FIGURE 2.1.2.1

AN EXAMPLE OF THE OCCURRENCE OF ALIASING

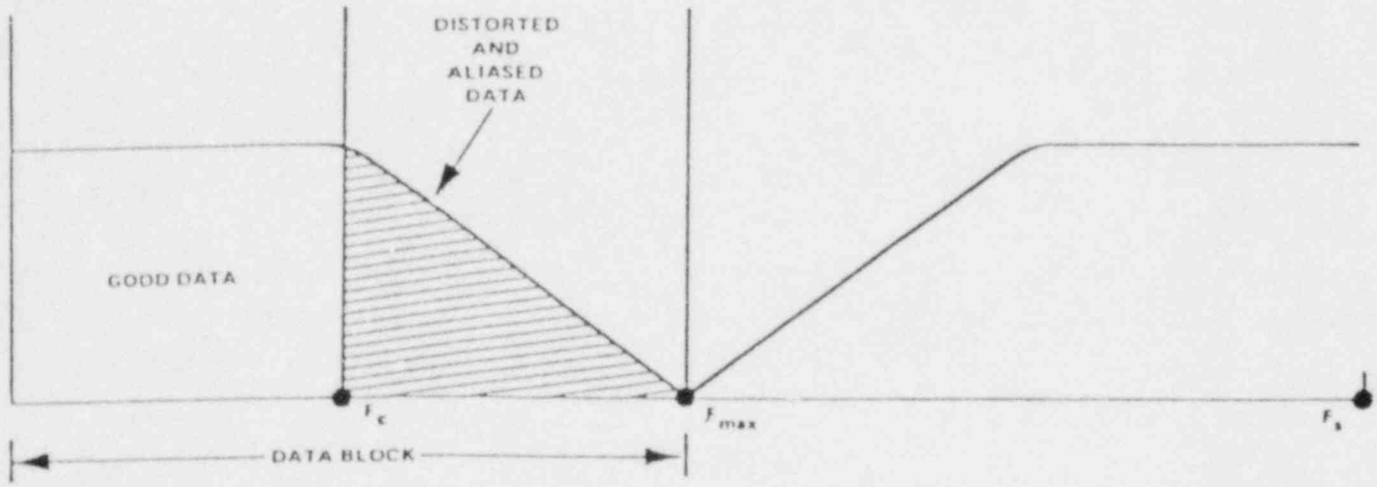

FIGURE 2.1.2.2

A DIAGRAM SHOWING ALIASED AND DISTORTED DATA
RELATIVE TO SIGNAL ANALYSIS PARAMETERS

These processes are handled automatically and correctly by the MPLUS[1] computer code

Once we have FFT's of the input, it is possible to compute a number of functions more useful to modal analysis. These, and the storage locations of each in the computer, are listed in Table 2.1.2.1

TABLE 2.1.2.1

FUNCTIONS GENERATED BY MPLUS

Function Name	Symbol	Storage Block	Definition
Input Auto Power Spectrum	Gxx(f)	2	Average Input Power Spectrum Gx(f)* G*x(f) Generally of the force
Response Power Spectrum	Gyy(f)	3	Any Response Power Spectrum Gy(f) * Gy(f)
Transfer Function	H(f)	1	$H_{(f)} = \frac{Gyx(f)}{Gxx(f)} = \frac{Gy(f)*G*x(f)}{Gx(f)*G*x(f)}$ The ratio of input to output in both phase and amplitude. The ratio of the output power spectrum that is linearly related to input power.
Coherence	γ^2	4	$0 \leq \gamma^2 \leq 1 = \frac{\lvert Gyx(f) \rvert^2}{\lvert Gxx(f) \rvert \cdot \lvert Gyy(f) \rvert}$

Of the four functions listed, only the transfer function is critical to the modal analysis. The others "support" the transfer function measurement by serving as tools with which we can examine its quality and diagnose problems in the data collection.

2.1.3 Frequency Content of Impulses and Random Force Excitation

The impulse is an ideal forcing function for modal analysis for the following reasons:

A. The frequency content of an impulse is very uniform as shown in Figure 2.1.3.1.

B. The break frequency and general shape of the frequency content of triangular or square impulses are approximately the same as that of the half sine and depend mostly on the pulse duration. In other words, we do not have to worry too much about the shape of the pulse.

C. The uniform distribution of the force in frequency gives each resonance equal excitation out to the break frequency of the pulse.

D. Impulses can be applied quickly and easily with a small hammer. A large number of points can be tested in a short period of time.

E. We can easily control the pulse width of the applied force by changing the mass of the hammer and hardness of the tip. Figure 2.1.3.2 shows examples of different hammer tips.

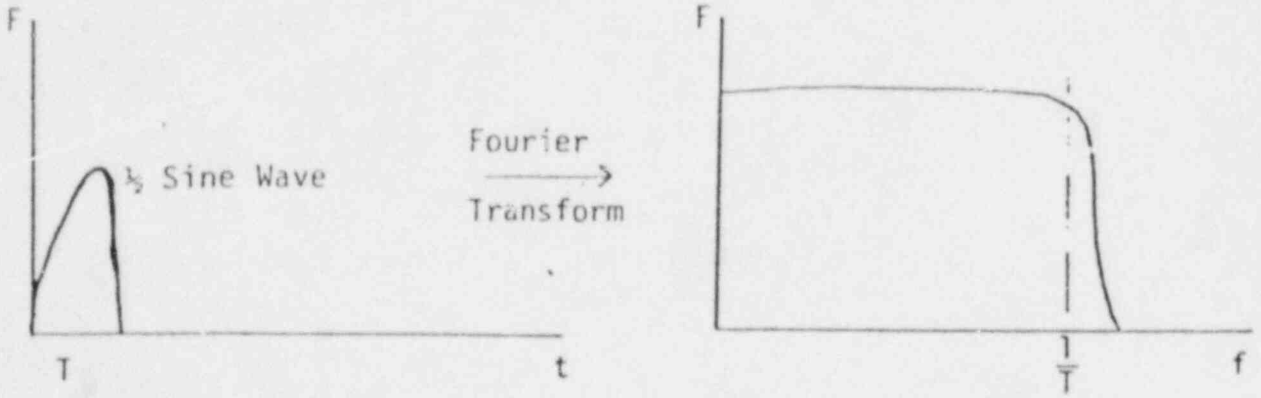

FIGURE 2.1.3.1

TIME HISTORY AND FREQUENCY CONTENT OF
A ONE-HALF SINE PULSE OF DURATION T

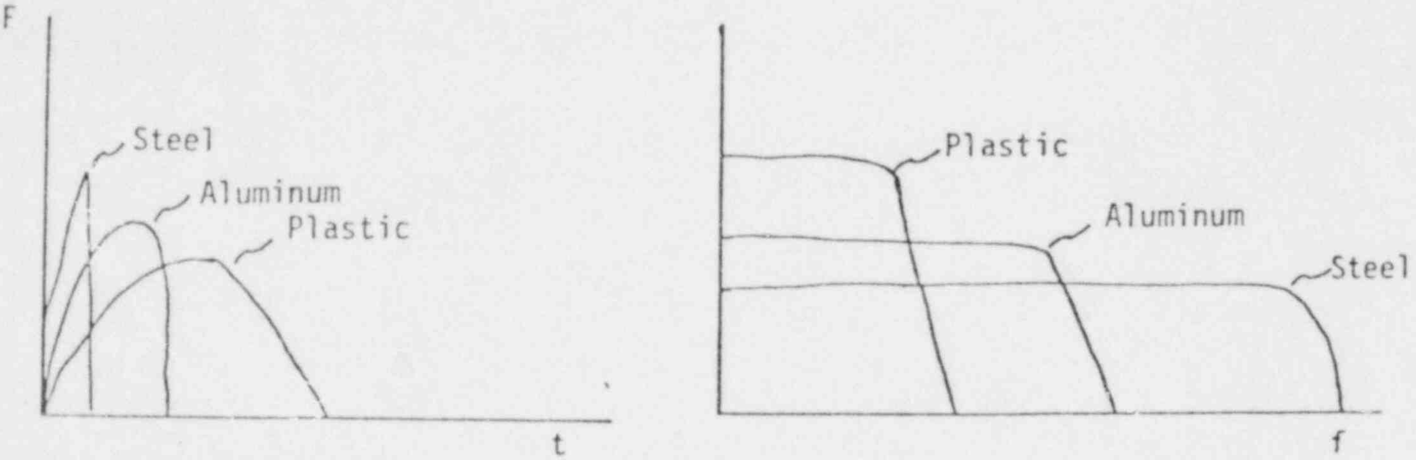

FIGURE 2.1.3.2

INFLUENCE OF HAMMER TIP MATERIAL ON
FORCE FREQUENCY CONTENT

In the structures tested by impulse technique, the hammer tip was a very soft rubber to provide approximately 125 hz break frequency.

There are several points about the way the force time history looks when acquired through the anti-aliasing filters and the A/D converter that should be noted. First, as shown in Figure 2.1.3.3, the filters may introduce a small amount of ringing into the time history. This is acceptable as long as the response is treated similarly in a matched filter. The GenRad anti-aliasing filters pay careful attention to matching to assure that this does not develop into a problem.

Another feature of the force that requires attention is the trigger level. It is necessary that the trigger level be set as low as possible to reflect accurately the true phase and amplitude of the pulse. The effect of a "too high" trigger level or a "soft tap" on frequency content is shown in Figure 2.1.3.4.

A clean, single pulse is the best form of excitation. On occasion, the hammer will slip and enter multiple taps. The consequence in the frequency domain is shown in Figure 2.1.3.5.

Here we see that ittle excitation is provided at some frequencies. In severe cases, this can cause the transfer function to appear to have additional resonances.

The best procedure, which followed consistently in this program, is to discard this data and reacquire with "clean" impulses.

A final consideration is the selection of pulse width and frequency range for analysis. Examples of digitized force pulse signals are shown in Figure 2.1.3.6.

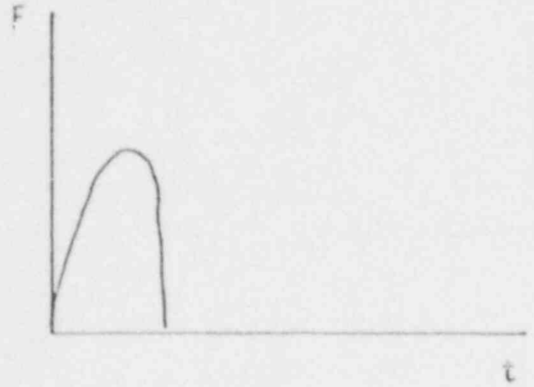

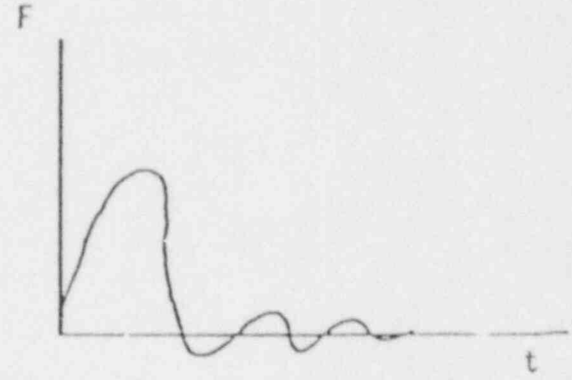

FIGURE 2.1.3.3

THE EFFECT OF THE A/D FILTERS ON
FORCE SIGNAL APPEARANCE

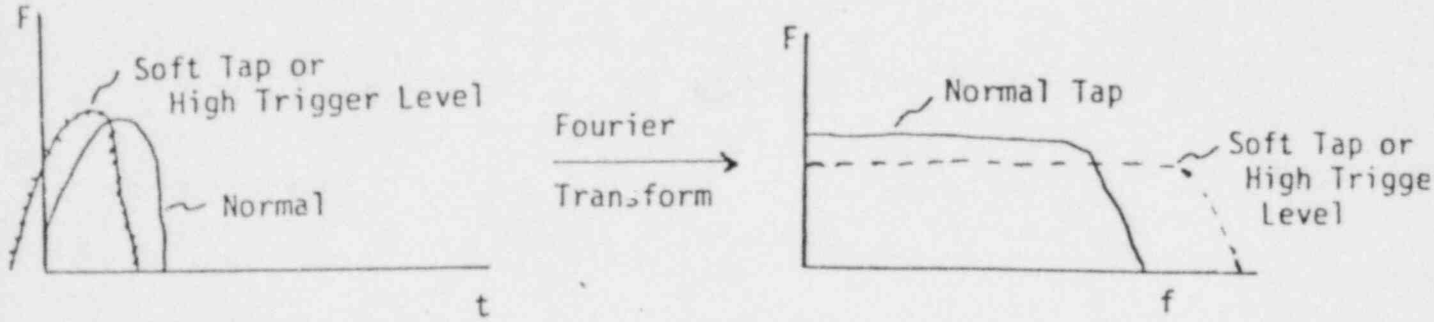

FIGURE 2.1.3.4

THE "SOFT TAP" OR "HIGH TRIGGER LEVEL" PROBLEM

A trigger level of 2% of the peak was used in this program and is sufficient to eliminate spurious triggers but avoid distorting the pulse.

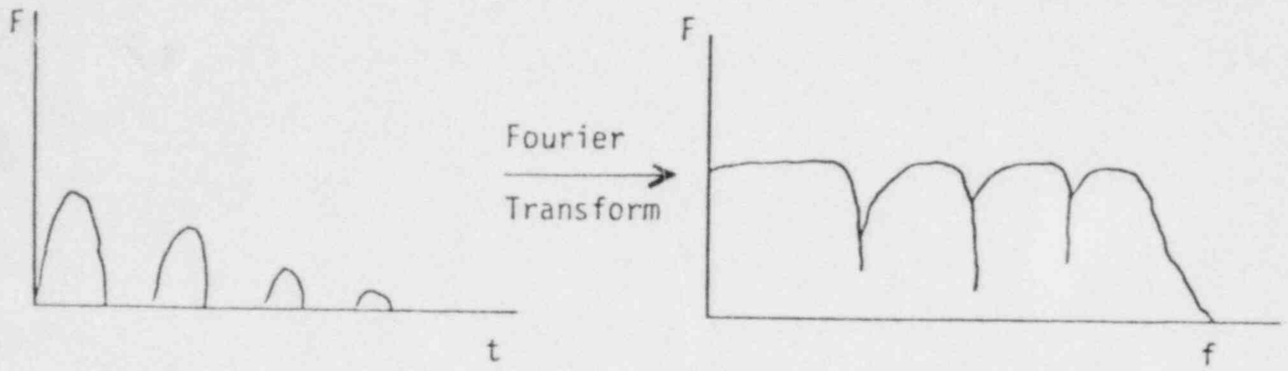

FIGURE 2.1.3.5

THE "MULTIPLE TAP" PROBLEM

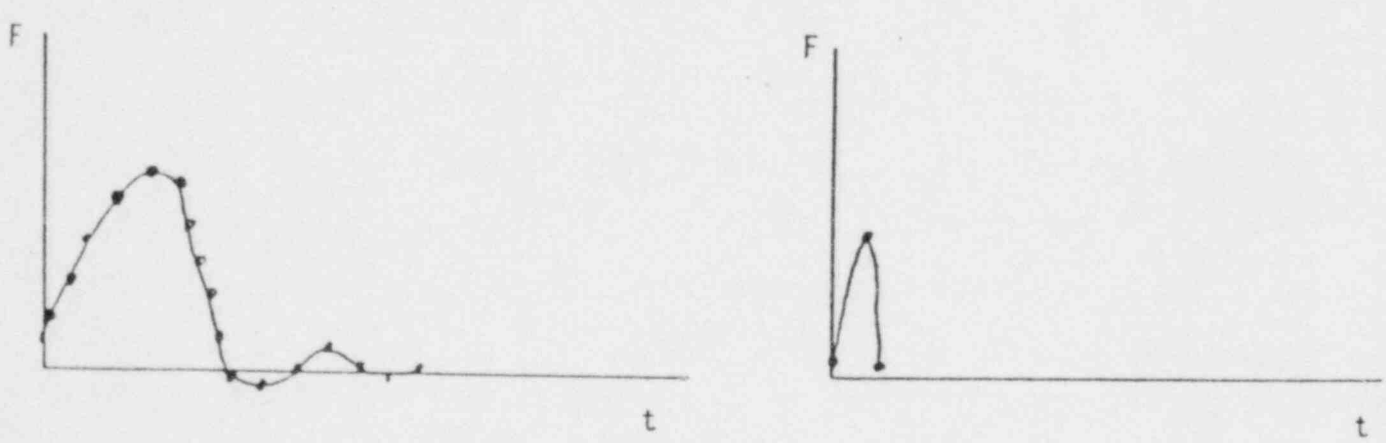

FIGURE 2.1.3.6

EXAMPLES OF SAMPLE RATE ON PULSE DEFINITION

In this program we used sampling rates of 1048 hz to give excellent definition to the pulse.

To resolve the difficulty of too narrow a pulse, a higher sampling rate or a greater hammer force pulse width should be chosen. This must be done with some attention to the resolution of the response as described in Section 2.1.4.

Similar consideration exists for random force excitation, the significant features for consideration are:

1. The forces shall be approximately uniform in frequency over the entire frequency range of analysis.
2. Clipping of the signal will introduce spurious high frequency content. Avoid this by using a "Sampling Abort" option at all times as is done in MPLUS.

The advantage of random force excitation is that the impulse equivalent (force times time) of a relatively small shaker is equivalent to a large hammer in providing continuous excitation. With a four channel analysis system, the rate of data acquisition is approximately equal to that of the hammer test.

2.1.4 Frequency Response of Structures

The dynamic response of structures depends on its geometric and material properties as well as the excitation. If the modal properties (resonant frequencies, dampings and mode shapes) are known, the response can be predicted for any force at any location on the structure.

The responses of real structures have three elements that describe the response. First is the rigid movement of the mass as a solid body. This mode dominates at the lowest frequencies and can be thought of as the inertia of the structure.

The second element of the structural response is governed by resonances. Generally, these dominate the response for the kind of forces that are encountered in real problems because the frequency content of the forcing functions are aligned with the areas of greatest dynamic response.

The third element of the structural behavior is treated as a residual compliance of all other modes outside the range of measurement or interest. Real structures have infinitely more responses, but only the few major ones are of interest.

The three elements of a response are shown in Figure 2.1.4.1.

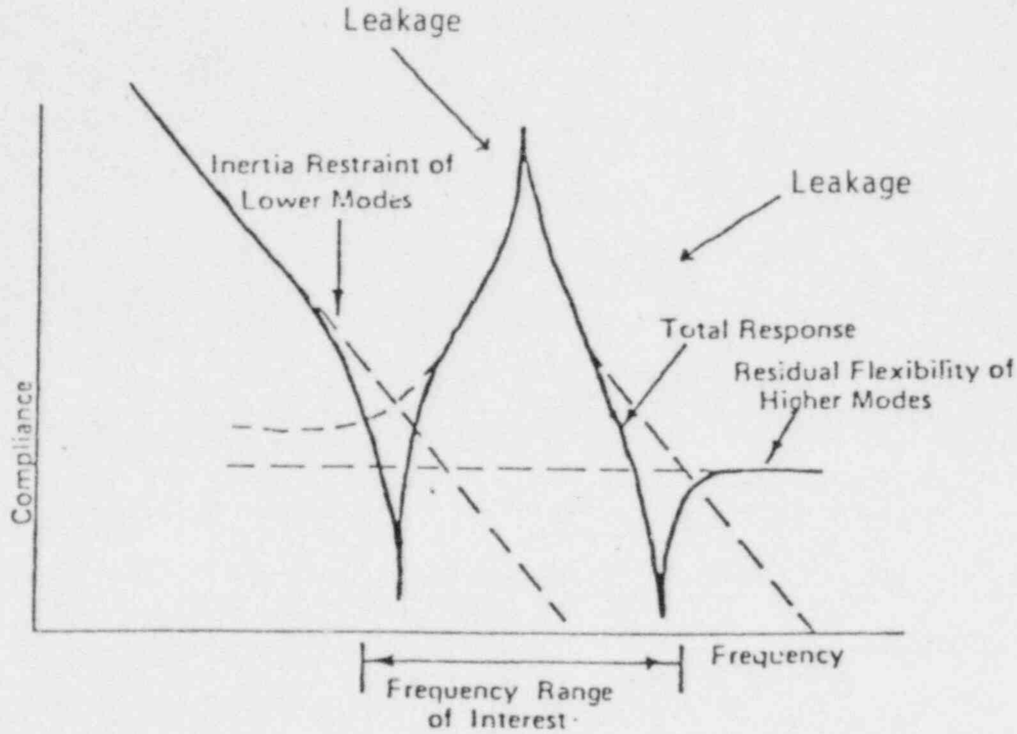

FIGURE 2.1.4.1

CONCEPT OF INERTIA RESTRAINT AND RESIDUAL FLEXIBILITY APPLIED TO A FREQUENCY RANGE OF INTEREST

The key element of structural response that influences the quality of a measurement is the sharpness (damping) of a resonance. If the sampling rate is too high (or the resolution too low) for a particular resonance, two things will happen to degrade the quality of the measurement. First, the resonance will be poorly resolved and fitted. For example, only three or so frequency lines will describe the resonance. Because of leakage, the data from the highest response will tend to "leak" into the lower lines, and an incorrect estimate of the damping will result. Efforts to circle fit the data will also be frustrated because not enough points are available to describe the resonances as shown in Figure 2.1.4.2. (For definitions of circle fit, see Section 3.2).

The next section shows the importance of each of these elements in the measurement of transfer functions which contain the modal properties.

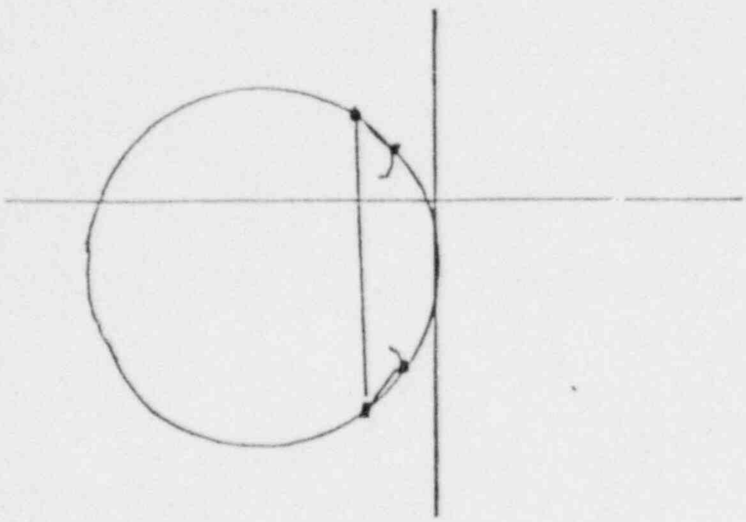

Circle Fit to Data
With Inadequate Resolution

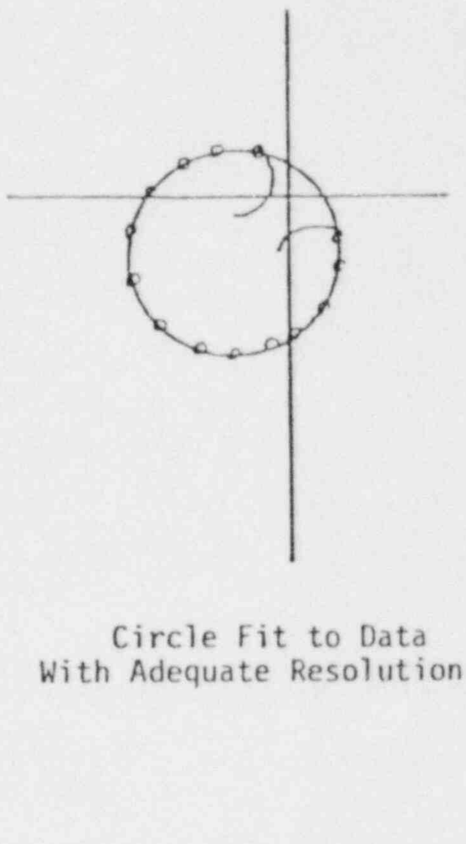

Circle Fit to Data
With Adequate Resolution

FIGURE 2.1.4.2

EXAMPLES OF CIRCLE FITS WITH
DIFFERENT SAMPLING RATES

2.1.5 Transfer Functions

The modal analysis of structures relies on the measurement of the transfer of force to a variable of the structural response. Common names for each of the commonly used transfer functions are listed in Table 2.1.5.1

TABLE 2.1.5.1

COMMON NAMES OF TRANSFER FUNCTIONS

Variables	Common Name
Acceleration/Force	Inertance, acceleration admittance
Force/Acceleration	Apparent mass, acceleration impedance
Velocity/Force	Mobility, velocity admittance
Force/Velocity	Mechanical impedance, velocity impedance
Displacement/Force	Compliance
Force/Displacement	Stiffness

The real art of modal analysis is in the interpretation of transfer functions. Through long experience, the following has been developed as an interpretation and ways to use transfer function data.

MEANING OF TRANSFER FUNCTION DATA FROM A SYSTEM DYANAMIC ANALYSIS POINT OF VIEW

1. For driving point transfer functions, the resonances and anti-resonances must alternate as one goes up the frequency range.
2. The addition of a single mass to a system decreases all non-zero resonances where the connection point participates. The resonances of the higher modes tend to be shifted more and as the frequency becomes large the new frequencies approach the anti-resonances of the original component at that location.
3. The addition of a single spring to a component increases all resonances in which the connection point participates. The frequencies of lower modes tend to be shifted more and as the frequency approaches zero the new resonances approach the anti-resonances of the original system.
4. If a sprung mass is added to a component such that its anti-resonances occurs between two successive resonances (i.e., ω_a and ω_b) of the original system, all resonant frequencies of the original system below ω_a will be decreased and all resonant frequencies above ω_b will be increased. In addition, a resonance of the combined system will occur between the anti-resonance of the sprung mass and the anti-resonance of the original system which lies between ω_a and ω_b.

5. If a constrained single degree of freedom system of natural frequency ω_a is connected to a system, the natural frequencies of that system will be shifted toward ω_a. In general, the farther a resonance is from ω_a the more it will tend to be shifted toward ω_a.
6. If a component is altered by means of a single interconnection to another system then resonances of the original system cannot be shifted from their original positions farther than the anti-resonances adjacent to each original resonant frequency.
7. If one component is connected to another component, at a single location, one and only one resonance of the combined system will lie between the resonances of the unconnected components, and one and only one resonance will lie between the anti-resonances of the unconnected components.
8. When anti-resonances of two separate systems coincide, a mode of the combined system in which the point of interconnection has zero displacement exists at that frequency.
9. If two components are rigidly interconnected at n points, the number of modes in the connected systems is n less than the number of modes in the separate systems.
10. When a system with two or more degrees of freedom is rigidly constrained at one point, the lowest resonance is raised and between every pair of resonances in the unconstrained system there will be a resonance of the constrained system. Also, the resonances of the constrained system will be at the anti-resonances of the unconstrained system viewed at the point of constraint.

11. When a strong and a weak system are rigidly interconnected at a single point, the modes of the combined system lie near the resonances of the strong system and the anti-resonances of the weak system.
12. If a resonance of the strong system and a resonance of the weak system lie close together, the combined system will have a pair of modes in this neighborhood. Furthermore, one of these modes will occur at a lower value of frequency than either the anti-resonance or the resonance and one will occur at a higher value of frequency.
13. When two systems of comparable strength are rigidly connected at a single point and a resonance of one lies near an anti-resonance of the other, the natural frequencies of the combined system will be displaced from that neighborhood by a substantial fraction of the maximum allowed by statement 7.
14. When two systems are connected together through a single weak spring, the resonances of the combined system will occur near and at slightly higher frequencies than the resonances of the separate systems. If two resonances of the separate systems lie close together, two corresponding resonant frequencies of the combined system result, of which one lies between the two separate resonances and the other lies slightly higher than either.

15. When two systems are connected together by means of a single large mass, the resonances of the combined system will lie near and slightly higher than the anti-resonances of the separate systems. If two anti-resonances of the separate system lie close together, but do not coincide two corresponding resonances of the combined system result, of which one lies between the anti-resonances of the separate systems and one lies higher than either.

16. When two systems of comparable strength are connected together at a single location by a weak coupling element, whose transfer function varies slowly with frequency, the two systems will have little effect on one another unless a resonance of one system is nearly coincident with a resonance of the other. In that case, a pair of modes will exist which will have a large participation of each component.

17. When two systems of comparable strength are interconnected by a general stiff coupling element, whose transfer function varies slowly with frequency, the two systems will have little effect on one another unless an anti-resonance of one is nearly coincident with an anti-resonance of the other. In this case a pair of modes will exist which will have a large participation of each component.

2.1.5.1 Criteria for Good Transfer Function Measurements

The following criteria will generally result in high quality measurements:

TABLE 2.1.5.1.1

EXCITATION CRITERIA
FOR HIGH QUALITY TRANSFER FUNCTION MEASUREMENTS

1. The excitation signal level should be 40-60 db above the background noise.
2. The frequency content of the excitation should be uniformly distributed (± 15 db) over the range of interest.
3. The excitation should contain no zeros at any frequency over the frequency range of interest. Dividing by zero will improperly range the transfer function.
4. The force should be appropriately ranged to the mass of the structure. The force should not permanently deform the structure or produce a non-linear response.
5. The analyzer input should be ranged appropriately for the peak signal level. (If a 2 volt peak is produced by the force, the analyzer should be set for 2 or 4 volt but not 8 volt signals).
6. [illegible] mpulse testing is used, the trigger level should be set as l[illegible] as possible.

The following response criteria will generally produce high quality transfer function measurements:

TABLE 2.1.5.1.2

RESPONSE CRITERIA
FOR HIGH QUALITY TRANSFER FUNCTION MEASUREMENTS

1. The response signal should be 40 - 60 db above the background noise.

2. The sensor should be appropriately selected for the modes of interest. Generally, displacement, strain or velocity are preferred for low frequency modes (below 5.0 Hz). Further, the sensor weight should be small compared to the weight of the structures (less than 1%).

3. The range of the response input should be correctly set to allow full use of the dynamic range of the instrument.

4. The mounted resonant frequency of the sensor should be at best five times that of the highest mode of interest.

5. There should be no major resonances just outside the range of analysis. The residual compliance of a large resonance can greatly distort the measurement of modal properties of a small adjacent resonance.

The criteria for coherence in obtaining usable transfer functions for modal analysis are described in Table 2.1.5.1.3

TABLE 2.1.5.1.3

COHERENCE CRITERIA FOR HIGH QUALITY TRANSFER FUNCTIONS

1. Coherence = .9 and above at resonances.
2. Coherence = .6 and above at all but antiresonance.
3. Partial coherence for indirect transfer functions are above .8 and well understood.

These criteria were met throughout this program.

If the coherence is less than .8 in the vicinity of an important resonance or over any substantial frequency interval, it is an indication that:

- The signal-to-noise ratio of either or both signals is too low (this could be caused by insufficient excitation at the input or response point, or by faulty measurement equipment).
- Extraneous inputs are entering the structure.
- Excitations are not being measured properly (i.e., transducers are loose or mounted in the wrong place or in the wrong direction).
- Not enough averages are being taken for each measurement (i.e., the more noise sources inherently associated with the structure, the more averages that should be taken).
- Aliasing of the data is taking place.
- Resolution of the measurement is not adequate.
- The response of the structure at a non-resonant frequency is extremely low relative to the response of resonant coherence at non-resonant frequencies.

2.2 Hammer Test Procedure

The equivalence of hammer (impulse) testing to shaker testing is described in Reference 4.

This section describes only the data acquisition activity for hammer testing as it differs from shaker testing. The analysis procedure for impulse generated data is described in Section 3.0.

First, the response measuring accelerometer is attached to the structure under test at a point where all modes can be measured. Generally an end or edge point is best. Next, the hammer is used to hit the structure at several points and the accelerometer moved to new points to assure that all modes are sensed at the final accelerometer position. This determination is made by observation of the data.

Several steps precede the acquisition and analysis of data. The first steps establish a "project file" on the magnetic disc. The project file is a framework in which all of the testing and analysis can take place in an orderly manner and which allows easy information retrieval.

In this example (a fuze), the project was initiated by the command:

IZ "FUZE"

I implies initiate.

Z implies project.

(The word in quotation marks is the title of the project.)

Next we attached Associated Data Files (ADF's) to have stored on the discs. The commands are:

AP 'FUZP' for modal parameter storage.

AS 'FINTS' for mode shapes of the interior compenents.

AG 'FUZG' for the fuze geometry (all points).

AH 'FUZH' for the fuze transfer functions.

AT 'FUZT' for the fuze trace links and coordinate traces.

A readout of the project status is possible using the ?Z command. For our example, the computer responded as follows:

```
#?Z
 CHECKPOINT 092278-000000
Z FUZE     091878-000000           0/MODAL SURVEY PATRIOT DUMMY FUZE
P FUZP     091878-000000          10/FUZE PARAMETERS
S FINTS    092178-000000          10/FUZE INTERNAL SHAPE
G FUZG     080878-000000       1/FUZE GEOM
H FUZH     091878-000000     150/FUZE TRANSFER FUNCTIONS
T FUZT     080878-000000      12/FUZE SEQUENCES
```

The next step was to enter a description of the geometric location of each point for which we would test into the geometry file using the RG@K command, entering the data as follows:

Point No.	X Dimension	Y Dimension	Z Dimension	
1	0	0	0	Return
2	300	0	0	Return

and so on for each point. The units are in inches and no decimals are allowed in the geometry.

We saved the geometry with the "WG" command and recall it with the "RG" command when needed for listing on the disc or changing.

Next, the trace links are entered into the computer using the "RTL@K" command. The trace links represent lines from one point of the geometry to the next to show how the model is formed. After the trace link was formed as described, it is saved by the WTL command. Generally, we make the trace link file in several sections to avoid excessive re-type work to accommodate errors.

The final step preparatory to data acquisition is the building of a condition file in the /D (data acquisition) subtask. By using the MC (modify condition) command, we communicate to the computer the methods we will use to perform the tests. An example is given in the following listing.

```
LC                                      CODE DEFINITION
 1 TRIGGER TYPE       1     EXTERNALLY GENERATED TRANSIENT, AS OPPOSED TO
                              RANDOM OR OTHER EXCITATION.
 2 TRIGGER LEVEL      5     TRIGGER AT 5% oF THE LEVEL SET IN CHANNEL 1 RANGE
                              (CONDITION 21)
 3 COUPLING CODE      0     AC AS OPPOSED TO DC
 4 HANNING CODE       0     NO HANNING WEIGHTING
 5 ENSEMBLE SIZE      4     AVERAGE 4 HAMMER TAPS
 6 MAXIMUM FREQ    2994.2   MAX. FREQUENCY
 7 A-A FILTERS     3000.0
 8 EXCITATION         1     TRANSIENT
 9 FREQRESP   1      21     CHANNEL 2/CHANNEL 1
10 FREQRESP   2       C
11 FREQRESP   3       0
12 OVERRANGES         0     OVERRANGES ALLOWED PER FRAME OF DATA
13 CLEAR FREQ   L 0.00000
14 CLEAR FREQ   U  2994.2
15 MINIMUM FREQ   0.00000
19 MASTER IDENT      10     *INT. PLATE*
20 AUXIL  SCALE   1.0000
21 CH 01  RANGE  0.50000    PEAK VOLTAGE ON CHANNEL 1 (FORCE SIGNAL)
22 CH 02  RANGE   1.0000    PEAK VOLTAGE ON CHANNEL 2 (ACCELERATION SIGNAL)
23 CH 03  RANGE   8.0000
24 CH 04  RANGE   8.0000
25 CH 01  SCALE   100.00    100 LBF/VOLT (10 MV/LBF)
26 CH 02  SCALE   100.00    100 G/VOLT   (100 MV/G)
27 CH 03  SCALE   1.0000
28 CH 04  SCALE   1.0000
29 CH 01  SIGNAL      4     FORCE
30 CH 02  SIGNAL      3     ACCELERATION
31 CH 03  SIGNAL      3     ACCELERATION
32 CH 04  SIGNAL      3     ACCELERATION
#
```

Finally, we are prepared for preliminary data acquisition. To confirm that our signal form and amplitude are correct, using the "ES" command, we impact the fuse one time and observe the signal level using the ∧#1 command for observing the force signal and ∧#2 for the response. Examples of each are shown in Figures 2.2.1 and 2.2.2. These examples show that we are correctly ranged for this test.

Finally, we gather data into transfer function format. The transfer function we use is acceleration per pound of force at each frequency. It is in this format that the data is stored onto magnetic media for later analysis.

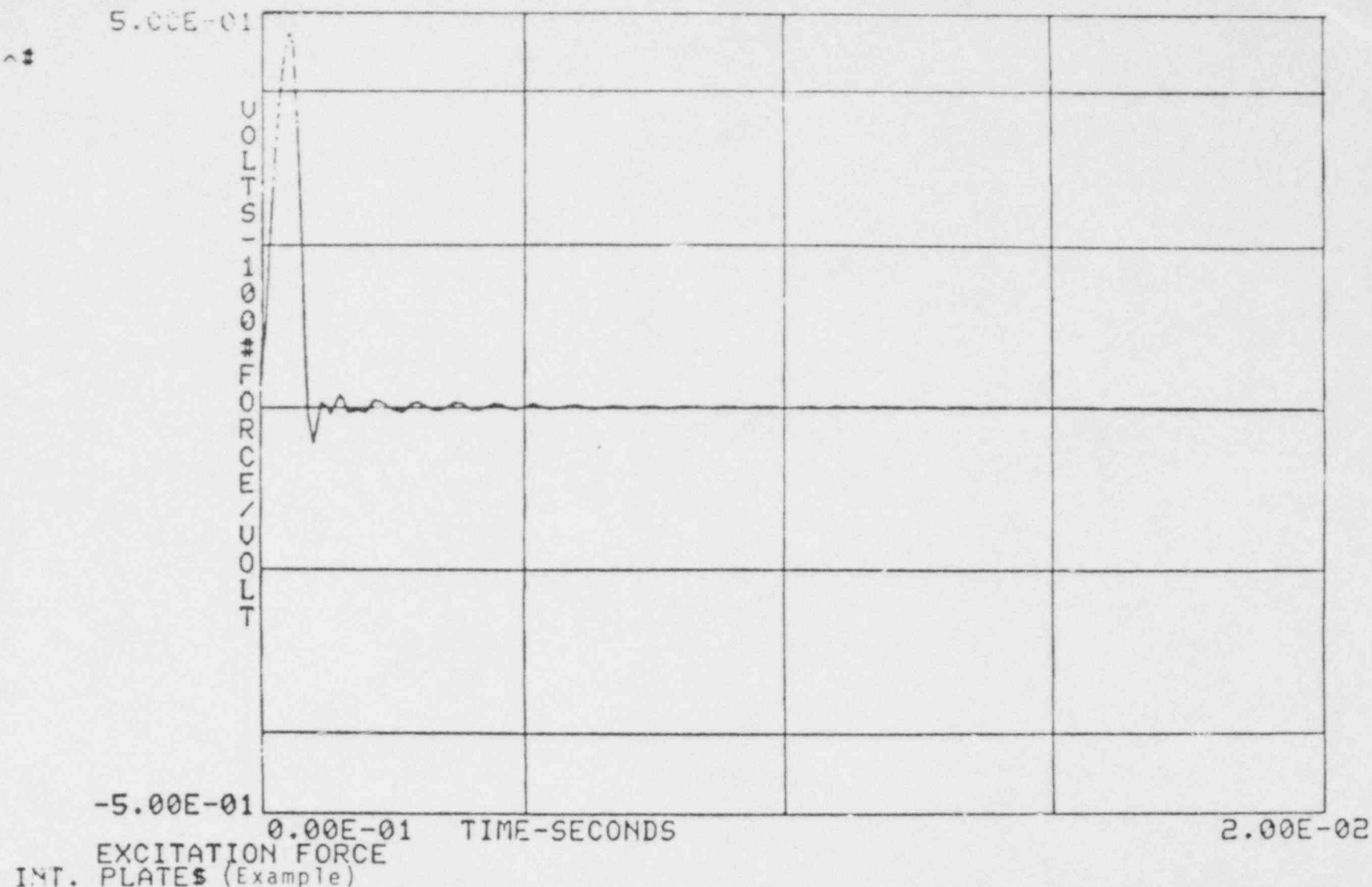

FIGURE 2.2.1

FORCE SIGNAL OBSERVED USING "ES" COMMAND

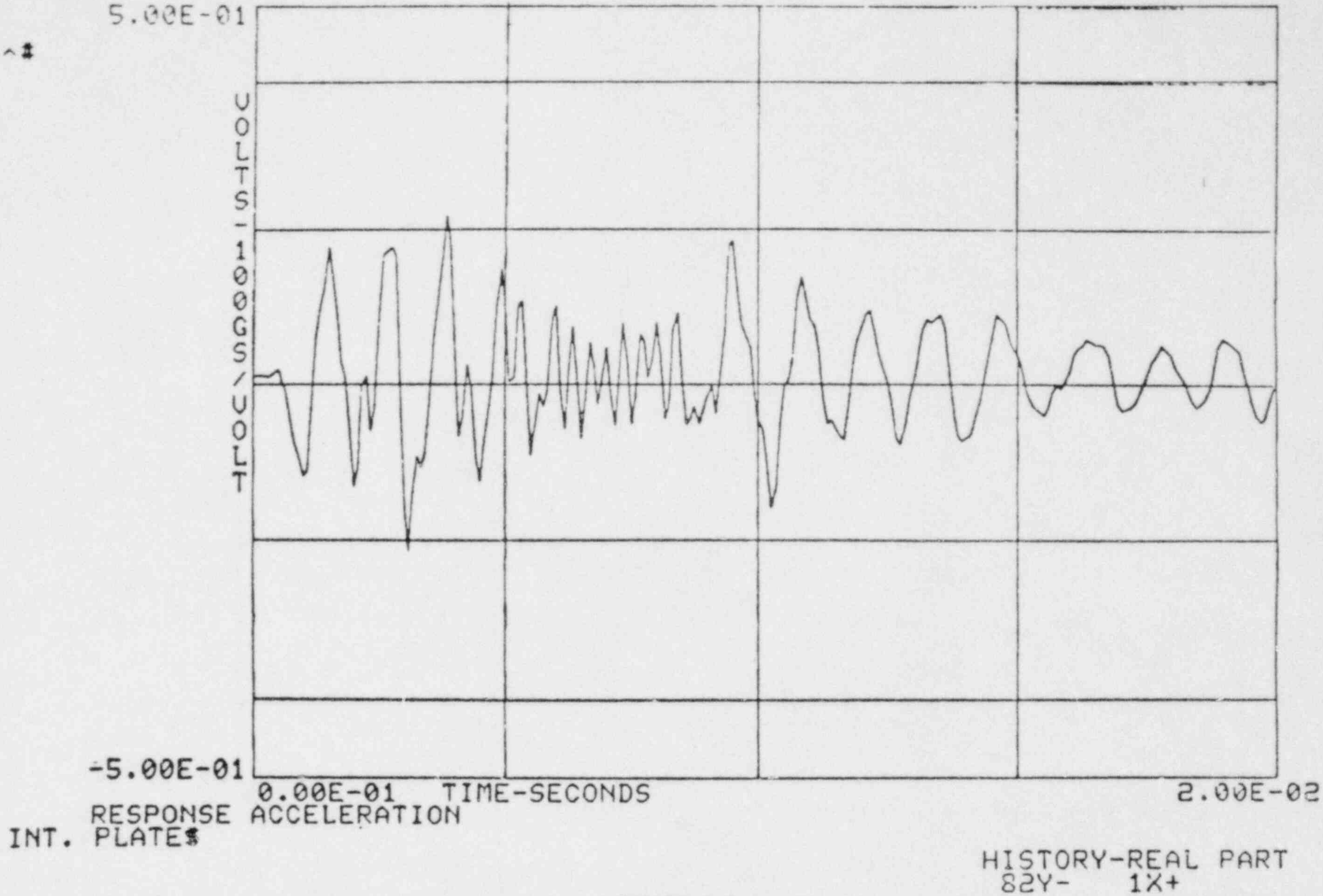

FIGURE 2.2.2

ACCELEROMETER SIGNAL OBSERVED USING "ES" COMMAND

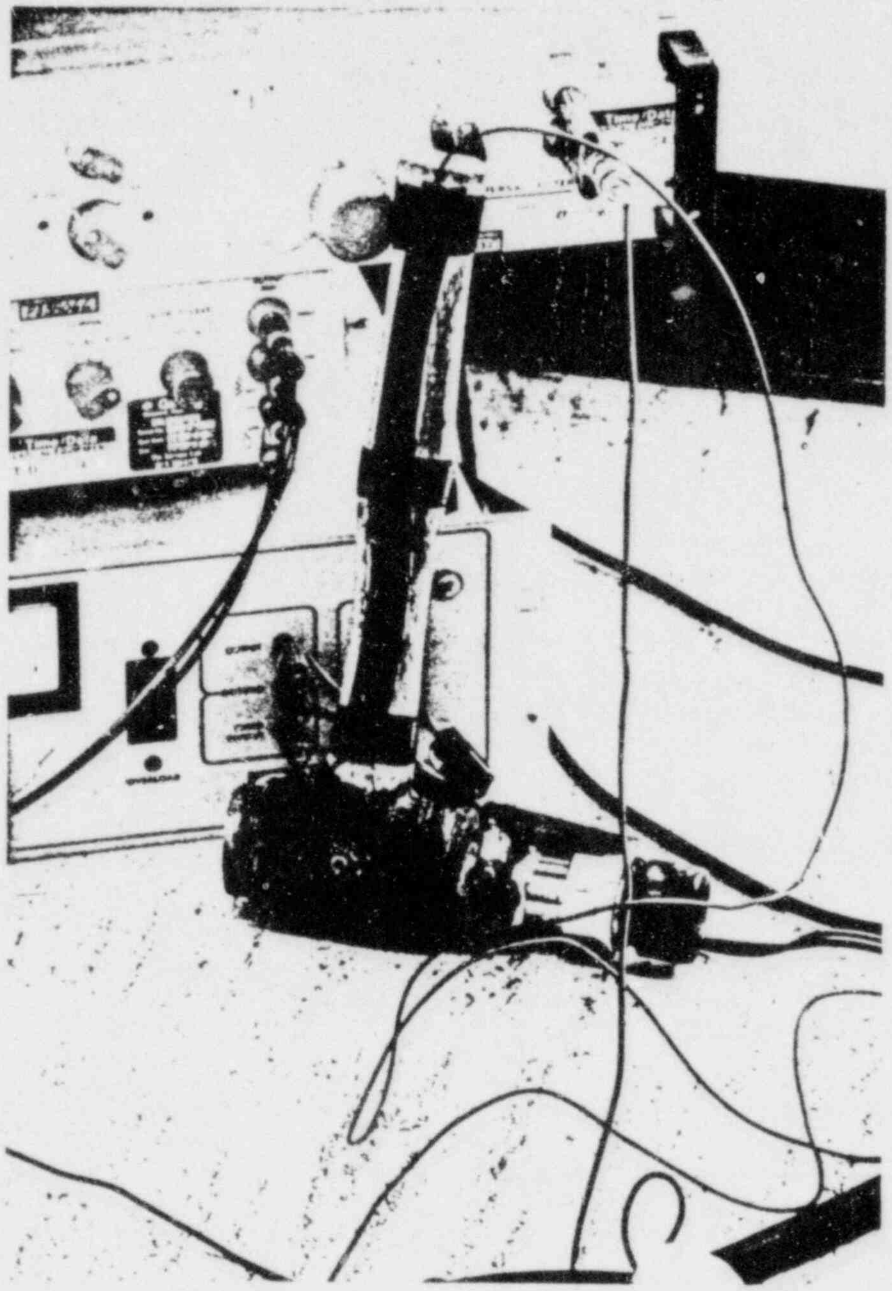

FIGURE 2.?.3

A PHOTOGRAPH OF THE TRANSITEK HAMMER

2.3 Electro Magnetic (E-M) Shaker Test Procedure

A typical E-M shaker test set-up is shown in Figure 2.3.1. The force signal is a broad band random signal with approximately equal input from 1 to 100 Hz. The accelerometers are moved from point to point until data is collected at each point for which a measurement has been specified.

Prior to start of testing, the force signal is examined by oscilloscope for smoothness and amplitude to confirm that the force transducer is not rattling and that the shaker armature is not bottomed out. This step assures us that all of the shaker energy is going into the desired frequency range. A complete set-up similar to that discussed in Section 2.2 is performed and verified.

The accelerometer signals are examined at each measurement point to assure that the range of the A/D converter is set to utilize the full dynamic range of the analyzer.

Once the shaker has been started, the force signal is not changed throughout the entire test. For this reason a representative sample of the force spectra is adequate to characterize the force at all times throughout the test.

Analagous to the repeated blows of the hammer, repeated samples of the time histories are analyzed to provide improved statistical estimates of the transfer function. In these tests 16-30 frames (samples) were analyzed, or about 3 minutes per measurement.

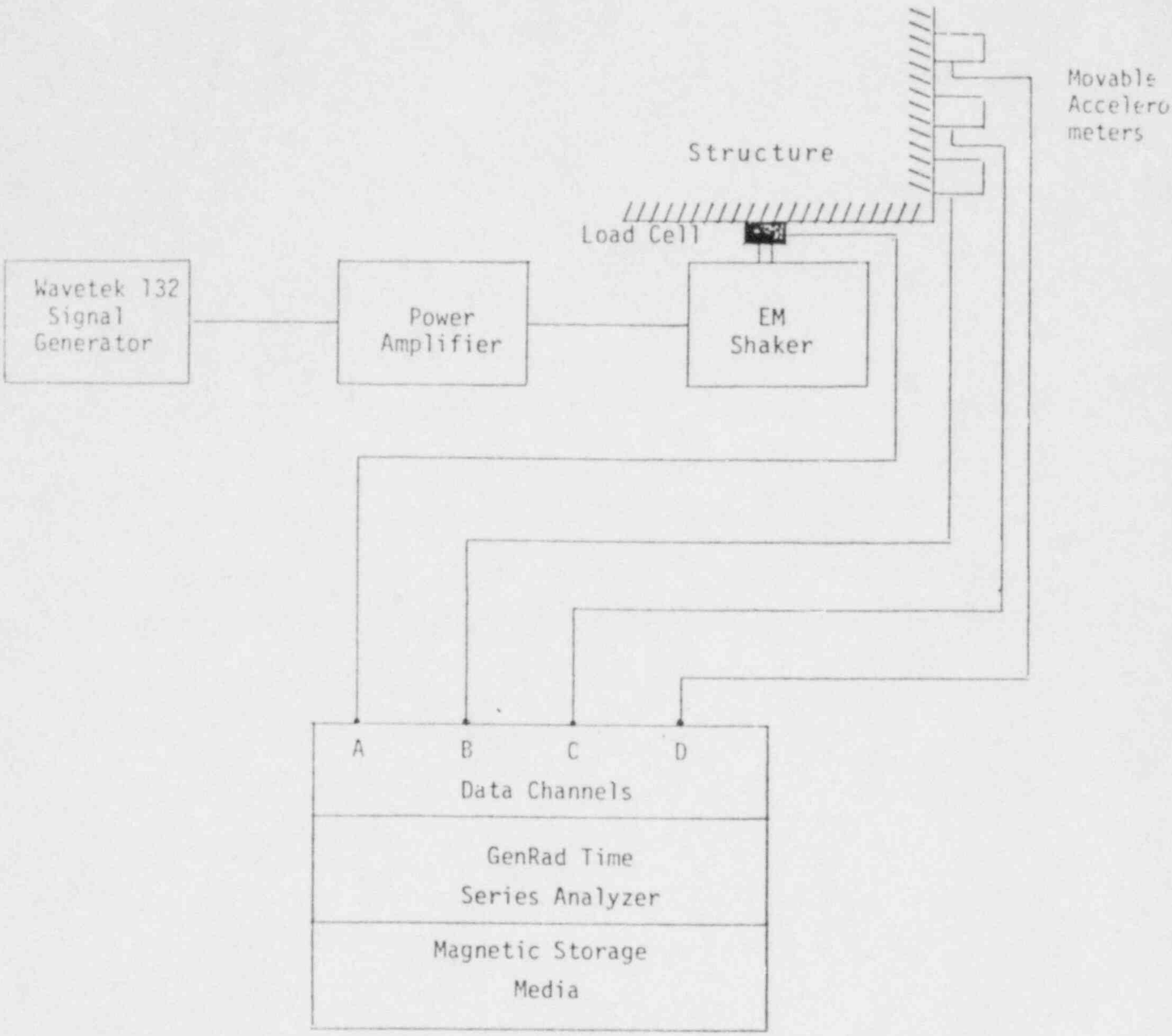

FIGURE 2.3.1

ELECTROMAGNETIC SHAKER TEST SET-UP

2.4 Hydraulic Shaker Test Procedure

In theory, the hydraulic shaker test is identical to that of the EM shaker. In practice, the measurement of force must be altered radically due to the bulk of the brackets involved in mounting the shaker.

Figure 2.4.1 shows a typical haudraulic shaker test set-up. The shaker force is measured by an accelerometer on the reaction mass. The shaker force is directly proportional to the reaction mass and to the acceleration of the mass. The advantage of this method is that no brackets or fixtures are required for anchoring the shaker to a wall or floor and no static load is applied to the structure by the actuator.

The oscilloscope (Figure 2.4.1) is used to observe the force to assure that no bottoming out is occurring and that the bearings supporting the mass are not binding. The accelerometer signals are observed upon starting the force to assure that the acceleration does not exceed reasonable levels on special equipment. Also, this observation assures that the signal levels are set into the computer to provide the maximum dynamic range for analysis.

At each measurement point, the accelerometer position gain and signal level were recorded and saved as part of the permanent test records.

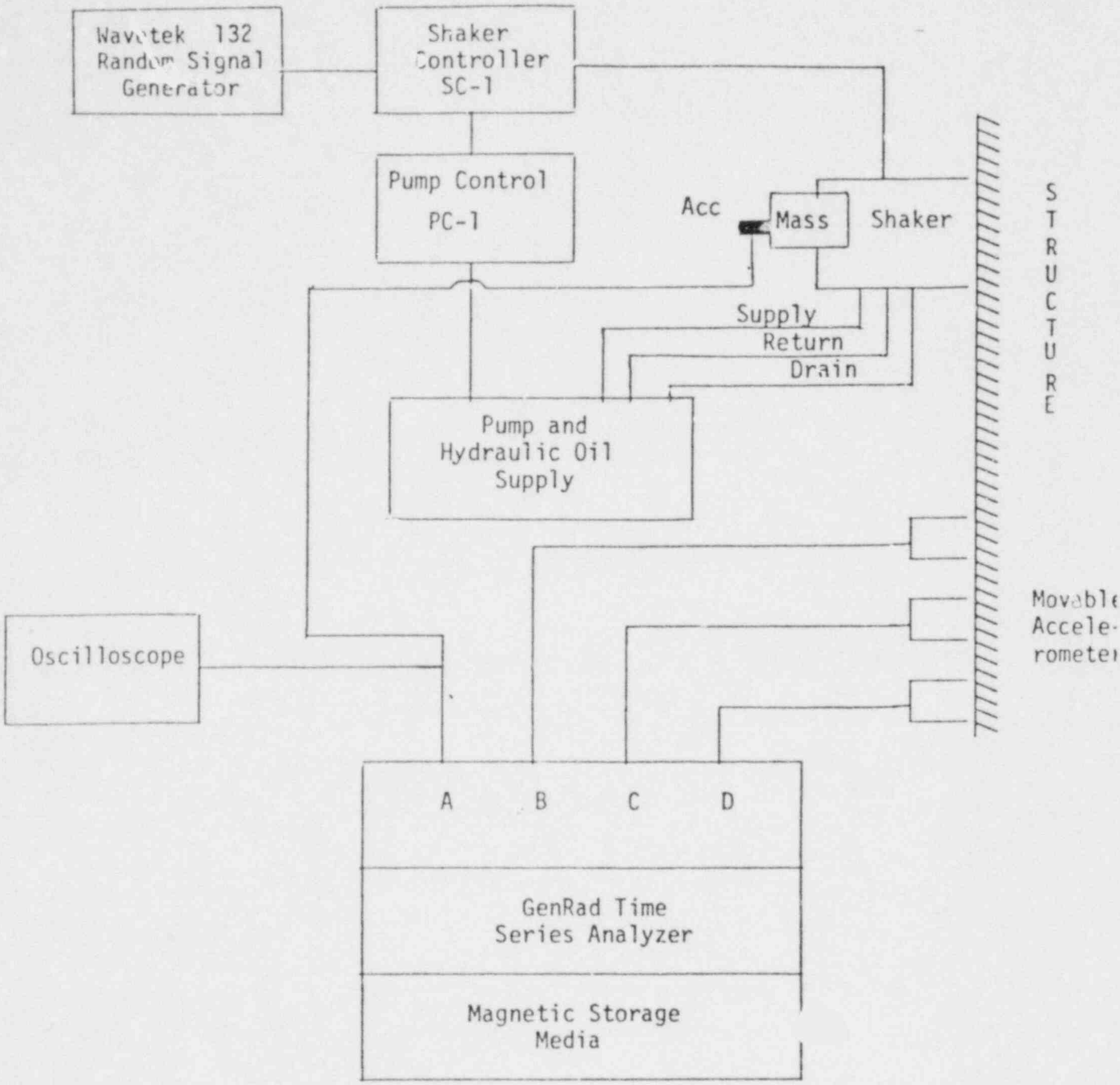

FIGURE 2.4.1

HYDRAULIC SHAKER TEST SET-UP

3.0 ANALYSIS METHODS:

The methods for analysis are based on the MPLUS program. To understand the theoretical background as developed for analysis, we first present the general relationship of data from Reference (1) as Section 3.1. Next, the methods of obtaining resonant frequency and dampings from transfer functions are presented in Section 3.2 and 3.3. Section 3.4 discusses circle fitting, the method of mode shapes calculation.

3.1 Theoretical Background for Analysis of Transfer Functions(1)

The theory behind modal analysis via frequency response functions can be examined by referring to the equations of motion for an N degree of freedom system with viscous damping:

$$[M][\ddot{q}] + [C][\dot{q}] + [K][q] = [f] \quad (1)$$

where

[M] = mass matrix

[C] = viscous damping matrix

[K] = stiffness matrix

[q] = time history of the displacement of system

[f] = time history of excitation to system

$[\dot{q}]$ = time history of velocity of system

$[\ddot{q}]$ = time history of acceleration of system

This equation is inconvenient to handle with standard methods of eigenvalue analysis if [C] is not proportional to [M] or [K]. However, a method has been proposed by Duncan[7] which reduces these equations to a standard eigenvalue form. In this method combine the identity:

$$[M][\dot{q}] - [M][\dot{q}] = [0]$$

with Equation 1 to obtain:

$$\begin{bmatrix} [0] & [M] \\ [M] & [C] \end{bmatrix} \begin{bmatrix} [\ddot{q}] \\ [\dot{q}] \end{bmatrix} + \begin{bmatrix} -[M] & [0] \\ [0] & [K] \end{bmatrix} \begin{bmatrix} [\dot{q}] \\ [q] \end{bmatrix} = \begin{bmatrix} [0] \\ [f] \end{bmatrix} \quad (2)$$

Represent this equation in the following manner:

$$[A][\dot{y}] + [B][y] = [z] \quad (3)$$

where

$$[A] = \begin{bmatrix} [0] & [M] \\ [M] & [C] \end{bmatrix}$$

$$[B] = \begin{bmatrix} -[M] & [0] \\ [0] & [K] \end{bmatrix}$$

$$[y] = \begin{bmatrix} [\dot{q}] \\ [q] \end{bmatrix}$$

$$[z] = \begin{bmatrix} [0] \\ [f] \end{bmatrix}$$

In order to find the solution to Equation 3 for the case of harmonic inputs, first consider the solution to the homogeneous equation found by letting $[z] = [0]$

$$[A][\dot{y}] + [B][y] = [0] \qquad (4)$$

Seek a solution of the form $[y] = [Y]\, e^{st}$

therefore $[\dot{y}] = s\, [Y]\, e^{st}$

Hence, Equation 4, becomes,

$$s[A][y] + [B][y] = [0] \text{ or}$$

$$\left[[B] + s[A]\right]\ [y] = [0]$$

This set of equations only have a solution if the determinant of the coefficient matrix is zero.

$$\det \left\{[B] + s[A]\right\} = 0$$

This leads to a set of 2N roots or eigenvalues s_1, s_2, s_{2_n} ..., which satisfy the above equation. For a resonant system, these eigenvalues will occur in conjugate pairs. Corresponding to each eigenvalue s_r, there exists an eigenvector $[\Psi^r]$ having 2N components satisfying the following equation:

$$[B] + s_r[A]\ \ [\Psi^r] = [0] \qquad (5)$$

In the case where the eigenvalues of a system are complex, in which case they occur in conjugate pairs, the eigenvectors will be complex and will also occur in conjugate pairs,

The above eigenvectors have important orthogonality conditions which can be easily shown. Consider the r^{th} and p^{th} eigenvectors $[\Psi^{r}]$ and $[\Psi^{p}]$ both of which satisfy Equation 5. First write Equation 5 for the r^{th} mode and premultiply by the transposed vector $[\Psi^{p}]^{T}$, to obtain:

$$[\Psi^{p}]^{T}[B][\Psi^{r}]-s_{r}[\Psi^{p}]^{T}[A][\Psi^{r}]=[0] \qquad (6)$$

Using the reversal law for transposed matrix products and recalling that [A] and [B] are symmetric matrices, transpose Equation 6 to obtain:

$$[\Psi^{r}]^{T}[B][\Psi^{p}]+s_{r}[\Psi^{r}]^{T}[A][\Psi^{p}]=[0] \qquad (7)$$

Next write Equation 5 for the p^{th} mode and premultiply by $[\Psi^{r}]^{T}$

$$[\Psi^{r}]^{T}[B][\Psi^{p}]+s_{p}[\Psi^{r}]^{T}[A][\Psi^{p}]=[0] \qquad (8)$$

If Equation 8 is subtracted from Equation 7, the result is:

$$(s_{r}-s_{p})\ [\Psi^{r}]^{T}[A][\Psi^{p}] = 0$$

If eigenvalues s_r and s_p are different, the following orthogonality properly relates the two eigenvectors:

$$[\Psi^{r}]^{T}[A][\Psi^{p}] = 0 \qquad (9)$$

It follows that these vectors are also orthogonal with respect to matrix [B]

$$[\Psi^{r}]^{T}[B][\Psi^{p}] = 0 \qquad (10)$$

Equations 9 and 10 are important orthogonality conditions which shows that the 2N vectors $[\Psi]$ form a linearly independent set, and therefore any vector in 2N space can be expressed as a linear combination of these 2N vectors. Since we are interested in frequency response information, let

$$[z(t)]=[Z]\,e^{j\omega t} \tag{11}$$

and seek a solution in the form:

$$[y(t)] = [Y]e^{j\omega t} \tag{12}$$

Substitute Equation 11 and Equation 12 into Equation 3 and divide by $e^{j\omega t}$ to obtain:

$$j\omega[A][Y] + [B][Y] = [Z] \tag{13}$$

Since the eigenvectors defined by Equation 5 form a linearly independent set over 2N space, write the solution to Equation (13) as a linear combination of these 2N vectors

$$[Y] = \sum_{r=1}^{2N} \gamma_r[\Psi^r] \tag{14}$$

Substitute Equation 14 into Equation 13 and multiply by $[\Psi^p]^T$ to obtain:

$$j\omega[\Psi^p]^T[A]\sum_{r=1}^{2N}\gamma_r[\Psi_r]+[\Psi^p]^T[B]\sum_{r=1}^{2N}\gamma_r[\Psi^r]=[\Psi^p]^T[Z]$$

From the orthogonality conditions, we obtain:

$$j\omega a_p(\gamma_p) + b_p(\gamma_p)=[\Psi^p]^T[Z] \tag{15}$$

where

$$a_p = [\Psi^p]^T[A][\Psi^p]$$
$$b_p = [\Psi^p]^T[B][\Psi^p]$$

Hence, we can solve Equation 15 for γ_p to obtain:

$$\gamma_p = \frac{[\Psi^p]^T[Z]}{j\omega a_p + b_p} \tag{16}$$

Substituting Equation 16 into Equation 14, we obtain:

$$[Y] = \sum_{r=1}^{2N} \frac{[\Psi^r]^T[Z][\Psi^r]}{j\omega a_r + b_r} \tag{17}$$

However, from Equation 7, we obtain

$$b_r + s_r a_r = 0$$

$$s_r = \frac{-b_r}{a_r}$$

Therefore, Equation 17 can be written

$$[Y] = \sum_{r=1}^{2N} \frac{[\Psi^r]^T[Z][\Psi^r]}{a_r(j\omega - s_r)} \tag{18}$$

Frequently the complex eigenvalues s_r are written in the following form:

$$s_r = -\zeta_r \omega_r \pm j\ \omega_r \sqrt{1-\zeta_r^2}$$

Where

ζ_r = damping ratio

ω_r = undamped natural frequency

In terms of [Q] and [F], Equation 18 becomes:

$$\begin{bmatrix} j\omega Q \\ Q \end{bmatrix} = \sum_{r=1}^{2N} \frac{[\Psi^r]^T \begin{bmatrix} 0 \\ F \end{bmatrix} [\Psi^r]}{a_r(j\omega - \zeta_r \omega_r \pm j\,\omega_r\sqrt{1-\zeta_r^2})}$$

Therefore the frequency response function recorded from excitation applied at location k and response monitored at location i is:

$$H_{ik} = \sum_{r=1}^{2N} \frac{\Psi_k^{\,r} \quad \Psi_i^{\,r}}{a_r(j\omega + \zeta_r\,\omega_r \pm j\,\omega_r\sqrt{1-\zeta_r^2})} \tag{19}$$

Since the eigenvalues occur in conjugate pairs, Equation 19 can be written as:

$$H_{ik} = \sum_{r=1}^{N} \frac{\Psi_k^{\,r} \quad \Psi_i^{\,r}}{a_r(j\omega + \zeta_r\,\omega_r + j\,\omega_r\sqrt{1-\zeta_r^2}} + \frac{\Psi_k^{\,r*} \quad \Psi_i^{\,r*}}{a_r^*(j\omega + \zeta_r\,\omega_r - j\,\omega_r\sqrt{1-\zeta_r^2})} \tag{20}$$

Equation 19 is an extremely valuable relationship between Frequency Response Functions and modal characteristics. It relates motion at any point i due to a force at point k. Notice that Equation 19 implies that the frequency response between response at i and excitation at k is the same as the function between response at k and excitation at i. Equation 19 is frequently written in the form:

$$H_{ik} = \sum_{r=1}^{2N} \frac{A_{ik}^{r}}{(s - s_r)} = \sum_{r=1}^{N} \frac{A_{ik}^{r}}{(s-s_r)} + \frac{A_{ik}^{r*}}{(s-s_r^*)} \tag{21}$$

where

$$A_{ik}^{r} = \text{Residue at pole } s_r (\text{i.e. } \frac{\Psi_i^r \ \Psi_k^r}{a_r})$$

The impulse response of the system can be obtained from Equation 21 by performing an inverse transform to obtain:

$$H_{ik}(t) = \sum_{r=1}^{2N} A_{ik}^{r} \ e^{s_r t} \tag{22}$$

Since the roots occur in conjugate pairs, Equation 22 can be written in the form:

$$H_{ik}(t) = 2 \sum_{r=1}^{N} \left| A_{ik}^{r} \right| \epsilon^{-\zeta_r \omega_r t} \cos[(\omega_r \sqrt{1-\zeta_r^{2}}) + \phi_{ik}^{r}] \tag{23}$$

where

$$\phi_{ik}^{r} = \measuredangle A_{ik}^{r}$$

Equation 23 indicates that the impulse response of the system can be represented by a summation of the number of damped cosine waves times the appropriate modal parameters.

The multi-degree-of-freedom (MDOF) curve fitting procedures in the modal analysis program calculates the value of A^r_{ik} in the above equations. Therefore, in the case where A^r_{ik} was determined from a displacement/force frequency response function, the value of a_r can be determined from the equation:

$$a_r = \frac{\Psi^r_i \quad \Psi^r_k}{A^r_{ik}}$$

where

A^r_{ik} is determined from a displacement/force function.

In the case where a velocity/force frequency response function was curve fit with the MDOF procedure, the parameter a_r is determined from the following:

$$a_r = \frac{\Psi^r_i \qquad \Psi^{\dot{r}}_k}{A^r_{ik}} \times j\ \omega_r$$

where: ω_r is in the units of rad/sec and

A^r_{ik} is determined from a velocity/force function

Sim .rly, if an acceleration/force frequency response function is used, a_r is determined from the equation:

$$a_r = \frac{\Psi^r_i \quad \Psi^{\ddot{r}}_k}{A^r_{ik}} \times (-\omega_r{}^2)$$

where

ω_r is in units of rad/sec and

A^r_{ik} is determined from an acceleration/force function.

If an analytical model is to be created from the test data, the parameters a_r, Ψ^r, ω_r and ξ_r are all that is necessary to describe the component with complex normal modes. However, in some cases an analyst would like to use a "real" mode approximation with the associated effective mass or effective stiffness in order to describe the component under test via the following equation:

$$H_{ik} = \sum_{r=1}^{N} \frac{\Psi_i^r \quad \Psi_k^r}{m_r[\omega_r^2 - \omega^2 + j\, 2\, \xi_r \omega \omega_r]} \qquad (24)$$

In that case it is recommended that this approximate representation be determined by setting the magnitude of the mode shape coefficient equal to the magnitude of the complex mode shape value and the sign of the mode shape coefficient from one of the following procedures:

1) Inverse of the sign of the imaginary portion of the mode shape coefficient when a displacement/force frequency response function is used to determine the mode shape coefficients.
2) The sign of the real portion of the mode shape coefficient when a velocity/force frequency response function is used to define the mode shape coefficients.
3) Sign of the imaginary portion of the mode shape coefficient when an acceleration/force frequency response function is used to determine the mode shape coefficients.

The effective mass necessary to approximate the actual frequency response with that described by Equation 24 can be determined from one of the following equations:

$$m_r = \frac{(\text{Approx. } \Psi_i^r)(\text{Approx. } \Psi_k^r)}{2\omega_r \left| A_{ik}^r \right|}$$

where A_{ik}^r is determined from a displacement/force function

$$m_r = \frac{(\text{Approx. } \Psi_i^r)(\text{Approx. } \Psi_k^r)}{2 \left| A_{ik}^r \right|}$$

where A_{ik}^r is determined from a velocity/force function

$$m_r = \frac{(\text{Approx. } \Psi_i^r)(\text{Approx. } \Psi_k^r)}{2 \left| A_{ik}^r \right|} \times \omega_r$$

where A_{ik}^r is determined from an acceleration/force function

In order to represent a component in an overall system model via a "real" mode approximation, the following approach can frequently be used. The uncoupled equations of motion for the component in terms of modal coordinates $[\gamma]$ are:

$$\left\{ -\omega^2 [\ulcorner m \lrcorner] + j\omega [\ulcorner c \lrcorner] + [\ulcorner k \lrcorner] \right\} [\gamma] = [F_\gamma]$$

where $[\ulcorner m \lrcorner]$ is a diagonal matrix of effective masses

$[\ulcorner c \lrcorner]$ is a diagonal matrix of effective damping

$[\ulcorner k \lrcorner]$ is a diagonal matrix of effective stiffnesses

The motion of the physical coordinates [Q] is related to the motion of the modal coordinates by:

$$[Q] = [\Psi][\gamma]$$

Symbolically, this can be represented by the following diagram:

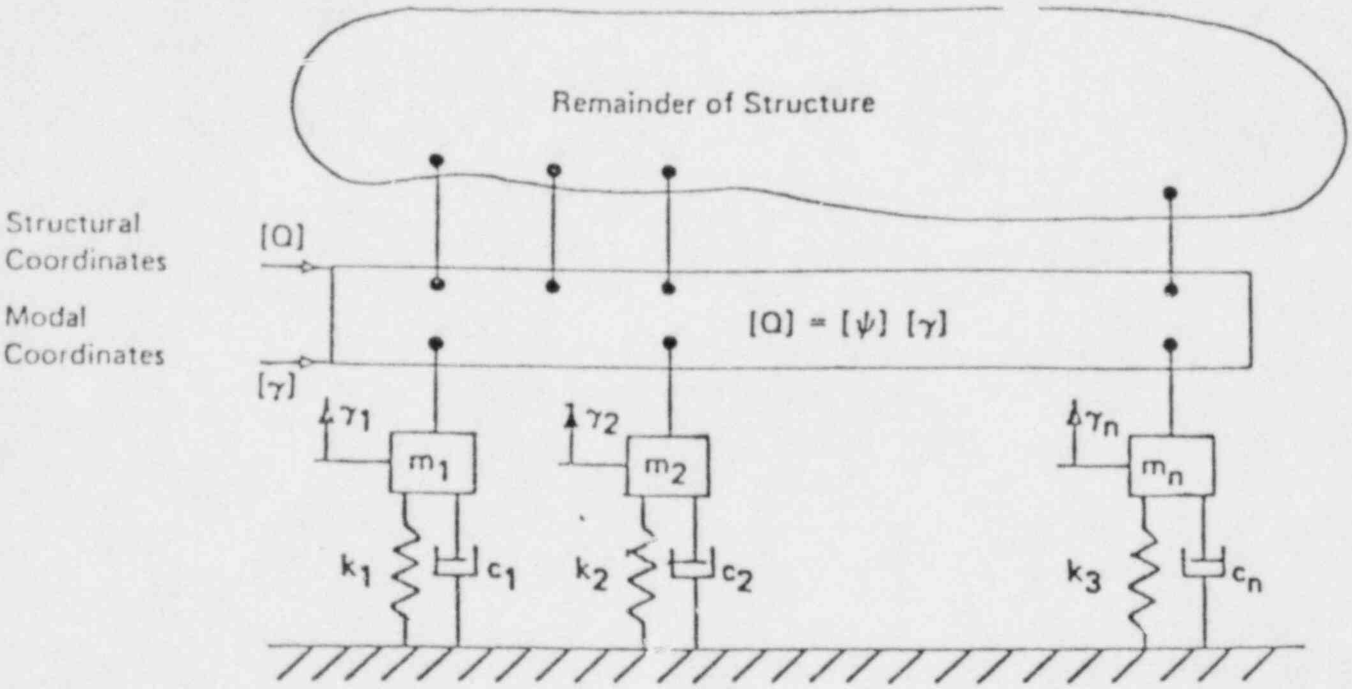

Therefore, a component can be represented analytically from test data in an overall system model by a set of springs, masses, dampers and equations of constraint which relate the motion of the physical coordinates to the motion of the modal coordinates. Since the equations of constraint can be quite voluminous, the NASTRAN input and MATRIX Generation task provides the capability to generate NASTRAN Multi Point Constraint (MPC) equations in a relatively automatic manner.

RESIDUAL INERTANCE AND COMPLIANCE

The frequency response in a specified range can be approximately described in terms of the following quantities:

1) "Residual Inertance" of the modes of vibration below the range of interest.
2) The modes of vibration which are resonant in the specified frequency range.
3) "Residual Compliance" of the modes of vibration above the range of interest.

Mathematically this can be expressed as:

$$H_{ik} = \frac{X_{ik}}{\omega^2} + \sum_{r=1}^{2N} \frac{\Psi_k^r \Psi_i^r}{a_r(j\omega + \zeta_r\omega_r \pm j\omega_r\sqrt{1-\zeta_r^2})} + Z_{ik}$$

This concept is shown graphically in the following figures:

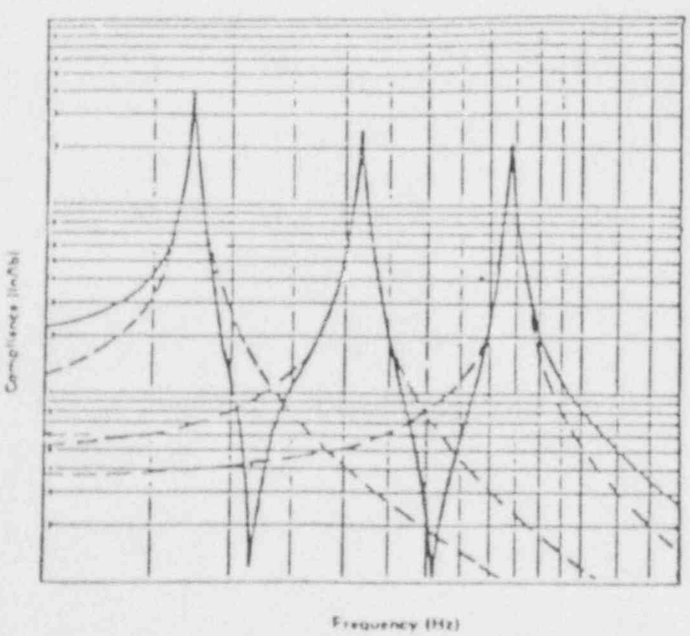

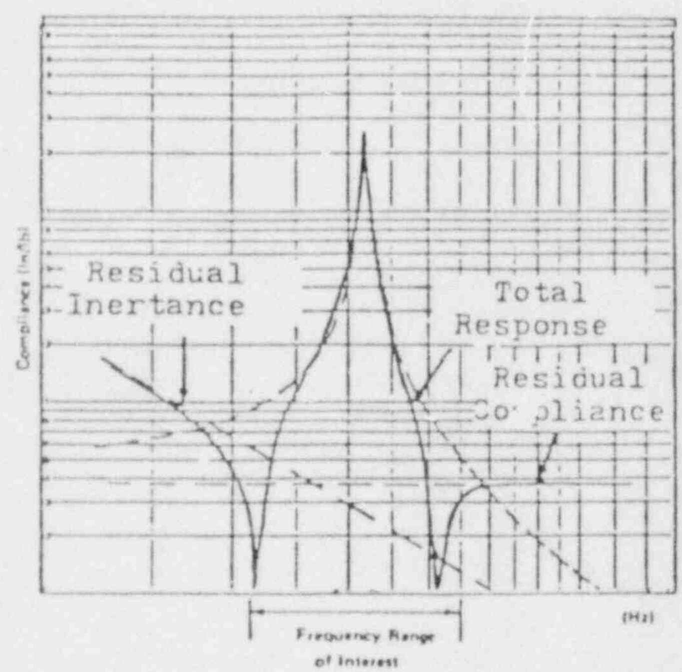

The SDOF and MDOF curve fitting procedures available in the Estimation task are used to evaluate the contribution due to the modes which are resonant in the frequency range under investigation. In order to determine the contribution of the residual effects the Generate Residual command in the Frequency Response Synthesis task is used.

3.2 Identification of Resonant Frequencies

Resonant frequencies can be estimated in any of the following ways:

1) Peak identification from the transfer function.
2) Zero crossing of the real component with simultaneous peaking of the imaginary component of the transfer function.
3) Estimation from the inverse Fourier transform of the transfer function by the GE command.

Examples of results of each method are shown in Figures 3.2.1 through 3.2.3

Throughout this test program resonant frequencies were determined by the third method which is described in great detail in Reference 2.

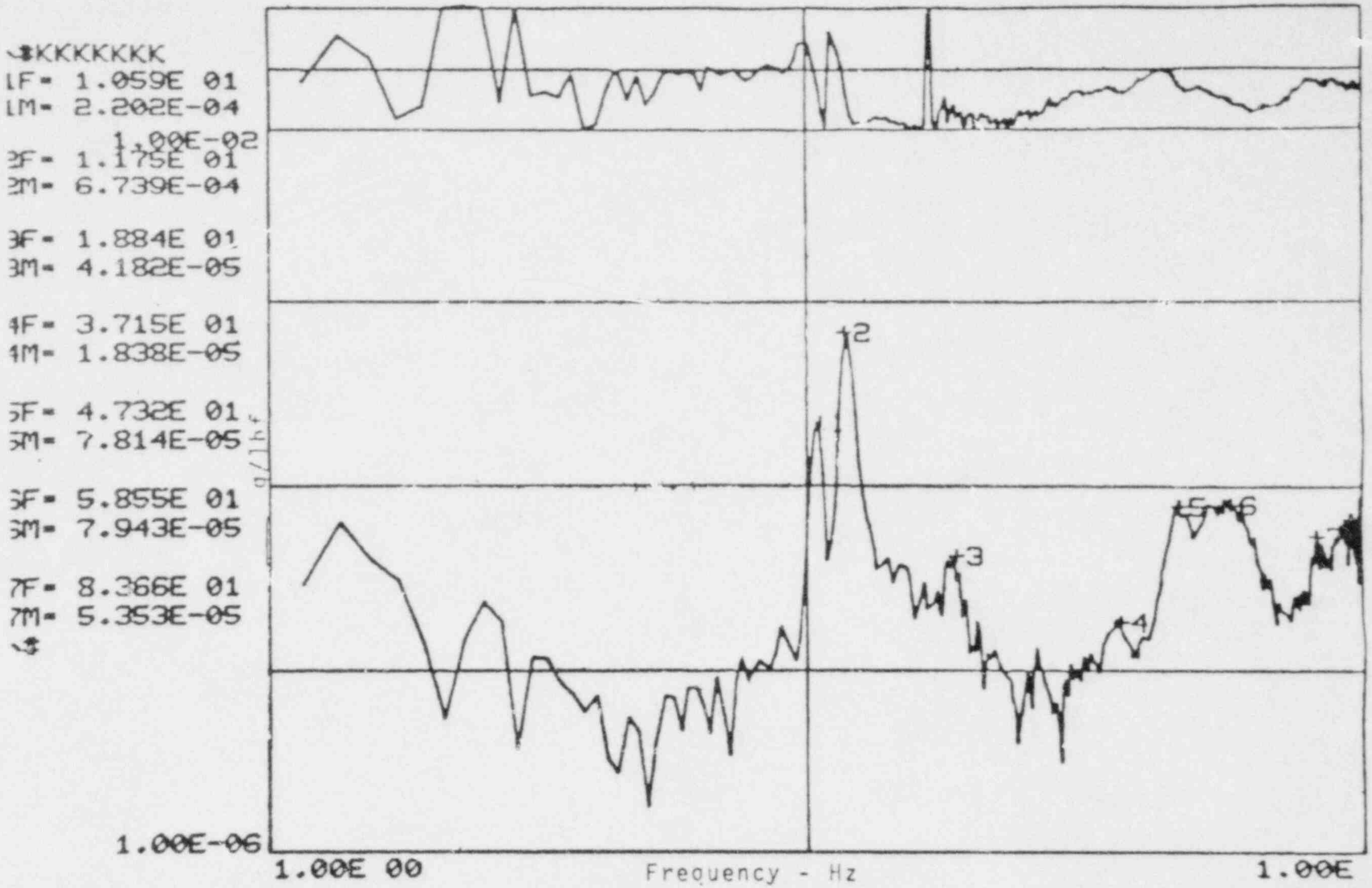

A1:LO PR CORE SPRA PUMP$

FREQRESP-BODE
37Z+ 31X+
072480-000000
092580-000000

FIGURE 3.2.1

An example of Resonant Frequency Identification by "peak picking". The numbered frequencies and amplitudes are listed to the left.

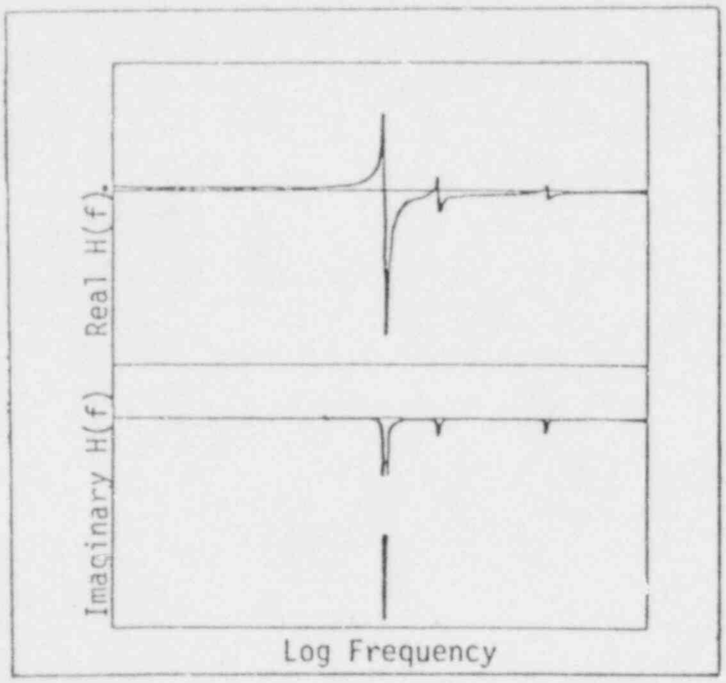

FIGURE 3.2.2

FREQUENCIES AT WHICH REAL VALUES OF THE TRANSFER FUNCTION GO TO ZERO AND THE IMAGINARY COMPONENT IS A MAXIUMUM, UNIQUELY IDENTIFY RESONANCES

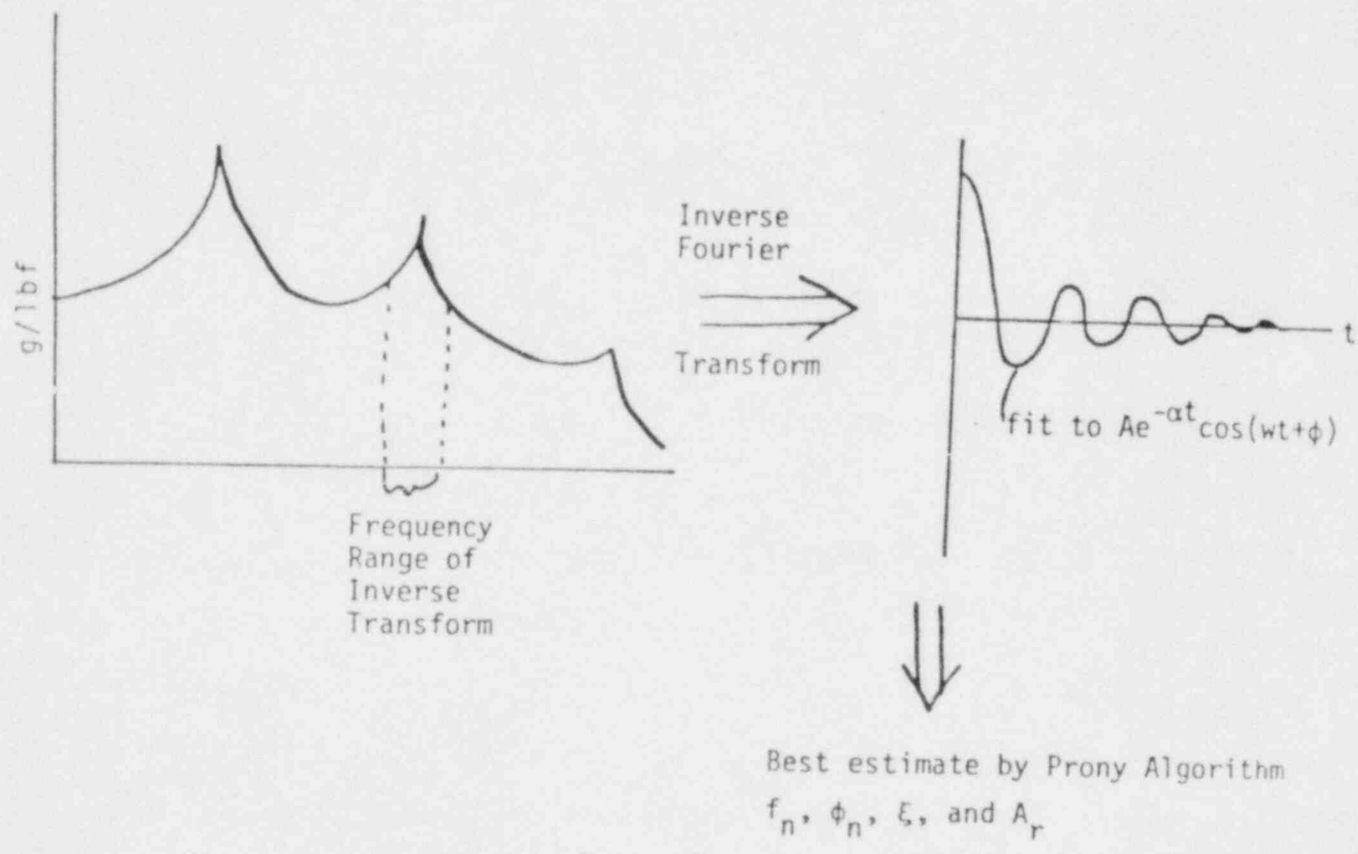

FIGURE 3.2.3

FLOW DIAGRAM FOR ESTIMATING MODAL PARAMETERS
BY INVERSE FOURIER TRANSFORM

(See Reference 2)

3.3 Estimation of Dampings

There are four commonly applied methods of estimation of damping. Each has advantages and limitations as discussed in the following sections.

3.3.1 Exponential Decay Rate: (5)

If a mode can be excited in such a way as to not excite modes other than the mode of interest, measurement of the decay rate is a valid means of estimating damping. The variables involved are illustrated in Figure 3.3.1.

This method is generally limited to damping estimates of the fundamental or lowest frequency mode due to difficulty in exciting individual modes.

3.3.2 Forced Vibration Response

When modes are well separated from one another, two independent methods of estimating damping can be developed from the resonance curve whose parameters are shown in Figure 3.3.2.

This method is successful provided the modes are well separated and the amplitude of the mode for which an estimate of damping is desired is not substantially smaller than a nearby mode. In these cases, estimation by either circle fitting or Inverse Fourier least squares curve fitting is necessary.

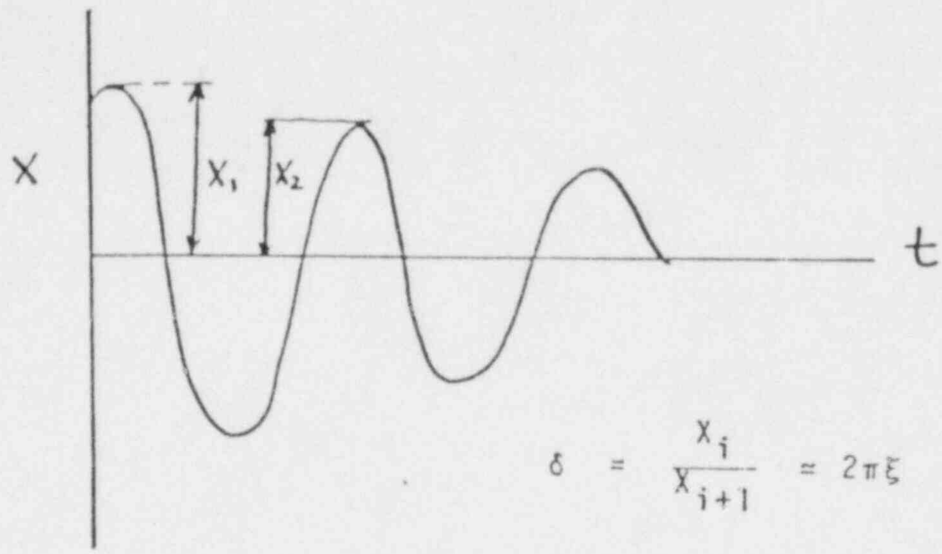

$$\delta = \frac{X_i}{X_{i+1}} = 2\pi\xi$$

FIGURE 3.3.1

ESTIMATION OF DAMPING FROM TIME DOMAIN DATA

This method often fails because other modes are als excited.

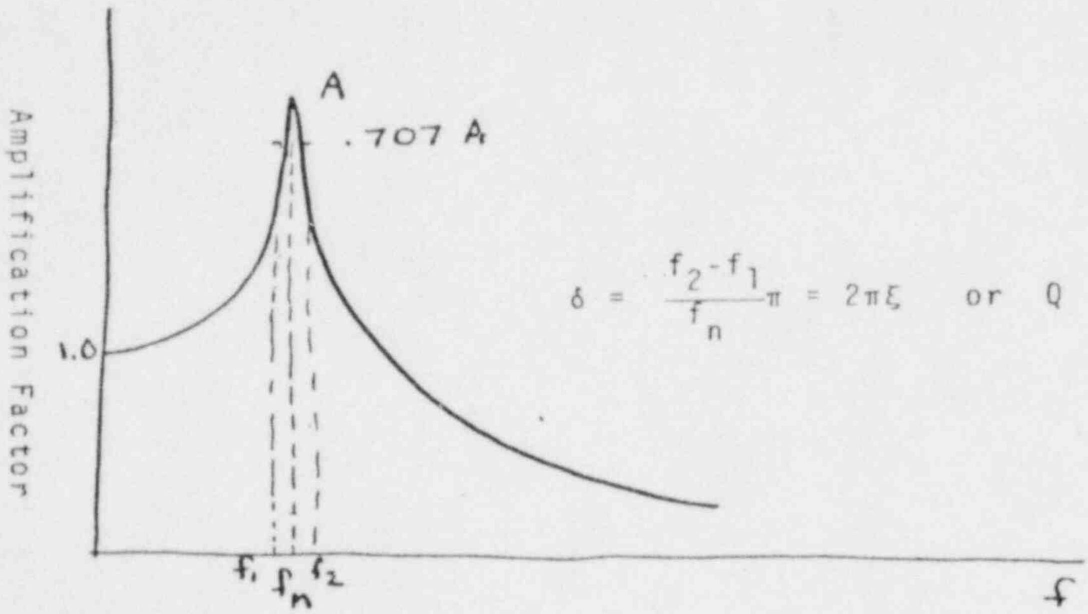

$$\delta = \frac{f_2 - f_1}{f_n}\pi = 2\pi\xi \quad \text{or} \quad Q = \frac{f_n}{f_2 - f_1} =$$

FIGURE 3.3.2

METHODS OF ESTIMATING DAMPING FROM FORCED VIBRATION

3.3.3 Damping Estimation by Circle Fitting

The original approach for this method was developed by Kennedy and Pancu (6) for systems with hysteretic damping characteristics. As shown below, the method can be extended to the viscous damping cases and has been extended to include complex modes by David Brown with the following assumptions:

1) The modes are only weakly coupled in the range where one mode is predominant. The contribution of lower and higher modes can be approximated by a complex constant (R + jI).

2) The system is relatively lightly damped.

These conditions are frequently met, so circle fitting is very useful.

The frequency response of the structure in the frequency range where the r-th mode is predominant is obtained from Equation 1 as:

$$\frac{X_p}{F_q} = \frac{U_{pqr} + jV_{pqr}}{-\delta_r + j(\omega - \omega_{dr})} + R + jI$$

where R+jI includes the contribution of the term associated with the conjugate eigenvalue. If the complex constant is neglected and the magnitude of the mode is set to unity, ($U_{pg} \rightarrow 0$ and $V_{pg} \rightarrow -1$ for a single degree of freedom, $\omega > 0$) the following relations is obtained:

$$\mathrm{Re}\left\{\frac{X_p}{F_q}\right\} = -\frac{(\omega-\omega_{dr})}{\left(\omega-\omega_{dr}\right)^2 + \delta_r^{\,2}}$$

$$\mathrm{Im}\left\{\frac{X_p}{F_q}\right\} = \frac{\delta_r}{\left(\omega-\omega_{dr}\right)^2 + \delta_r^{\,2}}$$

and thus,

$$\left[\mathrm{Re}\left\{\frac{X_p}{F_q}\right\}\right]^2 + \left[\mathrm{Im}\left\{\frac{X_p}{F_q}\right\} - \frac{1}{2\delta_r}\right]^2 = \left[\frac{1}{2\delta_r}\right]^2$$

In other words, the contribution of one mode to the general response can be represented in the Argand plane as a circle (Figure 3.3.3.1). Taking into coordinates of the center is calculated as:

$$\left(R = \frac{U_{pqr}}{2\delta_r}\;,\; I = \frac{V_{pqr}}{2\delta_r}\right)$$

and the diameter as:

$$d = \frac{\sqrt{U_{pqr}^2 + V_{pqr}^2}}{\delta_r}$$

The complex modal displacement vector expands or reduces the diameter and rotates the circle in the Argand plane. On the other hand, the complex constant (R+jI) will translate the center of the circle in the Argand plane (Figure 3.3.3.2).

A measure of the accuracy of this method is given by the shape of the frequency response in the region of the resonance: the more circular the curve, the more accurate the result.

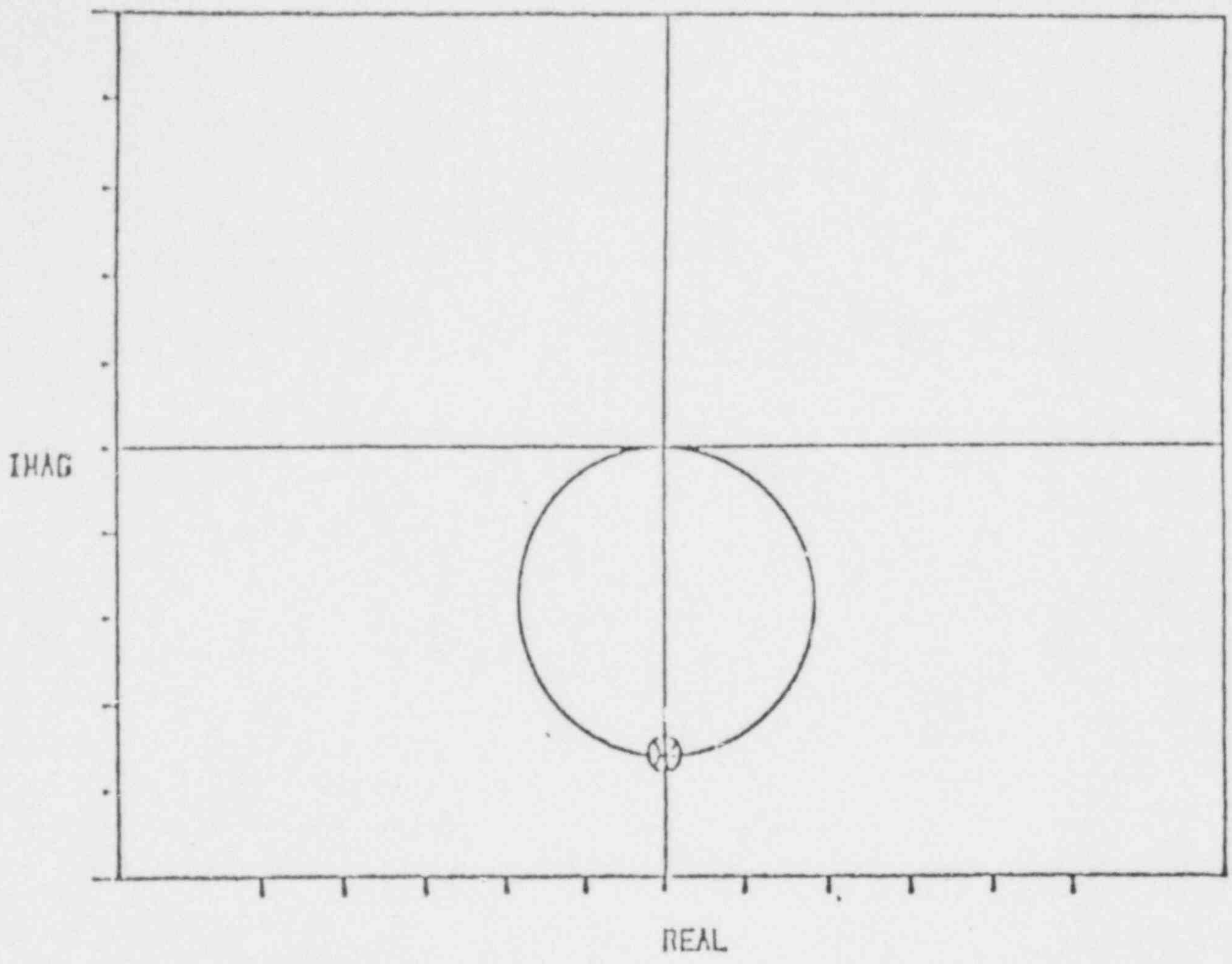

FIGURE 3.3.3.1

AN ARGAND DIAGRAM OF A TRANSFER FUNCTION
IN THE VICINITY OF A RESONANCE

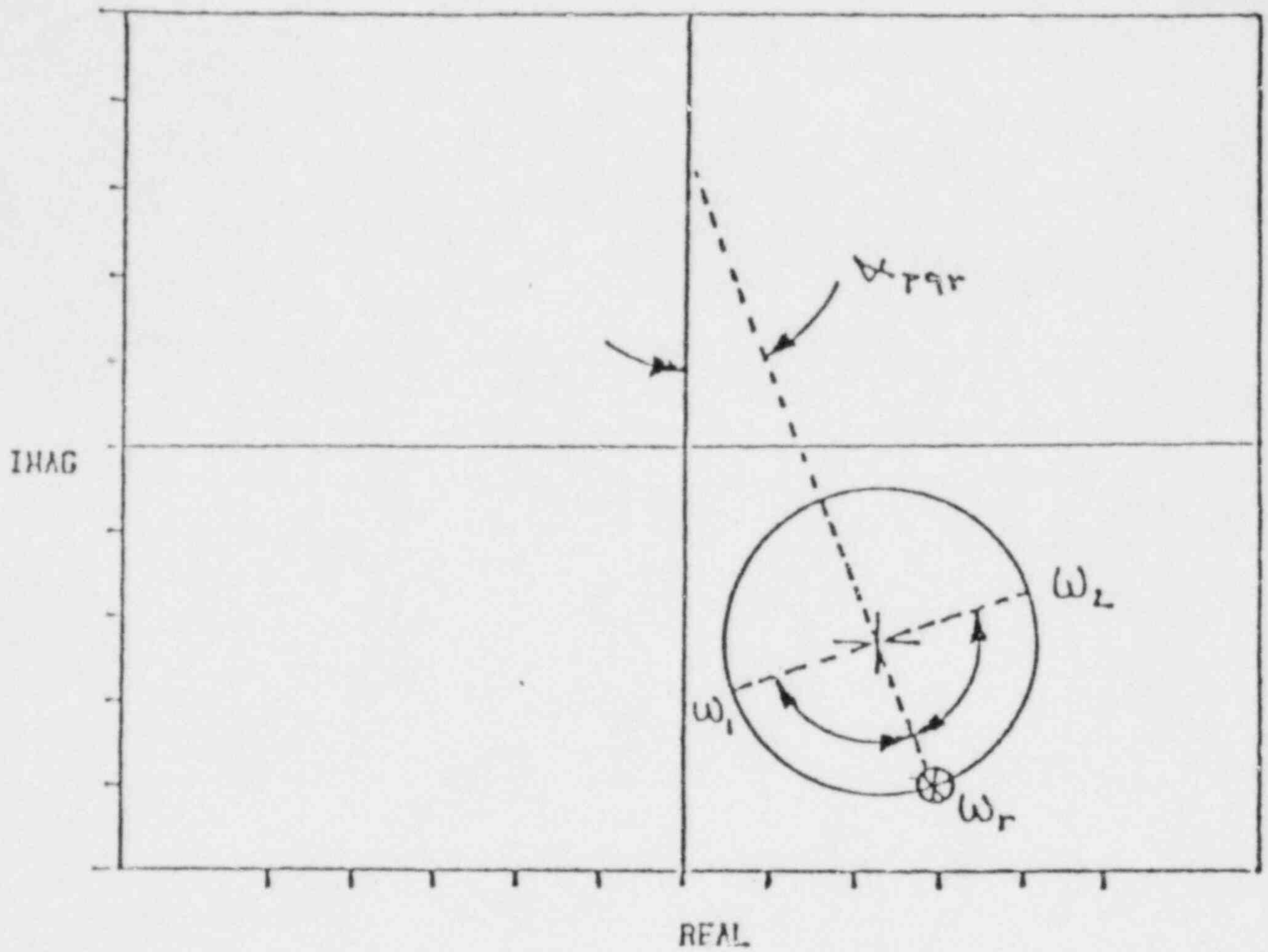

FIGURE 3.3.3.2

ESTIMATION OF MODAL PARAMETERS FROM AN ARGAND DIAGRAM

It was shown in Reference 2 that the resonant frequency could be found where the variation of the phase angle as a function of frequency is a maximum:

$$\frac{\partial^2 \phi}{\partial \omega^2} = 0$$

The damping ratio, ζ_r, can also be determined from the fitted circle. By locating the two frequencies ω_1 and ω_2 at $\pm$ 90 degrees with respect to the damped natural frequency (Figure 3.3.3.2), the damping can be calculated by the following relation:

$$\zeta_r = \left| \frac{\omega_1 - \omega_2}{2\omega_r} \right|$$

The diameter of the circle is proportional to the modulus of the residue:

$$d = \frac{1}{\delta_r} \left\| A_{pqr} \right\|^2$$

The phase angle α_{pqr}, of the complex modal coefficient can be calculated by passing a straight line through the point of the resonant frequency, ω_r, and the center of the circle. The angle this line makes with the imaginary axis is equal to the phase angle of the complex modal coefficient:

$$\alpha_{pqr} = \arctan\left(\frac{U_{pqr}}{V_{pqr}}\right) = \frac{\pi}{2} + \arg(A_{pqr})$$

Circle fitting typically is the next level of parameter estimation above quadrature response. It does a better job of separating coupled modes than the quadrature technique, but it, like most of the more sophisticated methods, can diverge and give very poor answers. In general, the method is fast and can be used to obtain complex modes but in order to get the best possible results it should be used interactively. The center frequency and bandwidth used in the circle fit can be varied depending upon the amount of noise, the coupling of modes, and the damping of the mode. This choice of data points utilized in the circle fit gives different answers and the best answer becomes a judgement. As a result, the best answers are obtained by a skillful operator with experience using the "GS" command of MPLUS.

The normal procedure for using the circle fit is to first determine the natural frequency of the system using the "GE" command procedures. Also, the peaks in the quadrature response or the peaks in a summation of power spectrums (constructed from the quadrature responses of all of the measurements) are very good indicators.

Using the following least squares Circle Fit algorithm, a circle can be interactively fit to the measured frequency response data at the designated natural frequency:

<u>Least Squares Error Fit of a Circle</u>

The general equation of a circle is

$$x^2 + y^2 + ax + by + c = 0$$

Setting this equation equal to an error function E, the least-squares error term is formed by a summation over the discrete frequencies in the area of the natural frequency.

$$\sum_{k=1}^{m} E^2 = \sum_{k=1}^{m} (x_k^2 + y_k^2 + ax_k + by_k + c)^2$$

The partial derivatives of the least-squares error term with respect to the constants, a, b, and c should be zero.

Writing these equations (while dropping the subscripts and summation interval for simplicity of notation):

$$\frac{\partial\Sigma(E^2)}{\partial a} = 2\Sigma(x^2 + y^2 + ax + by + c)\ x = 0$$

$$\frac{\partial\Sigma(E^2)}{\partial b} = 2\Sigma(x^2 + y^2 + ax + by + c)\ y = 0$$

$$\frac{\partial\Sigma(E^2)}{\partial c} = 2\Sigma(x^2 + y^2 + ax + by + c)\ 1 = 0$$

Rewriting these three equations in matrix form:

$$\begin{bmatrix} \Sigma(x^2) & \Sigma(xy) & \Sigma(x) \\ \Sigma(xy) & \Sigma(y^2) & \Sigma(y) \\ \Sigma(x) & \Sigma(y) & m \end{bmatrix} \begin{bmatrix} a \\ b \\ c \end{bmatrix} = \begin{bmatrix} -\Sigma(x^3 + xy^2) \\ -\Sigma(x^2 y + y^3) \\ -\Sigma(x^2 + y^2) \end{bmatrix}$$

Therefore, using these three equations a, b, and c can be found and the center of the circle and radius calculated (Figure 3.3.3.2):

$$x_{center} = -a/2$$

$$y_{center} = -b/2$$

$$\text{Radius} = \left(\left(\frac{a}{2}\right)^2 + \left(\frac{b}{2}\right)^2 - c \right)^{1/2}$$

The damping ratio (ζ_r) as well as the modal coefficient (amplitude and phase) are defined by the location, diameter and orientation of the circle.

In order to illustrate one of the more serious problems with circle fitting, the following example will be used. The first two modes of cantilever beam will be determined using circle fitting. The mode shapes for the beam are shown in Figure 3.3.3.3. If an excitation force is applied at point one on the beam, the measured frequency response plots between point one and all other points are shown in Figure 3.3.3.4. In this figure the resonance frequencies are marked with an X and the bandwidth used in the circle fit are shown by the double line. The problem which is being illustrated shows in the measurement at point 2. At point 2 the modal contribution of mode 2 is nearly zero. The circle fit in this case is really a fit of the skirt of the first mode. Instead of getting a value near zero, a very large value is obtained.

Due to this type of problem and due to bad estimates caused by noise, it is necessary to interactively fit the data with the circle fit algorithm.

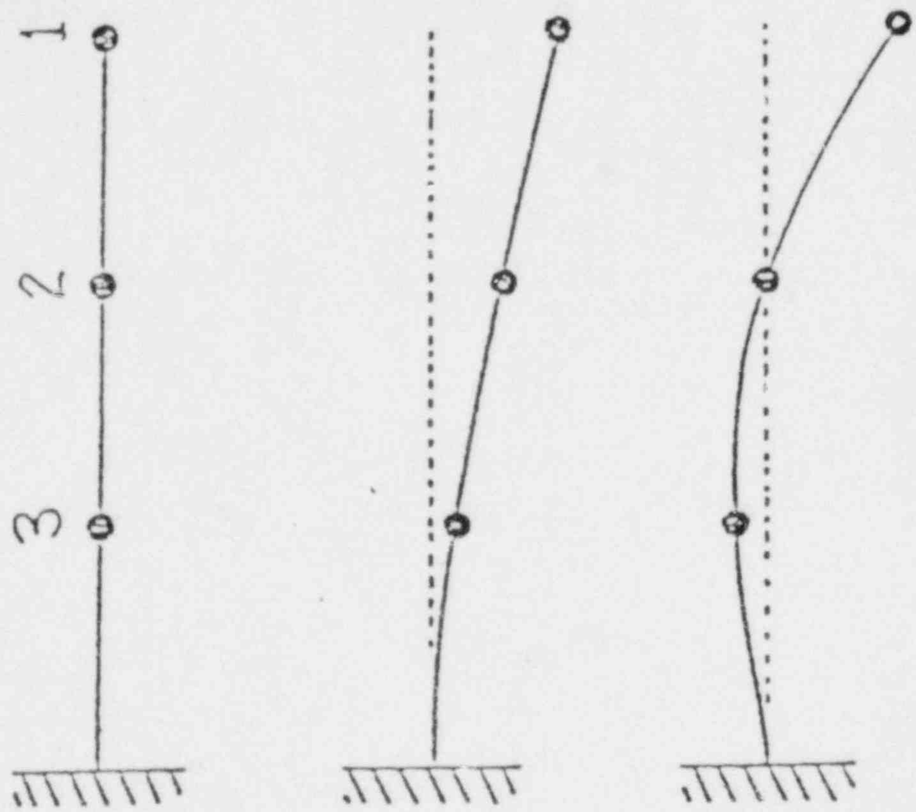

FIGURE 3.3.3.3

MODES OF A CANTILEVER BEAM

At point 2 of the Second Mode, only poor Circle Fits can be anticipated because it is at a Node Point of that Mode.

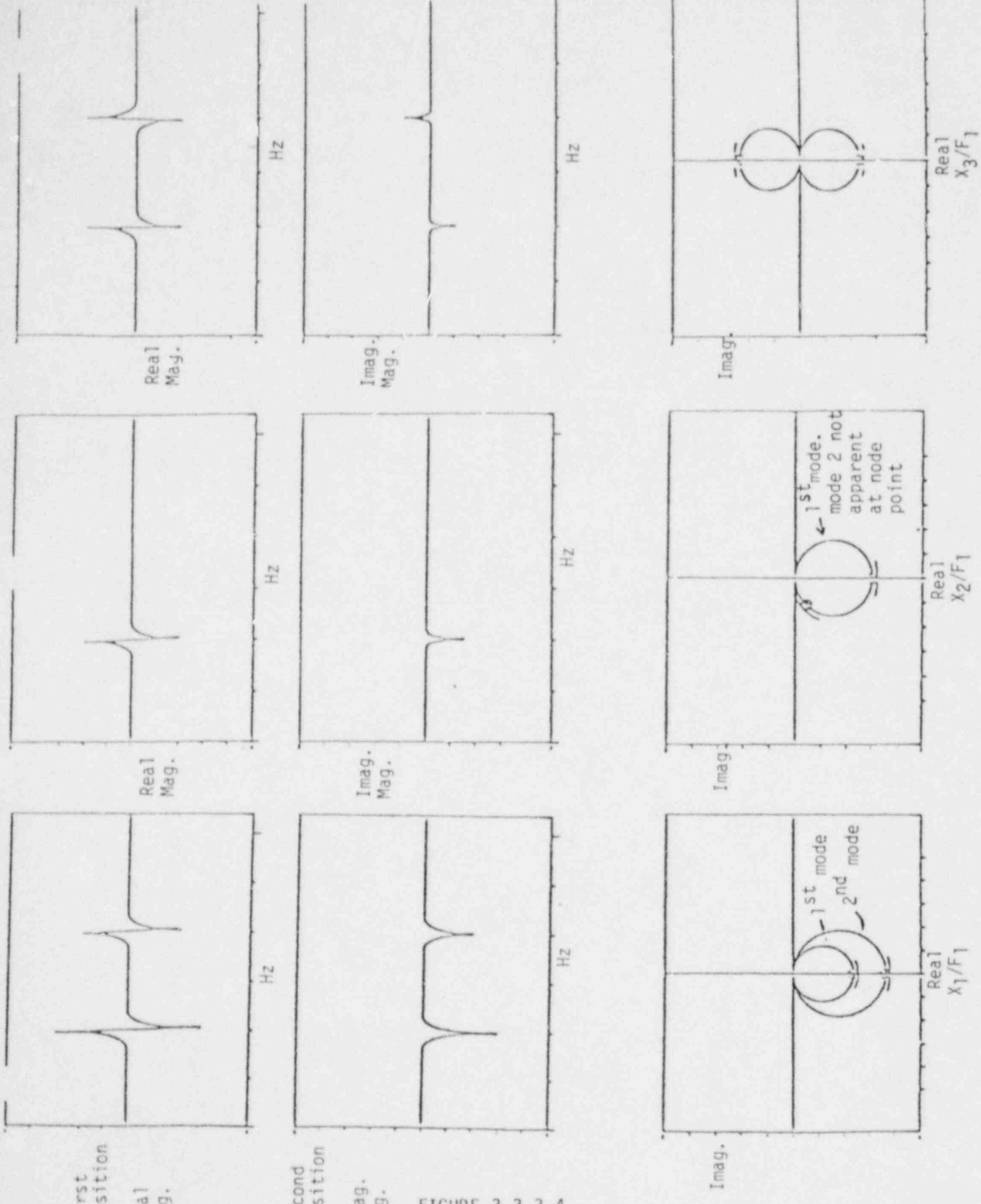

FIGURE 3.3.3.4

TRANSFER FUNCTIONS FOR THE STRUCTURE OF FIGURE 3.3.3.3

3.3.4 Estimation of Damping from Multidegree of Freedom Curve Fits of Inverse Fourier Transformed Data

Since the single degree of freedom equations are simply special cases of the multiple degree of freedom equations, all theoretical discussions will be made in terms of the multiple degree of freedom case.

In studies carried out by Klosterman,[2] Van Loon,[8] and Richardson,[4] a derivation is given for the general formula of the frequency response of a multiple degree of freedom system with viscous or hysteretic damping.

For general viscous damping, the frequency response for a multiple degree of freedom mechanical system can be written as:

$$\frac{X_p}{F_q} = \sum_{r=1}^{\infty} \left[\frac{A_{pqr}}{j\omega - S_r} + \frac{A^*_{pqr}}{j\omega - S^*_r} \right] \qquad (1)$$

where

x_p = response at point p,

F_q = input at point q,

j = $\sqrt{-1}$,

S_r = eigenvalue of r-th mode = $\delta_r + j\omega_{dr}$

ω_{dr} = damped natural frequency of the r-th mode,

δ_r = decay rate of the r-th mode (damping), exponential decay), and

A_{pqr} = complex residue of r-th mode = $U_{pqr} + jV_{pqr}$.

Continuous systems have an infinite number of degrees of freedom but, in general, only a finite number of modes can be used to describe the dynamic behavior of a system. The theoretical number of degrees of freedom can be reduced by using a finite frequency range (f_a, f_b). Therefore, for example, the frequency response can be broken up into three partial sums, each covering the modal contribution corresponding to modes located in the frequency ranges $(0, f_a)$, (f_a, f_b) and (f_b, ∞). (Figure 3.3.4.1). In the frequency range of interest, the modal parameters can be estimated to be consistent with Equation 1. In the lower and higher frequency ranges, residual terms can be included to handle modes in these ranges. In this case, Equation 1 can be rewritten as:

$$\frac{X_p}{F_q} = L_{pq} + \sum_{r=r_a}^{r_b} \left[\frac{A_{pqr}}{j\omega - S_r} + \frac{A^*_{pqr}}{j\omega - S^*_r} \right] + Z_{pq} \qquad (2)$$

where

r_a = lower mode index of the frequency range of interest,

r_b = upper mode index of the frequency range of interest,

L_{pq} = lower residual term, and

Z_{pq} = upper residual term.

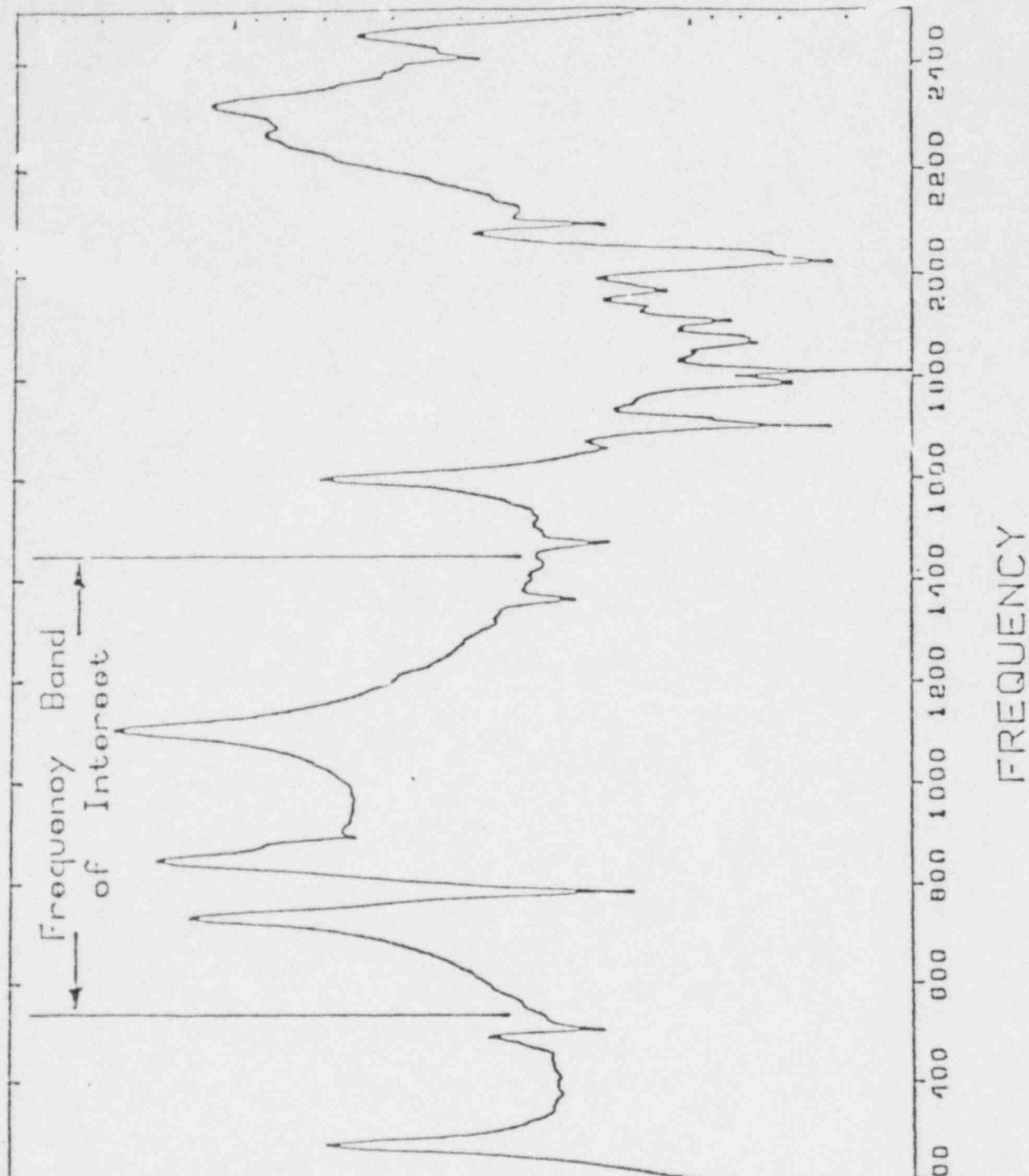
Frequency Band
of Interest
FREQUENCY
0
200
400
600
800
1000
1200
1400
1600
1800
2000
2200
2400
2
1
0
-1
-2

FIGURE 3.3.4.1

In many cases the lower residual term is called the inertia restraint, and the upper residual term is called the residual flexibility. These can be written as:

$$L_{pq} = -\frac{Y_{pq}}{\omega^2} = \text{Re}\left\{\sum_{r=1}^{r_a-1}\left[\frac{A_{pqr}}{j\omega - S_r} + \frac{A^*_{pqr}}{j\omega - S^*_r}\right]\right\} \tag{3}$$

$$Z_{pq} = \text{Re}\left\{\sum_{r=r_b+1}^{\infty}\left[\frac{A_{pqr}}{j\omega - S_r} + \frac{A^*_{pqr}}{j\omega - S^*_r}\right]\right\} \tag{4}$$

Where

Re z = real part of a complex number z

Y_{pq} = inertia restraint, and

Z_{pq} = residual flexibility

Therefore, Equation 1 can be rewritten as:

$$\frac{X_p}{F_q} = -\frac{Y_{pq}}{\omega^2} + \sum_{r=r_a}^{r_b}\left[\frac{A_{pqr}}{j\omega - S_r} + \frac{A^*_{pqr}}{j\omega - S^*_r}\right] + Z_{pq} \tag{5}$$

This concept is shown graphically in the following figures:

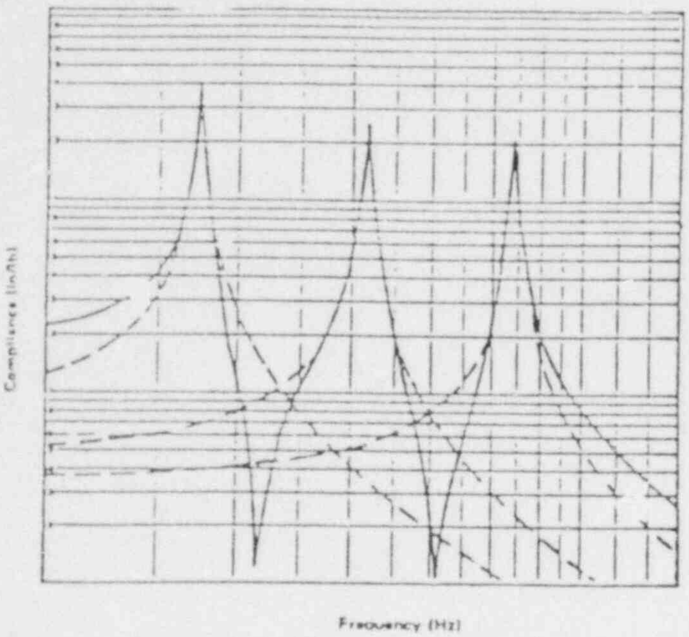

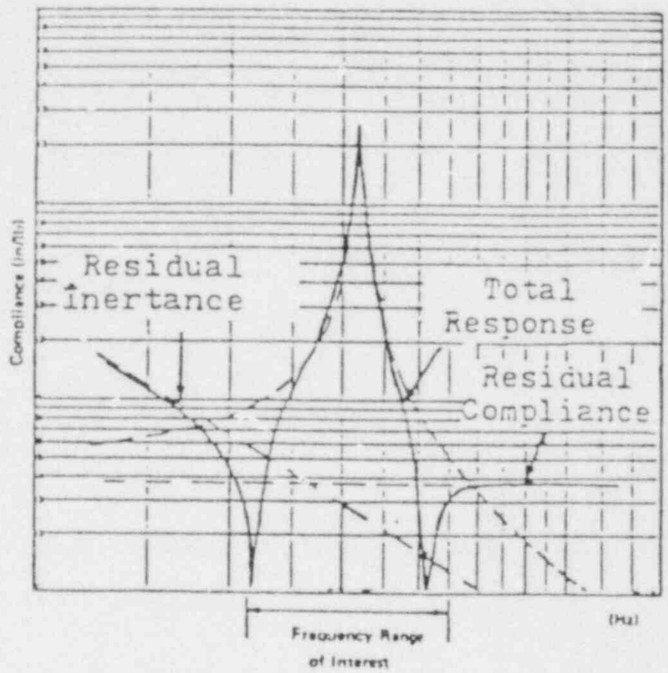

The SDOF and MDOF curve fitting procedure available in the Estimation task are used to evaluate the contribution due to the modes which are resonant in the frequency range under investigation.

An alternate way to write the frequency response in terms of its undamped natural frequency and damping coefficient is:

$$\frac{X_p}{F_q} = -\frac{Y_{pq}}{\omega^2} + \sum_{r=r_a}^{r_b} \frac{B_{pqr} + j\left(\frac{\omega}{\omega_r}\right) B'_{pqr}}{1 - \left(\frac{\omega}{\omega_r}\right)^2 + j2\zeta_r\left(\frac{\omega}{\omega_r}\right)} + Z_{pq} \qquad (6)$$

where, by definition,

$$\omega_r = \sqrt{\delta_r^2 + \omega_{dr}^2} \qquad B'_{pqr} = \frac{2U_{pqr}}{\omega_r} \tag{7}$$

$$\zeta_r = -\delta_r/\omega_r$$

$$B_{pqr} = -\frac{2\left(\delta_r U_{pqr} + \omega_{dr} V_{pqr}\right)}{\omega_r^2} \tag{8}$$

The above terms have the units of compliance and as a result the numerator of Equation 6 is the "complex compliance". For the case of proportional damping, the equation for the frequency response has the more classical form:

$$\frac{X_p}{F_q} = \frac{Y_{pq}}{\omega^2} + \sum_{r=r_a}^{r_b} \frac{B_{pqr}}{1 - \left(\frac{\omega}{\omega_r}\right)^2 + j2\zeta_r\left(\frac{\omega}{\omega_r}\right)} + Z_{pq} \tag{9}$$

where B_{pqr} is the modal compliance.

Many of the parameter estimation techniques that are used will assume that only one mode exists in the range of interest and all of the other modes appear as residual terms. For this case, Equation 2 can be rewritten as:

$$\frac{X_p}{F_q} = -\frac{Y'_{pq}}{\omega^2} + \frac{A_{pq}}{j\omega - S} + \frac{A^*_{pq}}{j\omega - S^*} + Z'_{pq} \tag{10}$$

or for the case of proportional damping as:

$$\frac{X_p}{F_q} = -\frac{Y'_{pq}}{\omega^2} + \frac{B_{pq}}{1-\left(\frac{\omega}{\omega_r}\right)^2 + j2\zeta_r\left(\frac{\omega}{\omega_r}\right)} + Z'_{pq} \qquad (11)$$

Several of the curve fitting cases which were discussed in this section utilized the unit impulse response of the system. The unit impulse response is the Fourier transform of the frequency response. Therefore, a mathematical expression for the unit impulse response can be obtained by a Fourier transform of Equation 1:

$$h_{pq}(t) = \sum_{r=1}^{\infty} \left[A_{pqr} e^{S_r t} + A^*_{pqr} e^{S^*_r t} \right] \qquad (12)$$

The method of estimation from inverse Fourier transform described in this section, was the method used exclusively in the analys for damping.

Generally damping was calculated from the driving point transfer function. In the case of complex structures, with strong local resonances, we also estimated damping from other points.

While the same method of curve fitting for damping estimation also gives modal coefficients, the circle fit technique developed in the following section is more efficient for estimating moda amplitudes.

3.4 Mode Shape Calculation

In the following sections two methods of mode shape calculation are discussed. The first method, circle fitting, was used exclusively in this report.

3.4.1 Mode Shape Calculation by Circle Fit

Once the transfer functions are safely stored on the disc, the data analysis can be begun. The procedure we prefer is to read in several of the transfer functions and use the "GE" command of the /E task to obtain the first estimate of modal parameters:

These rules apply to use of the "GE" command:

1) Choose a range for analysis that includes a minimum at a low frequency and at a high frequency.
2) Allow two degrees of freedom for each obvious mode over the range of analysis.
3) Check the fit with the "GA" command and compare fit to original data.
4) Store the appropriate modal parameters in the active modal parameter file.

Next, we estimate the mode shape for each real resonance using the MACROS to generate circle fits. The command to check the frequency range of the fit GS <u>LO</u>, <u>HI</u> where LO and HI are the low and high frequencies in hertz. The computer will respond with a circle fit as shown in the example below:

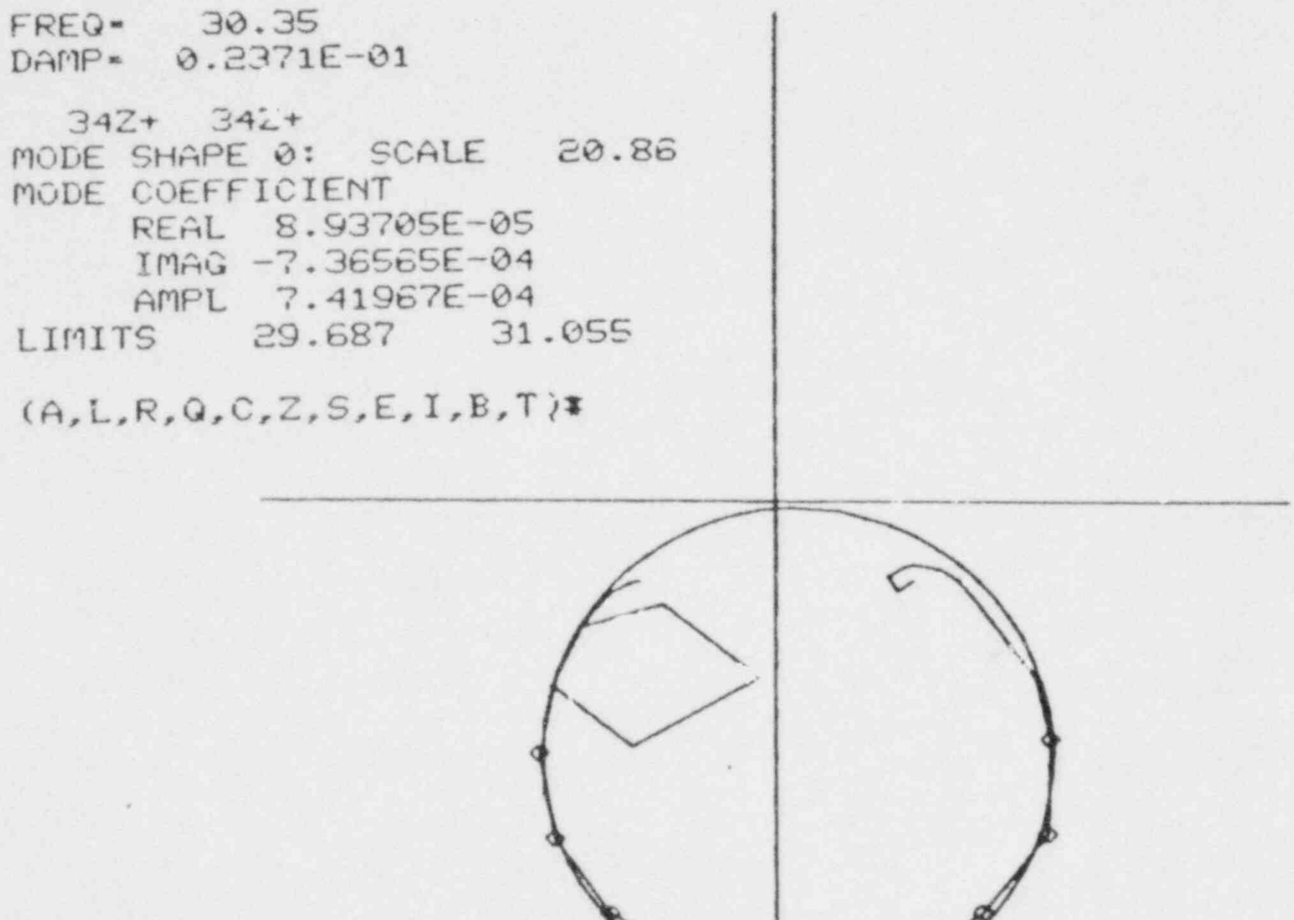

The example shown is an example of a good circle fit.

The following options are available as a response to the circle fit:

A	To accept the modal coefficient as displayed.
L<u>v1</u>,<u>v2</u>	To temporarily enter a new frequency limit between <u>v1</u> and <u>v2</u> for a new SDOF estimation.
R<u>v</u>	To use the measured response at frequency <u>v</u> for the mode shape definition.
Q<u>v</u>	To use the measured quadrature response (imaginary part) at frequency <u>v</u> for the mode shape definition.
C<u>v</u>	To use the measured coincident response (real part) at frequency <u>v</u> for the mode shape definition.
Z	To set the mode shape coefficient for the current coordinate to zero.
S	To skip this coordinate and leave the mode shape unmodified.
E	To leave the mode shape unmodified and force an exit from a macro, if the user has included the GS command inside a macro operation.
I	To accept the modal coefficient as displayed, but invert the sign before storage.

Now we are ready to run the macro program again for SDOF fitting of the data (Option 3). For this, the high and low frequencies are centered as we determined in the first circle fit at the reference coordinate. Of the SDOF options, 8 is preferred from the list below:

Code (i)	Analysis	Mode Shape Type	Rotation
1	Automatic	Real	Center
2	Interactive	Real	Center
3	Automatic	Complex	Center
4	Interactive	Complex	Center
5	Automatic	Real	Resonance
6	Interactive	Real	Resonance
7	Automatic	Complex	Resonance
8	Interactive	Complex	Resonance

Option 8 gives the interactive capability to change the frequency range or other steps to improve the mode shape estimate and uses the complex or total response. Options 1, 2, 3 and 6 use only the quadrature component of the response.

3.4.2 Mode Shape Calculation by MDOF Curve Fit

In order to generate mode shapes from either the circle fit or MDOF routines, the following prerequisites must be met:

1) There must be a mode shape file appended to the project file through the AS command.

2) A geometry file is in core.

3) A trace link file is in core.

When using circle fit, acceptance of a fit of the data (entering A to the query) automatically moves the numbers noted in Figure 3.4.2 to the active mode shape file.

The MDOF curve fit subroutine for generation of mode shapes is considerably more complex to use and subject to uncontrolled errors.

In this procedure the following steps are used:

1) The most agreeable result of a "GE" command listing is moved to a parameter file using the "MP" command.

2) The MDOF subroutine is selected from the MACRO subroutine.

3) Enter error bands for acceptance of resonant frequency (generally $\pm$ 5% of the resonant frequency) and damping (generally a range from .5% to 5% is adequate).

4) Enter the number of roots, frequency range, and trace coordinate file.

5) Execute the MACRO using the "XM commands.

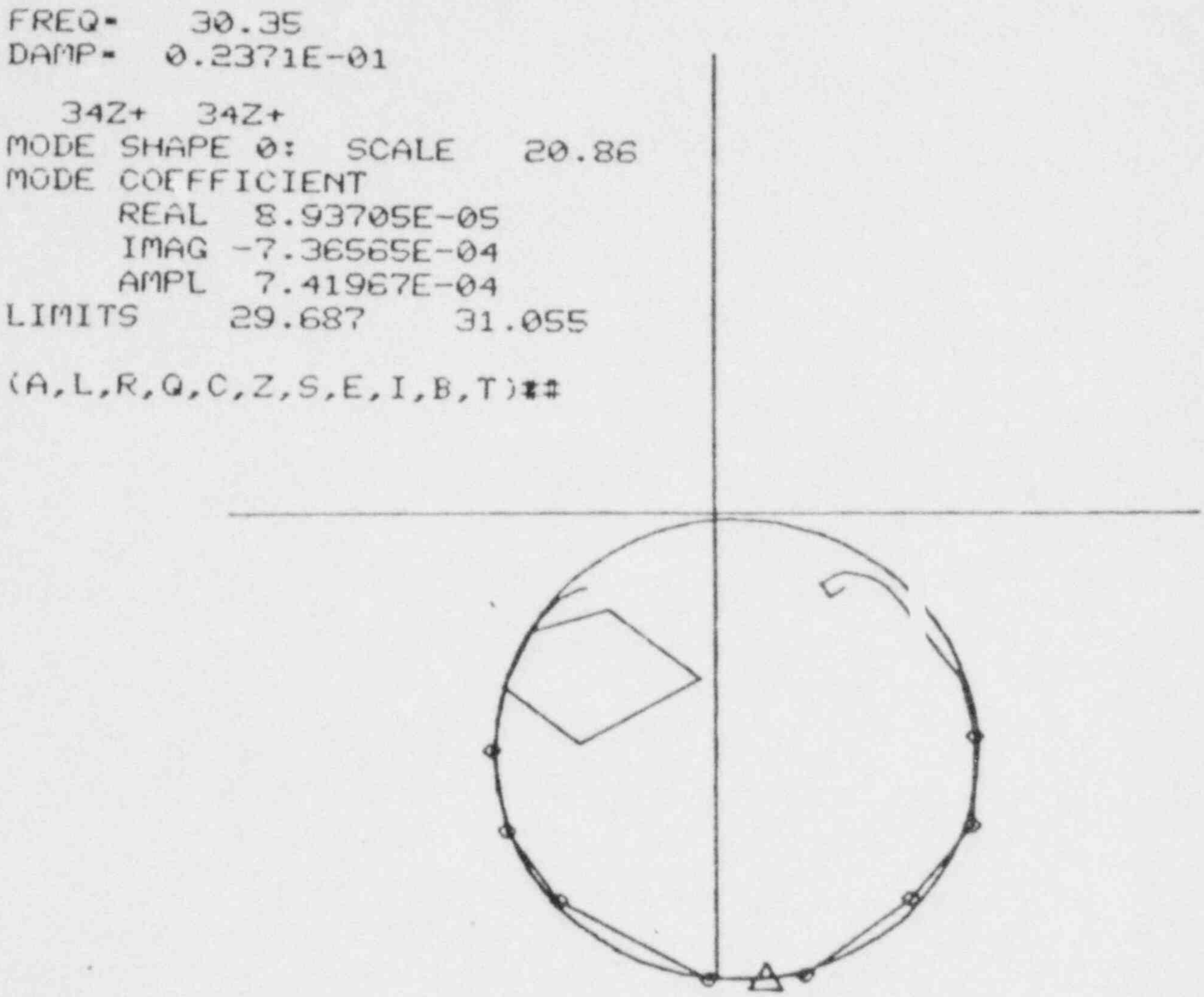

FIGURE 3.4.2

In this example, the circle fit results moved to the active mode shape file are the numbers labeled REAL (8.93705E-05) and IMAGINARY (-7.36565E-04).

The program will automatically move the amplitude and phase results (as real and imaginary numbers) to the active mode shape file.

The several dangers to this procedure are:

1) The curve fitting cannot find the mode.

2) The routine will not converge.

3) The time required for a long string of test points is inordinate.

For these reasons, generation of mode shape files by the MDOF option is not recommended. We recommend MDOF only for the odd occasion that circle fit does not adequately extract the modal coefficients at a particular point.

4.0 RESULTS:

The results of the testing are discussed separately for each component in the following sections.

The test program was generally very successful. The tests were conducted under a series of restrictions that influenced the outcome on some of the components.

Members of the Taipower organization, present to participate in the testing program, placed the restrictions on the test program in accordance with their concerns that the tests be nondestructive and not jeopardize the safety of the equipment. The restrictions under which these tests were performed are summarized as follows:

Component	Maximum Response (g's)	Maximum Frequency
3" Valve	.4	100
JPIP Panel	.4	100
RHR Pump	.3	33
RRFC Valve	.4	100
480V MCC Panel	.2	33

A compromise was reached on the MCC panel and RHR pump to 100 HZ by decreasing the force level over 100 HZ in proportion to the inverse of frequency.

The 3" valve testing was completed before any restrictions had been communicated and the levels of acceleration may have exceeded the restriction.

4.1 Reactor Recirculation Flow Control Valve (RRFCV):

4.1.1 Equipment Tested:

The reactor recirculation flow control valve, located in the inner containment, was tested using excitation from the hydraulic shaker. The maximum acceleration on the valve body which weighs about 5,000 lbs., was raised to .4 g's and provided adequate excitation for modal analysis. The frequency content of the excitation was broad band pseudo random to a maximum frequency of 100 Hz.

At the time of testing, the flow control valve line is believed to have been filled and all hydraulic and electrical connections had been made to the valve controls. At TRANSITEK's request, the mirror insulation on the valve body was removed to permit access to the valve body. Mirror insulation was not removed beyond approximately two feet from either side of the valve due to the time restrictions placed on the testing by the construction schedule of the biological shield. Generally, more detailed geometric models are constructed. In this case, the extreme time limitations required that we go to reduced geometric description of the valve. The number of points appears to be adequate for the number of modes measured.

4.1.2 Method of Testing:

The reactor recirculation flow control valve was excited to a level of .4 g's at the body of the valve. The acceleration limit was imposed at the request of Taipower. The force level required to produce this level of acceleration was approximately 1200 pounds peak. Random force excitation was used in the Z and Y directions. The valve was not tested in the X direction (which generally produces only minimal information) due to the extreme limitations of time imposed by the construction schedule.

Special brackets were constructed so that the shaker could be attached at point 7 in the Z direction and point 9 in the Y direction as shown in Figure 4.1.1. The acceleration response was measured at each of the numbered points shown in Figure 4.1.1. For more detail of the geometric model of the valve, see Figure 4.1.2. Table 4.1.1 lists the geometric location of each point of response measurement on the reactor recirculation flow control valve.

The response was measured using high sensitivity (1 v/g) PCB Model 308 accelerometers attached with beeswax. At each point, 16 frames of data were collected (this required about 3 minutes).

4.1.3 Modal Properties:

Driving point transfer functions are shown in Figure 4.1.3 for the Z direction and Figures 4.1.4A and 4.1.4B for the Y direction, respectively. The frequency listed to the le*t *f each figure identify each of the resonances found in this test. The modal properties e ted from the transfer functions are listed in Table 4.1.2. The range of damping values measured on this massive component range from 1.5% to 9% and are characteristic of TRANSITEK's measurements on similar equipment. Many of the resonances listed on this table are those of piping modes as noted in the following section.

4.1.4 Mode Shapes:

The mode shapes measured in the Y direction are shown in Figures 4.1.5 through 4.1.12. An attempt to identify each mode shape is indicated in the subtitle of each figure. The mode shapes measured in the Z direction are listed in Figures 4.1.13 through 4.1.17. The mode shapes are associated with measurements in the direction in which the excitation force was applied.

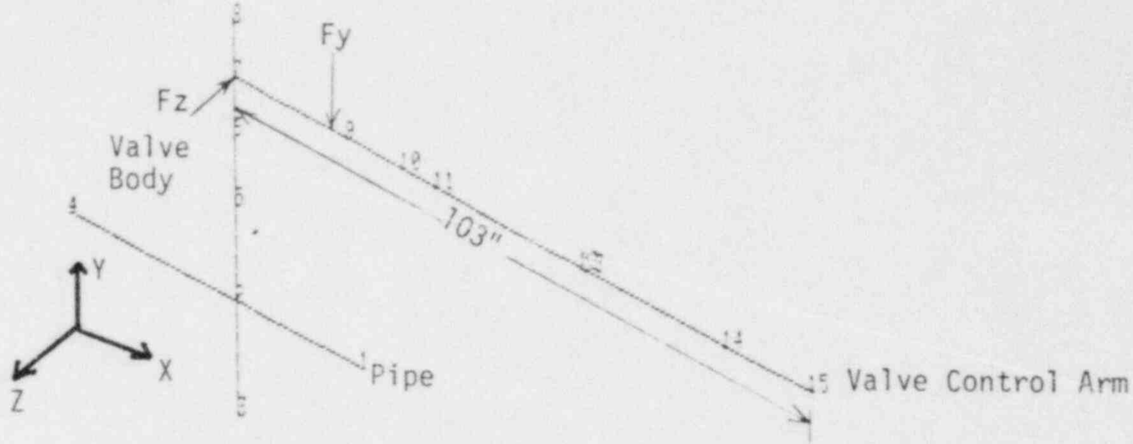

FIGURE 4.1.1

LABELED WIRE FRAME MODEL
REACTOR RECIRCULATION FLOW CONTROL VALVE (RRFCV)

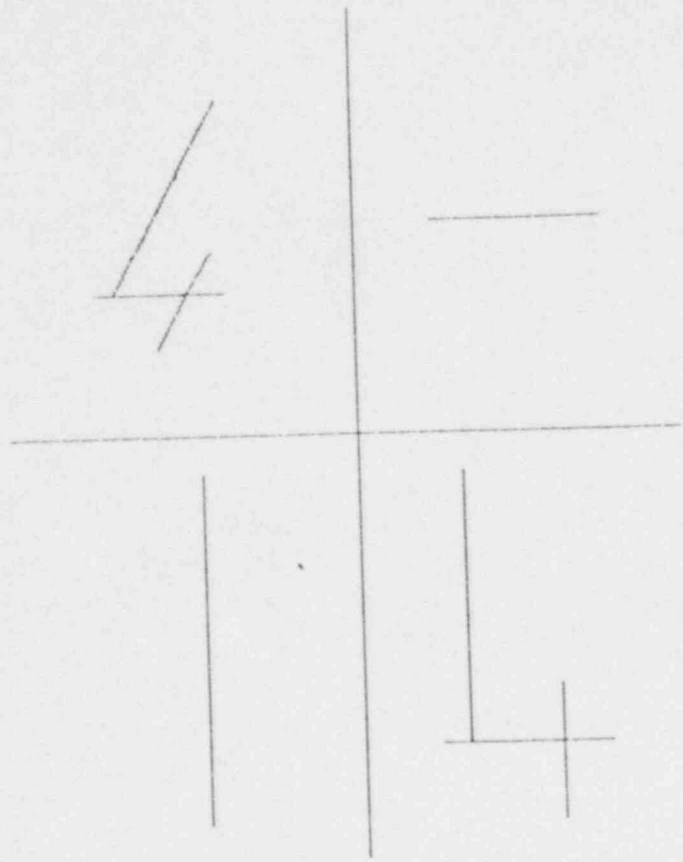

FIGURE 4.1.2

FOUR ORTHOGONAL VIEWS OF THE WIRE FRAME MODEL
REACTOR RECIRCULATION FLOW CONTROL VALVE (RRFCV)

TABLE 4.1.1

GEOMETRIC LOCATIONS OF POINTS OF RESPONSE MEASUREMENT
REACTOR RECIRCULATION FLOW CONTROL VALVE

Point No.	X (In.)	Y (In.)	Z (In.)
1	22	0	0
2	0	0	0
3	0	-18	0
4	-30	0	0
5	0	16	0
6	0	27	0
7	0	36	0
8	0	45	0
9	20	36	0
10	30	36	0
11	36	36	0
12	62	36	0
13	63	36	0
14	88	36	0
15	103	36	0

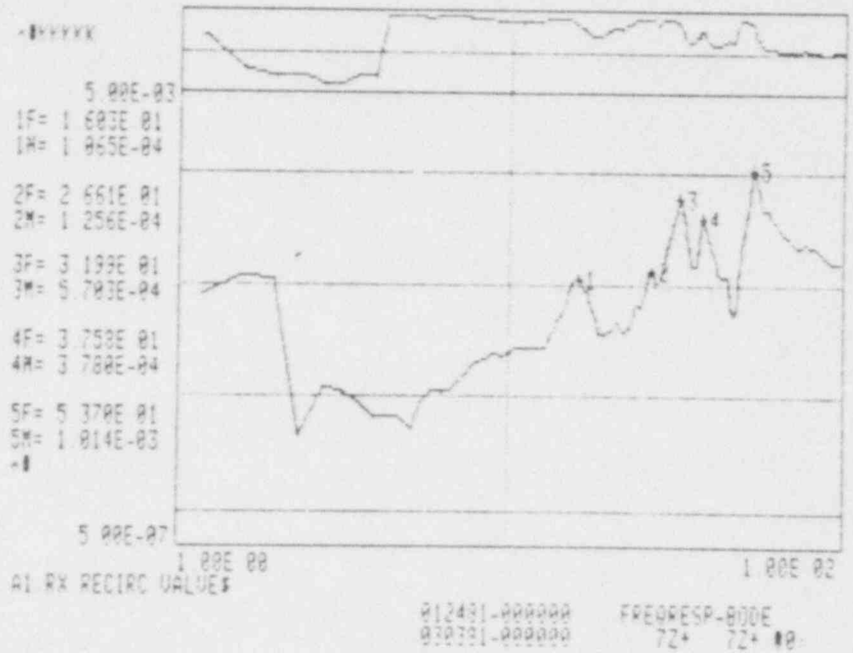

FIGURE 4.1.3

THE DRIVING POINT TRANSFER FUNCTION MEASURED IN THE Z DIRECTION
REACTOR RECIRCULATION FLOW CONTROL VALVE (RRFCV)

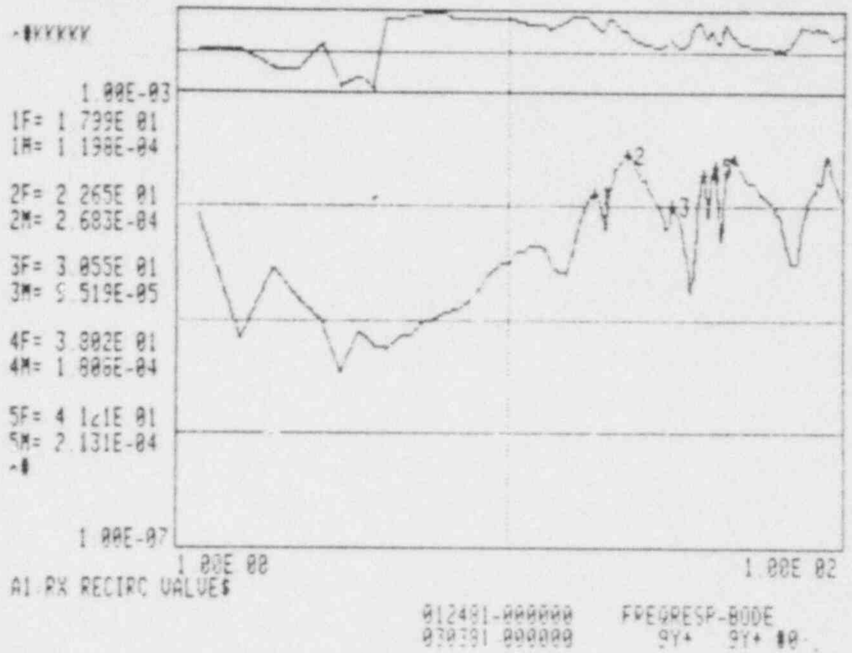

FIGURE 4.1.4A

THE DRIVING POINT TRANSFER FUNCTION MEASURED IN THE Y DIRECTION
REACTOR RECIRCULATION FLOW CONTROL VALVE (RRFCV)
SHOWING THE FIVE RESONANCES OF LOWEST FREQUENCY

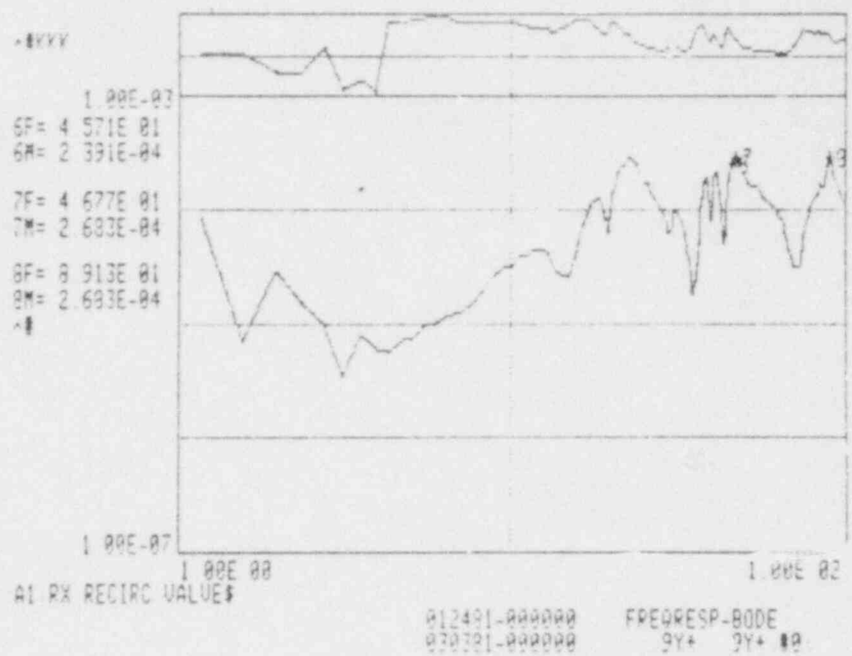

FIGURE 4.1.4B

THE DRIVING POINT TRANSFER FUNCTION MEASURED IN THE Y DIRECTION
REACTOR RECIRCULATION FLOW CONTROL VALVE (RRFCV)
SHOWING THE THREE RESONANCES OF HIGHEST FREQUENCY

TABLE 4.1.2

MODAL PROPERTIES MEASURED ON THE RRFCV

Mode Shape #	Frequency (HZ)	Damping (% Critical)
	Y DIRECTION	
1	18.97	3.8
2	22.57	8.5
3	30.69	1.5
4	38.36	2.1
5	40.86	2.3
6	45.20	2.5
7	47.96	1.5
8	89.99	1.9
	Z DIRECTION	
1	16.21	9.0
2	27.07	3.3
3	32.59	2.8
4	37.98	2.7
5	54.29	2.1

FIGURE 4.1.5

THE MODE SHAPE OF THE RRFCV ASSOCIATED WITH THE 18.97 HZ RESONANCE
MEASURED IN THE Y DIRECTION
THIS VIEW IS DIRECTLY INTO THE SIDE OF THE VALVE.
THIS MODE IS PROBABLY A PIPING RESONANCE.

FIGURE 4.1.6

THE MODE SHAPE OF THE RRFCV ASSOCIATED WITH THE 22.57 HZ RESONANCE
MEASURED IN THE Y DIRECTION
IT IS MOST LIKELY A PIPING MODE.

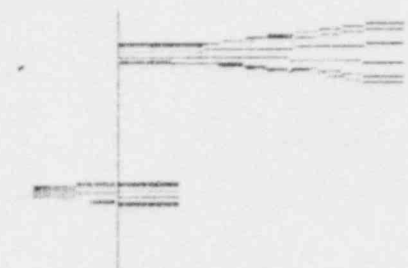

FIGURE 4.1.7

THE MODE SHAPE OF THE RRFCV ASSOCIATED WITH THE 30.7 HZ RESONANCE
MEASURED IN THE Y DIRECTION
IT IS A RIGID ROCKING OF THE CONTROL ARM.

FIGURE 4.1.8

THE MODE SHAPE OF THE RRFCV ASSOCIATED WITH THE 38.36 HZ RESONANCE
MEASURED IN THE Y DIRECTION
THIS IS THE FIRST TRUE CANTILEVER MODE OF THE CONTROL ARM.

FIGURE 4.1.9

THE MODE SHAPE OF THE RRFCV ASSOCIATED WITH THE 40.87 HZ RESONANCE
MEASURED IN THE Y DIRECTION
THIS IS A SECOND CANTILEVER MODE OF THE CONTROL ARM.

FIGURE 4.1.10

THE MODE SHAPE OF THE RRFCV ASSOCIATED WITH THE 45.21 HZ RESONANCE
MEASURED IN THE Y DIRECTION
THIS IS A THIRD CANTILEVER MODE OF THE CONTROL ARM.

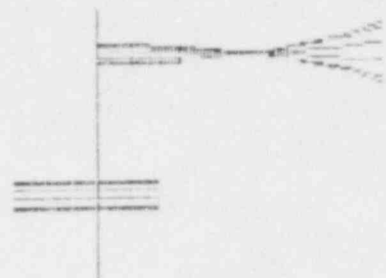

FIGURE 4.1.11

THE MODE SHAPE OF THE RRFCV ASSOCIATED WITH THE 47.97 HZ RESONANCE
MEASURED IN THE Y DIRECTION
THIS IS A PIPE MODE DRIVING THE CONTROL ARM.

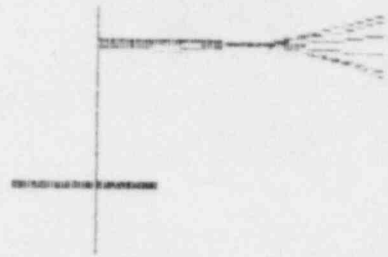

FIGURE 4.1.12

THE MODE SHAPE OF THE RRFCV ASSOCIATED WITH THE 89.9 HZ RESONANCE
MEASURED IN THE Y DIRECTION
THIS IS A CANTILEVER BENDING MODE OF THE SMALLER COMPONENTS AT THE END OF THE ARM.

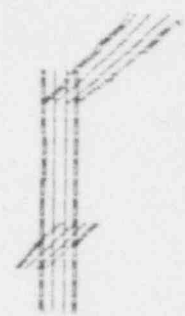

FIGURE 4.1.73

THE MODE SHAPE OF THE RRFCV ASSOCIATED WITH THE 16.21 HZ RESONANCE
MEASURED IN THE Z DIRECTION
THIS VIEW IS FROM THE SIDE OF THE VALVE AND OPPOSITE FROM THE CONTROL ARM.

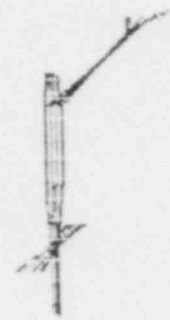

FIGURE 4.1.14

THE MODE SHAPE OF THE RRFCV ASSOCIATED WITH THE 27.07 HZ RESONANCE
MEASURED IN THE Z DIRECTION
THIS IS PROBABLY A PIPE TORSIONAL MODE.

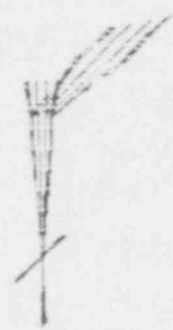

FIGURE 4.1.15

THE MODE SHAPE OF THE RRFCV ASSOCIATED WITH THE 32.59 HZ RESONANCE
MEASURED IN THE Z DIRECTION
THIS IS PROBABLY THE FIRST CANTILEVER MODE OF THE CONTROL ARM.

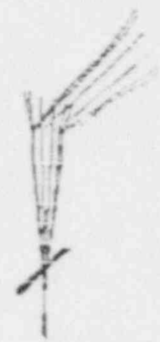

FIGURE 4.1.16

THE MODE SHAPE OF THE RRFCV ASSOCIATED WITH THE 37.98 HZ RESONANCE
MEASURED IN THE Z DIRECTION
THIS IS A SECOND CANTILEVER OR ROTATIONAL MODE OF THE VALVE BODY AND CONTROL ARM.

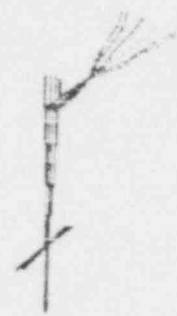

FIGURE 4.1.17

THE MODE SHAPE OF THE RRFCV ASSOCIATED WITH THE 54.29 HZ RESONANCE
MEASURED IN THE Z DIRECTION
THIS IS A CANTILEVER MODE INVOLVING THE SMALLER COMPONENTS OF THE CONTROL ARM.

4.1.5 Conclusions:

The results of this test show that large components such as the reactor recirculation flow control valve can be tested successfully using the restraint applied by Taipower for conduct of this program. The effort to measure dampings at higher acceleration levels was not permitted, but the damping values indicated in this test are quite reasonable for this type of structure.

4.? Residual Heat Removel (RHR) Pump:

4.2.1 Equipment Tested:

The residual heat removal pump, which we estimate weighs 3,000 lbs., was tested using the TRANSITEK hydraulic shaker at a force level of approximately 500 pounds. At the time of testing, the RHR line is presumed to have been filled with water. All hydraulic and electrical connections had been installed and completed at the time of testing. The pump located in the auxiliary building was properly secured to a base and foundation on the floor of the auxiliary building. The wire frame model of the RHR pump prepared by TRANSITEK is shown in Figures 4.2.1 and 4.2.2. The geometric location of points of response measurement on the RHR pump are listed in Table 4.2.1. The dimensions are given in inches.

4.2.2 Method of Testing:

The RHR pump was excited to an acceleration level of .3 g's at the point of excitation. The .3 g acceleration limit was imposed at the request of Taipower. The force level required to produce this level of acceleration was approximately 500 pounds force peak. Shaped pseudo random force excitation was used for both axes of testing. The spectrum was shaped to produce a one over frequency rolloff in the range of 30 to 100 Hz. This was done to satisfy the request of Taipower that we not shake the pump at greater than 33 Hz which was the upper previous limits of its level of qualification. The force level at the higher frequency proved to be adequate to excite the higher modes of the pump. Special brackets, which add approximately 70 lbs. of dead weight, were made to mount the shaker to the pump in both horizontal directions. The point of excitation for the X direction was 36 and point 48 for the Z direction.

The response was measured using high sensitivity (1g/volt) accelerometers (PCB Model 308) attached to the pump with beeswax. At each point 16 samples were taken, or about 3 minutes of continuous data collection.

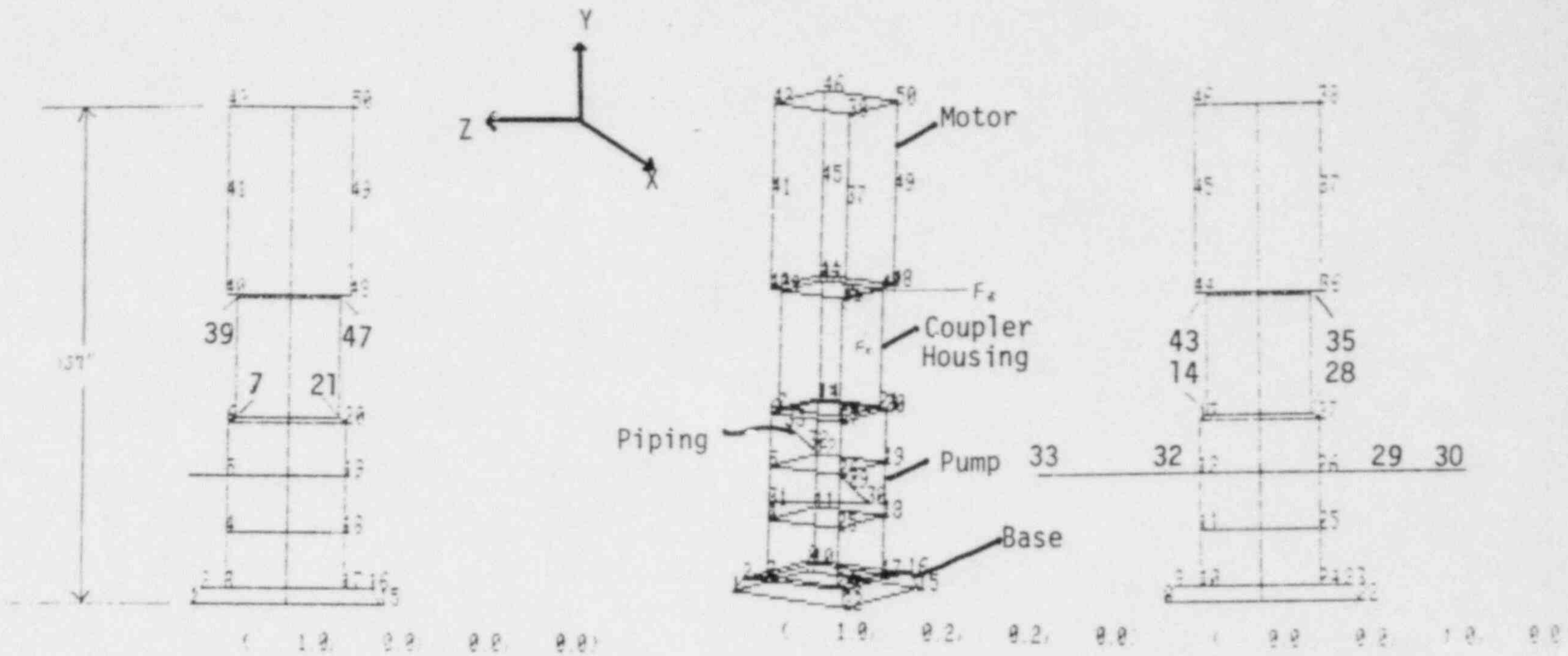

FIGURE 4.2.1

A LABELED WIRE FRAME MODEL OF THE RHR PUMP

LOOKING DIRECTLY ALONG THE X-A x 15

LOOKING DIRECTLY ALONG THE Z-A x 15

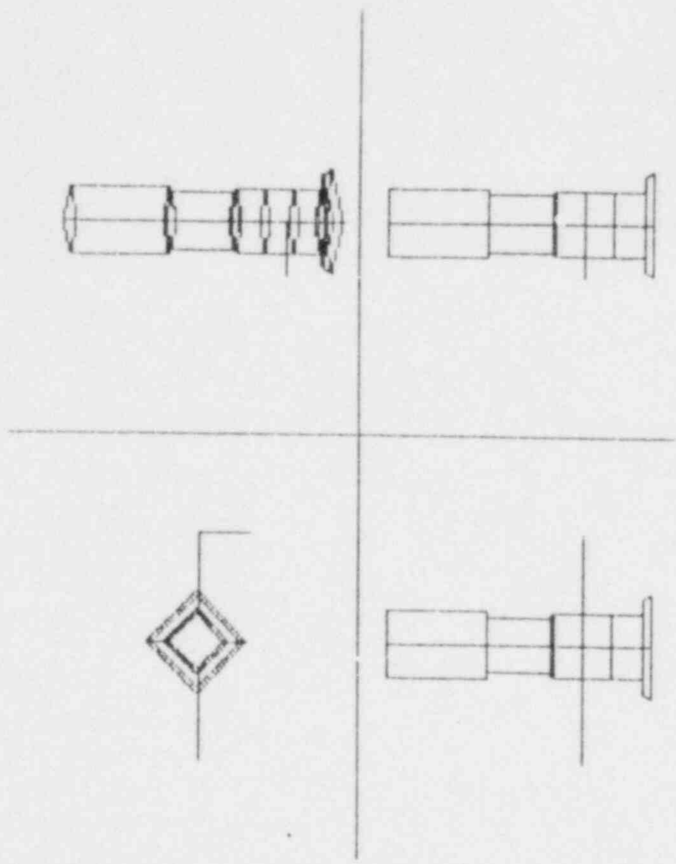

FIGURE 4.2.2

FOUR VIEWS OF THE WIRE FRAME MODEL OF THE RHR PUMP

TABLE 4.2.1

GEOMETRIC LOCATIONS OF POINTS OF RESPONSE MEASUREMENT - RHR PUMP

Point No.	X (In.)	Y (In.)	Z (In.)
1	0	0	26
2	0	4	23
3	0	4	16
4	0	20	16
5	0	35	16
6	0	50	16
7	0	51	14
8	-26	0	0
9	-23	4	0
10	-16	4	0
11	-16	20	0
12	-16	35	0
13	-16	50	0
14	-14	51	0
15	0	0	-26
16	0	4	-23
17	0	4	-16
18	0	20	-16
20	0	50	-16
21	0	51	-14
22	26	0	0
23	23	4	0
24	16	4	0
25	16	20	0
26	16	35	0
27	16	50	0
28	14	51	0
29	30	35	0
30	55	35	0
31	55	35	27
32	-28	35	0
33	-60	35	0
34	0	64	0
35	14	84	0
36	17	85	0
37	17	112	0
38	17	137	0
39	0	84	14
40	0	85	17
41	0	112	17
42	0	137	17
43	-14	84	0
44	-17	85	0
45	-17	112	0
46	-17	137	0
47	0	84	-14
48	0	85	-17
49	0	112	-17
50	0	137	-17
51	0	137	31
19	0	35	-16

4.2.3 Modal Properties:

The driving point transfer functions are shown in Figures 4.2.3 and 4.2.4 for the X and Z directions, respectively. Only two resonances were apparent in either transfer function. The slight difference in the resonant frequencies measured in the two directions are believed to be due to differences in the stiffness of the coupling housing between the motor and pump in the different directions. Table 4.2.2 lists the modal parameters estimated from the transfer functions shown in Figures 4.2.3 and 4.2.4.

4.2.4 Mode Shapes:

The mode shapes measured in the X direction are shown in Figures 4.2.5 and 4.2.6. The mode shapes are identified in the subtitle of each figure. The mode shapes measured in the Z direction are shown in Figures 4.2.7 and 4.2.8. The mode shapes are entirely those that would be predicted for equipment of this type.

4.2.5 Conclusions:

The results of this test show that even with relatively low levels of excitation and sharply reduced forces over 33 Hz, the mode shapes and modal properties of this type of equipment can be successfully measured. The damping values ranging from 1.7% to 3.0% are entirely believable and appropriate for equipment of this nature and is consistent with previous TRANSITEK experience.

The measurement of dampings at more than one force level was impractical on this piece of equipment for the extremely low levels of excitation to which we were restricted. The values stated, however, are a good indication that both structural and some acoustic damping would occur beyond the low values associated with hysteresis type damping.

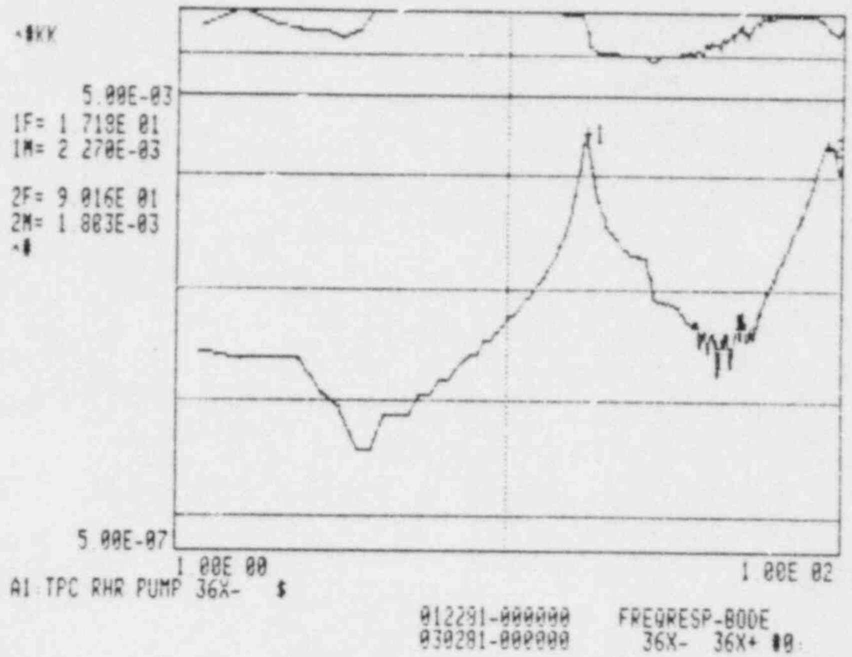

FIGURE 4.2.3

THE DRIVING POINT TRANSFER FUNCTION MEASURED IN THE X DIRECTION ON THE RHR PUMP

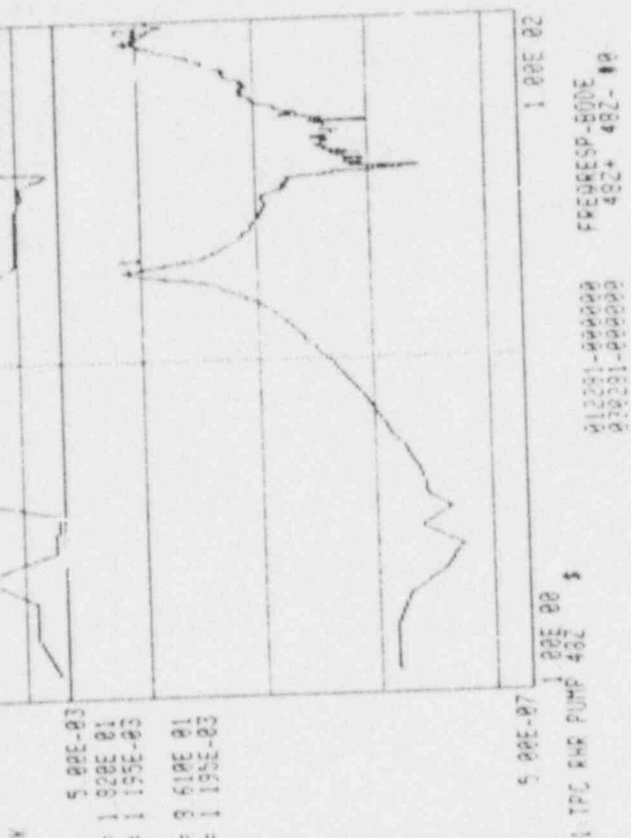

FIGURE 4.2.4

THE DRIVING POINT TRANSFER FUNCTION MEASURED IN THE Z DIRECTION ON THE RHR PUMP

TABLE 4.2.2

MODAL PROPERTIES MEASURED ON THE RHR PUMP

Mode Shape #	Frequency (Hz)	Damping (% Critical)
	X DIRECTION	
1	17.34	2.3
3	92.12	3.1
	Z DIRECTION	
7	18.3	2.4
5	87.0	1.7

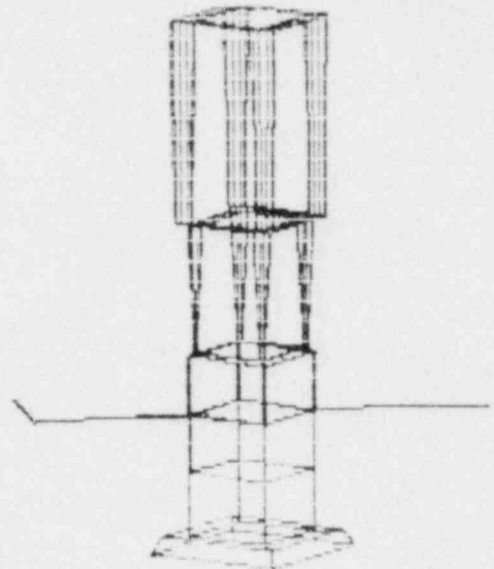

FIGURE 4.2.5

THE MODE SHAPE ASSOCIATED WITH THE 17.39 HZ RESONANCE
MEASURED IN THE X DIRECTION ON THE RHR PUMP
IS A FIRST ORDER CANTILEVER BEAM MODE

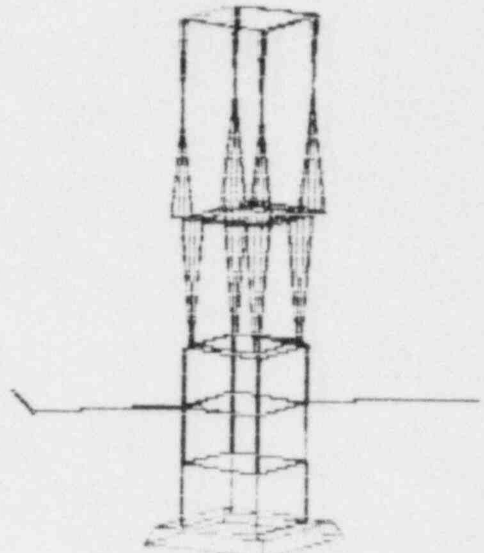

FIGURE 4.2.6

THE MODE SHAPE ASSOCIATED WITH THE 92.12 HZ RESONANCE
MEASURED IN THE X DIRECTION ON THE RHR PUMP
IS A SECOND ORDER CANTILEVER BEAM MODE

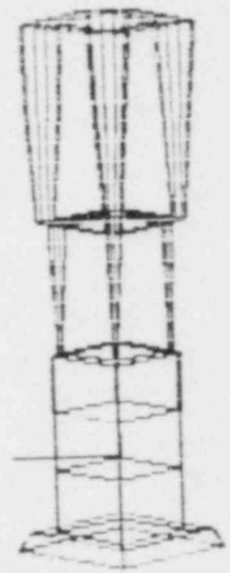

FIGURE 4.2.7

THE MODE SHAPE ASSOCIATED WITH THE 18.2 HZ RESONANCE
MEASURED IN THE Z DIRECTION ON THE RHR PUMP
IS A FIRST ORDER CANTILEVER BEAM MODE

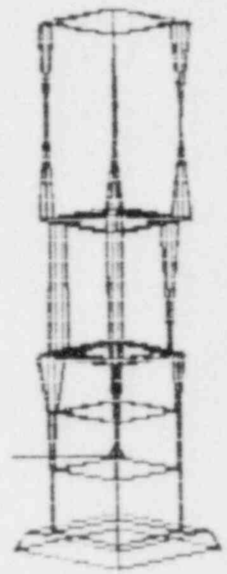

FIGURE 4.2.8

THE MODE SHAPE ASSOCIATED WITH THE 87 HZ RESONANCE
MEASURED IN THE Z DIRECTION ON THE RHR PUMP
IS A SECOND ORDER CANTILEVER BEAM MODE

4.3 Motor Control Center (1C1D):

4.3.1 Equipment Tested:

The motor control center 1C1D was tested to an acceleration level of .2 g's maximum. A high ambient background vibration (up to .05 g's) frustrated this test in the high frequency range in particular.

At the time of testing, all electrical connections and instrumentation of the control center, which is located in the auxiliary building, were completed. The cabinet was properly attached to the cement floor. The wire frame model of the control center prepared by TRANSITEK is shown in Figure 4.3.1. Four other views of the motor control center wire frame model are shown in Figure 4.3.2. The model is extremely detailed in an effort to make the very most of the possible mode shapes at the low level of excitation. The location of each point of response measurement is described in Table 4.3.1.

4.3.2 Method of Testing:

The motor control center was excited by the TRANSITEK hydraulic shaker to a maximum acceleration of .2 g's with wide band shaped pseudo random excitation. Above 30 Hz, the force spectrum was rolled off at approximately one over frequency rate of decrease. The actual rate of decrease was, in fact, higher due to the softness of the structure. The force level required to produce this level of excitation was approximately 300 pounds of force peak. The panel was tested only in the Z direction, or along the narrow dimension because previous TRANSITEK experience has shown that both vertical shaking and axial shaking tend to excite only the resonance of the narrow dimension with no new resonances. A special bracket which added approximately 100 lbs. of dead weight held the shaker at the top of the motor control center at point 92.

Thirty frames or samples of data were collected at each point to minimize the effects of the low level of excitation and high ambient vibration. The response was measured using high sensitivity (1 g/volt) accelerometers (PCB Model 308) attached to the structure with beeswax.

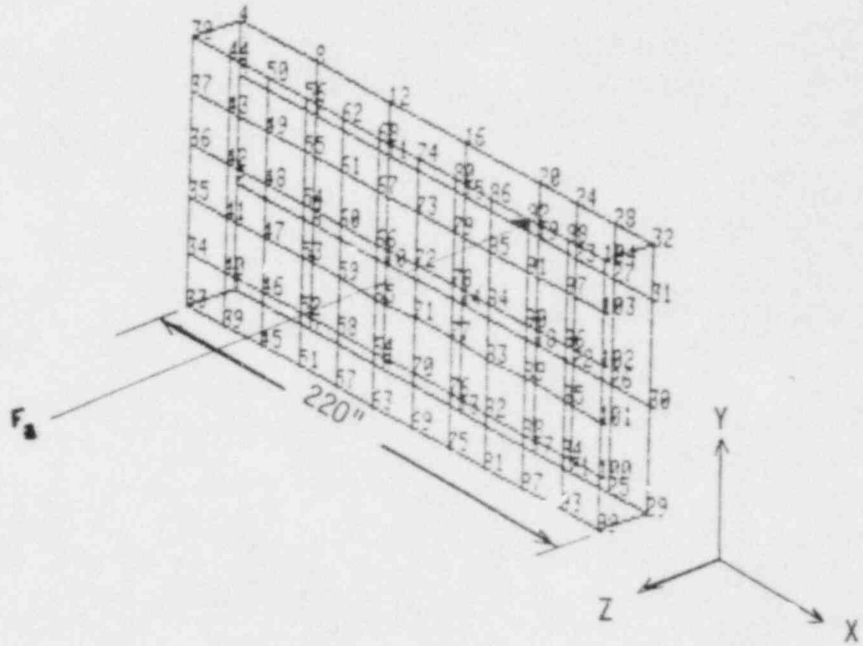

FIGURE 4.3.1

A LABELED WIRE FRAME MODEL
MOTOR CONTROL CENTER (1C1D)

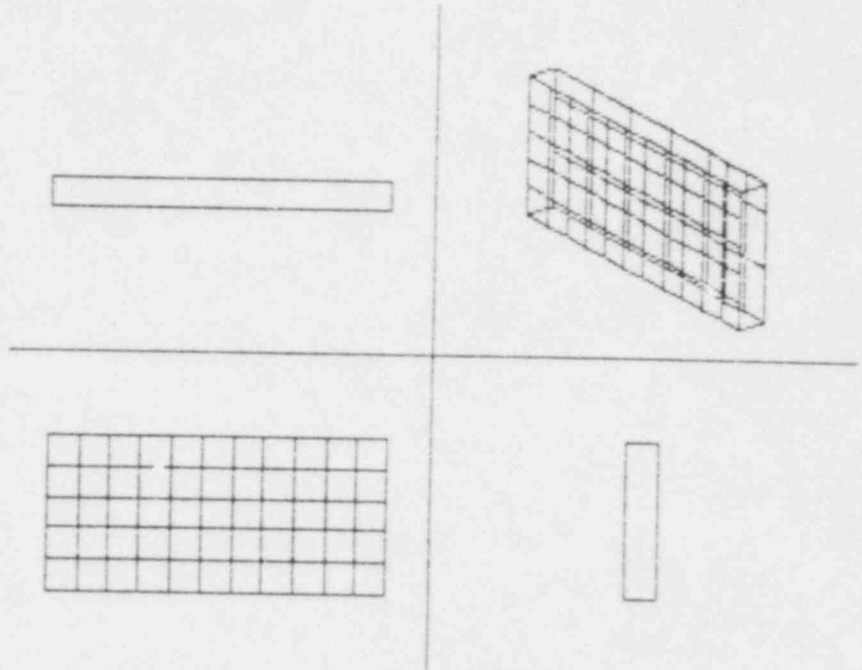

FIGURE 4.3.2

FOUR VIEWS OF THE WIRE FRAME MODEL
MOTOR CONTROL CENTER (1C1D)

TABLE 4.3.1

GEOMETRIC LOCATIONS OF POINTS OF RESPONSE MEASUREMENT
MOTOR CONTROL CENTER 1C1D

Point No.	X (In.)	Y (In.)	Z (In.)
1	0	0	0
2	0	40	0
3	0	80	0
4	0	100	0
5	40	0	0
6	40	40	0
7	40	80	0
8	40	100	0
9	80	0	0
10	80	40	0
11	80	80	0
12	80	100	0
13	120	0	0
14	120	40	0
15	120	80	0
16	120	100	0
17	160	0	0
18	160	40	0
19	160	80	0
20	160	100	0
21	180	0	0
22	180	40	0
23	180	80	0
24	180	100	0
25	200	0	0
26	200	40	0
27	200	80	0
28	200	100	0
29	220	0	0
30	220	40	0
31	220	80	0
32	220	100	0
33	0	0	20
34	0	20	20
35	0	40	20
36	0	60	20
37	0	80	20
38	0	100	20
39	20	0	20
40	20	20	20
41	20	40	20
42	20	60	20
43	20	80	20
44	20	100	20
45	40	0	20
46	40	20	20
47	40	40	20
48	40	60	20
49	40	80	20
50	40	100	20
61	80	80	20
51	60	0	20
52	60	20	20
53	60	40	20
54	60	60	20
55	60	80	20
56	60	100	20
57	80	0	20
58	80	20	20
59	80	40	20
60	80	60	20
62	80	100	20
63	100	0	20
64	100	20	20
65	100	40	20
66	100	60	20
67	100	80	20
68	100	100	20
69	120	0	20
70	120	20	20
71	120	40	20
72	120	60	20
73	120	80	20
74	120	100	20
75	140	0	20
76	140	20	20
77	140	40	20
78	140	60	20
79	140	80	20
80	140	100	20
81	160	0	20
82	160	20	20
83	160	40	20
84	160	60	20
85	160	80	20
86	160	100	20
87	180	0	20
88	180	20	20
89	180	40	20
90	180	60	20
91	180	80	20
92	180	100	20
93	200	0	20
94	200	20	20
95	200	40	20
96	200	60	20
97	200	80	20
98	200	100	20
99	220	0	20
100	220	20	20
101	220	40	20
102	220	60	20
103	220	80	20
104	220	100	20

4.3.3 Modal Properties:

The driving point impedance function is shown in Figures 4.3.3A and 4.3.3B. It will be noted that resonant frequencies range from 7.4 to 63 Hz. There is the possibility that more resonances exist at higher frequencies, but, due to the extremely low level of excitation, the quality of the data is inadequate for modal analysis. The modal properties derived from the driving point transfer functions shown in Figure 4.3.3A and B are listed in Table 4.3.2. The values of damping presented in this table are generally lower than TRANSITEK's experience on similar equipment in which higher levels of excitation were applied. The ambient vibration at the motor control center is between .01 and .04 g's, and this high ambient vibration also inhibited the measurement process.

4.3.4 Mode Shapes:

The mode shapes measured on the motor control center and associated with the resonances of Table 4.3.2 are shown in Figures 4.3.4 through 4.3.9. The resonance at 69.65 Hz had no discernible mode shape due to the low level of excitation.

4.3.5 Conclusions:

The results of this test were somewhat marginal indicating that higher levels of excitation are essential to the success of measurements of this type. TRANSITEK experience on similar structures using excitations to the 1 to 3 g level show significantly higher values of damping and greater clarity of the mode shapes.

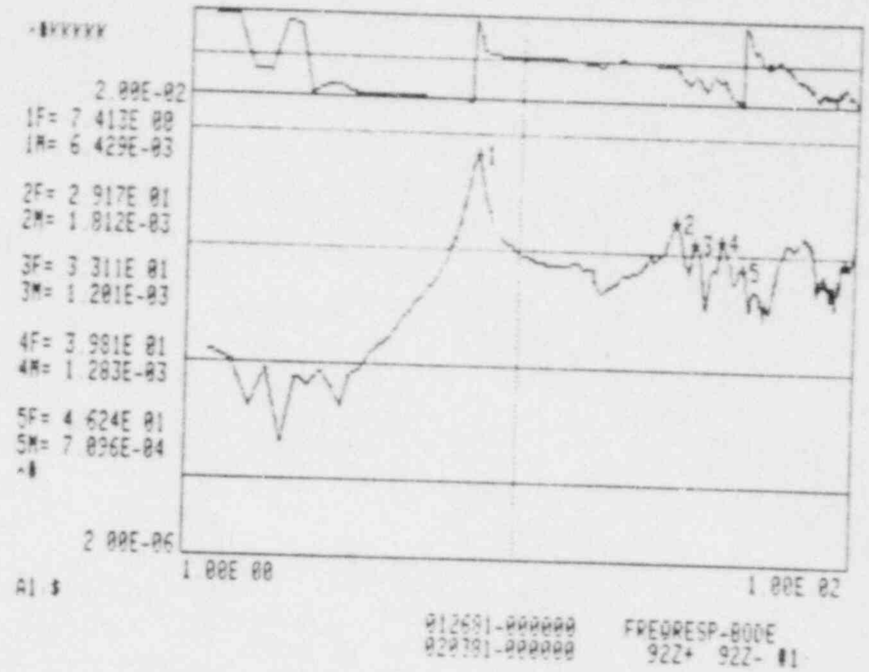

FIGURE 4.3.3A

THE DRIVING POINT TRANSFER FUNCTION SHOWING THE FIVE RESONANCES OF LOWEST FREQUENCY
MOTOR CONTROL CENTER (1C1D)

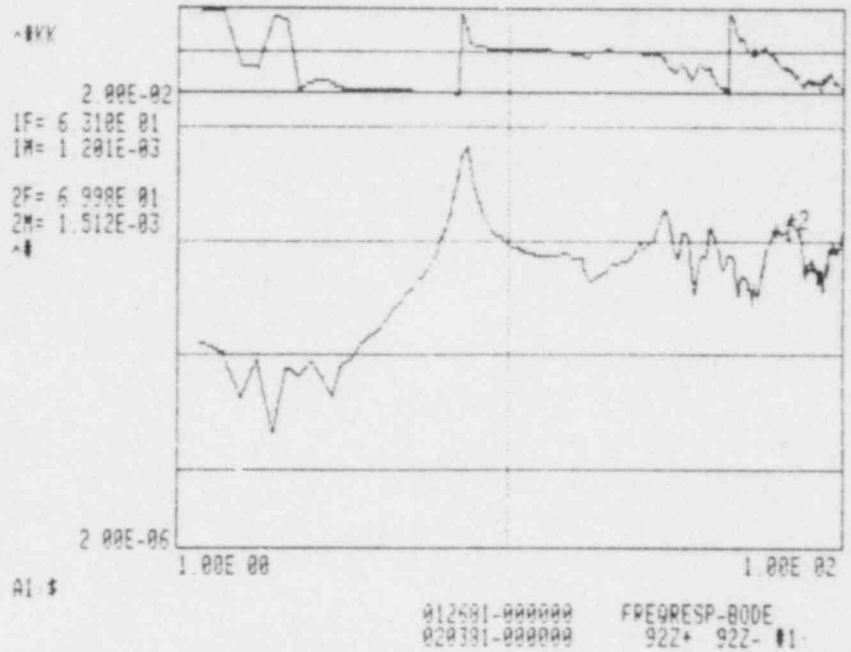

FIGURE 4.3.3B

THE DRIVING POINT TRANSFER FUNCTION SHOWING THE TWO RESONANCES OF HIGHEST FREQUENCY.
MOTOR CONTROL CENTER (1C1D)
THE "FUZZY" APPEARANCE OF THE DATA AT HIGH FREQUENCY IS DUE TO INADEQUATE FORCE LEVELS.

TABLE 4.3.2

MODAL PROPERTIES MEASURED ON THE MOTOR CONTROL CENTER (1C1D)

Mode Shape	Frequency (Hz)	Damping (% Critical)
1	7.4	2.4
2	29.19	2.6
3	33.93	4.4
4	39.72	1.4
5	47.42	1.4
6	62.98	1.3
No Shape Found	69.65	5.4

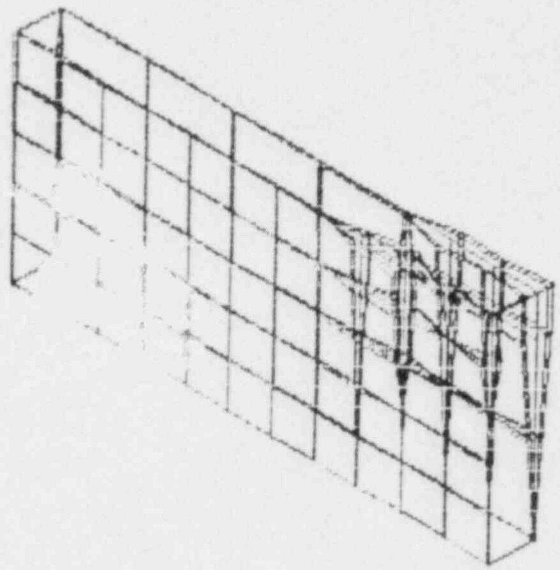

FIGURE 4.3.4

THE MODE SHAPE ASSOCIATED WITH THE 7.4 HZ RESONANCE
IS A TORSIONAL MODE OF THE ENTIRE PANEL - MOTOR CONTROL CENTER (1C1D)
THE LOW EXCITATION LEVEL AND TWO MASSIVE CONNECTOR PENETRATIONS FROM CABLE TRAYS
DISTORT THIS MODE AND ALL OTHERS.

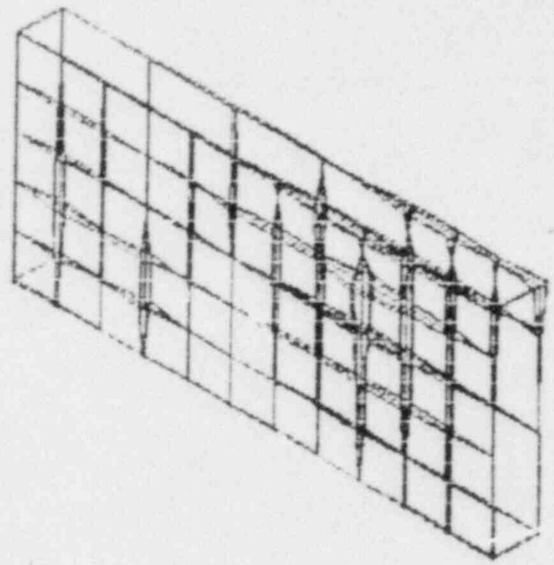

FIGURE 4.3.5

THE MODE SHAPE ASSOCIATED WITH THE 29.2 HZ RESONANCE
IS A LATERAL BENDING OF THE RIGHT SIDE OF THE PANEL
WITH SOME INTERACTION OF SIMILAR COMPONENTS AT THE LEFT SIDE.
(MOTOR CONTROL CENTER (1C1D)

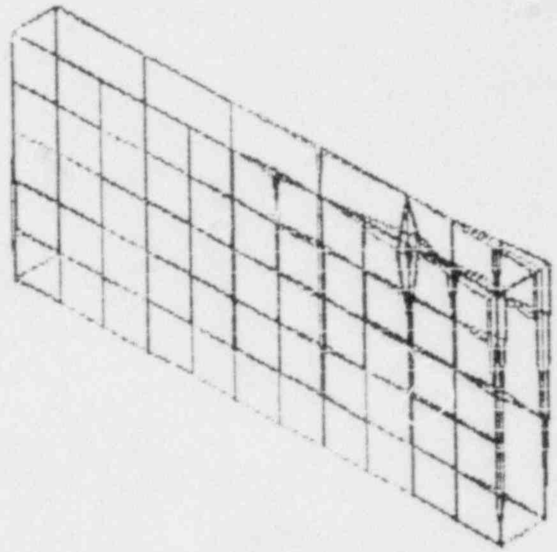

FIGURE 4.3.6

THE MODE SHAPE ASSOCIATED WITH THE 33.9 HZ RESONANCE
CONSISTS ONLY OF BENDING AT THE RIGHT END CORNER.
A SIMILAR MODE POSSIBLY EXISTS AT THE LEFT END, BUT, BECAUSE OF THE LOW EXCITATION
LEVEL ABOVE 33 HZ, IT COULD NOT BE DETECTED.
MOTOR CONTROL CENTER (1C1D)

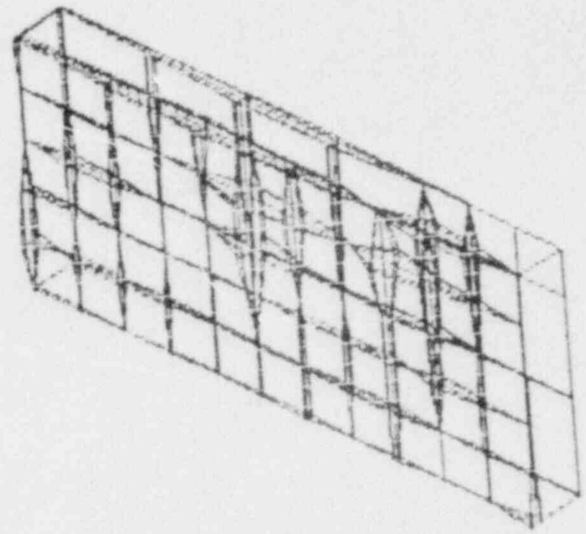

FIGURE 4.3.7

THE MODE SHAPE ASSOCIATED WITH THE 39.7 HZ RESONANCE
IS A BENDING OF THE MID-SECTION OF THE PANEL BETWEEN THE LARGE CABLE TRAY PENETRATIONS.
MOTOR CONTROL CENTER (1C1D)

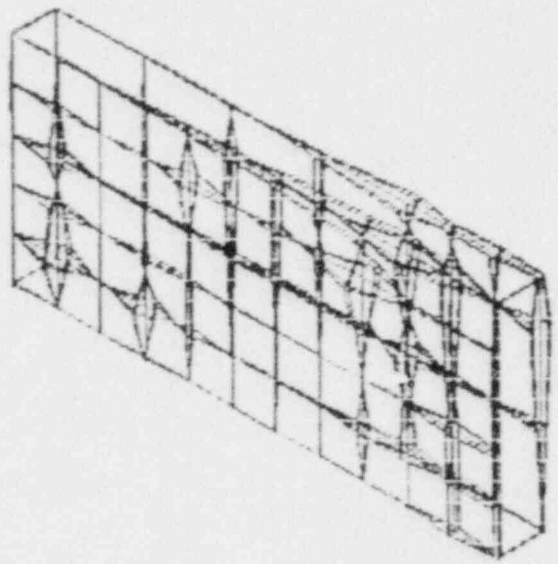

FIGURE 4.3.8

THE MODE SHAPE ASSOCIATED WITH THE 47.4 HZ RESONANCE
IS A COMPOSITE OF SEVERAL LOCAL MODES.
MOTOR CONTROL CENTER (1C1D)

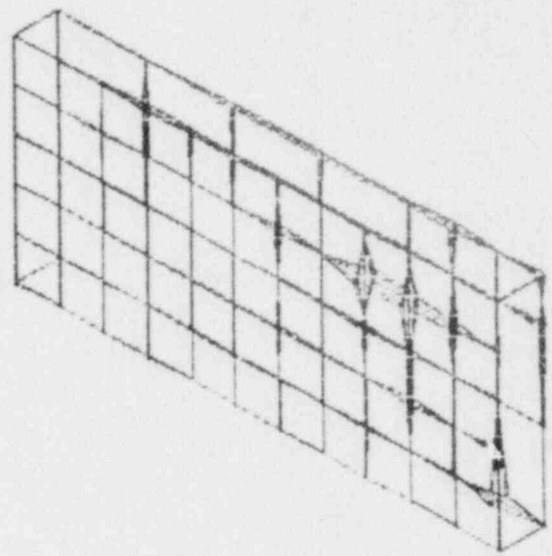

FIGURE 4.3.9

THE MODE SHAPE ASSOCIATED WITH THE 63.0 HZ RESONANCE IS STRICTLY LOCAL. INADEQUATE FORCE LEVELS MADE ANALYSIS OF HIGHER FREQUENCY MODES IMPOSSIBLE.
MOTOR CONTROL CENTER (1C1D)

4.4 Jet Pump Instrument Panel:

4.4.1 Equipment Tested:

The jet pump instrument panel was tested after it was completely installed and all electrical and hydraulic connections had been completed. All instruments and transmitters were in place and the panel was properly secured to the floor. Several individual and groups of small diameter (½") pipe connect to the top of the panel.

Wire frame models of the jet pump instrument panel are shown in Figures 4.4.1 and 4.4.2. Additional views of the panel are shown in Figure 4.4.3. Table 4.4.1 lists the geometric location of points of response measurement of the panel. Excitation was applied at point 59 in the Z direction. The panel, which weighs an estimated 1,000 lbs, is located in the inner containment.

4.4.2 Method of Testing:

Vibrations of the jet pump instrument panel were excited by the TRANSITEK electromagnetic shaker to an acceleration level of .4 g's maximum at the point of shaker attachment. The shaker excitation was broad band pseudo random with frequency content between 1 and 100 Hz. The panel was also tested by impulses (up to 300 lbf) applied in the X direction, or long dimension, of the panel. Response was measured using high sensitivity (1 g/volt) accelerometers (PCB Model 308) attached to the panel with beeswax.

4.4.3 Modal Properties:

The modal properties of the jet pump instrument panel measured in the X direction are shown in Figures 4.4.4A through 4.4.4D. The corresponding transfer function measurements for the Z direction are shown in Figures 4.4.5A and 4.4.5B. The modal properties deduced from these transfer functions are listed in Table 4.4.2.

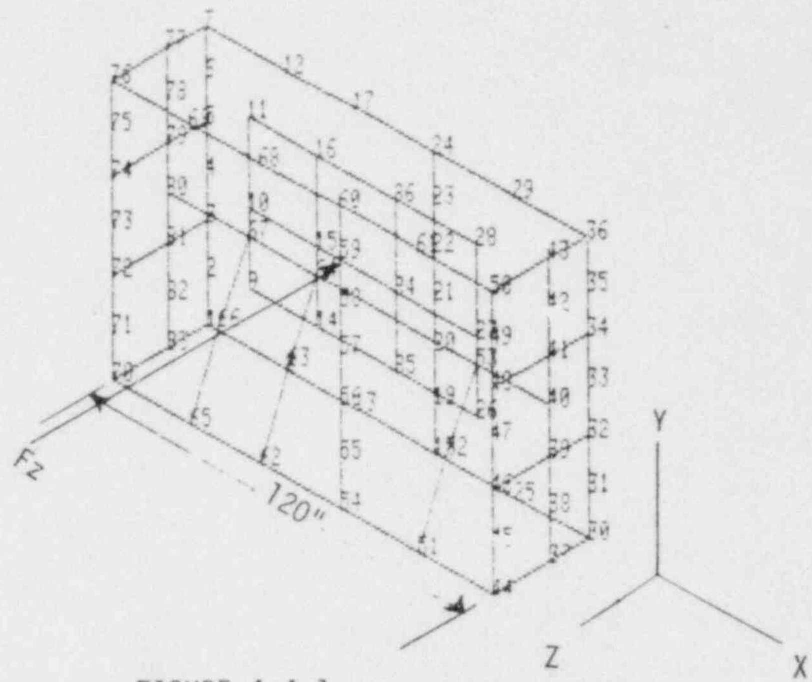

FIGURE 4.4.1

A LABELED WIRE FRAME MODEL OF THE ENTIRE WIRE FRAME MODEL OF THE JET PUMP INSTRUMENT PANEL

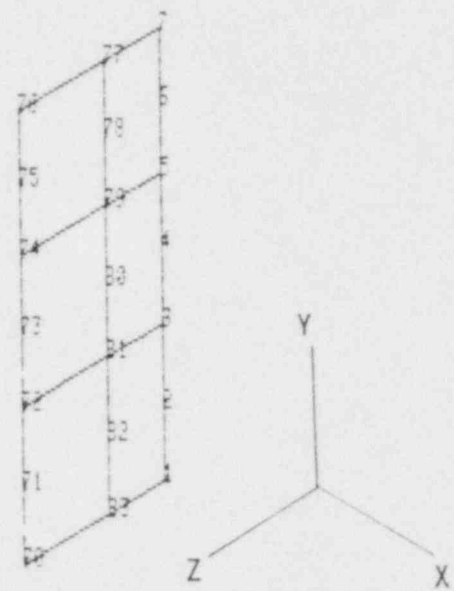

FIGURE 4.4.2

A LABELED WIRE FRAME MODEL OF THE END OF THE
JET PUMP INSTRUMENT PANEL WHICH IS TYPICAL OF ALL FOUR CROSS BRACED PANEL ENDS

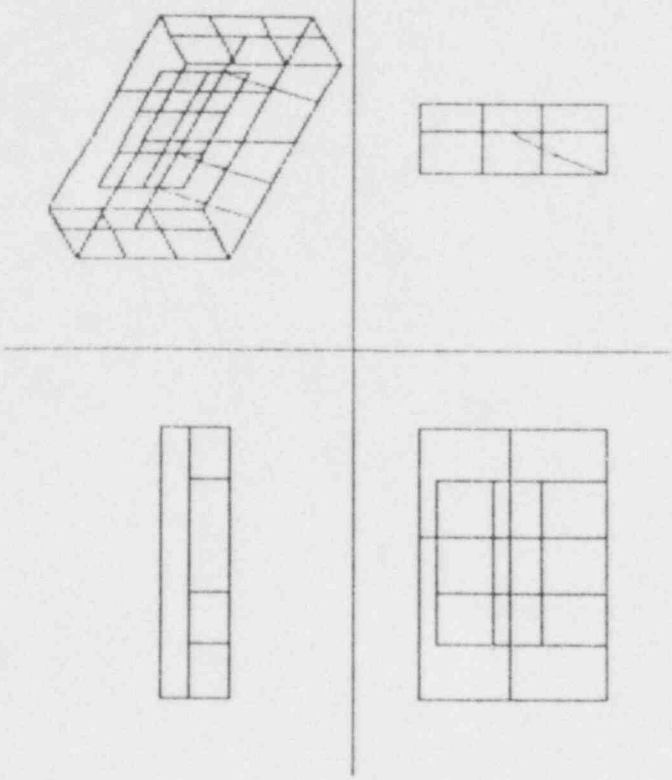

FIGURE 4.4.3

FOUR VIEWS OF THE WIRE FRAME OF THE JET PUMP INSTRUMENT PANEL

TABLE 4.4.1

GEOMETRIC LOCATIONS OF POINTS OF RESPONSE MEASUREMENT
JET PUMP INSTRUMENT PANEL

Point No.	X (In.)	Y (In.)	Z (In.)	Point No.	X (In.)	Y (In.)	Z (In.)
1	0	0	0	44	120	0	30
2	0	14	0	45	120	14	30
3	0	29	0	46	120	29	30
4	0	43	0	47	120	43	30
5	0	57	0	48	120	57	30
6	0	[illegible]	0	49	120	70	30
7	0	84	0	50	120	84	30
8	25	0	0	51	97	0	30
9	25	29	12	52	97	23	21
10	25	51	12	53	97	43	12
11	25	77	12	54	72	0	30
12	25	84	0	55	72	14	30
13	47	0	0	56	72	29	30
14	47	29	12	57	72	43	30
15	47	51	12	58	72	57	30
16	47	77	12	59	72	70	30
17	47	84	0	60	72	84	30
18	72	0	0	61	97	84	30
19	72	14	0	62	47	0	30
20	72	29	0	63	47	23	21
21	72	43	0	64	47	43	12
22	72	57	0	65	25	0	30
23	72	70	0	66	25	23	21
24	72	84	0	67	25	43	12
25	97	0	0	68	47	84	30
26	97	29	12	69	25	84	30
27	97	51	12	70	0	0	30
28	97	77	12	71	0	14	30
29	97	84	0	72	0	29	30
30	120	0	0	73	0	43	30
31	120	14	0	74	0	57	30
32	120	29	0	75	0	70	30
33	120	43	0	76	0	84	30
34	120	57	0	77	0	84	12
35	120	70	0	78	0	70	12
36	120	84	0	79	0	57	12
37	120	0	12	80	0	43	12
38	120	14	12	81	0	29	12
39	120	29	12	82	0	14	12
40	120	43	12	83	0	0	12
41	120	57	12	84	72	51	12
42	120	70	12	85	72	29	12
43	120	84	12	86	72	77	12

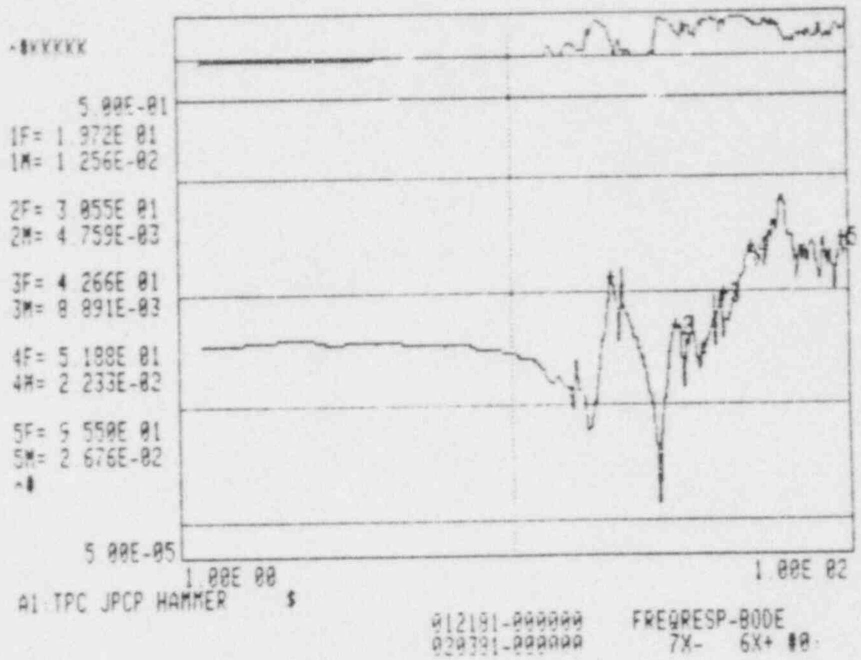

FIGURE 4.4.4A

A REPRESENTATIVE TRANSFER FUNCTION MEASURED ON THE JET PUMP INSTRUMENT PANEL IN THE X DIRECTION

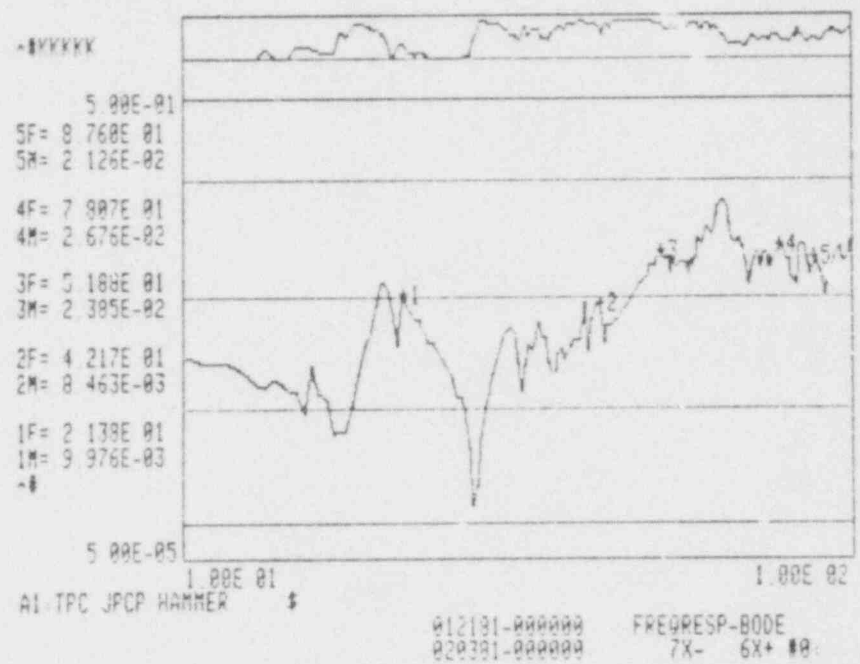

FIGURE 4.4.4B

FIGURES 4.4.4B, C AND D ARE EXPANDED VIEWS OF THE REPRESENTATIVE TRANSFER FUNCTION MEASURED IN THE X DIRECTION. IN ALL, A TOTAL OF 11 MODES WERE DETECTED IN THE X DIRECTION.

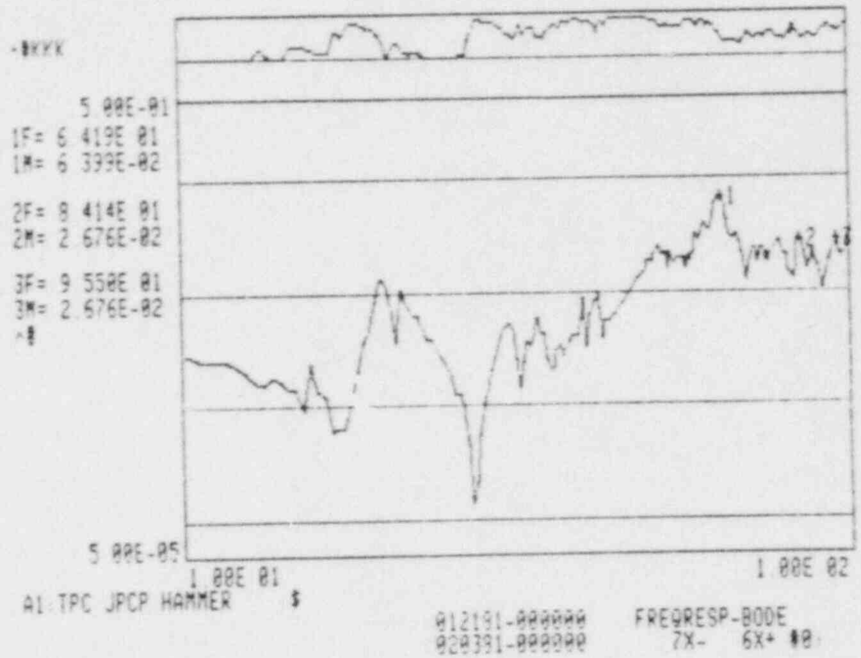

FIGURE 4.4.4C

REPRESENTATIVE TRANSFER FUNCTION MEASURED IN THE X DIRECTION

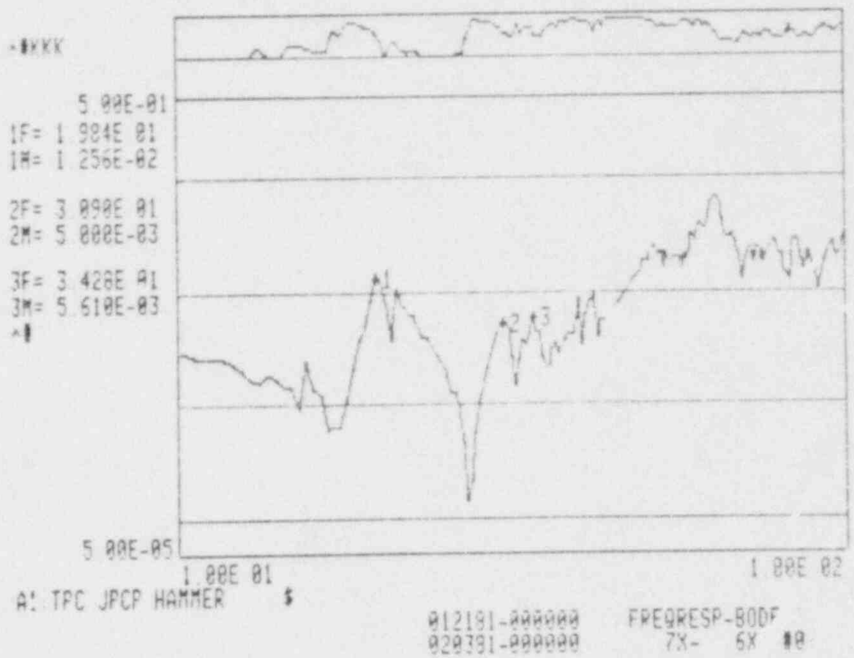

FIGURE 4.4.4D

REPRESENTATIVE TRANSFER FUNCTION MEASURED IN THE X DIRECTION.

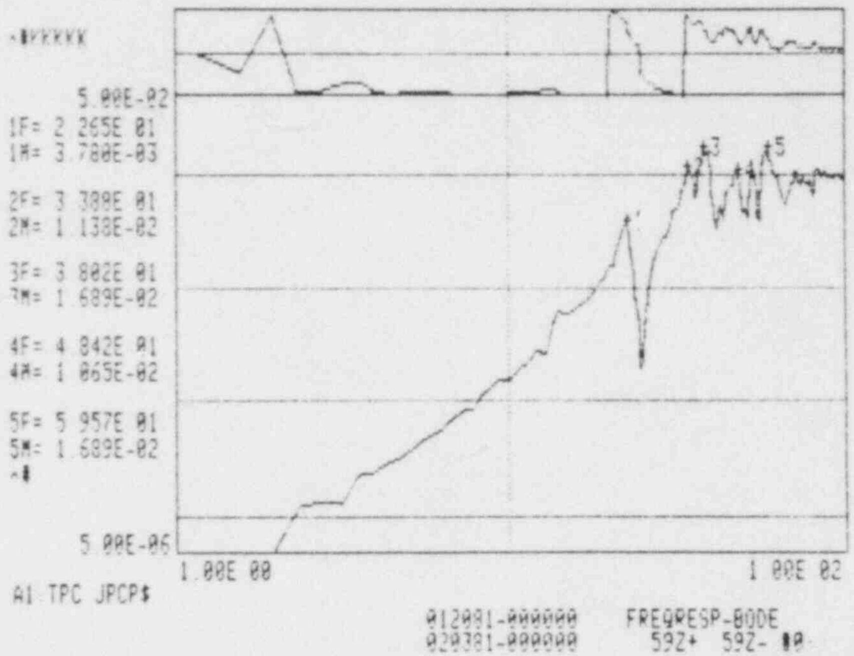

FIGURE 4.4.5A

THE DRIVING POINT TRANSFER FUNCTION MEASURED ON THE JET PUMP INSTRUMENT PANEL IN THE Z DIRECTION. A TOTAL OF 8 MODES ARE INDICATED IN FIGURES 4.4.5A AND 4.4.5B.

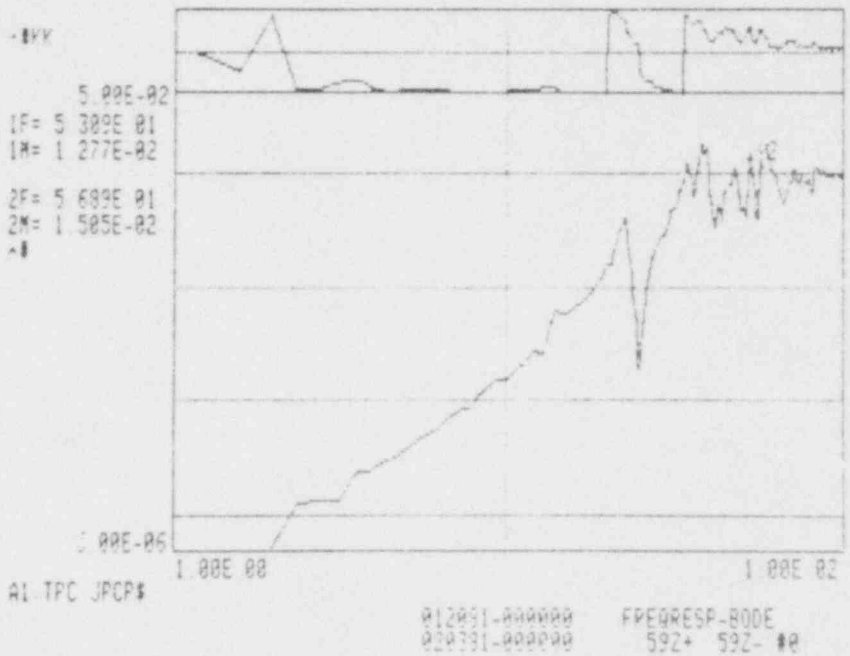

FIGURE 4.4.5B

THE DRIVING POINT TRANSFER FUNCTION MEASURED ON THE JET PUMP INSTRUMENT PANEL IN THE Z DIRECTION

TABLE 4.4.2

MODAL PROPERTIES MEASURED ON THE JET PUMP INSTRUMENT PANEL

Mode Shape	Frequency (Hz)	Damping (% Critical)
	X DIRECTION	
1	19.87	2.1
2	21.32	0.9
3	31.45	2.4
4	34.57	0.8
5	42.26	1.9
6	52.0	1.5
7	64.0	2.6
8	78.4	1.8
9	85.3	1.3
10	89.0	2.4
11	94.4	2.7
	Z DIRECTION	
1	22.7	3.7
2	35.0	2.8
3	38.4	3.7
4	44.9	8.8
5	48.2	3.8
6	53.8	3.8
7	58.5	2.4
8	60.1	0.9

4.4.4 Mode Shapes:

The mode shapes measured in the X direction on the end panel are shown in Figures 4.4.6 through 4.4.16. The mode shapes measured in the Z direction are shown in Figures 4.4.17 through 4.4.24. The mode shapes correspond to each of the modal parameters listed in Table 4.4.2.

4.4.5 Conclusions:

The results of this test show that structures such as the jet pump instrument panel are rich in both global and local modes of vibration, particularly in the frequency range of 30 to 100 Hz. The values of damping are similar to other structures TRANSITEK has tested and are appropriate for welded and bolted steel structures of this nature. Higher excitation levels would most likely raise the low estimates of damping observed at the 21 Hz and 34 Hz modes of vibration.

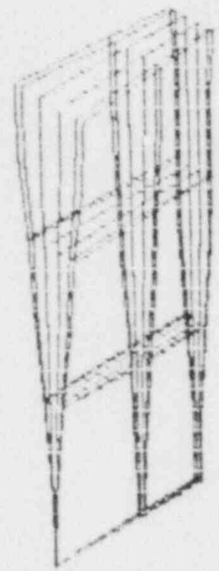

FIGURE 4.4.6

THE MODE SHAPE ASSOCIATED WITH 19.87 HZ RESONANCE
MEASURED ON THE JET PUMP INSTRUMENT PANEL IN THE X DIRECTION.

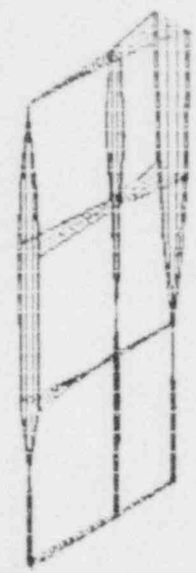

FIGURE 4.4.7

THE MODE SHAPE ASSOCIATED WITH 21.32 HZ RESONANCE
MEASURED ON THE JET PUMP INSTRUMENT PANEL IN THE X DIRECTION

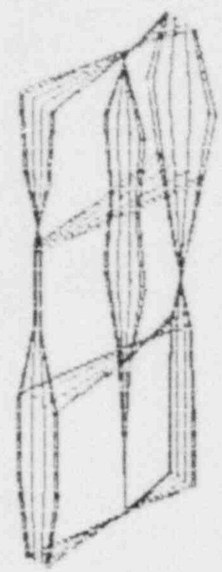

FIGURE 4.4.8

THE MODE SHAPE ASSOCIATED WITH 31.45 HZ RESONANCE
MEASURED ON THE JET PUMP INSTRUMENT PANEL IN THE X DIRECTION

FIGURE 4.4.9

THE MODE SHAPE ASSOCIATED WITH 34.57 HZ RESONANCE
MEASURED ON THE JET PUMP INSTRUMENT PANEL IN THE X DIRECTION

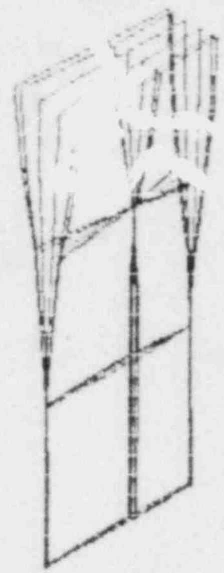

FIGURE 4.4.10

THE MODE SHAPE ASSOCIATED WITH 42.26 HZ RESONANCE
MEASURED ON THE JET PUMP INSTRUMENT PANEL IN THE X DIRECTION

FIGURE 4.4.11

THE MODE SHAPE ASSOCIATED WITH 52.0 HZ RESONANCE
MEASURED ON THE JET PUMP INSTRUMENT PANEL IN THE X DIRECTION

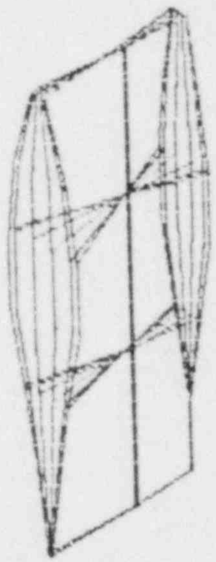

FIGURE 4.4.12

THE MODE SHAPE ASSOCIATED WITH 64.0 HZ RESONANCE
MEASURED ON THE JET PUMP INSTRUMENT PANEL IN THE X DIRECTION

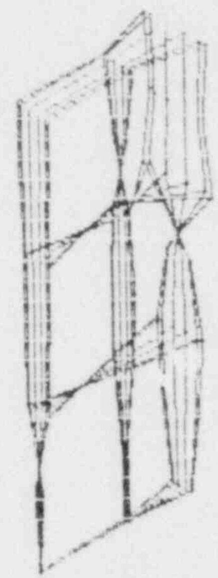

FIGURE 4.4.13

THE MODE SHAPE ASSOCIATED WITH 78.41 HZ RESONANCE
MEASURED ON THE JET PUMP INSTRUMENT PANEL IN THE X DIRECTION

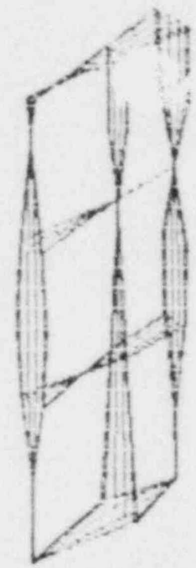

FIGURE 4.4.14

THE MODE SHAPE ASSOCIATED WITH 85.29 HZ RESONANCE
MEASURED ON THE JET PUMP INSTRUMENT PANEL IN THE X DIRECTION

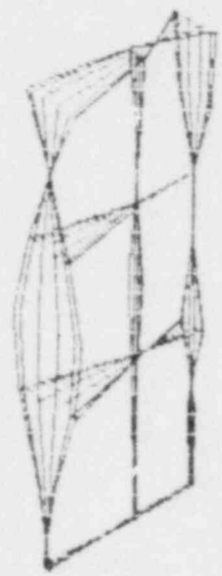

FIGURE 4.4.15

THE MODE SHAPE ASSOCIATED WITH 89.03 HZ RESONANCE
MEASURED ON THE JET PUMP INSTRUMENT PANEL IN THE X DIRECTION

FIGURE 4.4.16

THE MODE SHAPE ASSOCIATED WITH 94.35 HZ RESONANCE
MEASURED ON THE JET PUMP INSTRUMENT PANEL IN THE X DIRECTION

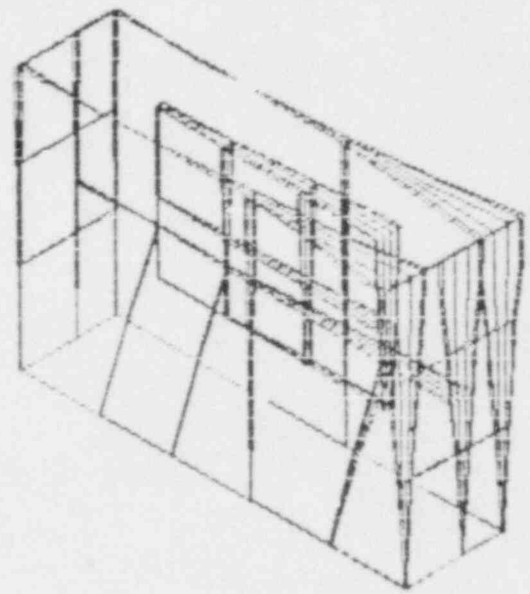

FIGURE 4.4.17

THE MODE SHAPE ASSOCIATED WITH 22.73 HZ RESONANCE
MEASURED ON THE JET PUMP INSTRUMENT PANEL IN THE Z DIRECTION

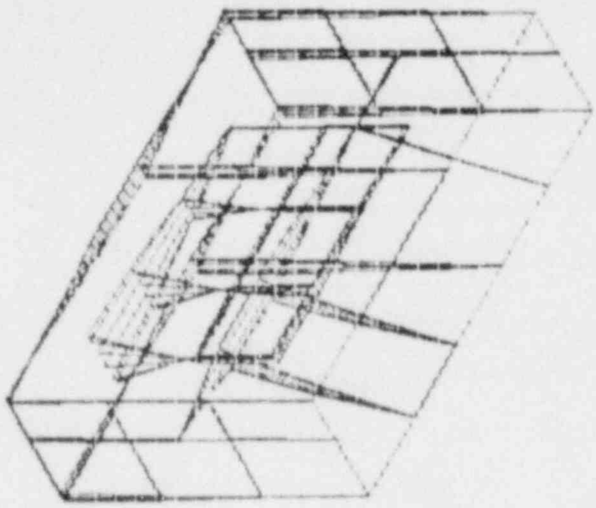

FIGURE 4.4.18

THE MODE SHAPE ASSOCIATED WITH 34.96 HZ RESONANCE
MEASURED ON THE JET PUMP INSTRUMENT PANEL IN THE Z DIRECTION

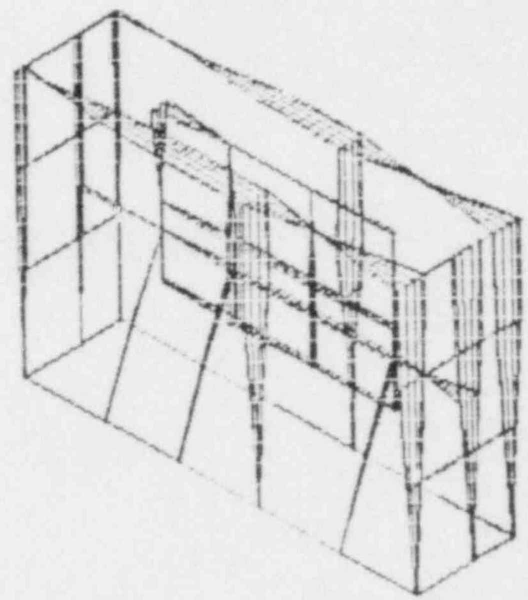

FIGURE 4.4.19

THE MODE SHAPE ASSOCIATED WITH 38.37 HZ RESONANCE
MEASURED ON THE JET PUMP INSTRUMENT PANEL IN THE Z DIRECTION

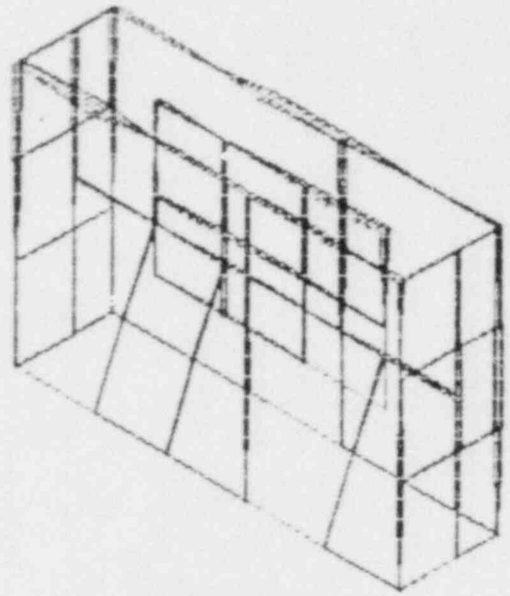

FIGURE 4.4.20

THE MODE SHAPE ASSOCIATED WITH 44.9 HZ RESONANCE
MEASURED ON THE JET PUMP INSTRUMENT PANEL IN THE Z DIRECTION

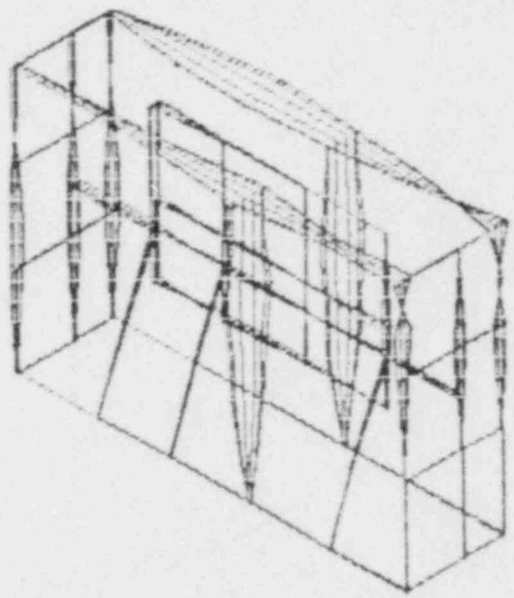

FIGURE 4.4.21

THE MODE SHAPE ASSOCIATED WITH 48.24 HZ RESONANCE
MEASURED ON THE JET PUMP INSTRUMENT PANEL IN THE Z DIRECTION

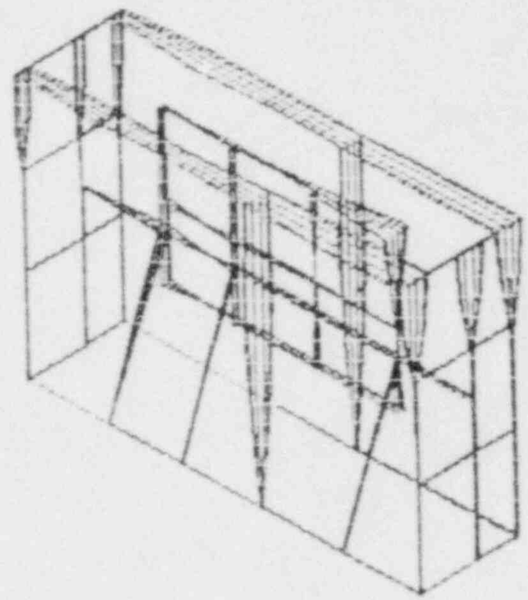

FIGURE 4.4.22

THE MODE SHAPE ASSOCIATED WITH 53.81 HZ RESONANCE
MEASURED ON THE JET PUMP INSTRUMENT PANEL IN THE Z DIRECTION

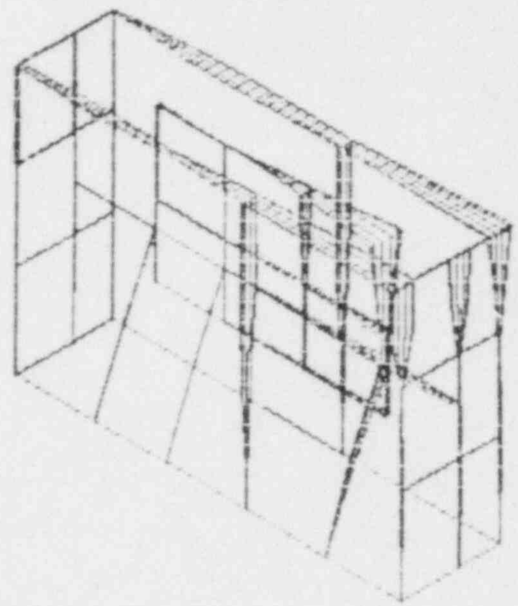

FIGURE 4.4.23

THE MODE SHAPE ASSOCIATED WITH 58.45 HZ RESONANCE
MEASURED ON THE JET PUMP INSTRUMENT PANEL IN THE Z DIRECTION

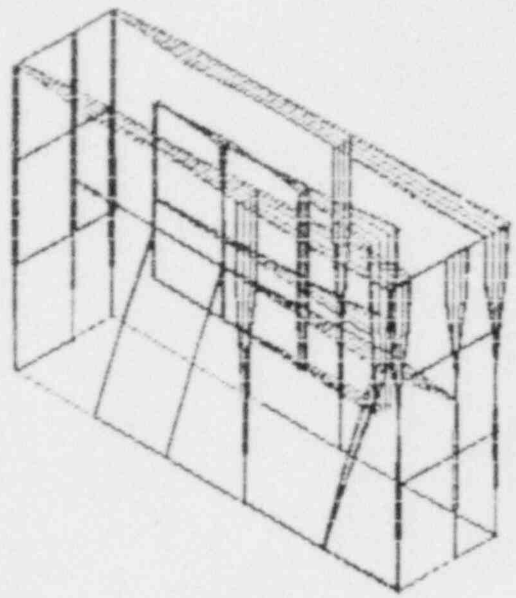

FIGURE 4.4.24

THE MODE SHAPE ASSOCIATED WITH 60.1 HZ RESONANCE
MEASURED ON THE JET PUMP INSTRUMENT PANEL IN THE Z DIRECTION

4.5 3 Inch Motor Operated Valve:

4.5.1 Equipment Tested:

The 3 inch motor operated valve was tested using impulse techniques. At the time of testing, the valve was completely installed and all hydraulic and electrical connections to the valve were completed. The pipes on which the valve was located are believed to have been empty. We estimate the valve to weigh nominally 300 lbs.

The geometric location of each point of response measurement is listed in Table 4.5.1. Figure 4.5.1 is a labeled wire frame model of the valve. Figure 4.5.2 shows additional views of the wire frame model.

4.5.2 Method of Testing:

The valve located on the inner wall of the inner containment was excited to an acceleration level of .2 to .3 g's in each of the three directions by hammer taps of nominally 200 lbf. Higher accelerations resulted from more forceful hammer taps up to 1,000 lbf in testing to determine if the damping changed appreciably with the level of excitation. Response was measured using sensitive (1 g/volt) accelerometers (PCB Model 308) attached to the valve with glued on mounting pads.

4.5.3 Modal Properties:

The driving point transfer function for the X direction is shown in Figure 4.5.3. Five modes are apparent in the transfer function. Figure 4.5.4 is a graph of the driving point transfer function measured in the Y direction. Again, five resonances are apparent in the transfer function. Figures 4.5.5A through D are the driving point transfer function measured in the Z direction. Eleven different modes are apparent in the expanded views (4.5.5B through D). The modal parameters derived from these transfer functions are listed in Table 4.5.2.

TABLE 4.5.1

GEOMETRIC LOCATIONS OF POINTS OF RESPONSE MEASUREMENT
3 INCH MOTOR OPERATED VALVE

Point No.	X (In.)	Y (In.)	Z (In.)
1	25	18	0
2	6	18	0
3	0	12	0
4	0	6	0
5	0	0	0
6	0	-6	0
7	0	-17	0
8	0	-28	0
9	4	0	7
10	0	-4	7
11	-4	0	7
12	0	4	7
13	2	0	14
14	-2	0	14
15	3	-3	21
16	-3	-3	21
17	3	-3	25
18	-3	-3	25
19	6	-1	21
20	13	-1	21
21	13	-1	25
22	6	-1	25
23	6	4	21
24	13	4	21
25	13	4	25
26	6	4	25
27	4	16	18
28	-3	16	18
29	4	16	24
30	-3	16	24
31	-4	3	21
32	-7	3	21

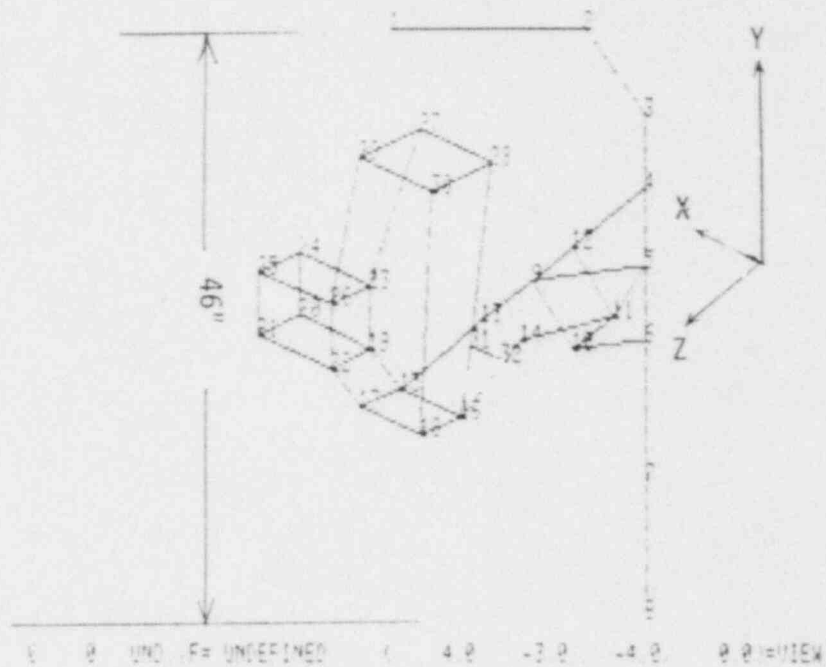

FIGURE 4.5.1

A WIRE FRAME MODEL OF THE 3 INCH MOTOR OPERATED VALVE

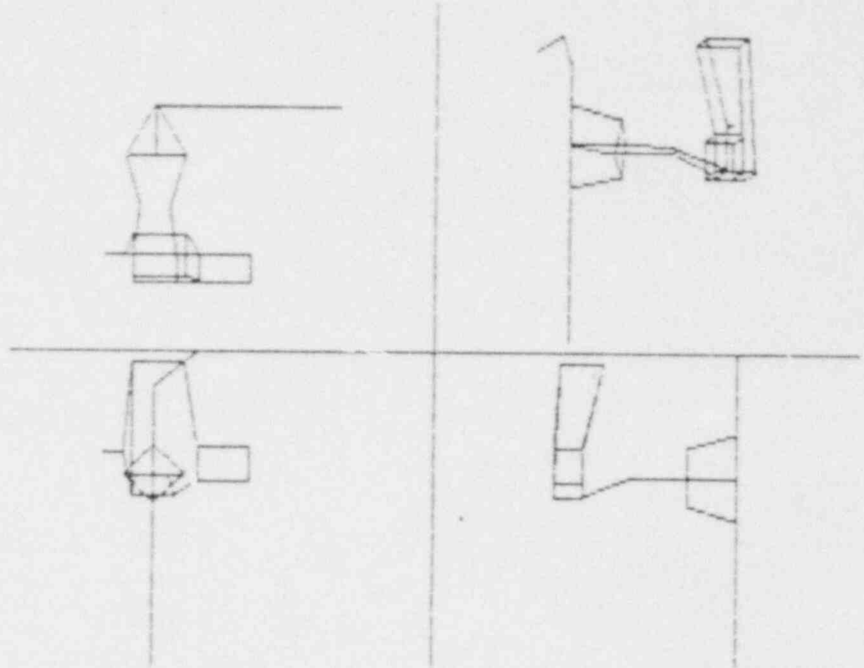

FIGURE 4.5.2

FOUR VIEWS OF THE 3 INCH MOTOR OPERATED VALVE

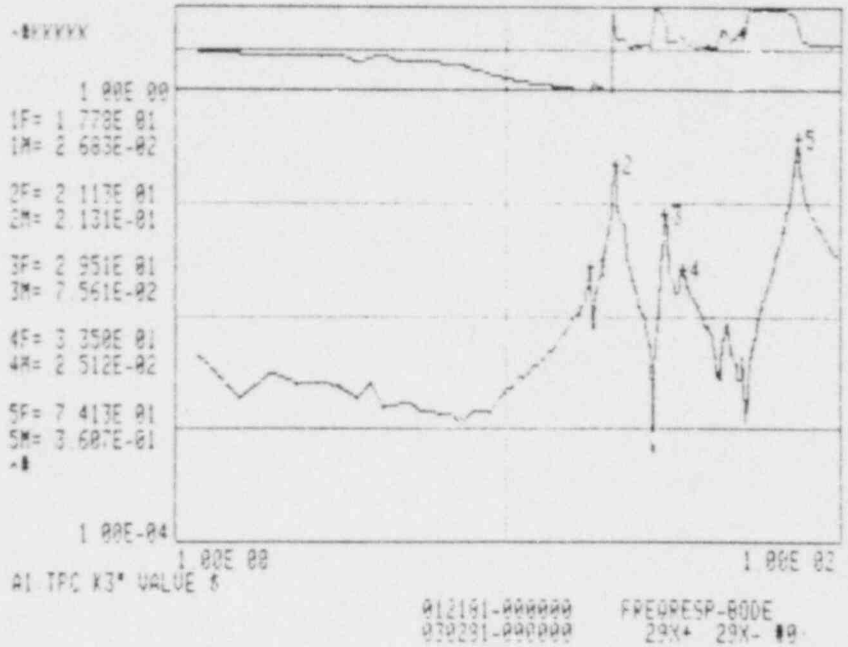

FIGURE 4.5.3

THE DRIVING POINT TRANSFER FUNCTION OF THE 3 INCH MOTOR OPERATED VALVE MEASURED IN THE X DIRECTION

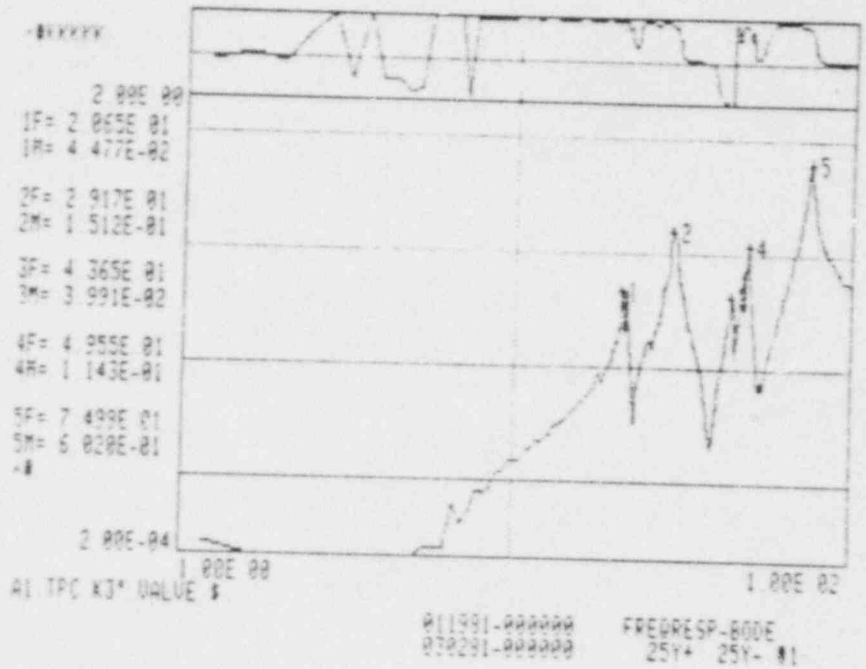

FIGURE 4.5.4

THE DRIVING POINT TRANSFER FUNCTION OF THE 3 INCH MOTOR OPERATED VALVE MEASURED IN THE Y DIRECTION

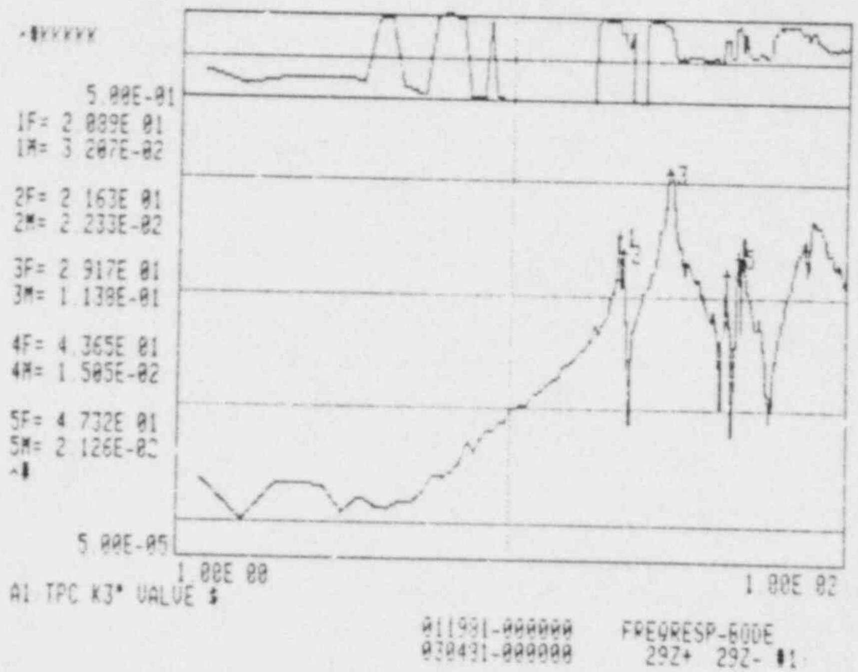

FIGURE 4.5.5A

THE DRIVING POINT TRANSFER FUNCTION OF THE 3 INCH MOTOR OPERATED VALVE MEASURED IN THE Z DIRECTION

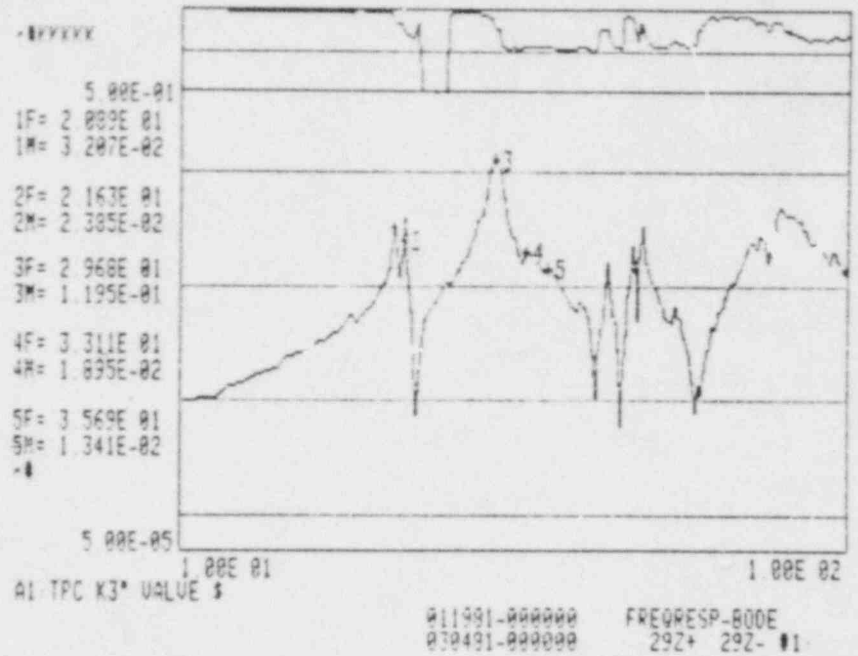

FIGURE 4.5.5B

AN EXPANDED VIEW OF THE DRIVING POINT TRANSFER FUNCTION
OF THE 3 INCH MOTOR OPERATED VALVE
MEASURED IN THE Z DIRECTION
DESIGNATING THE FIVE RESONANCES OF LOWEST FREQUENCY

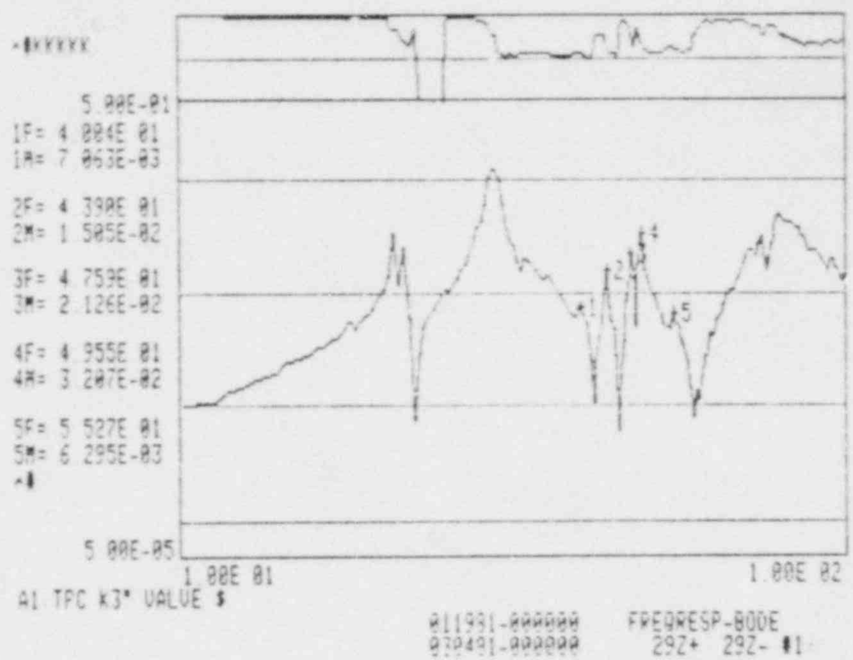

FIGURE 4.5.5C

AN EXPANDED VIEW OF THE DRIVING POINT TRANSFER FUNCTION OF THE 3 INCH MOTOR OPERATED VALVE MEASURED IN THE Z DIRECTION DESIGNATING THE FIVE RESONANCES BETWEEN 40 HZ AND 55 HZ

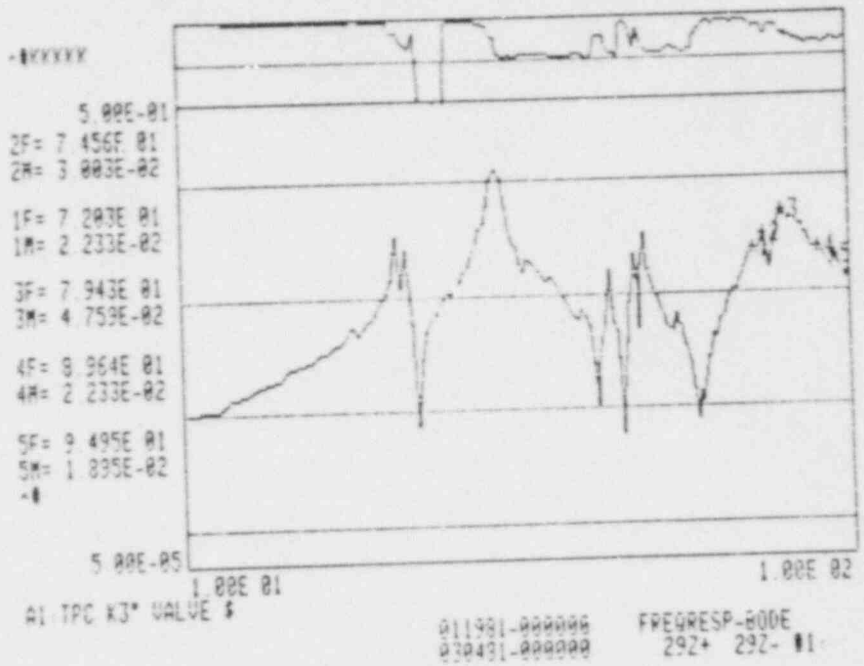

FIGURE 4.5.5D

AN EXPANDED VIEW OF THE DRIVING POINT TRANSFER FUNCTION
OF THE 3 INCH MOTOR OPERATED VALVE MEASURED IN THE Z DIRECTION
DESIGNATING THE FIVE RESONANCES OF HIGHEST FREQUENCY

TABLE 4.5.2

MODAL PROPERTIES MEASURED ON THE 3 INCH MOTOR OPERATED VALVE

Mode Shape #	Frequency (Hz)	Damping (% Critical)
	X DIRECTION	
1	18.2	1.1
2	21.4	1.0
3	30.1	1.3
4	33.4	9.7
5	74.6	1.9
	Y DIRECTION	
1	21.9	1.1
2	29.6	1.1
3	44.8	1.0
4	48.1	.9
5	49.5	.9
6	75.1	1.3
	Z DIRECTION	
1	20.6	4.1
9	29.6	.9
2	29.8	2.2
10	30.2	.4
3	44.1	.5
4	48.2	1.0
5	49.3	1.0
6	72.4	1.6
8	79.9	1.6
7	75.8	.7

4.5.4 Mode Shapes:

The mode shapes associated with the resonances listed in Table 4.5.2 for the X direction are shown in Figures 4.5.6 through 4.5.10. The mode shapes for the Y direction are shown in Figures 4.5.11 through 4.5.16, and the eight modes measured in the Z direction are shown in Figures 4.5.17 through 4.5.25.

4.5.5 Special Test Results:

The 3 inch valve was subjected to special tests consisting of impulses at greatly different force levels. The purpose of this special test was to measure the change in damping with excitation level and the tests were completed before we were advised of Taipower's desire to limit the response levels.

The results of the tests, listed in Table 4.5.3, show that generally the damping increases with the level of applied force. There are exceptions, however. The most frequent result is that damping increased a factor of 2 to 4 with a factor of 10 change in the force level.

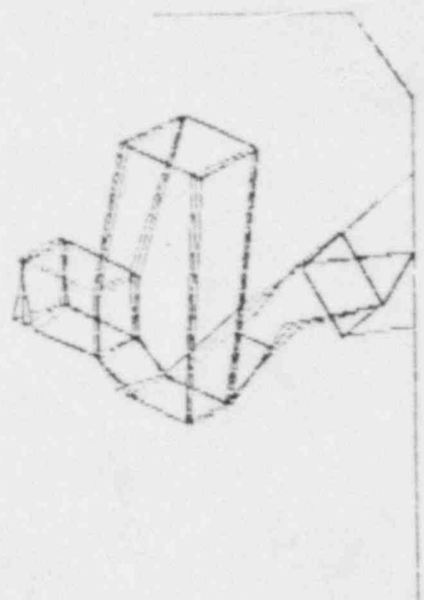

FIGURE 4.5.6

MODE SHAPE ASSOCIATED WITH THE 18.2 HZ RESONANCE OF THE 3 INCH MOTOR OPERATED VALVE
MEASURED IN THE X DIRECTION

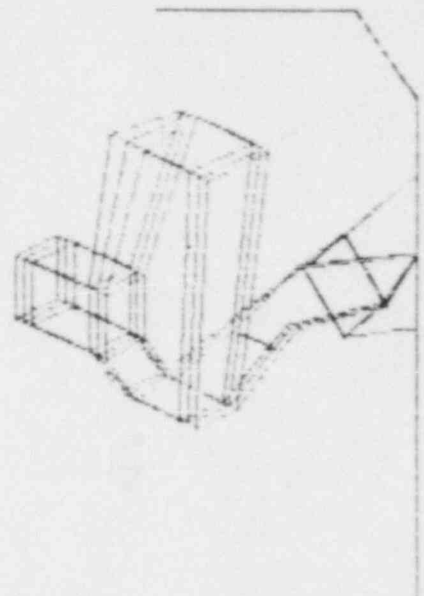

FIGURE 4.5.7

MODE SHAPE ASSOCIATED WITH THE 21.3 HZ RESONANCE OF THE 3 INCH MOTOR OPERATED VALVE
MEASURED IN THE X DIRECTION

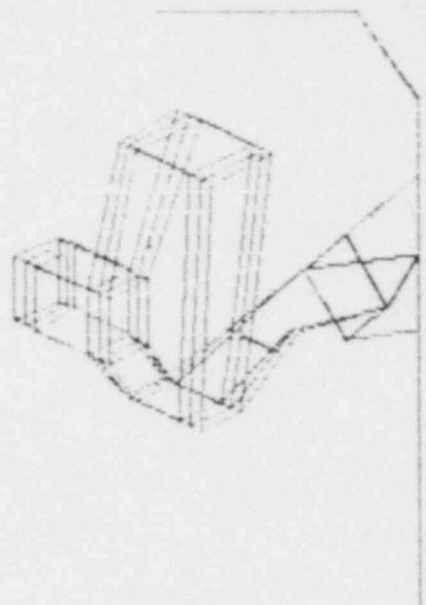

FIGURE 4.5.8

MODE SHAPE ASSOCIATED WITH THE 30.1 HZ RESONANCE OF THE 3 INCH MOTOR OPERATED VALVE MEASURED IN THE X DIRECTION

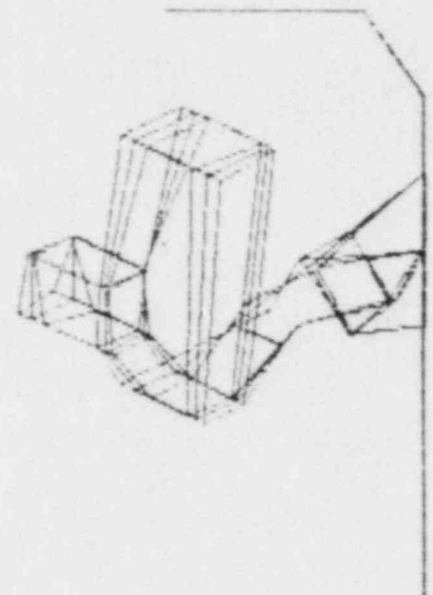

FIGURE 4.5.9

MODE SHAPE ASSOCIATED WITH THE 33.4 HZ RESONANCE OF THE 3 INCH MOTOR OPERATED VALVE
MEASURED IN THE X DIRECTION

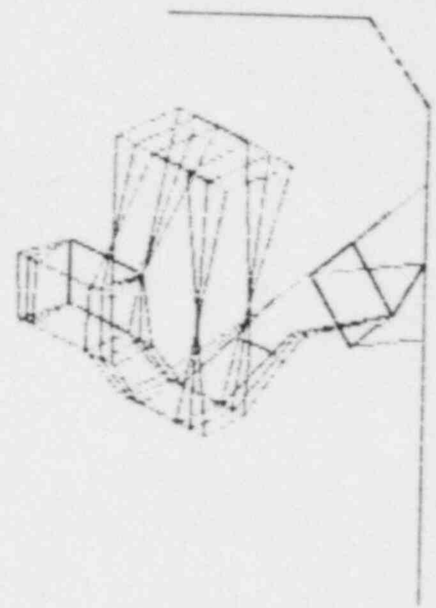

FIGURE 4.5.10

MODE SHAPE ASSOCIATED WITH THE 74.6 HZ RESONANCE OF THE 3 INCH MOTOR OPERATED VALVE
MEASURED IN THE X DIRECTION

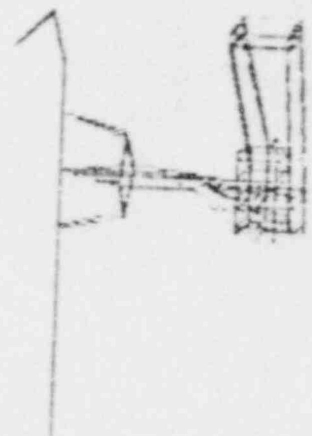

FIGURE 4.5.11

MODE SHAPE ASSOCIATED WITH THE 21.9 HZ RESONANCE OF THE 3 INCH MOTOR OPERATED VALVE
MEASURED IN THE Y DIRECTION

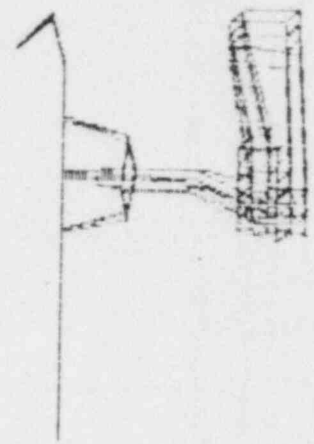

FIGURE 4.5.12

MODE SHAPE ASSOCIATED WITH THE 29.7 HZ RESONANCE OF THE 3 INCH MOTOR OPERATED VALVE
MEASURED IN THE Y DIRECTION

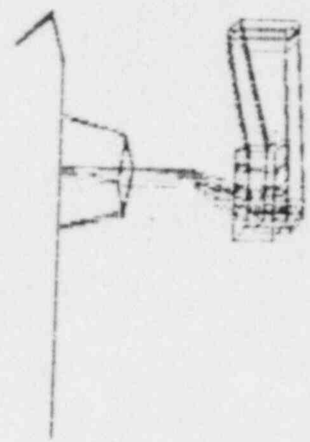

FIGURE 4.5.13

MODE SHAPE ASSOCIATED WITH THE 44.8 HZ RESONANCE OF THE 3 INCH MOTOR OPERATED VALVE
MEASURED IN THE Y DIRECTION

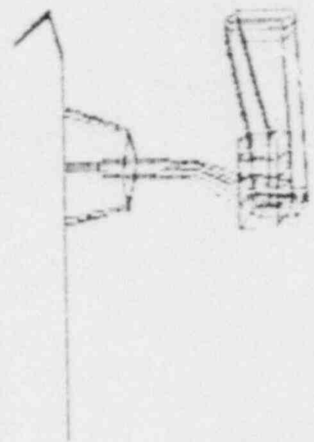

FIGURE 4.5.14

MODE SHAPE ASSOCIATED WITH THE 48.1 HZ RESONANCE OF THE 3 INCH MOTOR OPERATED VALVE
MEASURED IN THE Y DIRECTION

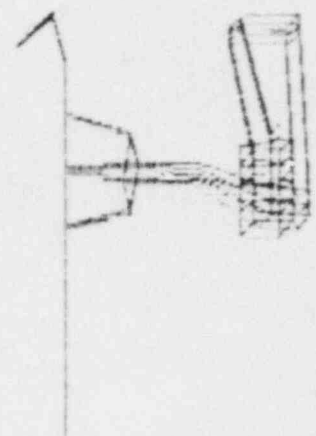

FIGURE 4.5.15

MODE SHAPE ASSOCIATED WITH THE 49.5 HZ RESONANCE OF THE 3 INCH MOTOR OPERATED VALVE
MEASURED IN THE Y DIRECTION

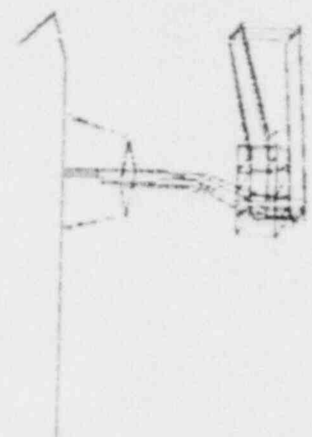

FIGURE 4.5.16

MODE SHAPE ASSOCIATED WITH THE 75.1 HZ RESONANCE OF THE 3 INCH MOTOR OPERATED VALVE
MEASURED IN THE Y DIRECTION

FIGURE 4.5.17

MODE SHAPE ASSOCIATED WITH THE 20.6 HZ RESONANCE OF THE 3 INCH MOTOR OPERATED VALVE
MEASURED IN THE Z DIRECTION

FIGURE 4.5.18

MODE SHAPE ASSOCIATED WITH THE 29.6 HZ RESONANCE OF THE 3 INCH MOTOR OPERATED VALVE MEASURED IN THE Z DIRECTION

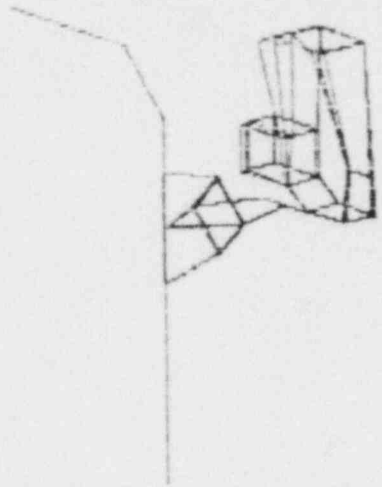

FIGURE 4.5.19

MODE SHAPE ASSOCIATED WITH THE 29.8 HZ RESONANCE OF THE 3 INCH MOTOR OPERATED VALVE
MEASURED IN THE Z DIRECTION

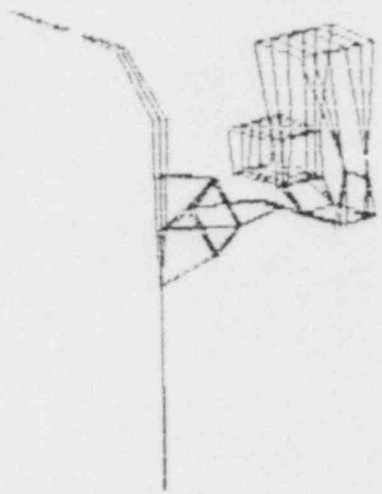

FIGURE 4.5.20

MODE SHAPE ASSOCIATED WITH THE 30.2 HZ RESONANCE OF THE 3 INCH MOTOR OPERATED VALVE
MEASURED IN THE Z DIRECTION

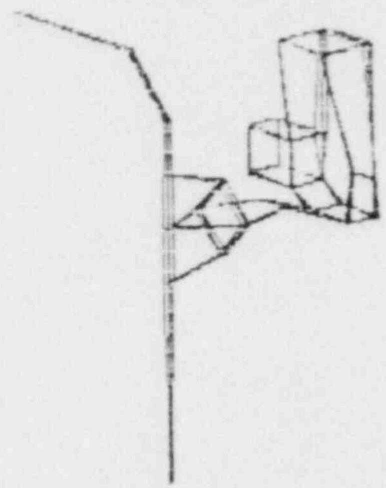

FIGURE 4.5.21

MODE SHAPE ASSOCIATED WITH THE 44.1 HZ RESONANCE OF THE 3 INCH MOTOR OPERATED VALVE MEASURED IN THE Z DIRECTION

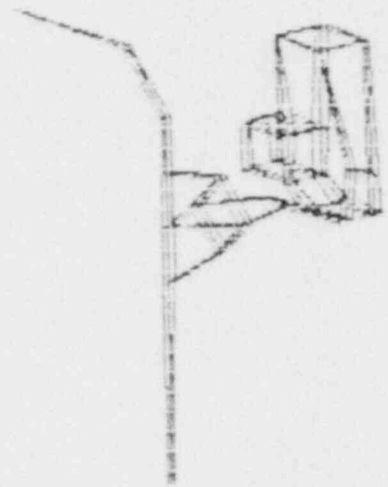

FIGURE 4.5.22

MODE SHAPE ASSOCIATED WITH THE 48.2 HZ RESONANCE OF THE 3 INCH MOTOR OPERATED VALVE
MEASURED IN THE Z DIRECTION

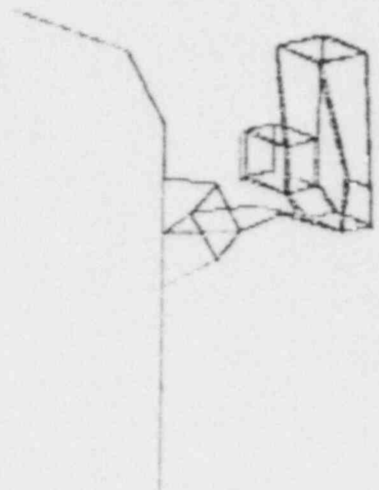

FIGURE 4.5.23

MODE SHAPE ASSOCIATED WITH THE 49.3 HZ RESONANCE OF THE 3 INCH MOTOR OPERATED VALVE
MEASURED IN THE Z DIRECTION

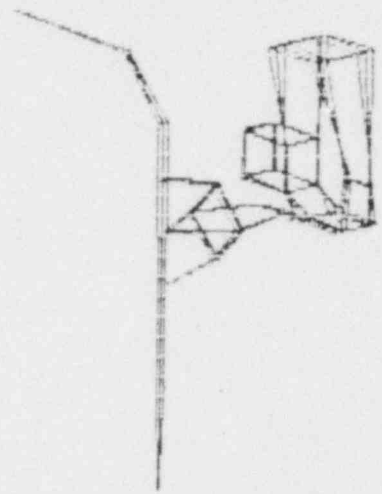

FIGURE 4.5.24

MODE SHAPE ASSOCIATED WITH THE 72.4 HZ RESONANCE OF THE 3 INCH MOTOR OPERATED VALVE
MEASURED IN THE Z DIRECTION

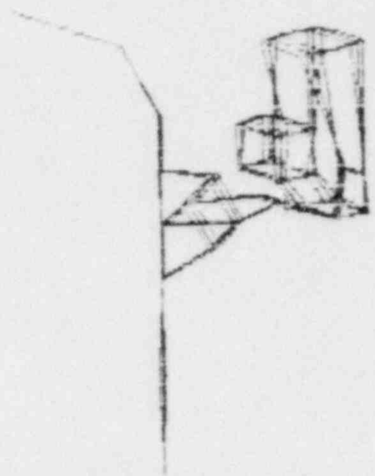

FIGURE 4.5.25

MODE SHAPE ASSOCIATED WITH THE 75.8 HZ RESONANCE OF THE 3 INCH MOTOR OPERATED VALVE
MEASURED IN THE Z DIRECTION

TABLE 4.5.3

SPECIAL TEST RESULTS
3 INCH MOTOR OPERATED VALVE

Hard (800-1000 lbf)		Soft (<100 lbf)	
Frequency (Hz)	Damping (% Critical)	Frequency (Hz)	Damping (% Critical)
	X DIRECTION		
18.56	1.52	18.10	0.2
21.11	[illegible].89	21.66	2.11
29.87	1.22	29.59	0.60
33.34	2.31	32.94	1.08
73.55	0.02	73.56	0.02
	Y DIRECTION		
21.18	2.20	21.07	0.60
21.73	0.66	21.82	0.42
29.88	1.13	28.59	3.55
44.99	0.69	45.19	0.63
47.17	2.21	47.31	1.22
49.55	0.98	48.83	0.58
73.98	1.17	74.64	0.13
	Z DIRECTION		
21.28	1.38	20.83	9.66
21.54	1.06	21.11	2.02
29.70	1.36	29.87	0.43
44.73	1.16	43.88	0.80
47.95	0.83	47.75	0.10
49.70	1.07	49.49	0.51
71.72	1.04	72.20	0.41
75.25	2.68	74.53	0.53
80.88	0.79	81.09	1.58

4.5.6 Conclusions:

The valve itself exhibits very few resonances. The greatest number of resonances experienced by the valve are associated with the pipe on which it is mounted. The values of damping are somewhat low for structures of this type and reflect the relatively low excitation levels applied.

5.0 CONCLUSIONS

The values of resonant frequency, dampings and modal coefficients are consistent with TRANSITEK experience on similar equipment. Many resonances were detected in the 1 to 100 Hz frequency range. While these resonances in and of themselves do not pose clear or potential hazards, they indicate that additional analysis is required to accurately assess the likelihood of failure in an event which produces a combination of seismic and high frequency loads.

The cooperation of station personnel (Taipower's C.C. Cheng, H.C. Lee and Hainan Hsiah) and EG&G personnel (Ira Hall and Bob Guenzler) enabled us to perform this program to the general extent of the original scope. The response levels to which the gram was limited ruled out the hoped-for measurement of variation in damping with response amplitude and limited severely the quality of data from the Motor Control Center. The data are, however, usable as the values of damping are in the range of expected and are characteristic values.

6.0 REFERENCES:

(1) "Modal Analysis Users Manual - The MPLUS Computer Program" SDRC, Cincinnati, Ohio, April 17, 1978 with revisions dating to March, 1980.

(2) Klosterman, A.L. "On the Experimental Determination and Use of Modal Representation of Dynamic Characteristics". A PhD Dissertation for the Dept. of Mech. Eng.; University of Cincinnati, Ohio 1971.

(3) W. G. Halvorsen and D.L. Brown, "Impulse Technique for Structural Response Testing" Sound and Vibration Magazine, November, 1977, pp. 8-21.

(4) M. Richardson and K. Ramsey, "Dynamic Testing of Mechanical Systems Using Impulse Testing Techniques" Hewlett-Packard Application Note 140-3.

(5) Baumeister & Marks, Eds. "Standard Handbook for Mechanical Engineers" 7th Ed., McGraw Hill, pp. 5-91.

(6) C.C. Kennedy and C.D.P. Pancu "Use of Vectors in Vibration Measurement and Analysis" Journal of Aeronautical Sciences, Vol. 14, No. 11, 19 and 7, pp. 603-625.

(7) W.J. Duncan, "Elementary Matrices" MacMillan Company, New York, 1946.

(8) "Modal Parameters of Mechanical Structures"
Van Loon, P.
PhD. Dissertation, Catholic University of Leuven, Leuven, Belgium 1974, 183 pp.

General References on Modal Analysis

"A Critical Introduction to Some Industrial Resonance Testing Techniques"
Pendered, J.W.; Bishop, R. E. D.
Journal of Mechanical Engineering Science, Vo. 5, No. 4 1963.
pp. 345-367.

"The Determination of Modal Shapes in Resonance Testing"
Pendered, J.W.; Biship, R. E. D.
Journal of Mechanical Engineering Science, Vol. 5, No. 4 1963,
pp. 379-385.

"An Investigation into the Theory of Resonance Testing:
Bishop, R.E.D.; Gladwell, G.M.L.
Philosophical Transactions, Royal Society of London, Series A,
Vol. 255, A 1055 1963, pp. 241-280.

"Modal Analysis Using Digital Test Systems"
Richardson, M.
Seminar on Understanding Digital Control and Analysis in Vibration Test Systems (Part 2) 1975, pp. 43-64.

General References on Modal Analysis (continued)

"Identification of the Modal Properties of an Elastic Structure from Measured Transfer Function Data"
Richardson, M.; Potter, R.
Instrument Society of America, ISA ASI 74250 1974, pp. 239-246

"Viscous vs. Structural Damping in Modal Analysis"
Richardson, M.; Potter, R.
46th Shock and Vibration Symposium 1975, 8 pp.

"Identifying Modes of Large Structures from Multiple Input and Response Measurements"
Richardson, M.; Kniskern, J.
SAE Paper No. 760875 1976, 12 pp

"Effective Measurements for Structural Dynamics Testing: Part I"
Ramsey, K.
Sound and Vibration, November 1975

"Effective Measurements for Structural Dynamics Testing: Part II"
Ramsey, K.
Sound and Vibraton, April 1976.

"Survey of Excitation Techniques Applicable to the Testing of Automotive Structures"
Brown, D. L.; Carbon, G.; Ramsey, K.
SAE Paper No. 770029 1977, 16 pp.

"Parameter Estimation Techniques for Modal Analysis"
Brown, D.L., et al
SAE Paper 790221 - Preliminary

General References on Digital Signal Processing

R. Otnes and L. Enochson "Applied Times Series Analysis Vol. 1." Wiley & Sons, 1978.

R. Otnes and L. Enochson "Digital Time Series Analysis." Wiley & Sons, 1972.

J. S. Bendat and A. G. Piersol, "Random Data", 1971.

APPENDIX B

FIGURES OF COMPONENTS TESTED

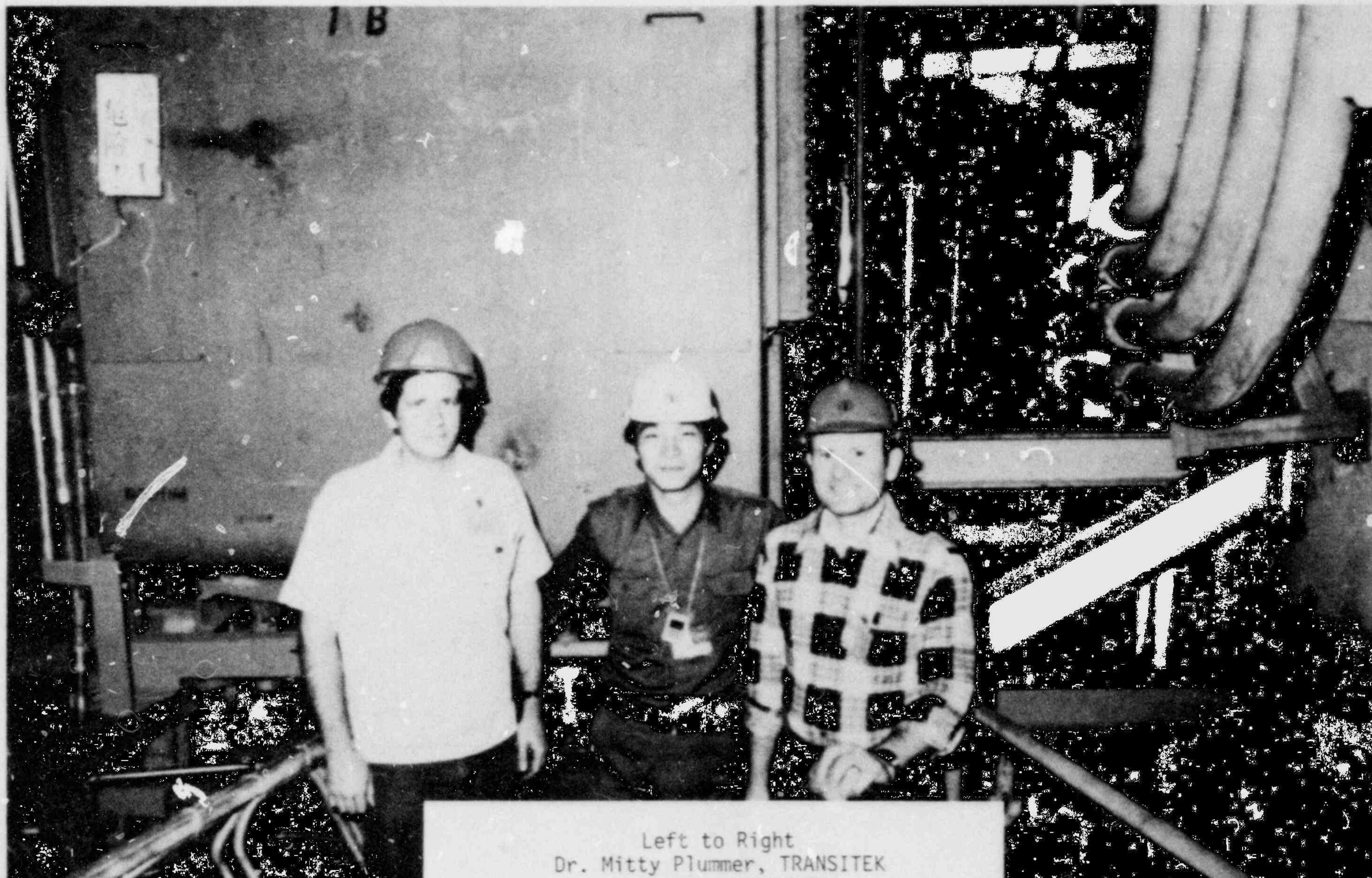

Left to Right
Dr. Mitty Plummer, TRANSITEK
H. C. Lee, TAIPOWER
Ira K. Hall, EG&G Idaho

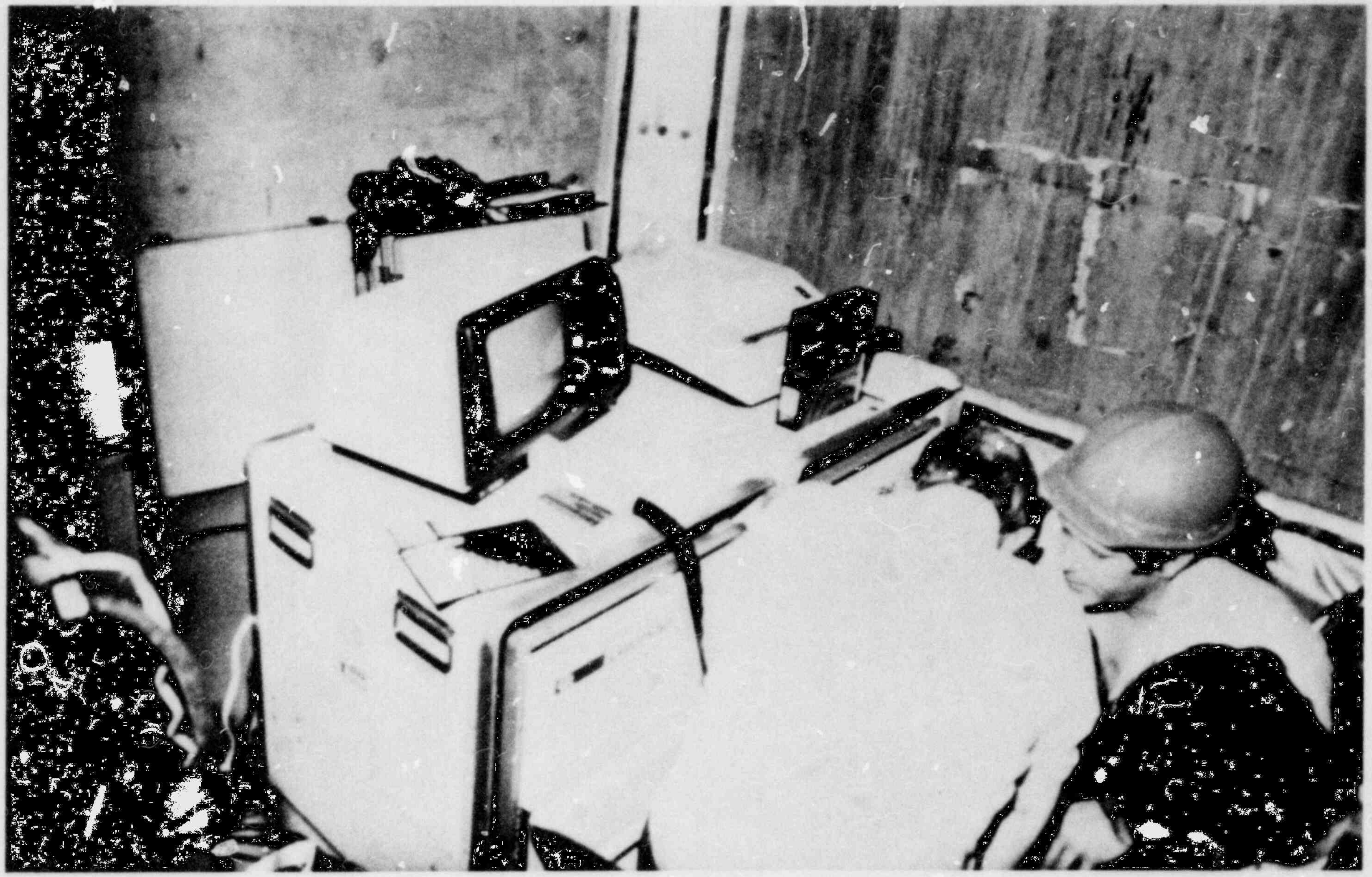

TRANSITEK Impedance Analyzer at Kuosheng

Kuosheng Impedance Test Analyzer Control

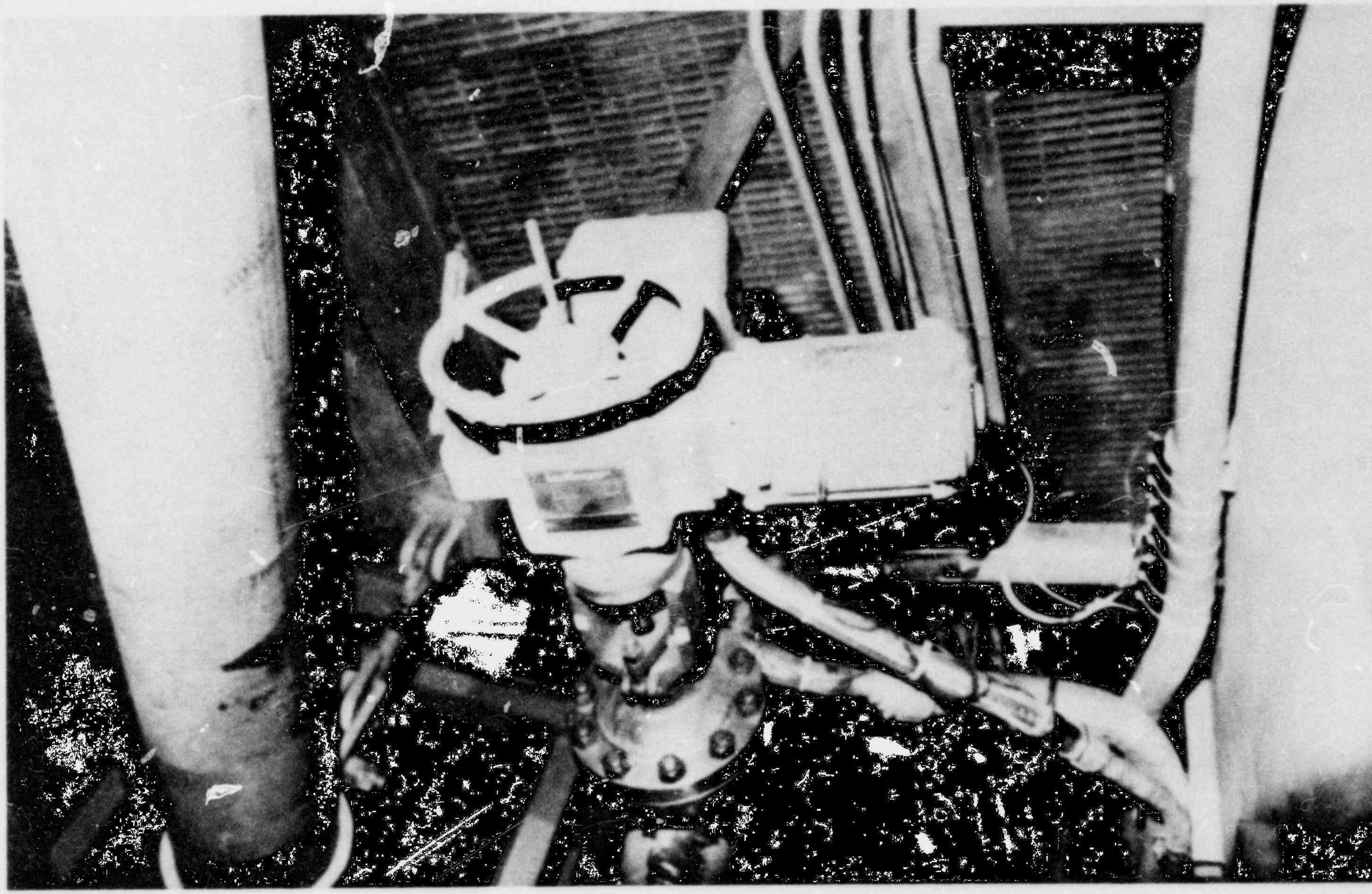

Kuosheng 3" Motor Operated Valve

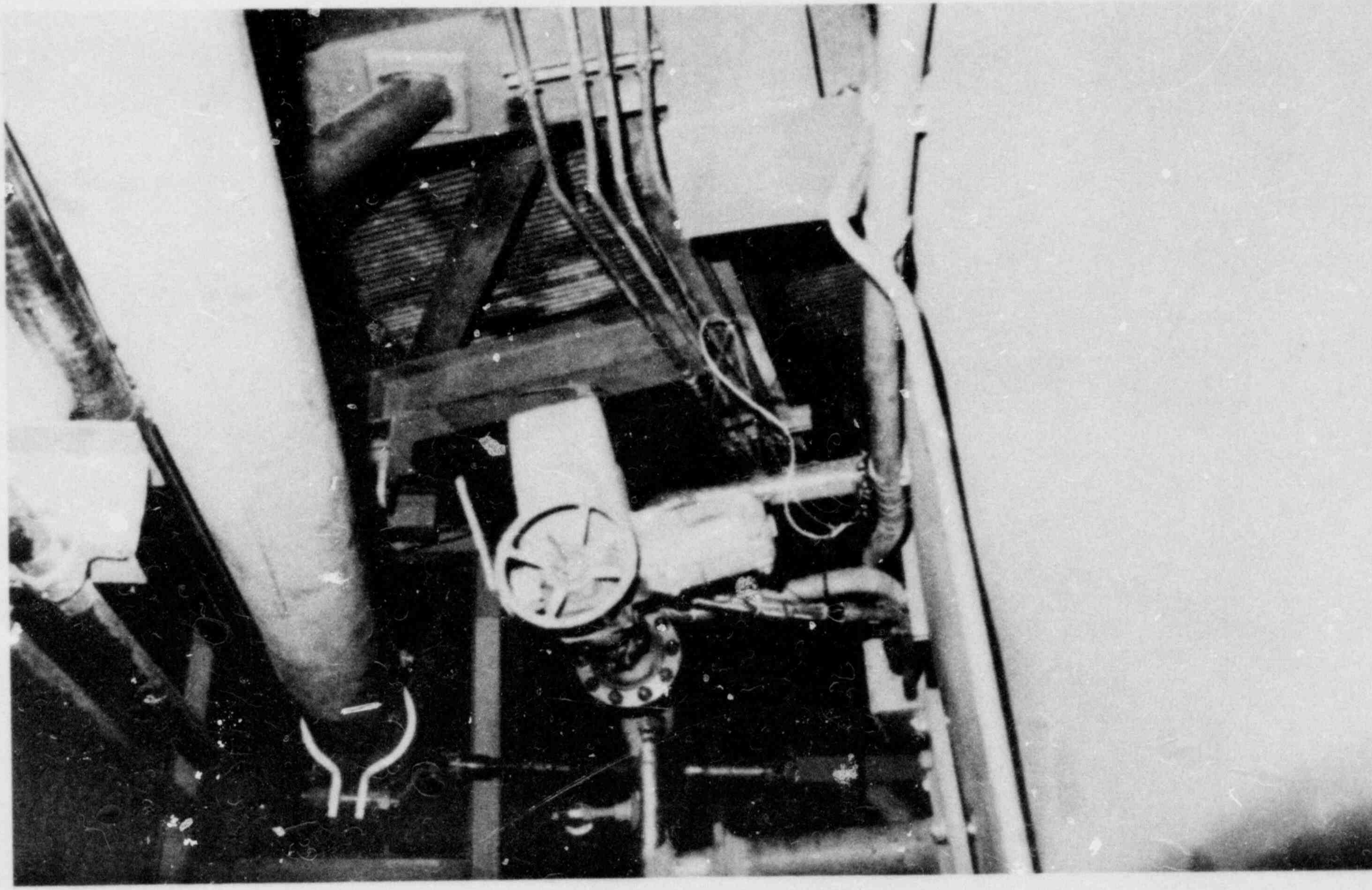

Kuosheng 3" Motor Operated Valve

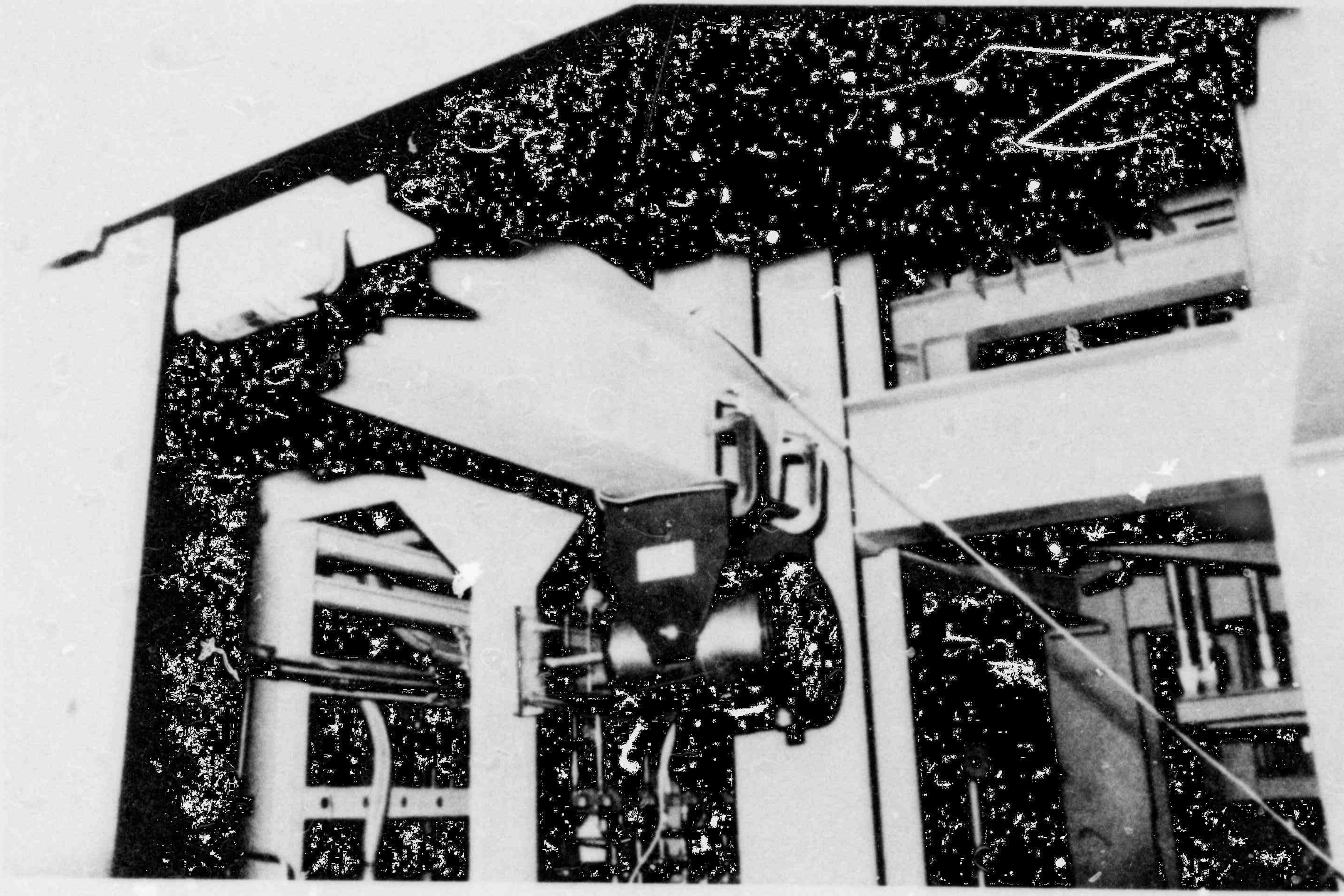

Horizontal Vibration of Kuosheng
Jet Pump Instrument Panel

Horizontal Vibration of Kuosheng
Jet Pump Instrument Panel

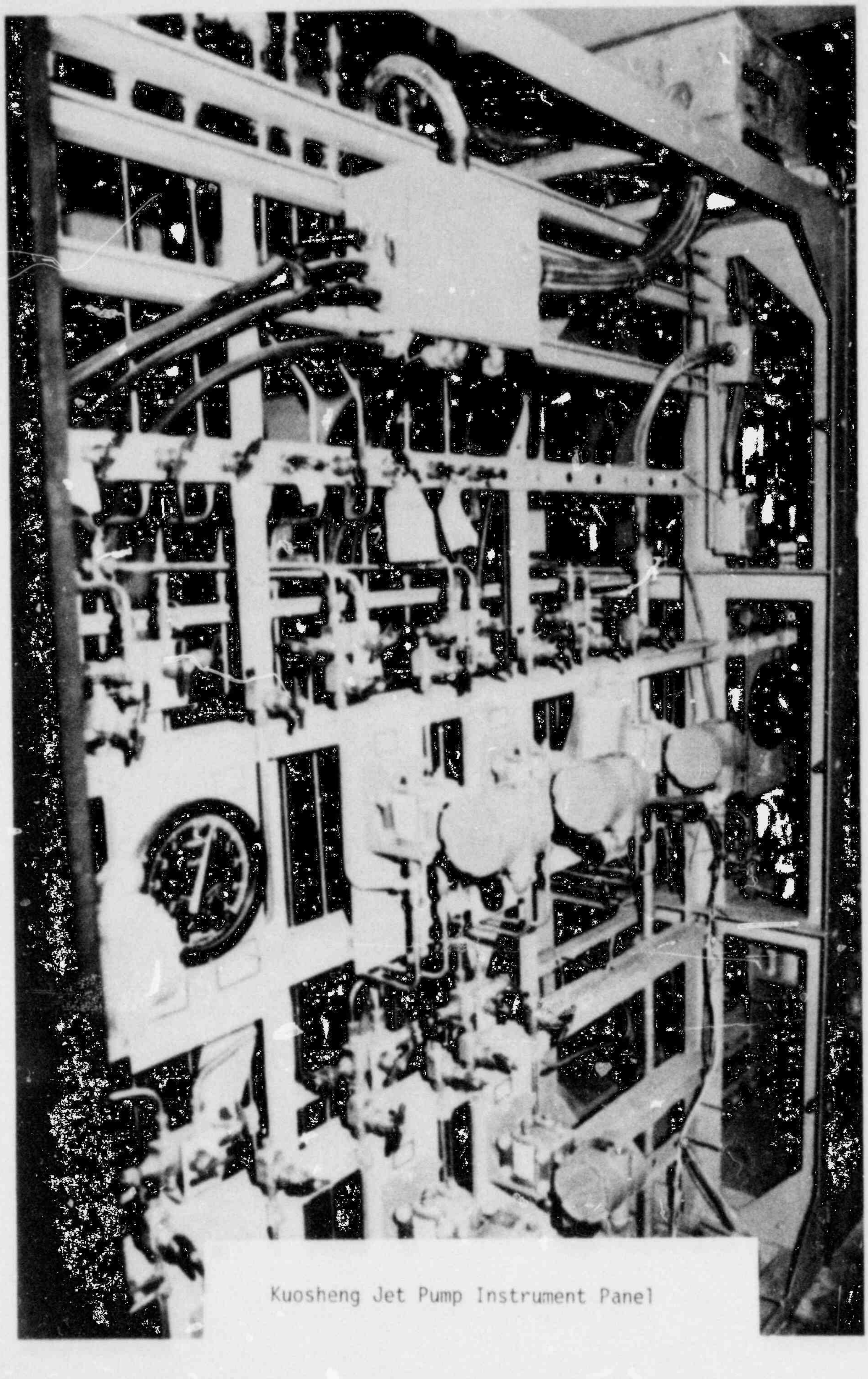

Kuosheng Jet Pump Instrument Panel

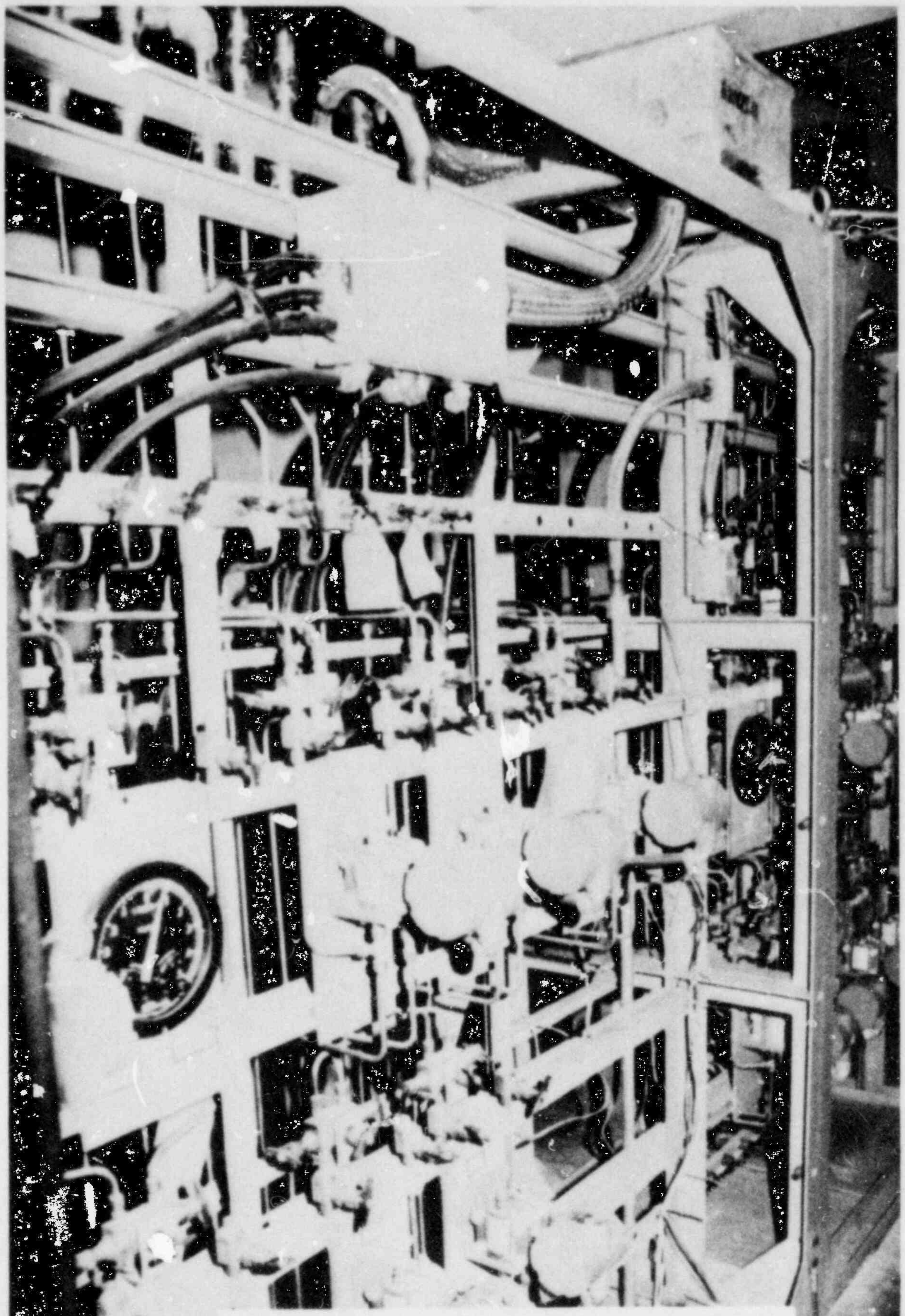
Kuosheng Jet Pump Instrument Panel

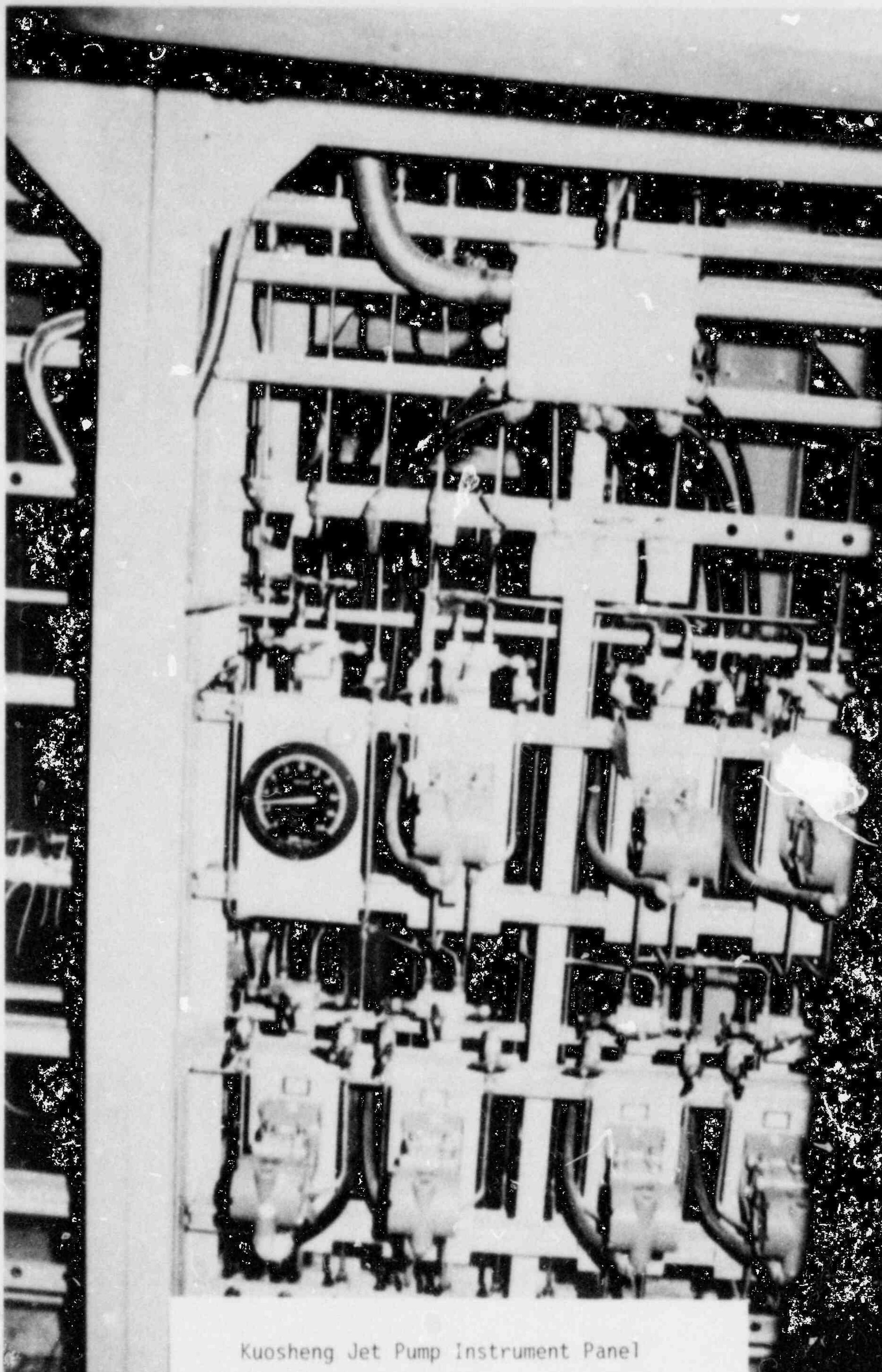

Kuosheng Jet Pump Instrument Panel

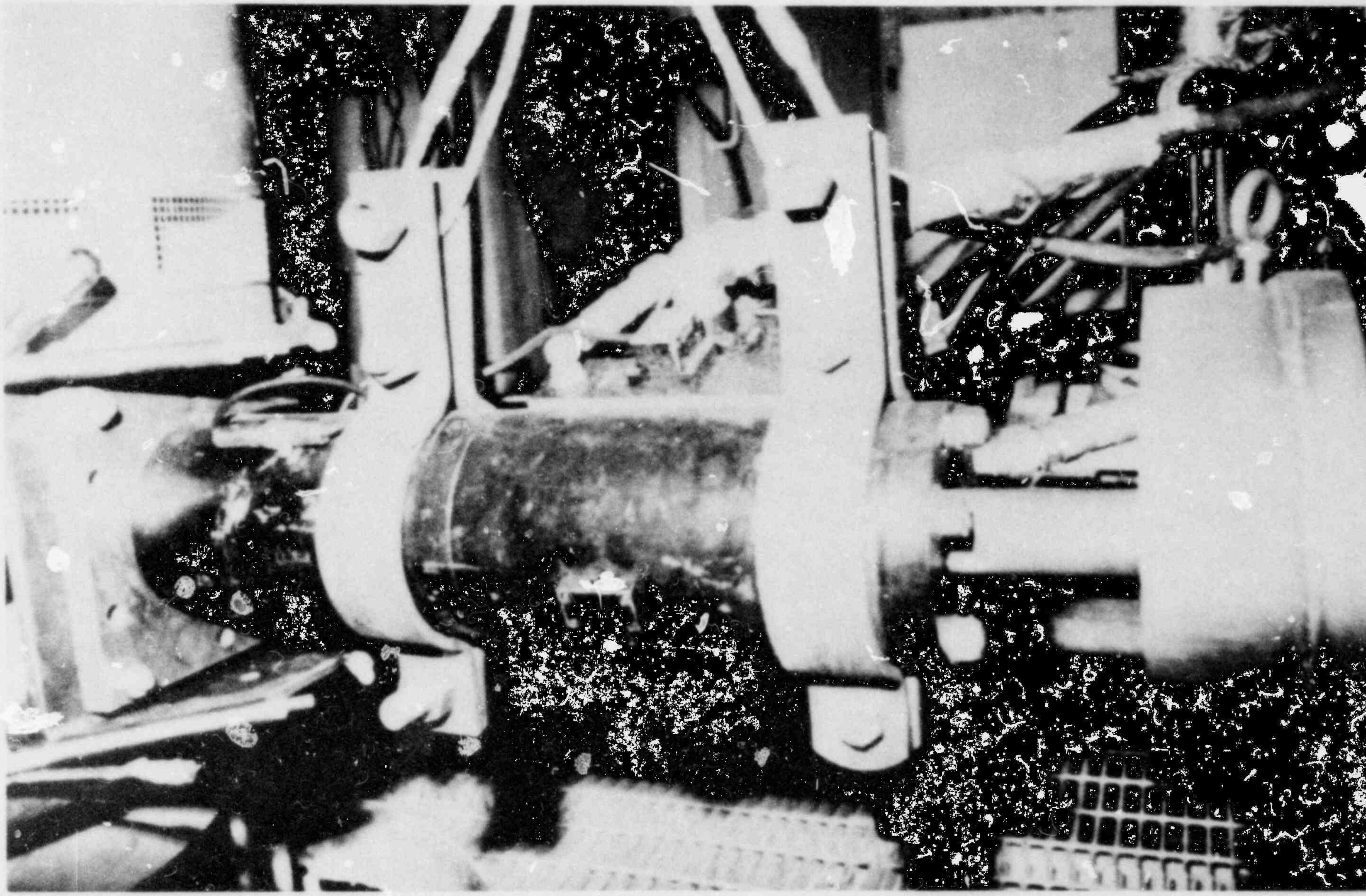

Hydraulic Shaker Installed On
Kuosheng RHR Pump (Horizontal)

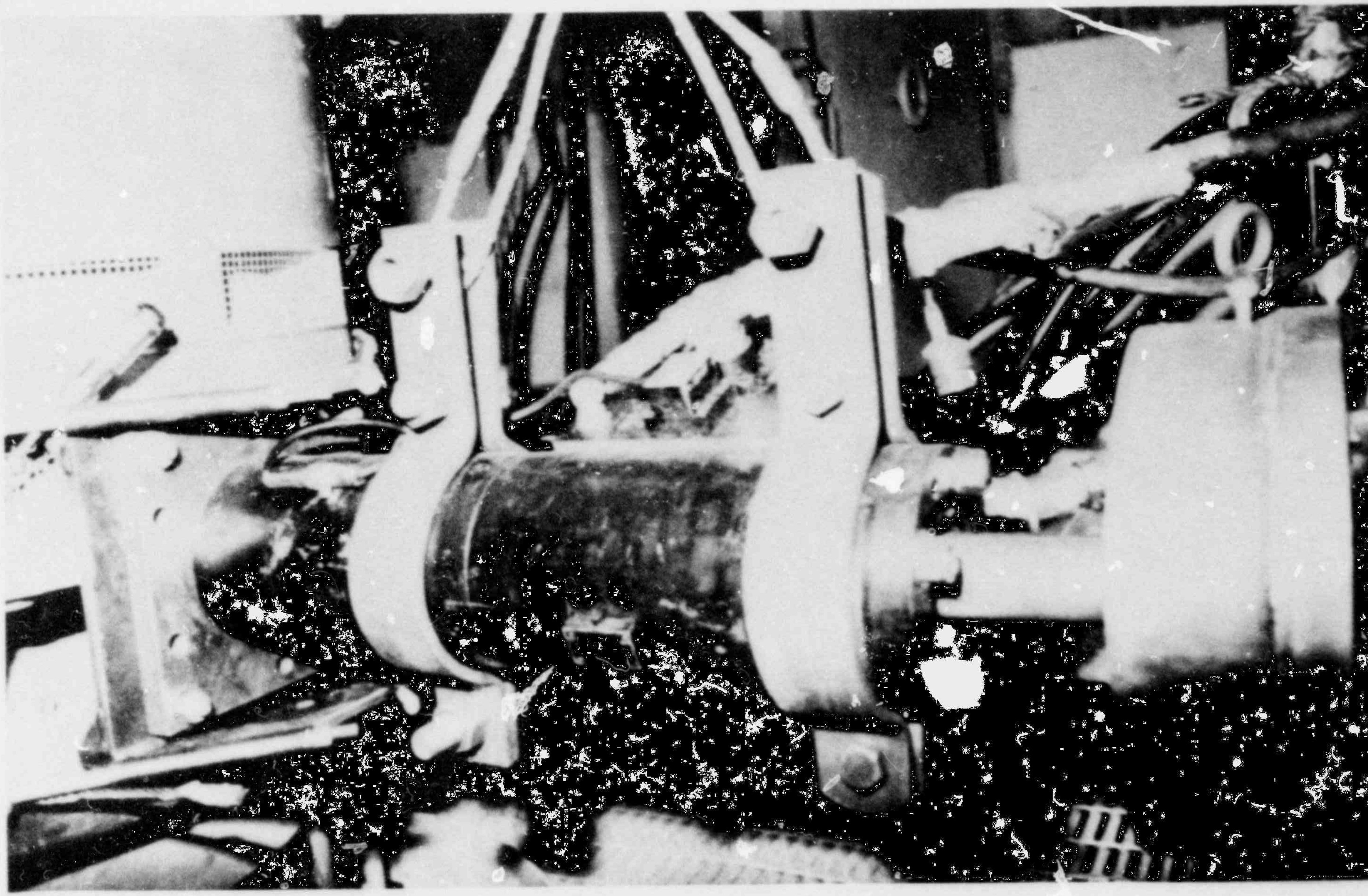

Hydraulic Shaker Installed Horizontally
On Kuosheng RHR Pump

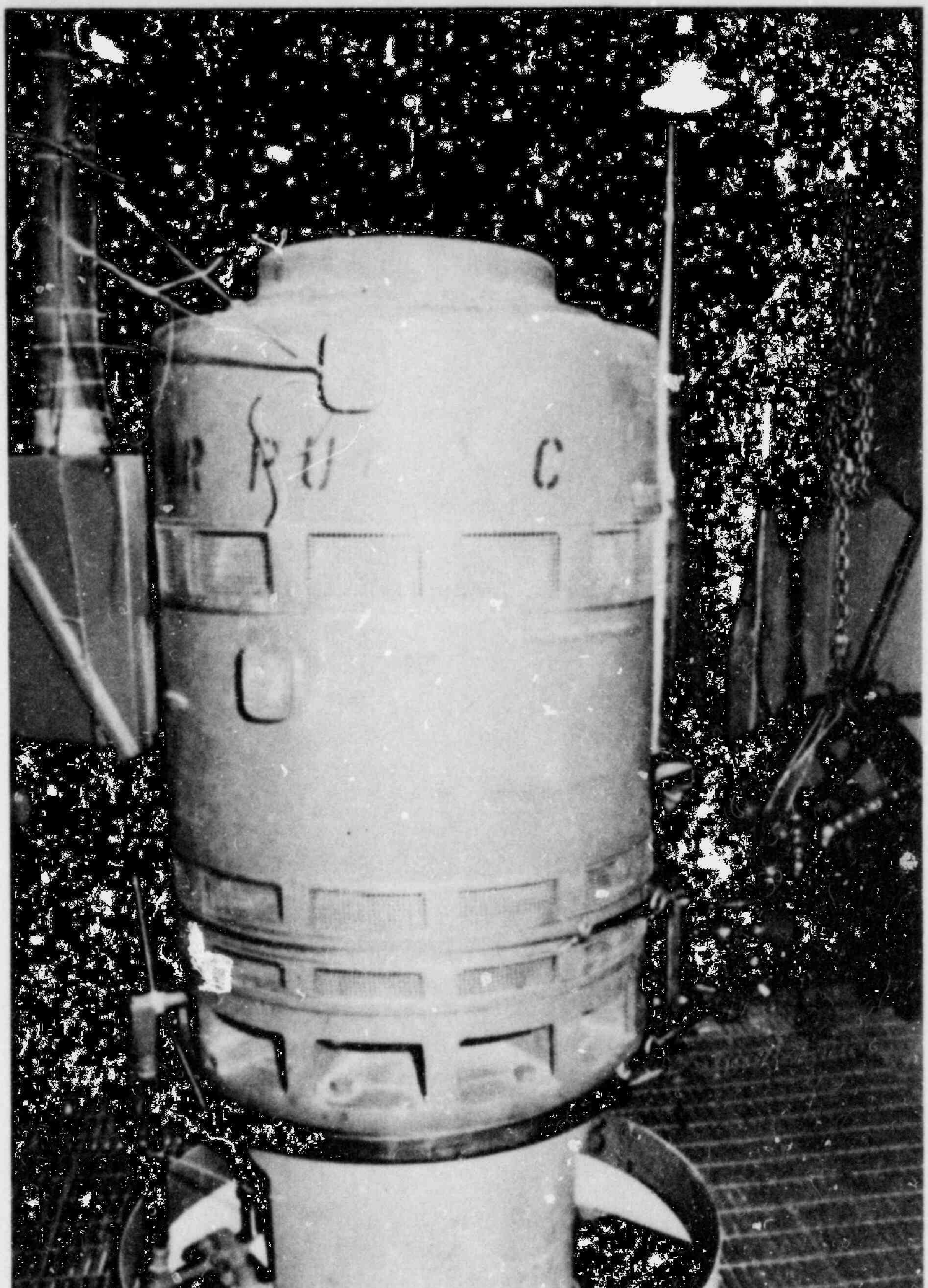

Horizontal Vibration of
Kuosheng RHR Pump

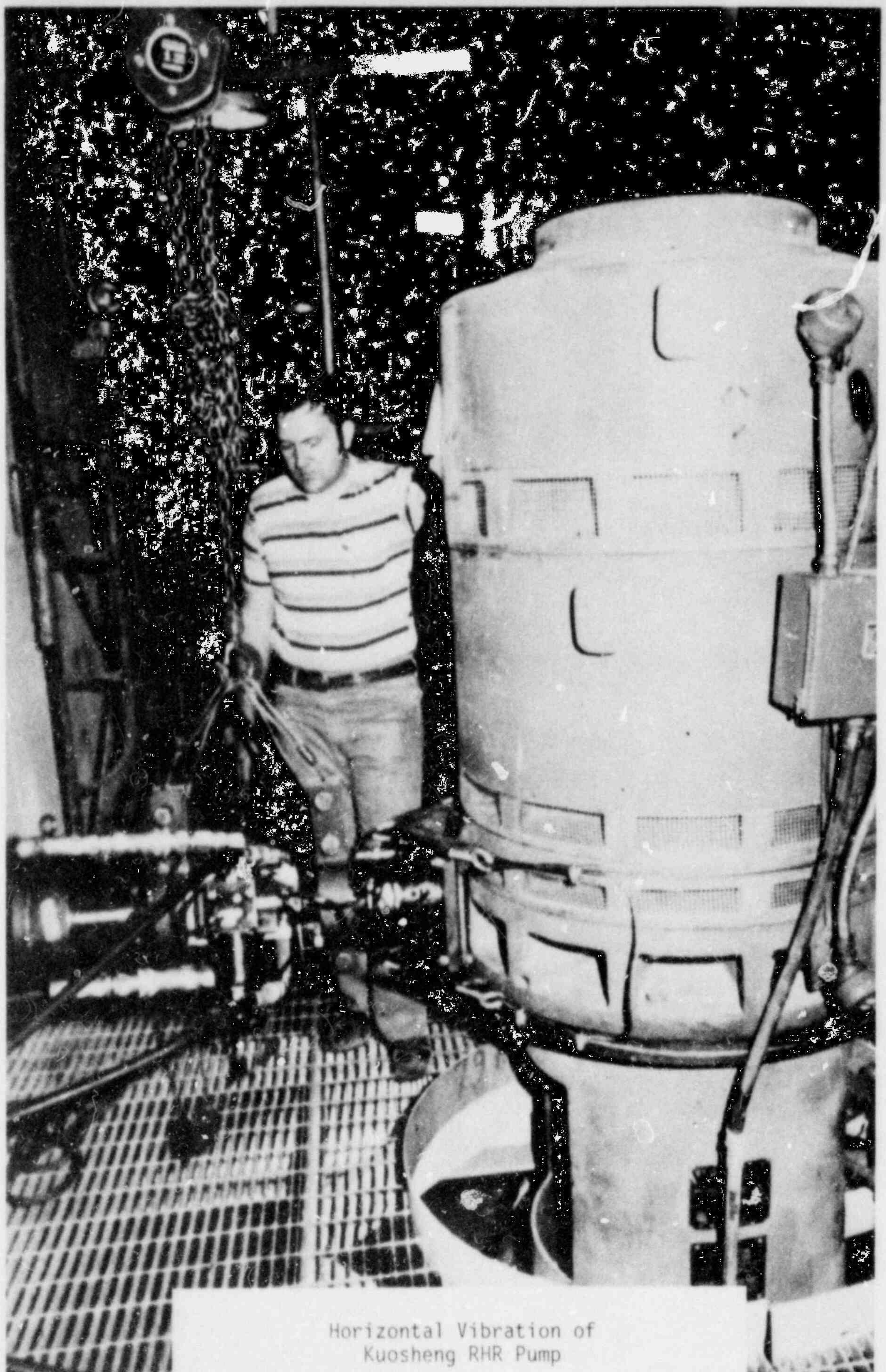

Horizontal Vibration of
Kuosheng RHR Pump

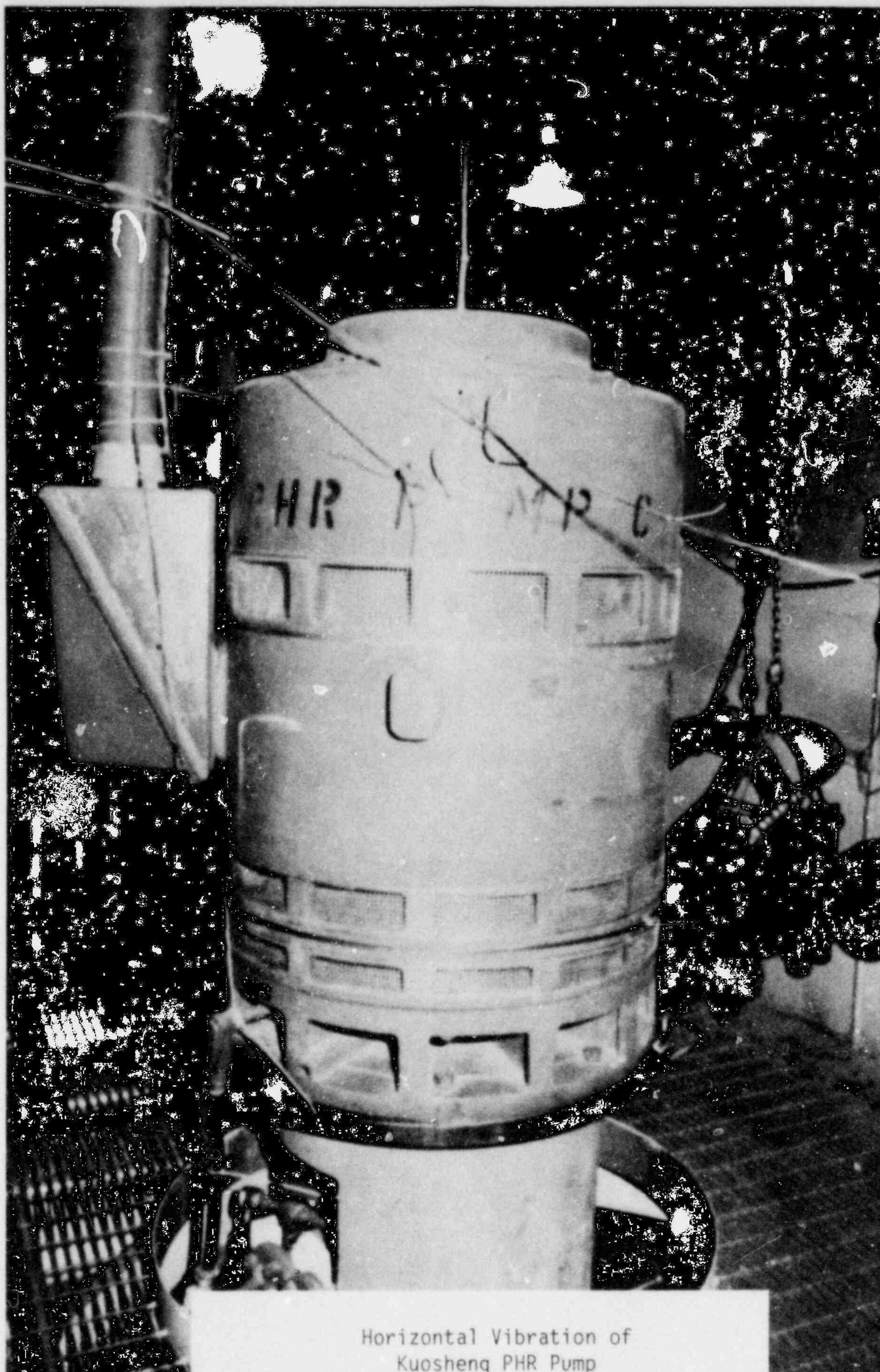

Horizontal Vibration of
Kuosheng PHR Pump

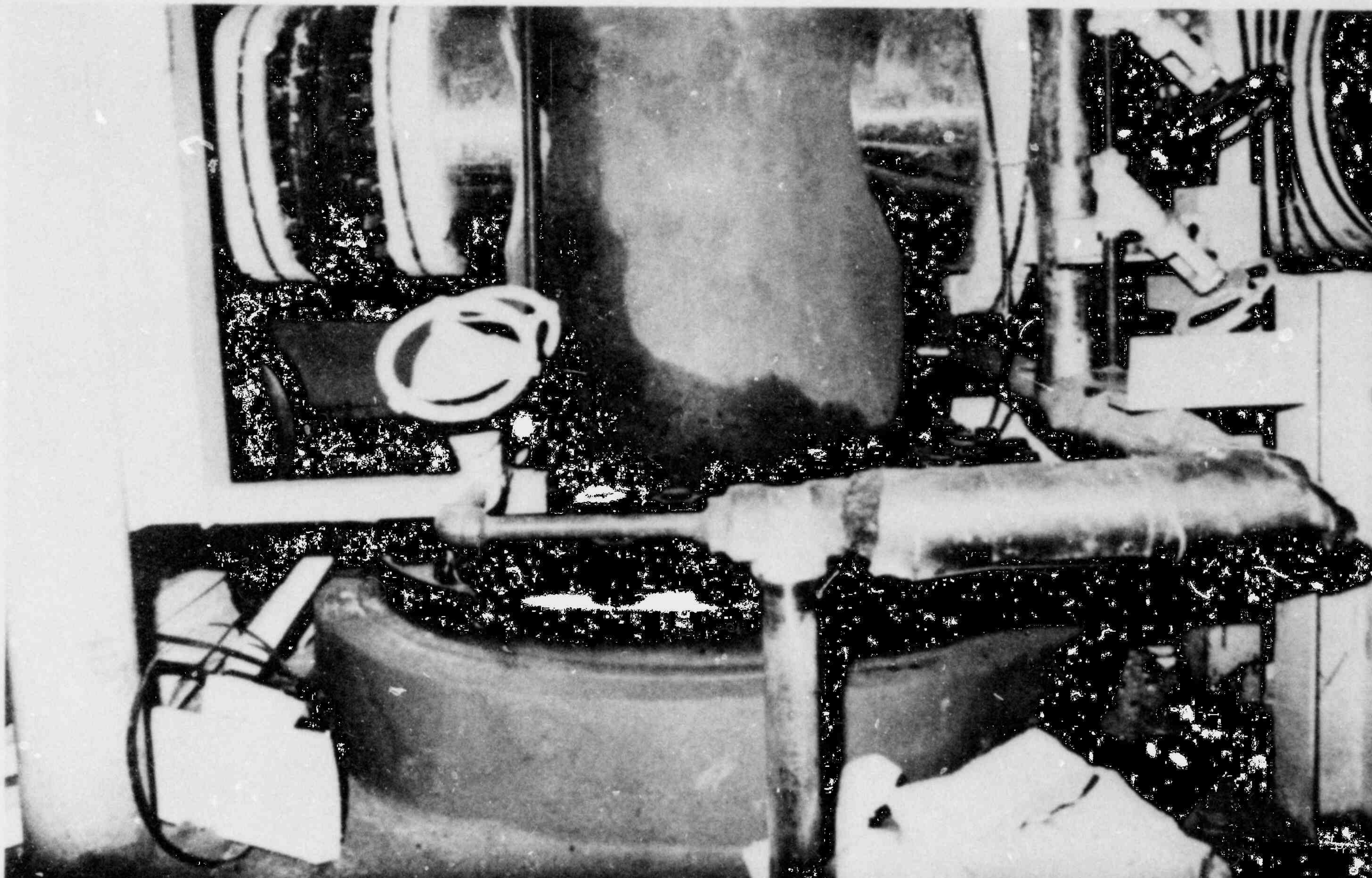

Kuosheng RHR Pump Base

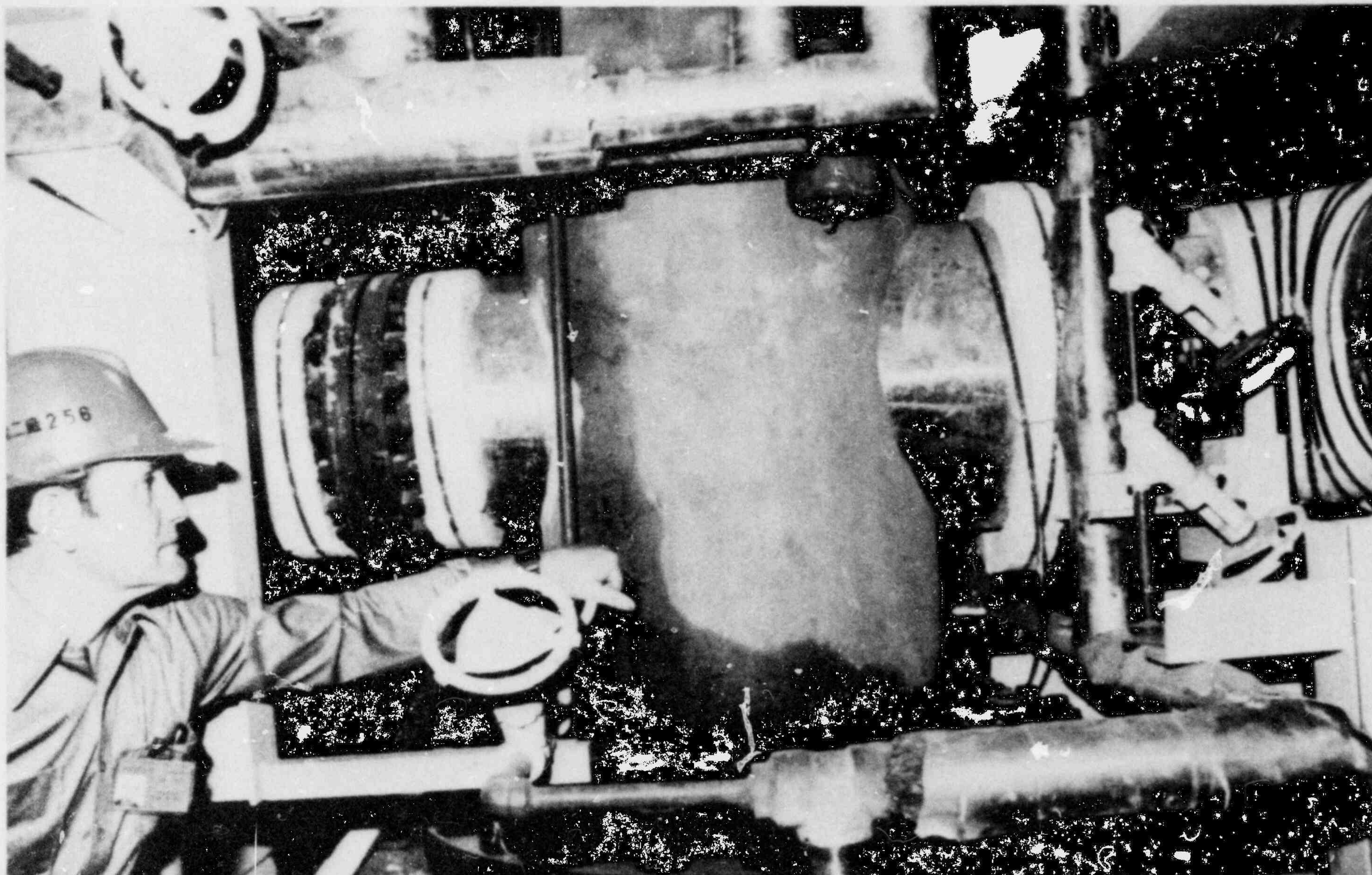

Kuosheng RHR Pump Base

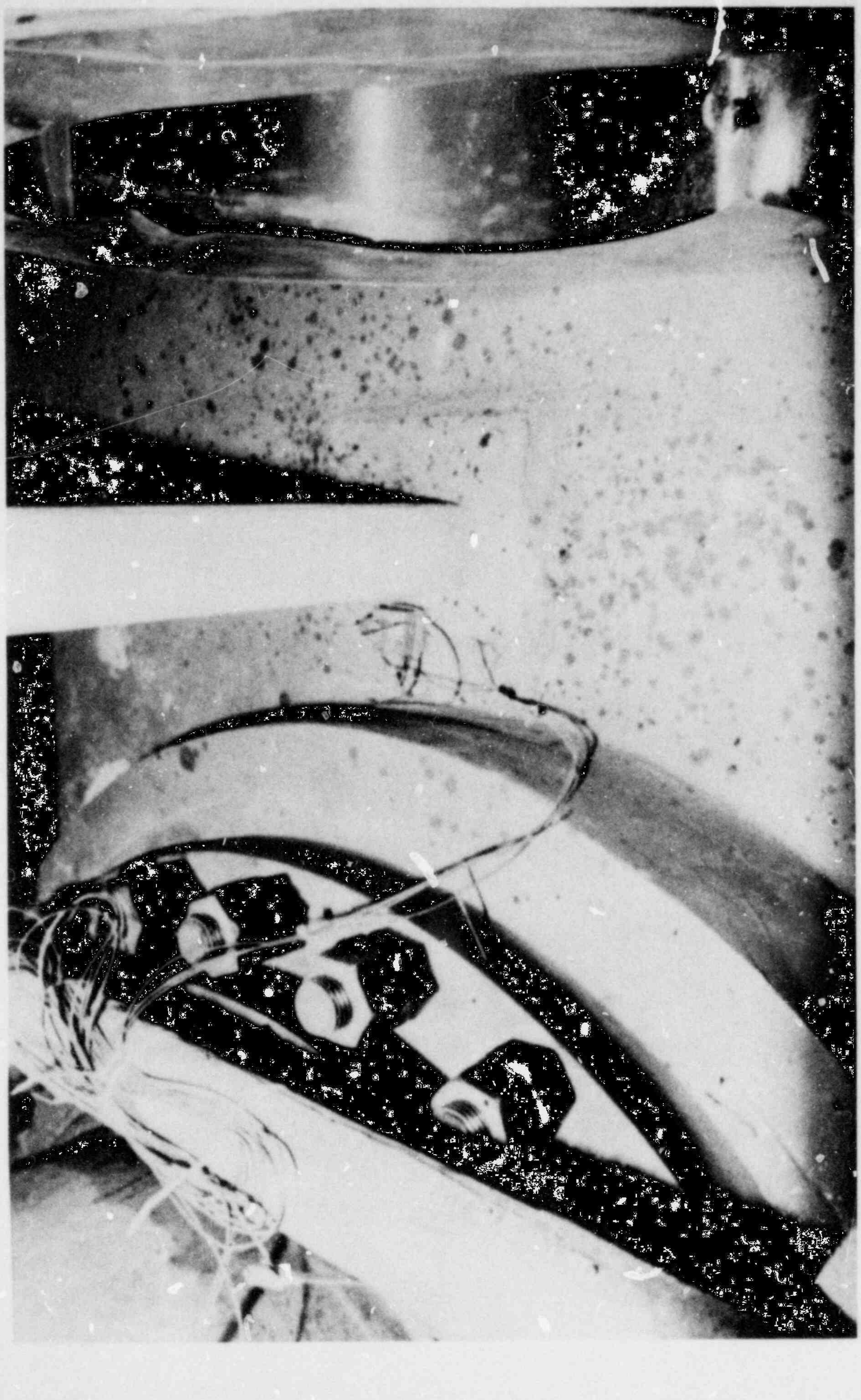

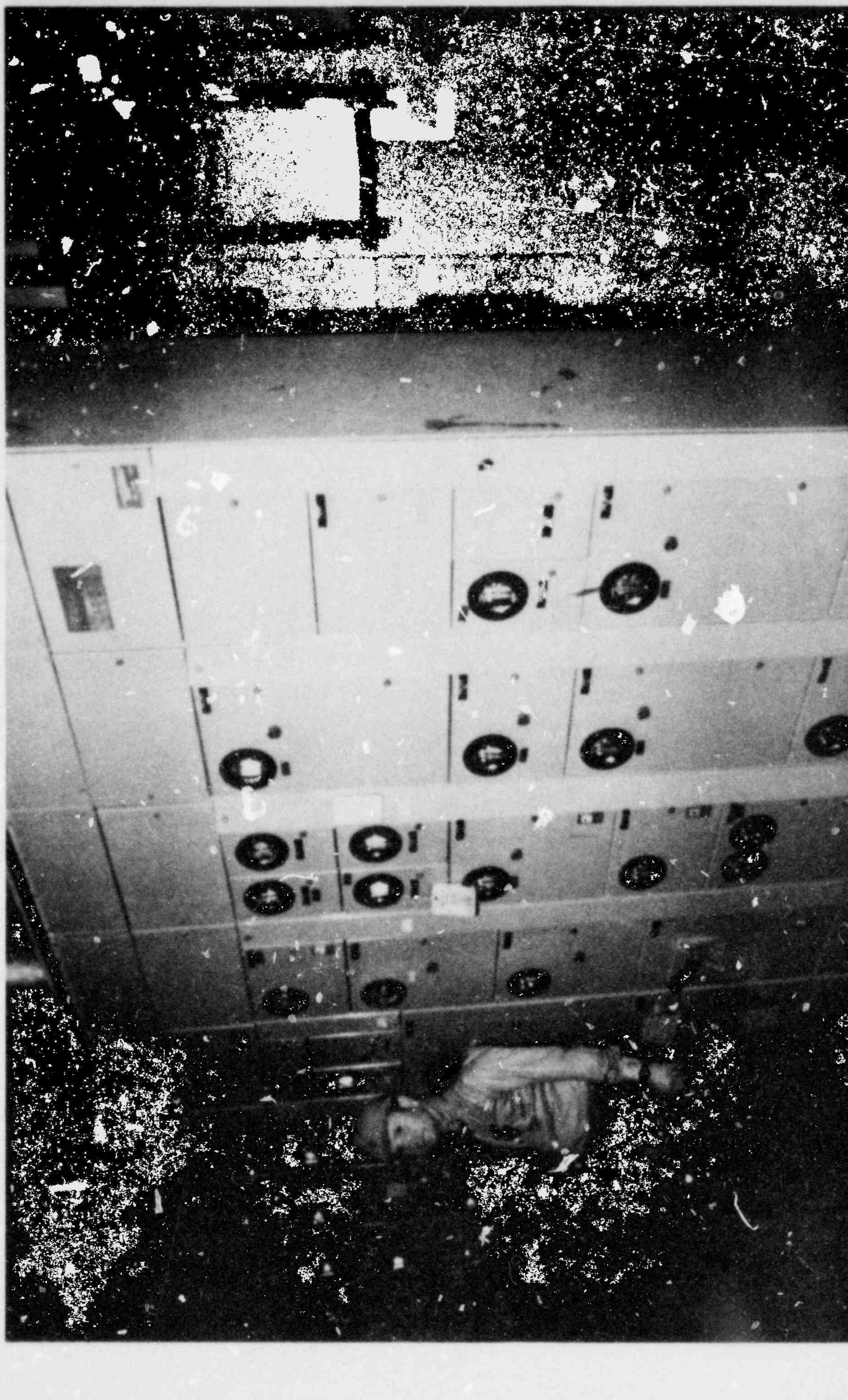

Kuosheng 480 V Motor Control Center

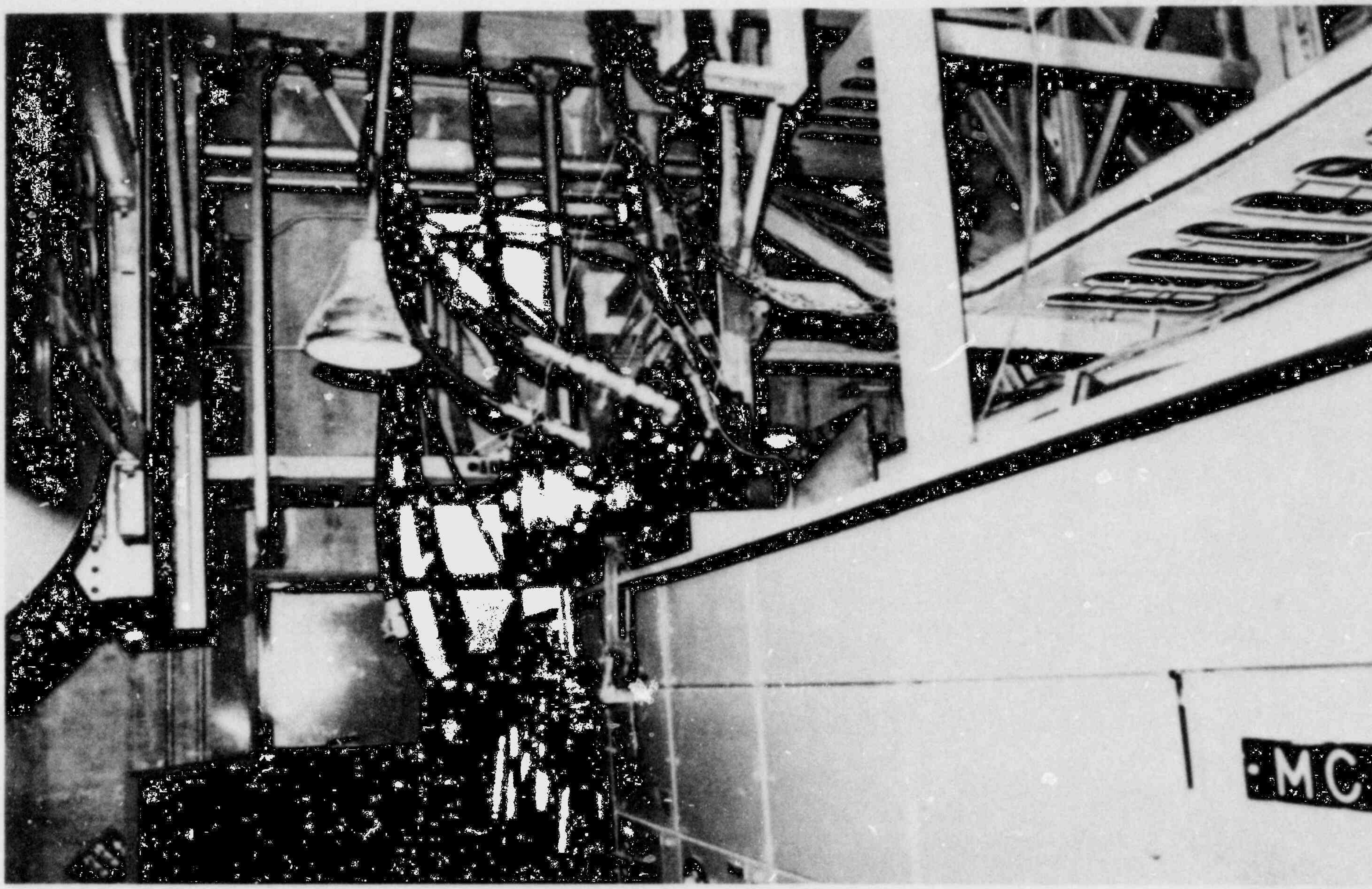

Horizontal Vibration of
Kuosheng 480 V Motor Control Center

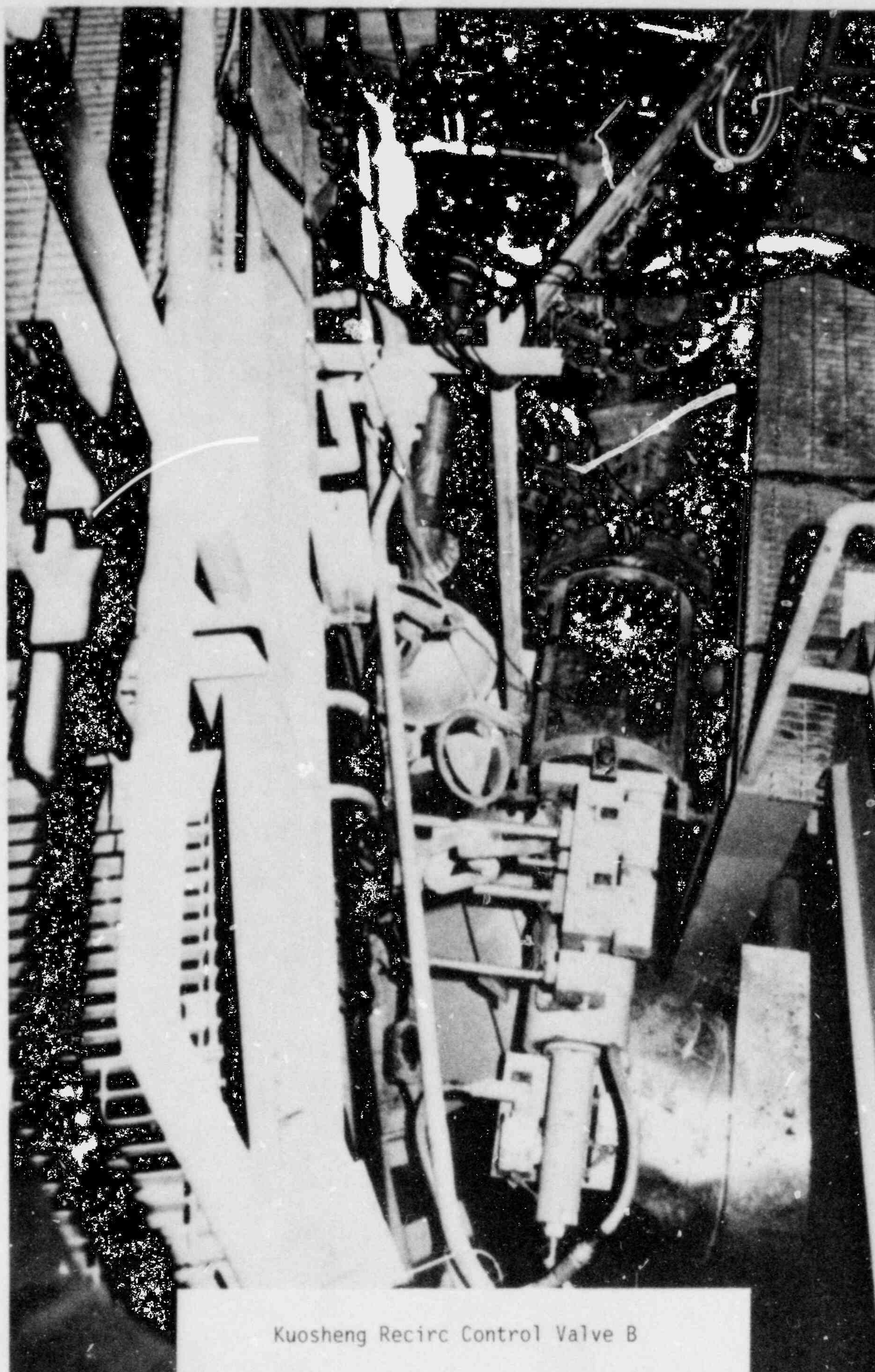

Kuosheng Recirc Control Valve B

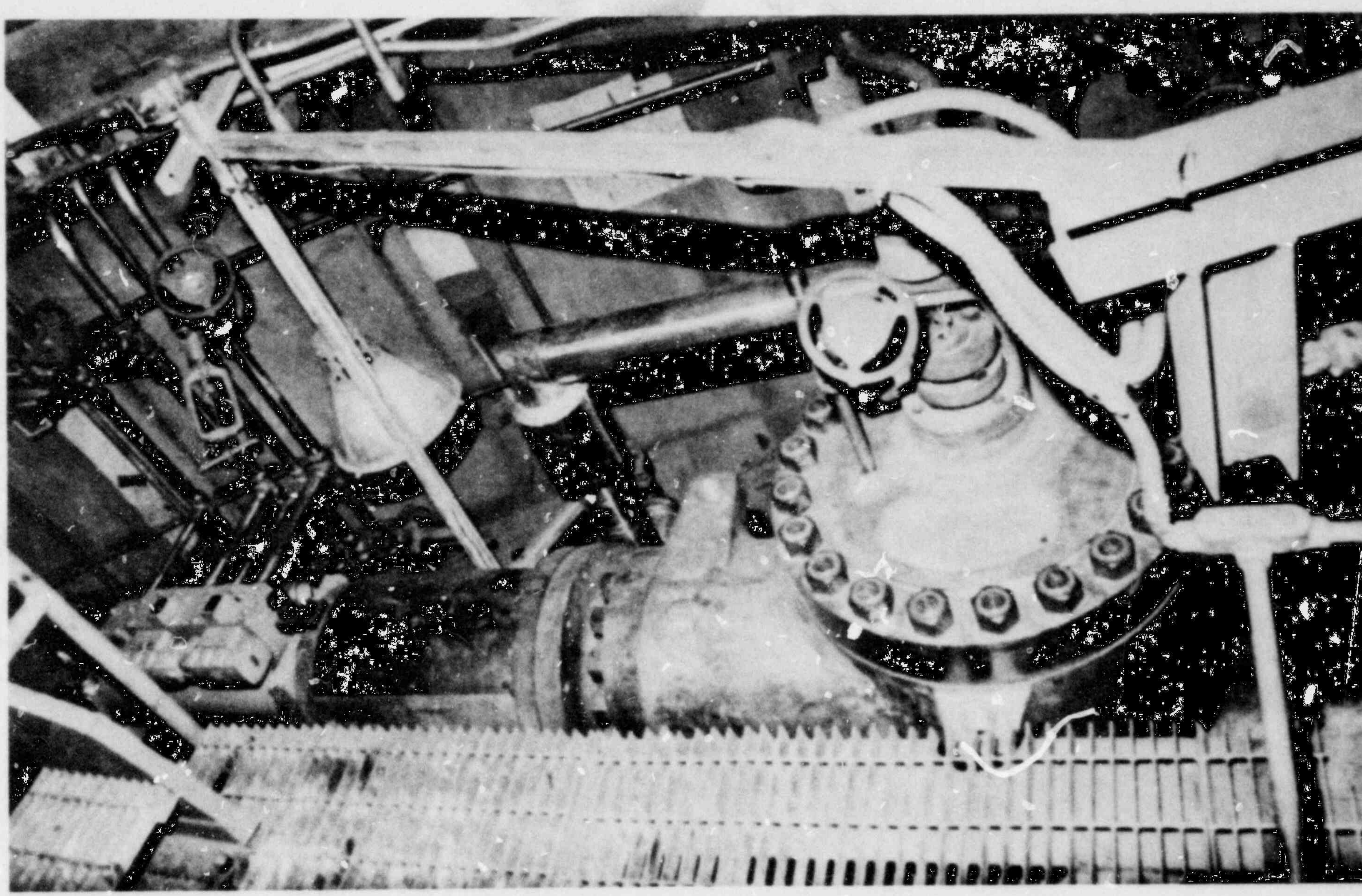

Kuosheng Recirc Control Valve B

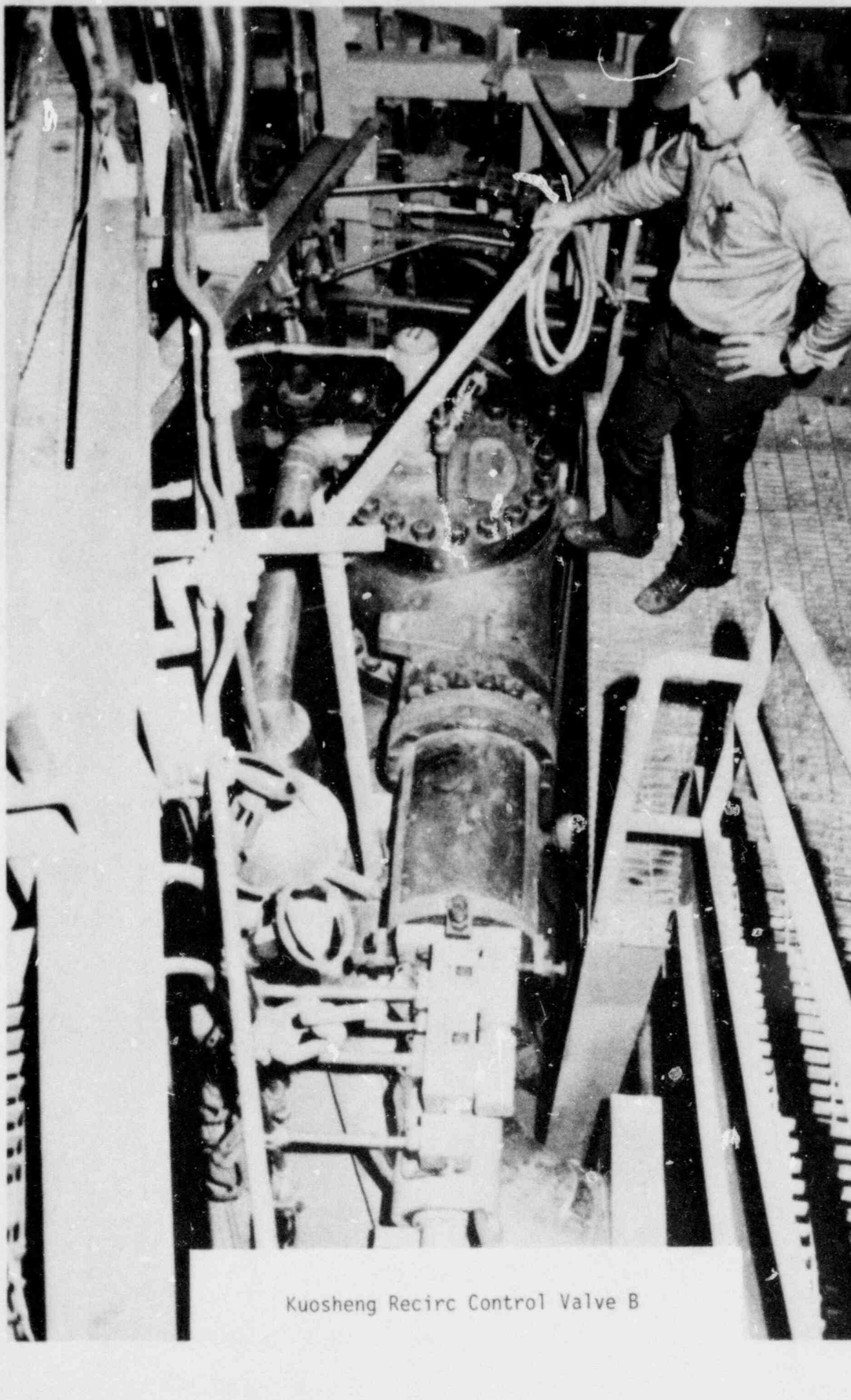

Kuosheng Recirc Control Valve B

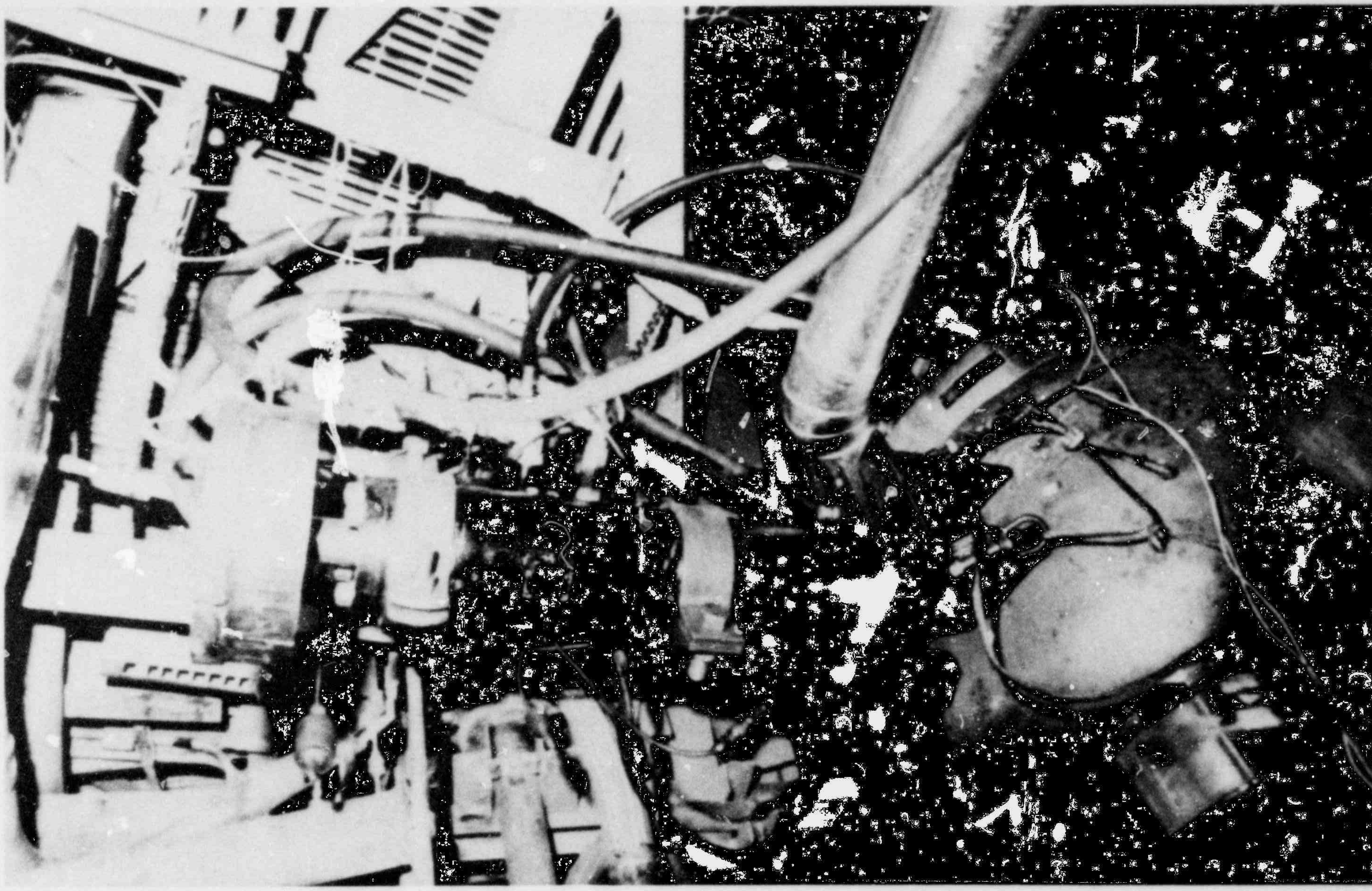

Horizontal Vibration of
Kuosheng Recirc Control Valve B

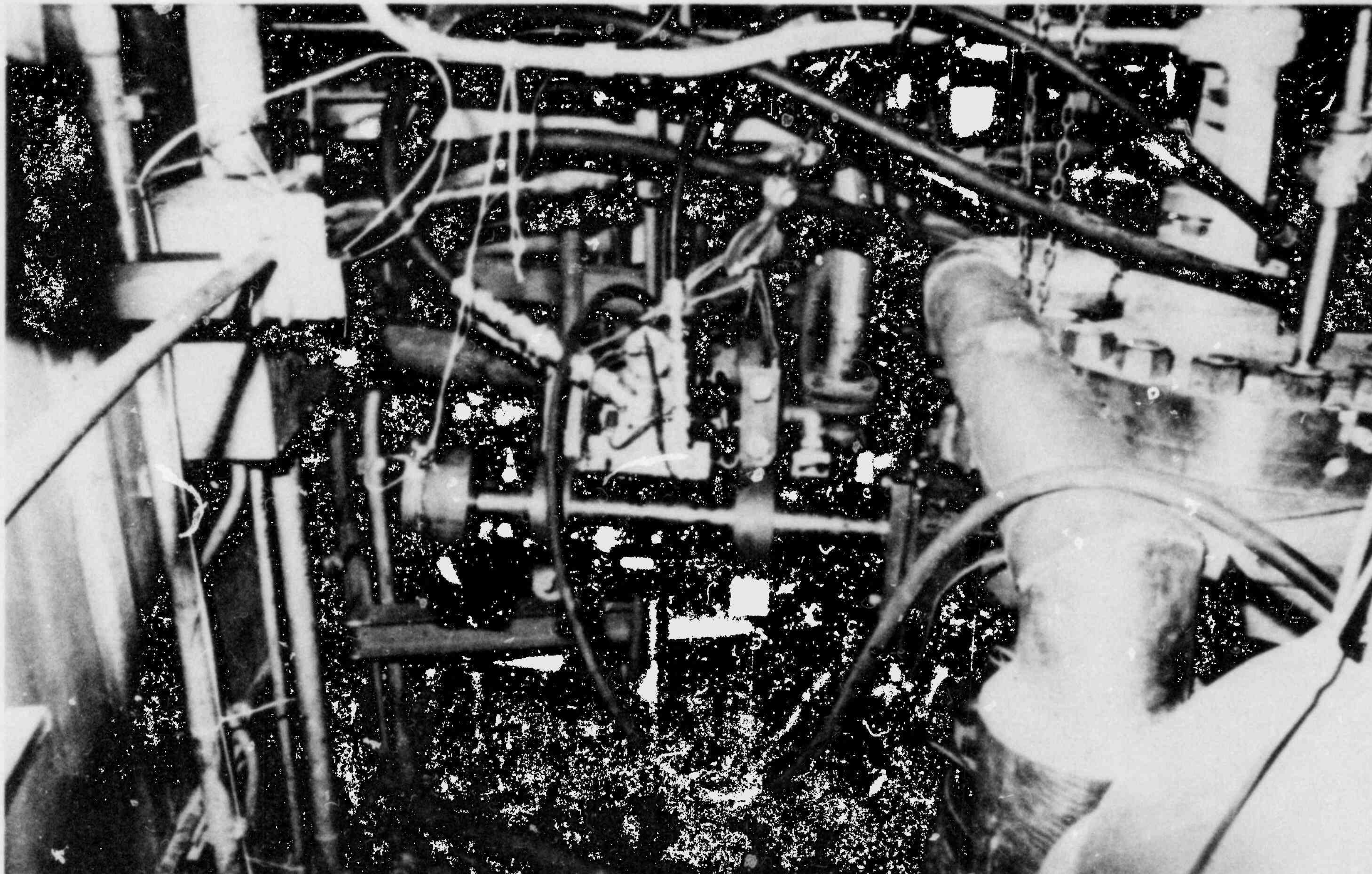

Horizontal Vibration of
Kuosheng Recirc Control Valve B

Vertical Vibration of
Kuosheng Recirc Control Valve B

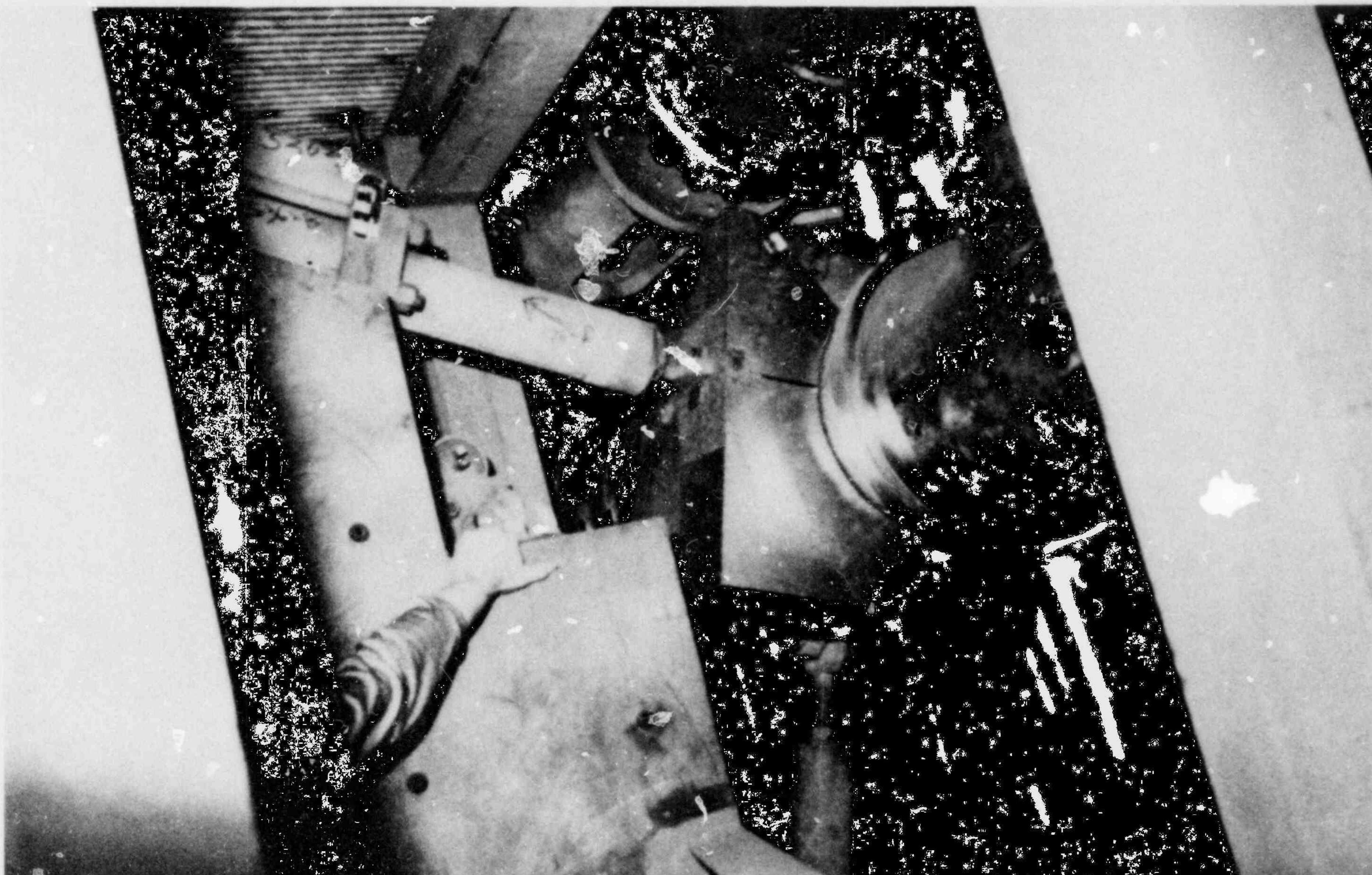

Kuosheng Recirc Control Valve B and Supports

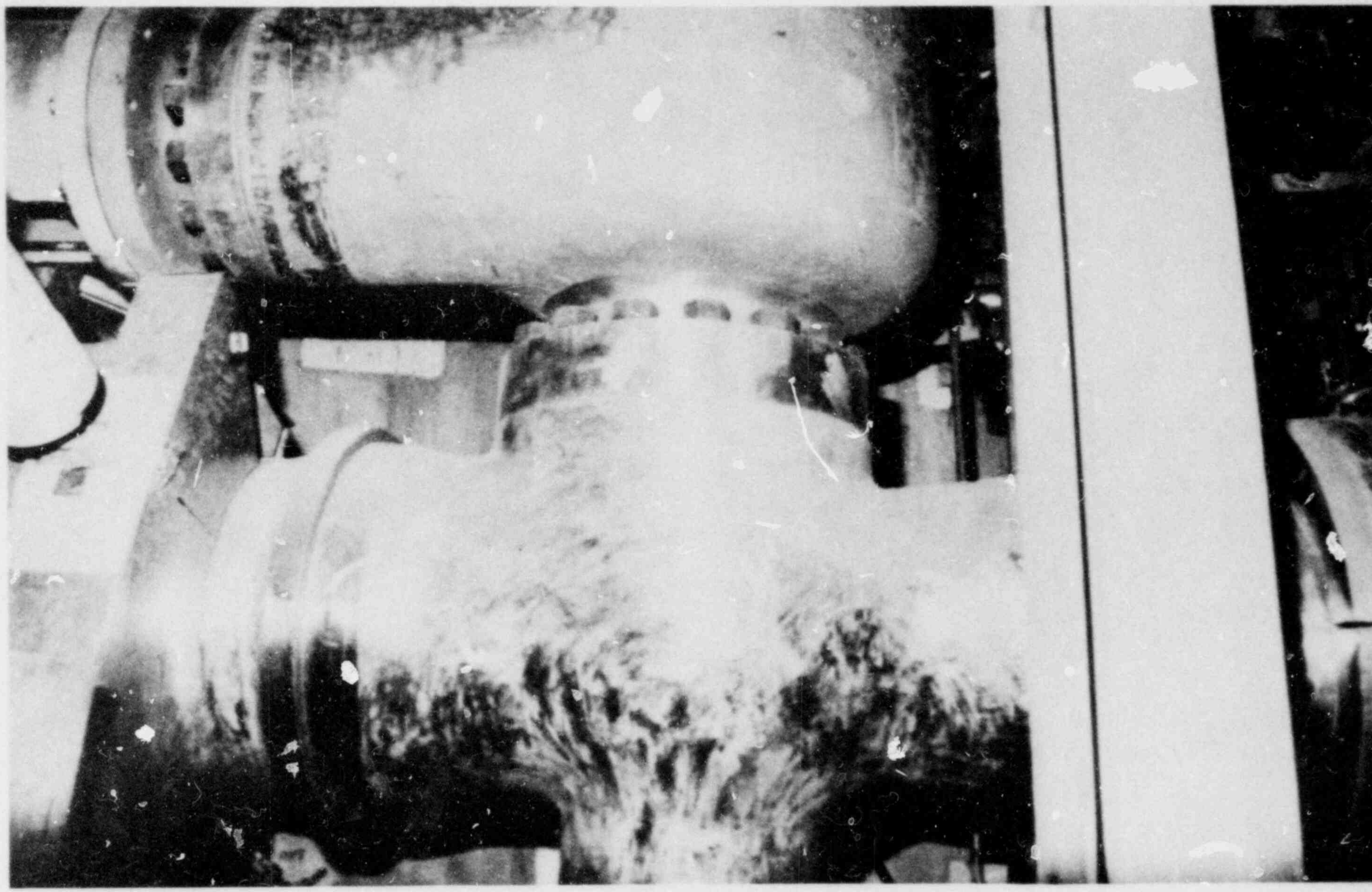

Kuosheng Recirc Control Valve B and Supports

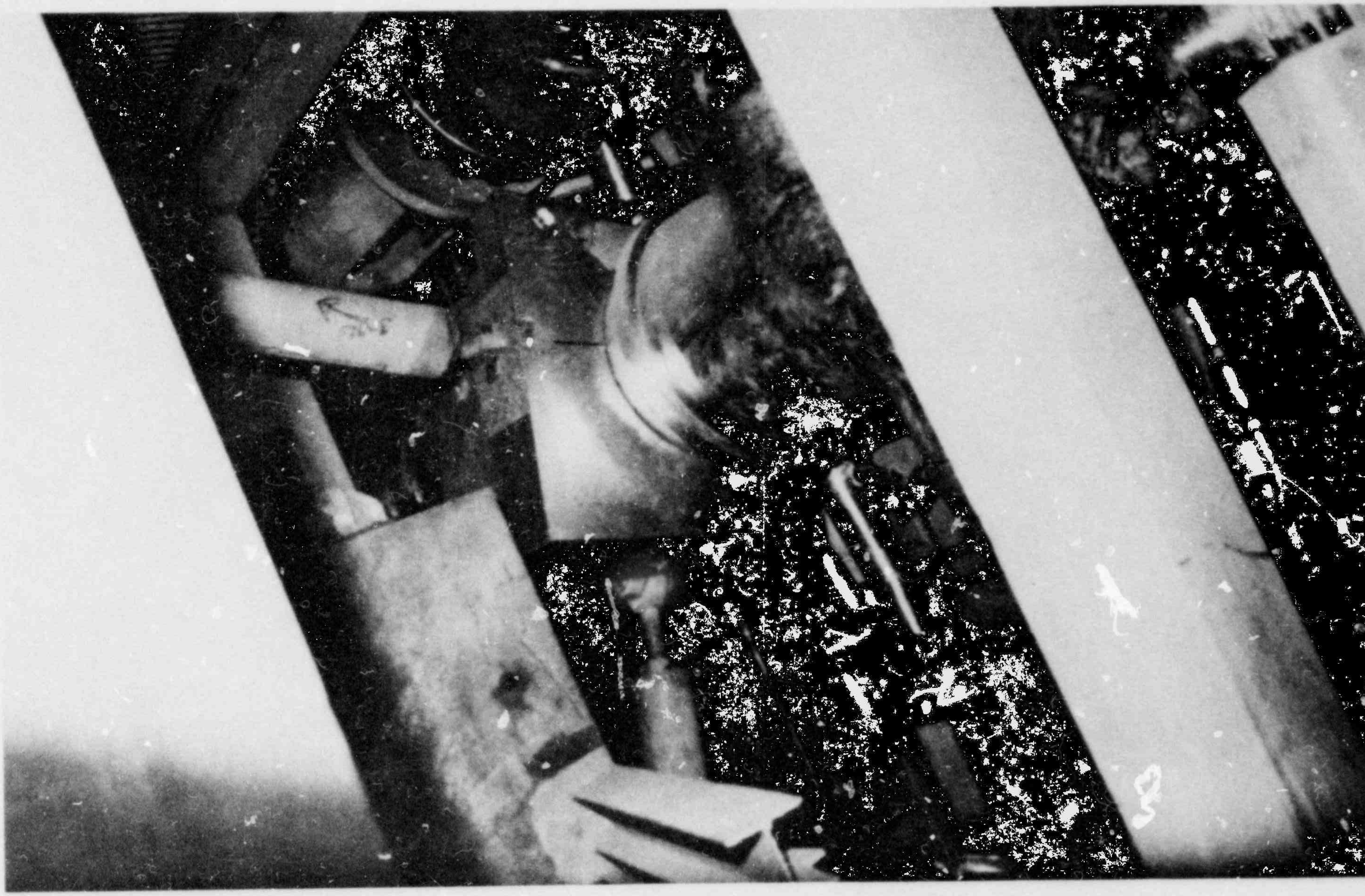

Kuosheng Recirc Control Valve B
and Pipe Supports

APPENDIX C

SUPPLEMENTARY TEST DATA

Transitek, Inc.

2328 J Walsh Avenue
Santa Clara, CA 95050
Telephone 408-246-1616

DATA TRANSMITTAL

MECHANICAL IMPEDANCE TESTS

ON

SELECTED COMPONENTS

KUOSHENG NUCLEAR POWER STATION

for

EG&G Idaho, Inc.
P.O. Box 1625
Idaho Falls, Idaho 83415

TRANSITEK Job No. 81035

May 15, 1981

Written by: *Gerald P. Coleman* — 5-15-81
Gerald P. Coleman — (Date)
Manager, Data Services

Reviewed by: *Mitty Plummer* — May 15, 1981
Mitty C. Plummer — (Date)
President

Transactions in Technology

81036
May 15, 1981

TABLE OF CONTENTS

8103б
May 15, 1981

Overview

Addendum to "Test Results, Mechanical Impedance Tests on Selected Components, Kuosheng Nuclear Power Station".

This addendum contains disk files from the above referenced test results. The raw data files are contained on both dual density floppy diskette and RK05 Hard Disk. In addition the hard disk contains all subsequent files generated during analysis and processing. Each file type is discussed in detail on pages 2 through 8. Pages 9 through 14 contain listings of each structure tested.

Format for Disk Files

1. The files are all in standard DEC RT-11 format.

Disk File Name	File Extension	Number of Blocks	Date File Created
6 characters maximum	3 characters maximum	256 Byte blocks	

Example:

K3INZ.DAT	52	08-May-81
File Name Extension	Blocks	Date Created

2. After each file the contents are identified.

Example:

K3INZ.DAT	52	08-May-81	Project

By looking in the appendix under 'Typical PROJECT FILE', you will find a break down of the contents of a PROJECT FILE.

3. Each Typical File or Typical record contains information which applies to that file type along with a more detailed description of the records within the file.

4. These files are structured around the FORTRAN based MPLUS structural analysis program written by SDRC (Structural Dynamics Research Corporation). FORTRAN listings are not supplied as a normal part of the program, we cannot go any deeper into the files.

5. Each of the five structures tested are broken down to the project file level with the listing of the records for each file.

TYPICAL PROJECT FILE

A PROJECT FILE is the master file for a given structure. Each PROJECT FILE contains Attached Data Files which may be moved in and out of the PROJECT FILE Any Data File may be attached to any PROJECT FILE.

PROJECT FILE

Check Point - A set of default conditions followed by the date and time of last update.

File Type	Code	File Name	Date Time	Records Identification
Project	Z	K3INZ	050881-000000	0/Taipower 3" Valve Project
Parameter	P	K3INP	011881-000000	4/Taipower 3" Valve Parameters
Mode Shape	S	K3INS1	012181-000000	10/Taipower 3" Valve Shapes 29X
Geometry	G	K3ING	011881-000000	1/Taipower 3" Valve Geometry
Function	H	K3INH3	011981-000000	45/Taipower 3" Valve Z-Functions
Traces	T	K3INT	011881-000000	6/Taipower 3" Valve Traces

Only one record is contained in a given project file although any data file may be attached to any project file.

```
 CHECKPOINT 050881-000000
Z K3INZ        050881-000000    0/Taipower 3" Valve Project
P K3INP        011881-000000    4/Taipower 3" Valve Parameters
S K3INSZ       030581-000000   20/Taipower 3" Valve Shapes 29Z
G K3ING        011881-000000    1/Taipower 3" Valve Geometry
H K3INH1       011981-000000   45/Taipower 3" Valve X-Functions
T K3INT        011881-000000    6/Taipower 3" Valve Traces
```

T RECORDS IN USE	Trace Records in File
REC 1:LC	L = Trace of Links
REC 2:LC	C = Trace of Coordinates
REC 3:C	

P RECORDS IN USE	Parameter Records in File
REC 1:5:	
REC 2:7:	
REC 3:9:	
REC 4:11:	

S RECORDS IN USE		Mode Shape Records in File
REC 1:	18.190 HZ Shape #1	
REC 2:	21.329 HZ Shape #2	
REC 3:	30.140 HZ Shape #3	
REC 4:	33.410 HZ Shape #4	
REC 5:	74.570 HZ Shape #5	
REC 6:	74.570 HZ Shape 5 Modified	
REC 7:	18..90 HZ Shape 1 Modified	
REC 8:	21.329 HZ Shape 2 Modified	
REC 9:	30.140 HZ Shape 3 Modified	
REC 10:	33.410 HZ Shape 4 Modified	

Only one Geometry record is included in any Geometry file so no record listing is included.

FUNCTION RECORDS IN FILE

H RECORDS IN USE

REC	1	29X+	3X-	0
REC	2	29X+	3X-	0
REC	3	29X+	4X-	0
REC	4	29X+	5X-	0
REC	5	29X+	6X-	0
REC	6	29X+	7X-	0
REC	7	29X+	8X+	0
REC	8	29X+	9X+	0
REC	9	29X+	11X+	0
REC	10	29X+	13X-	0
REC	11	29X+	14X+	0
REC	12	29X+	15X-	0
REC	13	29X+	17X-	0
REC	14	29X+	20X-	0
REC	15	29X+	21X-	0
REC	16	29X+	24X-	0
REC	17	29X+	25X-	0
REC	18	29X+	27X-	0
REC	19	29X+	29X-	3
REC	20	29X+	29X-	15
REC	21	29X+	29X-	16
REC	22	29X+	29X-	2
REC	23	29X+	28X+	0
REC	24	29X+	30X+	0
REC	25	29X+	31X+	0
REC	26	29X+	16X+	0
REC	27	29X+	18X+	0
REC	28	29X+	29Y-	0
REC	29	29X+	29Z-	0
REC	30	29X+	21Y+	0
REC	31	29X+	21Z-	0
REC	32	29X+	5Z+	0
REC	33	27X+	28X+	10
REC	34	27X+	28X+	11
REC	35	27X+	28X+	12
REC	36	27X+	28X+	13
REC	37	27X+	28X+	6
REC	38	27X+	29X+	7
REC	39	27X+	28X+	8
REC	40	27X+	28X+	9
REC	41	29X+	29X-	4
REC	42	29X+	29X-	1
REC	43	29X+	29X-	0

H = Function Records in Use

Record Number Reference Response Sequence Number User Assigned

The sequence numbers used for this report are as follows:

0 = Standard frequency response function
1 = Special frequency response function
2 = Response PSD
3 = Force PSD
4 = Coherence
5 = Not used
6 = Maximum force frequency response function
7 = Maximum response PSD
8 = Maximum force PSD
9 = Maximum Coherence
10= Minimum force frequency response function
11= Minimum response PSD
12= Minimum force PSD
13= Minimum Coherence
14= Not used
15= Force time history
16= Response time history

A Typical Record Taken From A Parameter File

LABEL	=	User identification for analysis
FREQ	=	Resonance frequency
DAMPING	=	Viscous damping ratio
AMPLITUDE	=	Modal amplitude
PHASE	=	Modal rotation
REF	=	Reference Coordinate
RES	=	Response Coordinate
MODE	=	Associated mode number
FLAGS	=	Processing flags for analysis

MODE PARAMETERS

LABEL	FREQ	DAMPING	AMPLITUDE	PHASE	REF	RES	MODE	FLAGS
1	21.250	0.014956	6.4277E-02	-1.4680	29Z+	29Z-	0	0 0 0 1 1
3	29.803	0.021740	0.4216	-1.4091	29Z+	29Z-	0	0 0 0 1 1
4	48.221	0.010247	8.1723E-02	-1.7421	29Z+	29Z-	0	0 0 0 1 1
5	44.067	0.005251	1.9301E-02	-2.2971	29Z+	29Z-	0	0 0 0 1 1
9	72.370	0.016246	0.1678	1.8579	29Z+	28Z+	0	0 0 0 1 1
10	75.784	0.007499	7.8523E-02	-2.1828	29Z+	29Z-	0	0 0 0 1 1
11	79.892	0.015758	0.2826	-1.6253	29Z+	29Z-	0	0 0 0 1 1
6	49.332	0.009690	0.4022	1.7980	29Z+	23Z+	0	0 0 0 1 1
2	20.552	0.040843	2.1412E-02	-0.4385	29Z+	29Z-	0	0 0 0 1 1

A Typical Record Taken From A Shape File

LOC = Geometry Location Followed by Coefficients for X, Y and Z Directions

MODE SHAPE

LOC	X REAL	X IMAG	Y REAL	Y IMAG	Z REAL	Z IMAG
1	0.000E-01	0.000E-01	0.000E-01	0.000E-01	-3.931E-03	-3.794E-03
2	0.000E-01	0.000E-01	3.397E-04	3.273E-03	-2.296E-02	-2.781E-02
3	-1.316E-03	-7.342E-03	0.000E-01	0.000E-01	-2.873E-02	-3.827E-02
4	0.000E-01	0.000E-01	0.000E-01	0.000E-01	-2.750E-02	-3.759E-02
5	0.000E-01	0.000E-01	0.000E-01	0.000E-01	-2.564E-02	-3.930E-02
6	0.000E-01	0.000E-01	0.000E-01	0.000E-01	-2.123E-02	-3.480E-02
7	0.000E-01	0.000E-01	0.000E-01	0.000E-01	-2.099E-02	-3.595E-02
8	0.000E-01	0.000E-01	0.000E-01	0.000E-01	-1.765E-02	-1.984E-02
9	0.000E-01	0.000E-01	0.000E-01	0.000E-01	-5.018E-03	-1.155E-02
10	0.000E-01	0.000E-01	0.000E-01	0.000E-01	0.000E-01	0.000E-01
11	0.000E-01	0.000E-01	0.000E-01	0.000E-01	-3.262E-02	-5.828E-02
12	0.000E-01	0.000E-01	0.000E-01	0.000E-01	0.000E-01	0.000E-01
13	0.000E-01	0.000E-01	0.000E-01	0.000E-01	0.000E-01	0.000E-01
14	0.000E-01	0.000E-01	0.000E-01	0.000E-01	0.000E-01	0.000E-01
15	0.000E-01	0.000E-01	0.000E-01	0.000E-01	2.071E-02	3.364E-02
16	0.000E-01	0.000E-01	0.000E-01	0.000E-01	-2.272E-02	-4.285E-02
17	0.000E-01	0.000E-01	0.000E-01	0.000E-01	0.000E-01	0.000E-01
18	0.000E-01	0.000E-01	0.000E-01	0.000E-01	0.000E-01	0.000E-01
19	0.000E-01	0.000E-01	0.000E-01	0.000E-01	2.419E-03	4.769E-03
20	0.000E-01	0.000E-01	0.000E-01	0.000E-01	1.505E-02	2.742E-02
21	0.000E-01	0.000E-01	0.000E-01	0.000E-01	-7.954E-03	-3.703E-03
22	0.000E-01	0.000E-01	0.000E-01	0.000E-01	-3.449E-02	-4.425E-02
23	0.000E-01	0.000E-01	0.000E-01	0.000E-01	-7.355E-03	-2.038E-02
24	0.000E-01	0.000E-01	0.000E-01	0.000E-01	3.478E-02	3.372E-02
25	0.000E-01	0.000E-01	0.000E-01	0.000E-01	8.940E-03	2.395E-02
26	0.000E-01	0.000E-01	0.000E-01	0.000E-01	-9.235E-03	-4.694E-03
27	-3.113E-02	-2.978E-02	6.819E-03	9.372E-03	-2.159E-02	-3.929E-02
28	0.000E-01	0.000E-01	0.000E-01	0.000E-01	-2.766E-02	-4.789E-02
29	0.000E-01	0.000E-01	0.000E-01	0.000E-01	-2.272E-02	-2.671E-02
30	0.000E-01	0.000E-01	0.000E-01	0.000E-01	-1.869E-02	-3.577E-02
31	0.000E-01	0.000E-01	0.000E-01	0.000E-01	-5.960E-02	-5.089E-02
32	0.000E-01	0.000E-01	0.000E-01	0.000E-01	0.000E-01	0.000E-01

A Typical Geometry File

GEOMETRY

LOC	X	Y	Z
1	25	18	0
2	6	18	0
3	0	12	0
4	0	6	0
5	0	0	0
6	0	-6	0
7	0	-17	0
8	0	-28	0
9	4	0	7
10	0	-4	7
11	-4	0	7
12	0	4	7
13	2	0	14
14	-2	0	14
15	3	-3	21
16	-3	-3	21
17	3	-3	25
18	-3	-3	25
19	6	-1	21
20	13	-1	21
21	13	-1	25
22	6	-1	25
23	6	4	21
24	13	4	21
25	13	4	25
26	6	4	25
27	4	16	18
28	-3	16	18
29	4	16	24
30	-3	16	24
31	-4	3	21
32	-7	3	21

Typical Frequency Response Function

Function Number = Data array from which function was listed.
29Z = Reference location, axis and sense
29Z- = Response location, axis and sense
Frequency = HERTZ followed by real and imaginary components, amplitude and phase.

FUNCTION 1: 29Z+ 29Z-

FREQUENCY	REAL	IMAG	AMPLITUDE	PHASE
0.0000	-4.1428E-03	0.0000	4.1428E-03	3.142
0.3906	-6.8665E-05	4.9591E-04	5.0064E-04	1.709
0.7812	-3.7384E-04	4.1962E-04	5.6199E-04	2.299
1.172	-9.1553E-05	2.1362E-04	2.3241E-04	1.976
1.562	6.1035E-05	8.3923E-05	1.0377E-04	0.9420
1.953	3.0518E-05	1.9836E-04	2.0070E-04	1.418
2.344	0.0000	2.2125E-04	2.2125E-04	1.571
2.734	1.5259E-05	1.9836E-04	1.9895E-04	1.494
3.125	1.5259E-05	1.2207E-04	1.2302E-04	1.446
3.516	6.8665E-05	1.5259E-04	1.6733E-04	1.148
3.906	1.2970E-04	-3.8147E-05	1.3519E-04	-0.2861
4.297	1.2970E-04	-2.2888E-05	1.3170E-04	-0.1747
4.687	1.0681E-04	1.0681E-04	1.5105E-04	0.7854
5.078	1.3733E-04	6.8665E-05	1.5354E-04	0.4636
5.469	1.6022E-04	9.9182E-05	1.8843E-04	0.5543
5.859	2.5940E-04	-2.2888E-05	2.6041E-04	-8.8007E-02
6.250	2.4414E-04	5.3406E-05	2.4991E-04	0.2154
6.641	2.6703E-04	-2.2888E-05	2.6801E-04	-8.5505E-02
7.031	3.1281E-04	-1.0681E-04	3.3054E-04	-0.3290
7.422	5.1117E-04	7.6294E-06	5.1123E-04	1.4924E-02
7.812	4.0436E-04	7.6294E-05	4.1149E-04	0.1865
8.203	5.4932E-04	1.5259E-05	5.4953E-04	2.7771E-02
8.594	5.9509E-04	-2.0599E-04	6.2974E-04	-0.3332

9.375	7.7820E-04	-1.5259E-05	7.7235E-04	-1.9605E-02
9.766	7.6294E-04	-1.5259E-05	7.6309E-04	-1.9997E-02
10.16	1.0071E-03	0.0000	1.0071E-03	0.0000
10.55	1.0071E-03	1.0681E-04	1.0127E-03	0.1057
10.94	1.1063E-03	2.2888E-05	1.1065E-03	2.0687E-02
11.33	1.0834E-03	7.6294E-05	1.0861E-03	7.0306E-02
11.72	1.2817E-03	-9.9182E-05	1.2856E-03	-7.7227E-02
12.11	1.3962E-03	-8.3923E-05	1.3987E-03	-6.0037E-02
12.50	1.4267E-03	-1.2207E-04	1.4319E-03	-8.5354E-02
12.89	1.6022E-03	-1.2970E-04	1.6074E-03	-8.0776E-02
13.28	1.7014E-03	-3.0518E-05	1.7016E-03	-1.7935E-02
13.67	1.8616E-03	-7.6294E-05	1.8631E-03	-4.0961E-02
14.06	1.9760E-03	-5.3406E-05	1.9767E-03	-2.7020E-02
14.45	2.2812E-03	-3.0518E-05	2.2814E-03	-1.3377E-02
14.84	2.4185E-03	-1.6022E-04	2.4238E-03	-6.6149E-02
15.23	2.6093E-03	-1.6022E-04	2.6142E-03	-6.1327E-02
15.62	2.7390E-03	-3.1281E-04	2.7569E-03	-0.1137
16.02	3.0746E-03	-1.2207E-04	3.0771E-03	-3.9681E-02
16.41	3.2578E-03	-2.6703E-04	3.2687E-03	-8.1784E-02
16.80	3.5934E-03	-2.4414E-04	3.6017E-03	-6.7836E-02
17.19	3.9444E-03	-3.1281E-04	3.9568E-03	-7.9138E-02
17.58	4.4174E-03	-6.1798E-04	4.4604E-03	-0.1390
17.97	5.2567E-03	-1.9913E-03	5.6212E-03	-0.3621
18.36	4.6463E-03	0.0000	[illegible]	0.0000
19.14	6.1139E-03	-7.7057E-04	[illegible]	-0.1257
19.53	6.9351E-03	-8.6212E-04	[illegible]	-0.1237
19.92	8.6517E-03	-1.1902E-03	8.7332E-03	-0.1367
20.31	9.9716E-03	-2.3651E-03	1.0248E-02	-0.2329
20.70	1.3130E-02	-5.0507E-03	1.4068E-02	-0.3672
21.09	9.5220E-03	-3.2906E-02	3.3991E-02	-1.317
21.48	7.4234E-03	-9.2010E-03	1.1822E-02	-0.8919
21.87	-5.8746E-03	-2.3460E-02	2.4185E-02	-1.816
22.27	-4.4022E-03	-3.8452E-03	5.8451E-03	-2.424
22.66	3.6621E-04	-6.9427E-04	7.8494E-04	-1.085
23.05	2.9602E-03	1.7548E-04	2.9654E-03	5.9209E-02
23.44	4.9438E-03	-1.6785E-04	4.9467E-03	-3.3939E-02
23.83	6.1722E-03	-6.1035E-04	6.2023E-03	-9.8567E-02
24.22	6.9580E-03	-1.7090E-03	7.1649E-03	-0.2408
24.61	8.6517E-03	-1.9757E-03	8.7184E-03	-0.1277
25.00	1.0071E-02	-2.4719E-03	1.0370E-02	-0.2407
25.39	9.0103E-03	-4.1962E-03	9.9395E-03	-0.4358
25.78	1.1284E-02	-1.7166E-03	1.1414E-02	-0.1510
26.17	1.3069E-02	-2.7771E-03	1.3361E-02	-0.2094
26.56	1.4915E-02	-2.4948E-03	1.5123E-02	-0.1657
26.95	1.7197E-02	-2.3804E-03	1.7361E-02	-0.1375
27.34	2.1759E-02	-3.0899E-03	2.1977E-02	-0.1411
27.73	2.7794E-02	-5.4779E-03	2.8329E-02	-0.1946
28.12	3.4119E-02	[illegible]	3.6105E-02	-0.3332

28.91	5.0752E-02	-2.6179E-02	5.7093E-02	-0.4755
29.30	7.5670E-02	-6.2195E-02	9.7919E-02	-0.6832
29.69	2.5177E-04	-0.1227	0.1227	-1.569
30.08	2.0927E-02	-0.1202	0.1219	-1.406
30.47	-3.2873E-02	-3.9948E-02	0.1007	-2.744
30.86	-5.9380E-02	-9.1934E-03	6.0087E-02	-2.988
31.25	-3.8033E-02	-2.3499E-03	3.8105E-02	-3.080
31.64	-2.5650E-02	-7.5760E-03	2.6745E-02	-2.854
32.03	-2.4780E-02	-9.6130E-04	2.4799E-02	-3.103
32.42	-1.8234E-02	-1.6022E-03	1.8305E-02	-3.054
32.81	-1.3260E-02	-5.8136E-03	1.4478E-02	-2.728
33.20	-1.7082E-02	-8.4229E-03	1.9046E-02	-2.683
33.59	-1.7433E-02	-6.9733E-03	1.8776E-02	-2.761
33.98	-1.6457E-02	-4.7531E-03	1.7129E-02	-2.860
34.37	-1.4961E-02	-4.3335E-03	1.5576E-02	-2.860
34.77	-1.4252E-02	-3.8681E-03	1.4767E-02	-2.877
35.16	-1.2909E-02	-3.3569E-03	1.3338E-02	-2.887
35.55	-1.2215E-02	-3.7689E-03	1.2783E-02	-2.842
35.94	-1.3237E-02	-3.9444E-03	1.3812E-02	-2.852
36.33	-1.2009E-02	-1.8616E-03	1.2152E-02	-2.988
36.72	-1.1421E-02	-1.2360E-03	1.1488E-02	-3.034
37.11	-1.0277E-02	-1.0910E-03	1.0335E-02	-3.036
37.50	-9.3307E-03	-6.1798E-04	9.3512E-03	-3.075
37.89	-8.4305E-03	-4.1962E-04	8.4409E-03	-3.092
38.67	-6.5002E-03	-9.7738E-04	6.5592E-03	-3.097
39.06	-6.1798E-03	-1.1291E-03	6.2821E-03	-2.961
39.45	-5.5161E-03	-1.6022E-03	5.7440E-03	-2.859
39.84	-6.9054E-03	-2.3880E-03	7.2122E-03	-2.804
40.23	-6.4316E-03	-1.6556E-03	6.6412E-03	-2.890
40.62	-6.0272E-03	-7.2479E-04	6.0706E-03	-3.022
41.02	-5.1804E-03	-6.1035E-05	5.1807E-03	-3.130
41.41	-4.0588E-03	5.3406E-04	4.0938E-03	3.011
41.80	-2.4872E-03	1.8311E-04	2.4939E-03	3.068
42.19	-7.6294E-04	-7.7057E-04	1.0844E-03	-2.351
42.58	5.0354E-04	-2.8076E-03	2.8524E-03	-1.393
42.97	8.3923E-05	-4.4937E-03	4.4945E-03	-1.552
43.36	1.1215E-03	-4.7226E-03	4.8539E-03	-1.338
43.75	1.4038E-03	-1.0460E-02	1.0554E-02	-1.437
44.14	-1.1299E-02	-1.0735E-02	1.5585E-02	-2.382
44.53	-6.7673E-03	-3.0060E-03	7.4049E-03	-2.724
44.92	-5.1575E-03	-2.3193E-03	5.6550E-03	-2.719
45.31	-4.5242E-03	-1.3046E-03	4.7086E-03	-2.861
45.70	-2.6321E-03	-5.3406E-04	2.6858E-03	-2.941
46.09	-5.1890E-04	-3.1281E-04	6.0580E-04	-2.599
46.48	1.3962E-03	-6.7902E-04	1.5525E-03	-0.4527
46.87	3.3569E-03	-1.5106E-03	3.6812E-03	-0.4229
47.27	7.3624E-03	-3.9179E-03	8.3390E-03	-0.4896
47.66	9.9417E-03	-9.6970E-03	1.3190E-02	-0.8259

48.44	-8.3694E-03	-1.0269E-02	1.3248E-02	-2.255
48.83	-7.6294E-04	-4.8218E-03	4.8818E-03	-1.728
49.22	9.6588E-03	-1.3316E-02	1.6940E-02	-0.9641
49.61	-1.1032E-02	-3.0823E-02	3.2738E-02	-1.915
50.00	-1.5594E-02	-1.3992E-02	2.0952E-02	-2.410
50.39	-1.2245E-02	-9.0561E-03	1.5230E-02	-2.505
50.78	-1.3504E-02	-6.4316E-03	1.4957E-02	-2.697
51.17	-1.0506E-02	-4.2801E-03	1.1344E-02	-2.755
51.56	-9.1476E-03	-3.6087E-03	9.8337E-03	-2.766
51.95	-7.9956E-03	-2.8610E-03	8.4921E-03	-2.798
52.34	-7.1640E-03	-2.7466E-03	7.6725E-03	-2.775
52.73	-6.5765E-03	-2.2278E-03	6.9436E-03	-2.815
53.12	-5.6381E-03	-2.2278E-03	6.0623E-03	-2.765
53.52	-4.8294E-03	-2.1286E-03	5.2777E-03	-2.726
53.91	-4.1428E-03	-2.4414E-03	4.8086E-03	-2.609
54.30	-3.7994E-03	-2.8534E-03	4.7516E-03	-2.497
54.69	-3.2120E-03	-3.4027E-03	4.6792E-03	-2.327
55.08	-3.6087E-03	-4.1733E-03	5.5172E-03	-2.284
55.47	-5.0507E-03	-4.0359E-03	6.4651E-03	-2.467
55.86	-4.5624E-03	-2.2507E-03	5.0873E-03	-2.683
56.25	-3.9444E-03	-2.7618E-03	4.8152E-03	-2.531
56.64	-4.4174E-03	-1.8463E-03	4.7877E-0[illegible]	-2.746
57.03	-3.1357E-03	-1.2360E-03	3.3705E-03	-2.766
57.42	-2.8763E-03	-1.2589E-03	3.1397E-03	-2.72[illegible]
58.20	-2.1057E-03	-1.2512E-03	2.4494E-03	-2.605
58.59	-1.1978E-03	-8.0872E-04	1.4453E-03	-2.548
58.98	-7.9346E-04	-8.5449E-04	1.1661E-03	-2.319
59.37	6.1035E-05	-8.0109E-04	8.0341E-04	-1.495
59.77	0.0000	-1.0376E-03	1.037[illegible]E-03	-1.571
60.16	6.1798E-04	-1.2436E-03	1.3887E-03	-1.110
60.55	6.4087E-04	-9.5367E-04	1.1490E-03	-0.9791
60.94	9.9182E-04	-1.0605E-03	1.4520E-03	-0.8188
61.33	2.0599E-03	-1.0605E-03	2.3169E-03	-0.4754
61.72	2.4109E-03	-1.1673E-03	2.6786E-03	-0.4509
62.11	2.8000E-03	-8.9264E-04	2.9388E-03	-0.3086
62.50	3.3798E-03	-1.3885E-03	3.6539E-03	-0.3898
62.89	4.1351E-03	-1.7395E-03	4.4861E-03	-0.3982
63.28	3.1891E-03	-2.7695E-03	4.2238E-03	-0.7151
63.67	4.020[illegible]E-03	-2.0142E-03	4.4970E-03	-0.4644
64.06	4.6463E-03	-1.9684E-03	5.0461E-03	-0.4007
64.45	5.2872E-03	-2.2964E-03	5.7644E-03	-0.4098
64.84	5.7755E-03	-2.3804E-03	6.2468E-03	-0.3909
65.23	5.6305E-03	-2.6093E-03	6.2057E-03	-0.4340
65.62	6.2943E-03	-2.1591E-03	6.6543E-03	-0.3305
66.02	7.4844E-03	-2.3193E-03	7.8356E-03	-0.3005
66.41	8.1711E-03	-[illegible].4719E-03	8.5368E-03	-0.2938
66.80	9.0256E-03	-[illegible].3646E-03	9.6323E-03	-0.3568
67.19	9.3842E-03	[illegible] 2953E-03	1.032[illegible]E-02	-0.4293

67.97	9.1858E-03	-4.5395E-03	1.0246E-02	-0.4590
68.36	9.7733E-03	-7.7308E-03	1.0461E-02	-0.3647
68.75	1.0788E-02	-4.0054E-03	1.1508E-02	-0.3555
69.14	1.2177E-02	-4.0741E-03	1.2840E-02	-0.3229
69.53	1.2642E-02	-4.5242E-03	1.3427E-02	-0.3437
69.92	1.3596E-02	-4.7989E-03	1.4418E-02	-0.3393
70.31	1.5236E-02	-5.9128E-03	1.6343E-02	-0.3702
70.70	1.7289E-02	-6.8054E-03	1.7653E-02	-0.3958
71.09	1.8471E-02	-8.0490E-03	2.0148E-02	-0.4110
71.48	1.8997E-02	-1.0948E-02	2.1926E-02	-0.5228
71.87	1.9493E-02	-1.3466E-02	2.3692E-02	-0.6045
72.27	1.7357E-02	-1.6479E-02	2.3934E-02	-0.7595
72.66	1.4442E-02	-1.7769E-02	2.2898E-02	-0.8883
73.05	1.3351E-02	-1.6716E-02	2.1394E-02	-0.8968
73.44	1.4229E-02	-1.4679E-02	2.0443E-02	-0.8010
73.83	1.6922E-02	-1.4587E-02	2.2342E-02	-0.7114
74.22	1.9287E-02	-1.6998E-02	2.5709E-02	-0.7224
74.61	2.0073E-02	-2.0744E-02	2.8866E-02	-0.8018
75.00	1.9119E-02	-2.5414E-02	3.1802E-02	-0.9258
75.39	1.5503E-02	-3.0540E-02	3.4250E-02	-1.101
75.78	2.6474E-03	-3.1784E-02	3.1894E-02	-1.488
76.17	7.8583E-04	-1.9897E-02	1.9913E-02	-1.531
76.56	5.8670E-03	-1.4709E-02	1.5836E-02	-1.191
76.95	1.1253E-02	-1.3351E-02	1.7461E-02	-0.8705
77.73	1.9249E-02	-1.6823E-02	2.5564E-02	-0.7182
78.12	2.2964E-02	-1.9295E-02	2.9994E-02	-0.6988
78.52	2.6176E-02	-2.4834E-02	3.6082E-02	-0.7591
78.91	2.7336E-02	-3.2379E-02	4.2375E-02	-0.8696
79.30	2.3689E-02	-4.0909E-02	4.7273E-02	-1.046
79.69	1.6640E-02	-4.7401E-02	5.0237F-02	-1.233
80.08	8.4457E-03	-4.8088E-02	4.8824E-02	-1.397
80.47	1.5640E-03	-4.4418E-02	4.4446E-02	-1.536
80.86	-2.9755E-04	-4.0436E-02	4.0437E-02	-1.578
81.25	-7.0953E-04	-3.9116E-02	3.9122E-02	-1.589
81.64	8.4686E-04	-4.0192E-02	4.0201E-02	-1.550
82.03	-8.8501E-04	-4.0665E-02	4.0674E-02	-1.593
82.42	-2.1591E-03	-4.1328E-02	4.1385E-02	-1.623
82.81	-6.8207E-03	-4.0726E-02	4.1293E-02	-1.737
83.20	-1.0071E-02	-3.8063E-02	3.9373E-02	-1.829
83.59	-1.1154E-02	-3.6209E-02	3.7888E-02	-1.870
83.98	-1.1688E-02	-3.4775E-02	3.6687E-02	-1.895
84.37	-1.3710E-02	-3.3531E-02	3.6226E-02	-1.959
84.77	-1.3390E-02	-3.2791E-02	3.5419E-02	-1.958
85.16	-1.4771E-02	-3.1128E-02	3.4455E-02	-2.014
85.55	-1.6251E-02	-2.9182E-02	3.3402E-02	-2.079
85.94	-1.6945E-02	-2.7046E-02	3.1916E-02	-2.130
86.33	-1.6884E-02	-2.5810E-02	3.0842E-02	-2.150
86.72	-1.7204E-02	-2.3453E-02	2.9086E-02	-2.204

87.50	-1.5938E-02	-1.9547E-02	2.5221E-02	-2.255
87.89	-1.3832E-02	-1.9449E-02	2.3059E-02	-2.214
88.28	-1.2962E-02	-1.8127E-02	2.2285E-02	-2.192
88.67	-1.1482E-02	-1.7891E-02	2.1259E-02	-2.141
89.06	-1.0475E-02	-1.7967E-02	2.0798E-02	-2.099
89.45	-9.5596E-03	-1.8890E-02	2.1172E-02	-2.039
89.84	-1.0063E-02	-1.9508E-02	2.1951E-02	-2.047
90.23	-1.0132E-02	-2.1141E-02	2.3444E-02	-2.019
90.62	-1.0002E-02	-2.0073E-02	2.2427E-02	-2.033
91.02	-1.0857E-02	-1.8936E-02	2.1828E-02	-2.091
91.41	-1.2703E-02	-1.9188E-02	2.3012E-02	-2.156
91.80	-1.2764E-02	-1.7059E-02	2.1306E-02	-2.213
92.19	-1.2383E-02	-1.5640E-02	1.9949E-02	-2.240
92.58	-1.1116E-02	-1.4282E-02	1.8098E-02	-2.232
92.97	-1.0223E-02	-1.4175E-02	1.7477E-02	-2.196
93.36	-9.4833E-03	-1.3733E-02	1.6689E-02	-2.175
93.75	-8.2626E-03	-1.3634E-02	1.5942E-02	-2.116
94.14	-6.9885E-03	-1.4374E-02	1.5983E-02	-2.023
94.53	-6.9122E-03	-1.5717E-02	1.7169E-02	-1.985
94.92	-6.5536E-03	-1.6747E-02	1.7983E-02	-1.944
95.31	-7.7820E-03	-1.7746E-02	1.9377E-02	-1.984
95.70	-8.6517E-03	-1.6937E-02	1.9019E-02	-2.043
96.09	-8.5907E-03	-1.6090E-02	1.8240E-02	-2.061
96.48	-8.7738E-03	-1.4191E-02	1.6684E-02	-2.125
97.27	-7.8430E-03	-1.3443E-02	1.5564E-02	-2.099
97.66	-7.1259E-03	-1.3229E-02	1.5026E-02	-2.065
98.05	-6.9351E-03	-1.2810E-02	1.4567E-02	-2.067
98.44	-6.8130E-03	-1.3412E-02	1.5044E-02	-2.041
98.83	-6.3477E-03	-1.1932E-02	1.3516E-02	-2.060
99.22	-5.2261E-03	-1.1360E-02	1.2505E-02	-2.002
99.61	-3.7689E-03	-1.3733E-02	1.4241E-02	-1.839
100.0	-4.2725E-03	-1.4832E-02	1.5435E-02	-1.951
100.4	-4.7760E-03	-1.5030E-02	1.5770E-02	-1.878
100.8	-4.7760E-03	-1.5480E-02	1.6200E-02	-1.870
101.2	-7.1716E-03	-1.5999E-02	1.6715E-02	-2.014
101.6	-6.1646E-03	-1.3390E-02	1.4741E-02	-2.002
102.0	-6.1189E-03	-1.3451E-02	1.4777E-02	-1.998
102.3	-6.6452E-03	-1.2009E-02	1.3725E-02	-2.076
102.7	-6.1417E-03	-1.0712E-02	1.2347E-02	-2.091
103.1	-5.3329E-03	-1.1086E-02	1.2302E-02	-2.019
103.5	-5.1193E-03	-1.0345E-02	1.1543E-02	-2.030
103.9	-3.1204E-03	-9.9792E-03	1.0456E-02	-1.874
104.3	-3.9520E-03	-1.0179E-02	1.0919E-02	-1.941
104.7	-3.1662E-03	-9.9869E-03	1.0477E-02	-1.878
105.1	-2.3880E-03	-1.0049E-02	1.0328E-02	-1.804
105.5	[illegible]	-9.2468E-03	9.4752E-03	-1.791
105.9	[illegible]	-9.5373E-03	[illegible]	[illegible]
[illegible]	[illegible]	-9.6517E-03	[illegible]	[illegible]

107.0	2.2507E-03	-[illegible]719E-03	9.3798E-03	-1.299
107.4	4.2419E-03	-7.9727E-03	9.0310E-03	-1.082
107.8	5.3482E-03	-8.6823E-03	1.0197E-02	-1.019
108.2	6.8359E-03	-8.4991E-03	1.0907E-02	-0.8934
108.6	8.7814E-03	-9.4833E-03	1.2925E-02	-0.8238
109.0	1.0155E-02	-1.0231E-02	1.4415E-02	-0.7891
109.4	1.1719E-02	-1.0818E-02	1.5949E-02	-0.7455
109.8	1.3390E-02	-1.3084E-02	1.8721E-02	-0.7739
110.2	1.3893E-02	-1.4343E-02	1.9969E-02	-0.8013
110.5	1.7014E-02	-1.4153E-02	2.2130E-02	-0.6939
110.9	1.8822E-02	-1.7586E-02	2.5759E-02	-0.7515
111.3	2.2179E-02	-1.8883E-02	2.9128E-02	-0.7053
111.7	2.4666E-02	-2.4834E-02	3.5002E-02	-0.7888
112.1	2.7634E-02	-3.4821E-02	4.4453E-02	-0.9000
112.5	2.5139E-02	-4.5898E-02	5.2332E-02	-1.070
112.9	1.6930E-02	-5.7083E-02	5.9541E-02	-1.282
113.3	4.3945E-03	-6.1363E-02	6.1520E-02	-1.499
113.7	-9.0485E-03	-5.8655E-02	5.9349E-02	-1.724
114.1	-2.0393E-02	-5.2757E-02	5.6562E-02	-1.940
114.5	-2.6421E-02	-4.1435E-02	4.9142E-02	-2.138
114.8	-2.6398E-02	-3.3112E-02	4.2346E-02	-2.244
115.2	-2.4948E-02	-2.7313E-02	3.6992E-02	-2.311
115.6	-2.2324E-02	-2.1576E-02	3.1046E-02	-2.373
116.0	-2.0607E-02	-1.9234E-02	2.7516E-02	-2.417

116.9	-1.5976E-02	-1.5297E-02	2.2118E-02	-2.378
117.2	-1.5152E-02	-1.5732E-02	2.1842E-02	-2.337
117.6	-1.3924E-02	-1.4854E-02	2.0292E-02	-2.320
118.0	-1.1551E-02	-1.3298E-02	1.7614E-02	-2.286
118.4	-1.1002E-02	-1.3496E-02	1.7412E-02	-2.255
118.8	-9.8267E-03	-1.3626E-02	1.6800E-02	-2.196
119.1	-1.0483E-02	-1.2794E-02	1.6540E-02	-2.257
119.5	-9.9792E-03	-1.0628E-02	1.4579E-02	-2.325
119.9	-8.4991E-03	-1.1009E-02	1.3908E-02	-2.228
120.3	-8.1177E-03	-1.1688E-02	1.4231E-02	-2.178
120.7	-7.2479E-03	-1.0796E-02	1.3003E-02	-2.162
121.1	-5.2185E-03	-9.6512E-03	1.0972E-02	-2.065
121.5	-5.3635E-03	-9.1705E-03	1.0624E-02	-2.100
121.9	-4.4250E-03	-8.5907E-03	9.6634E-03	-2.046
122.3	-3.2579E-03	-8.4839E-03	9.0879E-03	-1.937
122.7	-2.5864E-03	-9.0561E-03	9.4182E-03	-1.849
123.0	-1.2665E-03	-8.9935E-03	8.9931E-03	-1.712
123.4	-1.1902E-03	-8.7991E-03	8.8693E-03	-1.705
123.8	2.5177E-04	-8.2321E-03	8.2360E-03	-1.540
124.2	6.9665E-04	-8.3771E-03	8.4052E-03	-1.489
124.6	2.0447E-03	-9.0942E-03	9.3213E-03	-1.350
125.0	2.8000E-03	-1.0612E-02	1.0976E-02	-1.313
125.4	1.0223E-03	-1.1597E-02	1.1642E-02	-1.483
125.8	5.9509E-04	-9.6283E-03	9.6467E-03	-1.509

126.6	3.2806E-03	-9.0948E-03	8.7343E-03	-1.186
127.0	4.3030E-03	-7.9880E-03	9.0732E-03	-1.077
127.3	4.6692E-03	-8.2016E-03	9.4376E-03	-1.053
127.7	5.5923E-03	-7.8735E-03	9.6575E-03	-0.9532
128.1	6.8359E-03	-7.6210E-03	1.0238E-02	-0.8397
128.5	7.2098E-03	-7.1487E-03	1.0153E-02	-0.7811
128.9	9.6207E-03	-8.1406E-03	1.2603E-02	-0.7023
129.3	1.0209E-02	-8.2855E-03	1.3147E-02	-0.6813
129.7	1.0666E-02	-9.8572E-03	1.4523E-02	-0.7460
130.1	1.1070E-02	-1.0437E-02	1.5215E-02	-0.7560
130.5	1.2520E-02	-9.7198E-03	1.5850E-02	-0.6602
130.9	1.4694E-02	-9.8953E-03	1.7715E-02	-0.5927
131.3	1.3702E-02	-1.0780E-02	1.7435E-02	-0.6666
131.6	1.6014E-02	-1.0910E-02	1.9377E-02	-0.5980
132.0	1.7303E-02	-1.3145E-02	2.1730E-02	-0.6497
132.4	1.6441E-02	-1.2062E-02	2.0391E-02	-0.6330
132.8	1.8242E-02	-1.2665E-02	2.2207E-02	-0.6069
133.2	1.7815E-02	-1.4679E-02	2.3083E-02	-0.6892
133.6	1.9600E-02	-1.4297E-02	2.4261E-02	-0.6302
134.0	2.1111E-02	-1.5701E-02	2.6309E-02	-0.6395
134.4	2.1304E-02	-1.8196E-02	2.8476E-02	-0.6932
134.8	2.0432E-02	-1.8733E-02	2.7723E-02	-0.7422
135.2	1.8761E-02	-2.1263E-02	2.8356E-02	-0.8478
135.5	1.6823E-02	-2.1461E-02	2.7269E-02	-0.9060
136.3	1.7220E-02	-1.9066E-02	2.56[illegible]1E-02	-0.8362
136.7	1.7319E-02	-1.7960E-02	2.4878E-02	-0.8008
137.1	1.9714E-02	-1.9356E-02	2.7628E-02	[illegible]
137.5	2.2285E-02	-1.9142E-02	2.9378E-02	-0.7097
137.9	2.1988E-02	-2.0416E-02	3.0005E-02	-0.7484
138.3	2.1904E-02	-2.0363E-02	2.9907E-02	-0.7490
138.7	2.3026E-02	-2.3010E-02	3.2552E-02	-0.7851
139.1	2.1614E-02	-2.2133E-02	3.0936E-02	-0.7973
139.5	2.0943E-02	-2.1446E-02	2.9976E-02	-6.7973
139.9	2.2072E-02	-2.0851E-02	3.0363E-02	-0.7570
140.2	2.3376E-02	-1.9417E-02	3.0389E-02	-0.6931
140.6	2.5737E-02	-1.9211E-02	3.2157E-02	-0.6403
141.0	2.6566E-02	-2.0996E-02	3.3861E-02	-0.6688
141.4	2.9587E-02	-2.0439E-02	3.5960E-02	-0.6045
141.8	3.0411E-02	-2.0592E-02	3.6726E-02	-0.5952
142.2	3.1013E-02	-2.1942E-02	3.7991E-02	-0.6157
142.6	3.3905E-02	-2.3682E-02	4.1357E-02	-0.6097
143.0	3.7659E-02	-2.4651E-02	4.5009E-02	-0.5796
143.4	3.6079E-02	-2.9481E-02	4.5966E-02	-0.6852
143.8	3.9268E-02	-2.9694E-02	4.9231E-02	-0.6474
144.1	3.9135E-02	-3.2402E-02	5.0846E-02	-0.6909
144.5	3.9970E-02	-3.3890E-02	5.2404E-02	-0.7033
144.9	3.9345E-02	-3.3623E-02	5.1754E-02	-0.7071
145.3	3.9666E-02	-3.4959E-02	5.2126E-02	-0.7351

146.1	4.1214E-02	-3.7964E-02	5.6031E-02	-0.7444
146.5	4.1412E-02	-3.7636E-02	5.5959E-02	-0.7377
146.9	4.3221E-02	-4.0743E-02	5.9401E-02	-0.7560
147.3	4.[illegible]151E-02	-4.1870E-02	6.0848E-02	-0.7589
147.7	4.4945E-02	-4.7348E-02	6.5293E-02	-0.8114
148.0	4.7928E-02	-5.0217E-02	6.9418E-02	-0.8087
148.4	4.7966E-02	-5.2986E-02	7.1472E-02	-0.8351
148.8	5.1239E-02	-4.9698E-02	7.1381E-02	-0.7701
149.2	5.3482E-02	-5.6351E-02	7.7690E-02	-0.8115
149.6	5.1636E-02	-5.8884E-02	7.8317E-02	-0.8509
150.0	5.0026E-02	-6.5842E-02	8.2691E-02	-0.9211
150.4	4.9614E-02	-6.7520E-02	8.3789E-02	-0.9371
150.8	4.8462E-02	-6.6925E-02	8.2629E-02	-0.9441
151.2	5.3169E-02	-7.2617E-02	9.0001E-02	-0.9388
151.6	5.0018E-02	-7.5607E-02	9.0655E-02	-0.9863
152.0	5.3566E-02	-7.6653E-02	9.3514E-02	-0.9609
152.3	5.4520E-02	-8.2405E-02	9.8808E-02	-0.9863
152.7	4.6753E-02	-9.0378E-02	0.1018	-1.093
153.1	4.8698E-02	-9.5474E-02	0.1072	-1.099
153.5	4.3739E-02	-9.8671E-02	0.1079	-1.154
153.9	4.0161E-02	-9.9831E-02	0.1076	-1.188
154.3	3.2913E-02	-0.1929	0.1078	-1.269
154.7	3.2869E-02	-0.1086	0.1135	-1.277
155.1	3.3539E-02	-0.1111	0.1161	-1.279
155.9	3.2945E-02	-0.1226	0.1269	-1.309
156.2	2.9411E-02	-0.1179	0.1215	-1.326
156.6	2.0187E-02	-0.1139	0.1156	-1.395
157.0	1.4122E-02	-0.1275	0.1282	-1.460
157.4	1.0460E-02	-0.1300	0.1304	-1.491
157.8	7.4768E-03	-0.1260	0.1263	-1.512
158.2	9.2163E-03	-0.1281	0.1284	-1.499
158.6	1.4618E-02	-0.1328	0.1336	-1.461
159.0	2.1744E-03	-0.1362	0.1363	-1.555
159.4	4.4250E-04	-0.1450	0.1450	-1.568
159.8	-9.7580E-03	-0.1651	0.1654	-1.630
160.2	-2.9686E-02	-0.1601	0.1628	-1.754
160.5	-3.3752E-02	-0.1615	0.1650	-1.777
160.9	-5.0768E-02	-0.1649	0.1757	-1.924
161.3	-6.8756E-02	-0.1502	0.1652	-2.000
161.7	-6.4316E-02	-0.1492	0.1625	-1.978
162.1	-8.7585E-02	-0.1367	0.1623	-2.141
162.5	-8.4099E-02	-0.1216	0.1478	-2.176
162.9	-9.8737E-02	-0.1255	0.1537	-2.186
163.3	-9.2331E-02	-0.1064	0.1409	-2.295
163.7	-9.5007E-02	-0.1023	0.1330	-2.264
164.1	-9.0477E-02	-0.1007	0.1354	-2.303
164.5	-8.8959E-02	-9.8356E-02	0.1254	-2.360
164.9	-9.5335E-02	-8.2130E-02	0.1184	-2.375

165.6	-9.0792E-02	-7.4952E-02	0.1177	-2.452
166.0	-9.3343E-02	-6.9374E-02	0.1128	-2.479
166.4	-9.6342E-02	-5.9906E-02	0.1051	-2.535
166.8	-8.6493E-02	-5.7602E-02	0.1038	-2.554
167.2	-8.3443E-02	-5.3795E-02	9.9280E-02	-2.569
167.6	-8.2268E-02	-5.1254E-02	9.6928E-02	-2.584
168.0	-8.0276E-02	-5.1659E-02	9.5462E-02	-2.570
168.4	-7.5813E-02	-5.1636E-02	9.1727E-02	-2.544
168.8	-7.7118E-02	-4.7958E-02	9.0814E-02	-2.585
169.1	-7.5470E-02	-4.1656E-02	8.6203E-02	-2.637
169.5	-7.2685E-02	-3.9284E-02	8.2622E-02	-2.646
169.9	-7.5164E-02	-4.0184E-02	8.5178E-02	-2.650
170.3	-6.6261E-02	-3.6682E-02	7.5737E-02	-2.636
170.7	-6.2187E-02	-3.4317E-02	7.1027E-02	-2.637
171.1	-6.8214E-02	-3.5446E-02	7.6874E-02	-2.662
171.5	-6.4125E-02	-3.5858E-02	7.3470E-02	-2.632
171.9	-6.1348E-02	-3.9665E-02	7.3054E-02	-2.569
172.3	-5.9052E-02	-3.0701E-02	6.6[illegible]55E-02	-2.662
172.7	-5.5023E-02	-2.9671E-02	6.2513E-02	-2.647
173.0	-5.4939E-02	-3.4561E-02	6.4906E-02	-2.580
173.4	-5.6694E-02	-3.3371E-02	6.5786E-02	-2.610
173.8	-4.8149E-02	-2.9953E-02	5.6706E-02	-2.585
174.2	-4.8454E-02	-2.7855E-02	5.5890E-02	-2.620
174.6	-4.4708E-02	-2.7275E-02	5.2371E-02	-2.594
175.4	-4.4670E-02	-3.6957E-02	5.7976E-02	-2.450
175.8	-4.2801E-02	-3.0663E-02	5.2651E-02	-2.520
176.2	-4.2671E-02	-3.3890E-02	5.4492E-02	-2.470
176.6	-4.0283E-02	-3.4393E-02	5.2969E-02	-2.435
177.0	-3.8734E-02	-3.3432E-02	5.1167E-02	-2.430
177.3	-4.0718E-02	-3.3478E-02	5.2714E-02	-2.453
177.7	-4.1336E-02	-3.7468E-02	5.5790E-02	-2.405
178.1	-3.8612E-02	-3.7521E-02	5.3840E-02	-2.371
178.5	-3.7918E-02	-4.4479E-02	5.8448E-02	-2.277
178.9	-4.1183E-02	-4.0886E-02	5.8032E-02	-2.360
179.3	-4.3945E-02	-4.4548E-02	6.2576E-02	-2.349
179.7	-4.7470E-02	-4.0977E-02	6.2710E-02	-2.429
180.1	-4.5899E-02	-4.2076E-02	6.2266E-02	-2.400
180.5	-4.2404E-02	-4.1298E-02	5.9191E-02	-2.369
180.9	-4.1924E-02	-4.0260E-02	5.8125E-02	-2.376
181.3	-3.8651E-02	-3.4477E-02	5.1793E-02	-2.413
181.6	-3.8940E-02	-3.7575E-02	5.4113E-02	-2.374
182.0	-3.6987E-02	-3.9146E-02	5.3956E-02	-2.328
182.4	-3.6926E-02	-4.2404E-02	5.6229E-02	-2.287
182.8	-4.1046E-02	-4.4617E-02	6.0625E-02	-2.315
183.2	-4.2900E-02	-4.5181E-02	6.2304E-02	-2.330
183.6	-4.1649E-02	-4.4731E-02	6.1119E-02	-2.321
184.0	-4.4870E-02	-4.3266E-02	6.2304E-02	-2.374
184.4	-4.7920E-02	-4.4273E-02	6.5242E-02	-2.396

185.2	-4.3022E-02	-3.9574E-02	5.8455E-02	-2.338
185.5	-3.9040E-02	-4.0230E-02	5.6058E-02	-2.341
185.9	-3.7964E-02	-4.3358E-02	5.7629E-02	-2.290
186.3	-3.2677E-02	-4.1542E-02	5.2854E-02	-2.237
186.7	-3.7170E-02	-4.5685E-02	5.8896E-02	-2.254
187.1	-3.3279E-02	-4.8553E-02	5.8864E-02	-2.172
187.5	-3.4462E-02	-5.3528E-02	6.3662E-02	-2.143
187.9	-4.3549E-02	-5.4672E-02	6.9897E-02	-2.243
188.3	-4.9179E-02	-5.7335E-02	7.5537E-02	-2.280
188.7	-5.5573E-02	-5.5962E-02	7.8867E-02	-2.353
189.1	-5.7541E-02	-5.1933E-02	7.7511E-02	-2.407
189.5	-5.4169E-02	-4.9835E-02	7.3606E-02	-2.398
189.8	-5.6374E-02	-5.1468E-02	7.6334E-02	-2.402
190.2	-5.5420E-02	-4.5036E-02	7.1412E-02	-2.459
190.6	-5.5122E-02	-4.5197E-02	7.1283E-02	-2.455
191.0	-5.8846E-02	-4.5479E-02	7.4371E-02	-2.484
191.4	-5.5694E-02	-3.9795E-02	6.9267E-02	-2.530
191.8	-5.2155E-02	-4.5547E-02	6.9244E-02	-2.424
192.2	-5.5107E-02	-4.3381E-02	7.0133E-02	-2.475
192.6	-5.6236E-02	-4.8195E-02	7.4063E-02	-2.433
193.0	-5.5168E-02	-5.3246E-02	7.6672E-02	-2.374
193.4	-6.4201E-02	-5.8563E-02	8.6899E-02	-2.402
193.8	-7.0259E-02	-4.6219E-02	8.4098E-02	-2.560
194.1	-7.1678E-02	-5.3131E-02	8.9223E-02	-2.504
194.9	-7.2433E-02	-3.5446E-02	8.0641E-02	-2.686
195.3	-6.7795E-02	-3.5896E-02	7.6712E-02	-2.655
195.7	-6.8634E-02	-2.9884E-02	7.4858E-02	-2.731
196.1	-6.5613E-02	-2.8595E-02	7.1573E-02	-2.731
196.5	-6.6460E-02	-2.9350E-02	7.2652E-02	-2.726
196.9	-7.2754E-02	-2.8847E-02	7.8264E-02	-2.764
197.3	-6.6154E-02	-2.6604E-02	7.1303E-02	-2.759
197.7	-6.8329E-02	-2.4353E-02	7.2539E-02	-2.799
198.0	-6.6559E-02	-2.1400E-02	6.9915E-02	-2.831
198.4	-6.6582E-02	-1.5366E-02	6.8332E-02	-2.915
198.8	-6.7062E-02	-1.8501E-02	6.9568E-02	-2.872
199.2	-6.4407E-02	-2.1774E-02	6.7988E-02	-2.816
199.6	-6.2225E-02	-1.7326E-02	6.4593E-02	-2.870

A Typical Record Taken From A Trace File

Trace of locations

Locations = Connectivity sequence for geometry locations
0 = Pen lift
Numbers = A line drawn between locations

LOCATIONS

1	2	3	4	5	6	7	8	0	6	10	0
4	12	0	9	10	11	12	9	5	11	0	9
13	15	17	0	11	14	16	18	0	15	16	0
17	18	0	19	20	0	21	22	0	23	24	0
25	26	0	23	19	22	26	23	0	24	20	21
25	24	0	16	31	29	0	18	30	0	27	28
30	29	27	0	32	31	0	15	19	0	17	22
0	23	27	0	26	29	0					

Trace of coordinates

Coordinates = Sequence in which functions are accessed, includes axis and sense direction.

COORDINATES

1Z+	2Z+	3Z+	4Z+	5Z+	6Z+	7Z+	8Z+	9Z+	11Z+
15Z+	16Z+	31Z+	19Z+	20Z+	24Z+	23Z+	21Z-	22Z-	25Z-
26Z-	29Z-	30Z-	27Z+	28Z+	27Y-	27X-	2Y-	3X+	

Disk Files For RHR Pump A-3, Equipment No. IP-48C

```
KRHRT .DAT     11 21-Jan-81- Trace
KRHRG .DAT      5 21-Jan-81- Geometry
KRHRH2.DAT    279 21-Jan-81- Function-X
KRHRZ .DAT     52 08-May-81- Project
KRHRP .DAT      9 21-Jan-81- Parameter
KRHRH1.DAT    279 21-Jan-81- Function-Z
KRHRS .DAT     61 23-Jan-81- Shape
```

```
 CHECKPOINT 050881-000000
Z KRHRZ          050881-000000   0/TPC RHR PUMP
P KRHRP          012181-000000   4/TPC RHR PUMP PARAMETERS
S KRHRS          012381-000000  10/TPC RHR PUMP SHAPES
G KRHRG          012181-000000   1/TPC RHR PUMP GEOMETRY
H KRHRH2         012181-000000  65/TPC RHR PUMP FUNCTIONS 36X-
T KRHRT          012181-000000  10/TPC RHR PUMP TRACES

P RECORDS IN USE
REC 1/2
REC 2/2

KRHRS
S RECORDS IN USE
REC 1/      17.390 HZ  SHAPE 1
REC 2/      17.390 HZ  SHAPE 1 MODIFIED
REC 3/      89.201 HZ  SHAPE 3
REC 4/      89.201 HZ  SHAPE 3 MODIFIED
REC 5/      87.010 HZ  Z-AXIS
REC 6/      87.010 HZ  SHAPE 5 MODIFIED
REC 7/      18.300 HZ  Z-AXIS
REC 8/      18.300 HZ  SHAPE 7 MODIFIED

T RECORDS IN USE
REC 1/LC
REC 2/C
REC 3/LC
REC 4/C
REC 5/C
```

GEOMETRY

LOC	X	Y	Z
1	0	0	26
2	0	4	23
3	0	4	16
4	0	20	16
5	0	35	16
6	0	50	16
7	0	51	14
8	-26	0	0
9	-23	4	0
10	-16	4	0
11	-16	20	0
12	-16	35	0
13	-16	50	0
14	-14	51	0
15	0	0	-26
16	0	4	-23
17	9	4	-16
18	0	20	-16
20	0	50	-16
21	0	51	-14
22	26	0	0
23	23	4	0
24	16	4	0
25	16	20	0
26	16	35	0
27	16	50	0
28	14	51	0
29	30	35	0
30	55	35	0
31	55	35	27
32	-29	35	0
33	-60	35	0
34	0	64	0
35	14	84	0
36	17	85	0
37	17	112	0
38	17	137	0
39	0	84	14
40	0	85	17
41	0	112	17
42	0	137	17
43	-14	84	0
44	-17	85	0
45	-17	112	0
46	-17	137	0
47	0	84	-14
48	0	85	-17
49	0	112	-17
50	0	137	-17
51	0	137	31
19	0	35	-16

H RECORDS IN USE

REC	1	36X-	2Z+	0
REC	2	36X-	2Y+	0
REC	3	36X-	4Z+	0
REC	4	36X-	5Z+	0
REC	5	36X-	6Z+	0
REC	6	36X-	6Y+	0
REC	7	36X-	13X-	0
REC	8	36X-	13Y-	0
REC	9	36X-	12X-	0
REC	10	36X-	11X-	0
REC	11	36X-	9X-	0
REC	12	36X-	9Y-	0
REC	13	36X-	16Y+	0
REC	14	36X-	16Z-	0
REC	15	36X-	18Z-	0
REC	16	36X-	19Z-	0
REC	17	36X-	20Z-	0
REC	18	36X-	20Y+	0
REC	19	36X-	27Y+	0
REC	20	36X-	27X+	0
REC	21	36X-	26X+	0
REC	22	36X-	25X+	0
REC	23	36X-	23X+	0
REC	24	36X-	23Y+	0
REC	25	36X-	29X+	0
REC	26	36X-	29Z+	0
REC	27	36X-	29Y+	0
REC	28	36X-	30Z-	0
REC	29	36X-	31Y+	0
REC	30	36X-	31X-	0
REC	31	36X-	33X+	0
REC	32	36X-	32Y+	0
REC	33	36X-	32Z+	0
REC	34	36X-	34X+	0
REC	35	36X-	34Z+	0
REC	36	36X-	34Y-	0
REC	37	36X-	40Z+	0
REC	38	36X-	41Z+	0
REC	39	36X-	42Z+	0
REC	40	36X-	42Y+	0
REC	41	36X-	38Y+	0
REC	42	36X-	38X+	0
REC	43	36X-	37X+	0
REC	44	36X-	36X+	0
REC	45	36X-	48Z-	0
REC	46	36X-	49Z-	0
REC	47	36X-	50Z-	0
REC	48	36X-	51Y+	0
REC	49	36X-	46Y+	0
REC	50	36X-	46X-	0
REC	51	36X-	45X-	0
REC	52	36X-	44X-	0
REC	53	36X-	44Y-	0
REC	54	36X-	39Y-	0
REC	55	36X-	51X+	0
REC	56	36X-	51Y+	0
REC	57	36X-	51Z+	0
REC	58	36X-	36X+	1
REC	59	36X-	36X+	2
REC	60	36X-	36X+	3
REC	61	36X-	36X+	4

H RECORDS IN USE

REC	1	48Z+	4Z+	0
REC	2	48Z+	2Y+	0
REC	3	48Z+	2Z+	0
REC	4	48Z+	5Z+	0
REC	5	48Z+	6Z+	0
REC	6	48Z+	6Y+	0
REC	7	48Z+	13X-	0
REC	8	48Z+	13Y-	0
REC	9	48Z+	12X-	0
REC	10	48Z+	11X-	0
REC	11	48Z+	9X-	0
REC	12	48Z+	9Y-	0
REC	13	48Z+	16Y+	0
REC	14	48Z+	16Z-	0
REC	15	48Z+	18Z-	0
REC	16	48Z+	19Z-	0
REC	17	48Z+	20Z-	0
REC	18	48Z+	20Y+	0
REC	19	48Z+	27Y+	0
REC	20	48Z+	27X+	0
REC	21	48Z+	26X+	0
REC	22	48Z+	25X+	0
REC	23	48Z+	23X+	0
REC	24	48Z+	23Y+	0
REC	25	48Z+	29X+	0
REC	26	48Z+	29Z+	0
REC	27	48Z+	29Y+	0
REC	28	48Z+	30Z-	0
REC	29	48Z+	31Y+	0

REC	30	48Z+	31X-	0
REC	31	48Z+	33X+	0
REC	32	48Z+	32Y+	0
REC	33	48Z+	32Z+	0
REC	34	48Z+	34X+	0
REC	35	48Z+	34Z+	0
REC	36	48Z+	34Y-	0
REC	37	48Z+	40Z+	0
REC	38	48Z+	41Z+	0
REC	39	48Z+	42Z+	0
REC	40	48Z+	42Y+	0
REC	41	48Z+	38Y+	0
REC	42	48Z+	38X+	0
REC	43	48Z+	37X+	0
REC	44	48Z+	36X+	0
REC	45	48Z+	48Z-	0
REC	46	48Z+	49Z-	0
REC	47	48Z+	50Z-	0
REC	48	48Z+	50Y+	0
REC	49	48Z+	46Y+	0
REC	50	48Z+	46X-	0
REC	51	48Z+	45X-	0
REC	52	48Z+	44X-	0
REC	53	48Z+	44Y-	0
REC	54	48Z+	39Y-	0
REC	55	48Z+	51X+	0
REC	56	48Z+	51Y+	0
REC	57	48Z+	51Z+	0
REC	58	48Z+	51X+	4

81036
May 15, 1981

Disk Files For Jet Pump Instrumentation Panel B, Equipment No. R-53-H22-P009

```
JPCPP .DAT      9 20-Jan-81- Parameter
JPCPS .DAT    121 20-Jan-81- Shapes-Shaker
JPCPH1.DAT    556 20-Jan-81- Function-Z Shaker
JPCPH3.DAT    215 21-Jan-81- Function-X-Hammer
JPCPG .DAT      5 20-Jan-81- Geometry
JPCPT .DAT     11 20-Jan-81- Trace
JPCPS1.DAT    133 03-Feb-81- Shape-Hammer
JPCPH2.DAT     87 20-Jan-81- Function-Special Points
JPCPZ .DAT     52 08-May-81- Project
```

```
 CHECKPOINT 050881-000000
Z JPCPZ          050881-000000   0/TPC JET PUMP CONTROL PANEL
P JPCPP          012081-000000   4/TPC JET PUMP CNTL PNL PARAMETERS
S JPCPS          012081-000000  20/TPC JET PUMPCNTL PNL SHAPES
G JPCPG          012081-000000   1/TPC JET PUMP CNTL PNL GEOMETRY
H JPCPH1         012081-000000 130/TPC JET PUMP CNTL PNL FUNCS 59Z
T JPCPT          012081-000000  10/TPC JET PUMP CNTL PNL TRACES

P RECORDS IN USE
REC 1 11
REC 2 1
REC 3 8

JPCPS
S RECORDS IN USE
REC 1       22.730 HZ  Z-AXIS SHAPE 1
REC 2       34.957 HZ  Z-AXIS SHAPE 2
REC 3       38.370 HZ  Z-AXIS SHAPE 3
REC 4       44.899 HZ  Z-AXIS SHAPE 4
REC 5       48.240 HZ  Z-AXIS SHAPE 5
REC 6       53.810 HZ  Z-AXIS SHAPE 6
REC 7       58.450 HZ  Z-AXIS SHAPE 7
REC 8       60.080 HZ  Z-AXIS SHAPE 8
REC 9       22.730 HZ  Z-AXIS SHAPE 1 MODIFIED
REC 10       34.957 HZ  Z-AXIS SHAPE 2 MODIFIED
REC 11       38.370 HZ  Z-AXIS SHAPE 3 MODIFIED
REC 12       44.899 HZ  Z-AXIS SHAPE 4 MODIFIED
REC 13       48.240 HZ  Z-AXIS SHAPE 5 MODIFIED
REC 14       53.810 HZ  Z-AXIS SHAPE 6 MODIFIED
REC 15       58.450 HZ  Z-AXIS SHAPE 7 MODIF.ED
REC 16       60.080 HZ  Z-AXIS SHAPE 8 MODIFIED
```

```
JPCPS1
S RECORDS IN USE
REC 1      19.870 HZ  SHAPE 1
REC 2      21.720 HZ  SHAPE 2
REC 3      31.450 HZ  SHAPE 3
REC 4      34.570 HZ  SHAPE 4
REC 5      42.260 HZ  SHAPE 5
REC 6      52.000 HZ  SHAPE 6
REC 7      64.010 HZ  SHAPE 7
REC 8      78.410 HZ  SHAPE 8
REC 9      85.290 HZ  SHAPE 9
REC 10      89.030 HZ  SHAPE 10
REC 11      94.350 HZ  SHAPE 11
REC 12      19.870 HZ  HAMMER SHAPE 1 MODIFIED
REC 13      21.720 HZ  HAMMER SHAPE 2 MODIFIED
REC 14      31.450 HZ  HAMMER SHAPE 3 MODIFIED
REC 15      34.570 HZ  HAMMER SHAPE 4 MODIFIED
REC 16      42.260 HZ  HAMMER SHAPE 5 MODIFIED
REC 17      52.000 HZ  HAMMER SHAPE 6 MODIFIED
REC 18      64.010 HZ  HAMMER SHAPE 7 MODIFIED
REC 19      [illegible]8.410 HZ  HAMMER SHAPE 8 MODIFIED
REC 20      85.290 HZ  HAMMER SHAPE 9 MODIFIED
REC 21      89.030 HZ  HAMMER SHAPE 10 MODIFIED
REC 22      94.350 HZ  HAMMER SHAPE 11 MODIFIED

T RECORDS IN USE
REC 1 LC
REC 2 LC
REC 3 LC
REC 4 LC
REC 5 LC
REC [illegible] LC
REC [illegible] [illegible]C
REC 8 C
REC 9 C


H RECORDS IN USE
REC   1  59Z+  90X+   0
REC   2  59Z+  90Y+   0
REC   3  59Z+  90Z+   0
REC   4  59Z+  91X+   0
REC   5  59Z+  91Y+   0
REC   6  59Z+  91Z+   0
REC   7  59Z+  92X+   0
REC   8  59Z+  92Y+   0
REC   9  59Z+  92Z+   0
REC  10  59Z+  59Z+  15
REC  11  59Z+  59Z+   3
```

H RECORDS IN USE

REC	1	7X-	7X+	1
REC	2	7X-	7X+	2
REC	3	7X-	7X+	3
REC	4	7X-	7X+	4
REC	5	7X-	1X+	0
REC	6	7X-	2X+	0
REC	7	7X-	3X+	0
REC	8	7X-	3Z-	0
REC	9	7X-	4X+	0
REC	10	7X-	4Z-	0
REC	11	7X-	5X+	0
REC	12	7X-	5Z-	0
REC	13	7X-	6X+	0
REC	14	7X-	6Z-	0
REC	15	7X-	7Z-	0
REC	16	7X-	77X+	0
REC	17	7X-	77Z+	0
REC	18	7X-	78X+	0
REC	19	7X-	79X+	0
REC	20	7X-	80X+	0
REC	21	7X-	80Z+	0
REC	22	7X-	81X+	0
REC	23	7X-	82X+	0
REC	24	7X-	82Z+	0
REC	25	7X-	83X+	0
REC	26	7X-	70X+	0
REC	27	7X-	71X+	0
REC	28	7X-	71Z+	0
REC	29	7X-	72X+	0
REC	30	7X-	72Z+	0
REC	31	7X-	73X+	0
REC	32	7X-	73Z+	0
REC	33	7X-	74X+	0
REC	34	7X-	74Z+	0
REC	35	7X-	75X+	0
REC	36	7X-	75Z+	0
REC	37	7X-	76X+	0
REC	38	7X-	76Z+	0
REC	39	7X-	7X+	15
REC	40	7X-	7X+	16

H RECORDS IN USE

REC	1	59Z+	2Z+	0
REC	2	59Z+	3Z+	0
REC	3	59Z+	1Z+	0
REC	4	59Z+	2Z+	0
REC	5	59Z+	3Z+	0
REC	6	59Z+	4Z+	0
REC	7	59Z+	4X-	0
REC	8	59Z+	5Z+	0
REC	9	59Z+	5X-	0
REC	10	59Z+	6Z+	0
REC	11	59Z+	6X-	0
REC	12	59Z+	7Z+	0
REC	13	59Z+	7X-	0
REC	14	59Z+	7Y+	0
REC	15	59Z+	8Z+	0
REC	16	59Z+	9Z+	0
REC	17	59Z+	10Z+	0
REC	18	59Z+	11Z+	0
REC	19	59Z+	12Z+	0
REC	20	59Z+	12Y+	0
REC	21	59Z+	13Z+	0
REC	22	59Z+	14Z+	0
REC	23	59Z+	15Z+	0
REC	24	59Z+	16Z+	0
REC	25	59Z+	17Z+	0
REC	26	59Z+	17Y+	0
REC	27	59Z+	18Z+	0
REC	28	59Z+	19Z+	0
REC	29	59Z+	20Z+	0
REC	30	59Z+	21Z+	0
REC	31	59Z+	22Z+	0
REC	32	59Z+	23Z+	0
REC	33	59Z+	24Z+	0
REC	34	59Z+	24X+	0
REC	35	59Z+	24Y+	0
REC	36	59Z+	25Z+	0
REC	37	59Z+	26Z+	0
REC	38	59Z+	27Z+	0
REC	39	59Z+	28Z+	0
REC	40	59Z+	29Z+	0
REC	41	59Z+	29Y+	0
REC	42	59Z+	30Z+	0
REC	43	59Z+	31Z+	0
REC	44	59Z+	32Z+	0
REC	45	59Z+	33Z+	0
REC	46	59Z+	33X+	0
REC	47	59Z+	34Z+	0
REC	48	59Z+	34Z+	0
REC	49	59Z+	35Z+	0
REC	50	59Z+	34Y+	0
REC	51	59Z+	35X+	0
REC	52	59Z+	36Z+	0
REC	53	59Z+	36X+	0
REC	54	59Z+	36Y+	0
REC	55	59Z+	43Y+	0
REC	56	59Z+	43X+	0
REC	57	59Z+	42X+	0
REC	58	59Z+	41X+	0
REC	59	59Z+	49X+	0
REC	60	59Z+	39X+	0
REC	61	59Z+	38X+	0
REC	62	59Z+	37X+	0
REC	63	59Z+	44Z-	0
REC	64	59Z+	45Z-	0
REC	65	59Z+	46Z-	0
REC	66	59Z+	47Z+	0
REC	67	59Z+	47X+	0
REC	68	59Z+	48Z-	0
REC	69	59Z+	49X+	0
REC	70	59Z+	48X+	0
REC	71	59Z+	49Z-	0
REC	72	59Z+	50X+	0
REC	73	59Z+	50Z-	0
REC	74	59Z+	50Y+	0
REC	75	59Z+	51Z-	0
REC	76	59Z+	52Z-	0
REC	77	59Z+	53Z-	0
REC	78	59Z+	61Z-	0
REC	79	59Z+	61Y+	0
REC	80	59Z+	60X+	0
REC	81	59Z+	60Z-	0
REC	82	59Z+	60Y+	0
REC	83	59Z+	59Z-	0
REC	84	59Z+	59X+	0
REC	85	59Z+	58Z-	0
REC	86	59Z+	58X+	0
REC	87	59Z+	57Z-	0
REC	88	59Z+	57X+	0
REC	89	59Z+	56X+	0
REC	90	59Z+	56Z-	0
REC	91	59Z+	55Z-	0
REC	92	59Z+	54Z-	0
REC	93	59Z+	62Z-	0
REC	94	59Z+	63Z-	0
REC	95	59Z+	64Z-	0
REC	96	59Z+	65Z-	0
REC	97	59Z+	66Z-	0
REC	98	59Z+	67Z-	0
REC	99	59Z+	68Z-	0
REC	100	59Z+	68Y+	0
REC	101	59Z+	69Z-	0
REC	102	59Z+	69Y+	0
REC	103	59Z+	76Y+	0
REC	104	59Z+	76X-	0
REC	105	59Z+	76Z-	0
REC	106	59Z+	75Z-	0
REC	107	59Z	75X-	0
REC	108	59Z+	74Z-	0
REC	109	59Z+	74X-	0
REC	110	59Z+	73Z-	0
REC	111	59Z+	73X-	0
REC	112	59Z+	72X-	0
REC	113	59Z+	72Z-	0
REC	114	59Z+	71Z-	0
REC	115	59Z+	70Z-	0
REC	116	59Z+	71X-	0
REC	117	59Z+	83X-	0
REC	118	59Z+	82X-	0
REC	119	59Z+	81X-	0
REC	120	59Z+	80X-	0
REC	121	59Z+	79X-	0

GEOMETRY

LOC	X	Y	Z
1	0	0	0
2	0	14	0
3	0	29	0
4	0	43	0
5	0	57	0
6	0	70	0
7	0	84	0
8	25	0	0
9	25	29	12
10	25	51	12
11	25	77	12
12	25	84	0
13	47	0	0
14	47	29	12
15	47	51	12
16	47	77	12
17	47	84	0
18	72	0	0
19	72	14	0
20	72	29	0
21	72	43	0
22	72	57	0
23	72	70	0
24	72	84	0
25	97	0	0
26	97	29	12
27	97	51	12
28	97	77	12
29	97	84	0
30	120	0	0
31	120	14	0
32	120	29	0
33	120	43	0
34	120	57	0
35	120	70	0
36	120	84	0
37	120	0	12
38	120	14	12
39	120	29	12
40	120	43	12
41	120	57	12
42	120	70	12
43	120	84	12
44	120	0	30
45	120	14	30
46	120	29	30
47	120	43	30
48	120	57	30
49	120	70	30
50	120	84	30
51	97	0	30
52	97	23	21
53	97	43	12
54	72	0	30
55	72	14	30
56	72	29	30
57	72	43	30
58	72	57	30
59	72	70	30
60	72	84	30
61	97	84	30
62	47	0	30
63	47	23	21
64	47	43	12
65	25	0	30
66	25	23	21
67	25	43	12
68	47	84	30
69	25	84	30
70	0	0	30
71	0	14	30
72	0	29	30
73	0	43	30
74	0	57	30
75	0	70	30
76	0	84	30
77	0	84	12
78	0	70	12
79	0	57	12
80	0	43	12
81	0	29	12
82	0	14	12
83	0	0	12
84	72	51	12
85	72	29	12
86	72	77	12

81036
May 15, 1981

Disk Files For Recirculation Control Valve B, Equipment No. R-57-B33-V003

```
KRRVP .DAT      9 23-Jan-81- Parameter
KRRVG .DAT      5 23-Jan-81- Geometry
KRRVH2.DAT    194 23-Jan-81- Function - Z
KRRVH .DAT    215 27-Feb-81- Function - Y
KRRVZ .DAT     52 08-May-81- Project
KRRVT .DAT     11 23-Jan-81- Trace
KRRVS .DAT    121 23-Jan-81- Shape    - Y
KRRVS2.DAT     61 04-Mar-81- Shape    - Z
```

```
 CHECKPOINT 050881-000000
Z KRRVZ         050881-000000   0/TPC REACTOR RECIRC VALVE
P KRRVP         012381-000000   4/TPC REACTOR RECIRC VALVE PARAMS
S KRRVS         012381-000000  20/TPC REACTOR RECIRC VALVE SHAPES
G KRRVG         012381-000000   1/TPC REACTOR RECIRC VALVE GEOM
H KRRVH2        012381-000000  45/TPC REAC. RECIRC VALVE FUNCTIONS YZ
T KRRVT         012381-000000  10/TPC REACTOR RECIRC VALVE TRACES

P RECORDS IN USE
REC 1 8
REC 2 5

KRRVS
S RECORDS IN USE
REC 1       18.970 HZ  Y-DIR SHAPE #1
REC 2       22.570 HZ  Y-DIR SHAPE #2
REC 3       30.700 HZ  Y-DIR SHAPE #3
REC 4       38.360 HZ  Y-DIR SHAPE #4
REC 5       40.870 HZ  Y-DIR SHAPE #5
REC 6       45.210 HZ  Y-DIR SHAPE #6
REC 7       47.970 HZ  Y-DIR SHAPE #7
REC 8       89.900 HZ  Y-DIR SHAPE #8
REC 9       18.970 HZ  SHAPE #1 MODIFIED
REC 10       22.570 HZ  SHAPE #2 MODIFIED
REC 11       30.700 HZ  SHAPE #3 MODIFIED
REC 12       38.360 HZ  SHAPE #4 MODIFIED
REC 13       40.870 HZ  SHAPE #5 MODIFIED
REC 14       45.210 HZ  SHAPE #6 MODIFIED
REC 15       47.970 HZ  SHAPE #7 MODIFIED
REC 16       89.900 HZ  SHAPE #8 MODIFIED
```

```
KRRUS2
S RECORDS IN USE
REC 1     16.210 HZ  Z-DIR SHAPE #1
REC 2     27.070 HZ  Z-DIR SHAPE #2
REC 3     32.595 HZ  Z-DIR SHAPE #3
REC 4     37.980 HZ  Z-DIR SHAPE #4
REC 5     54.290 HZ  Z-DIR SHAPE #5
REC 6     16.210 HZ  SHAPE 1 MODIFIED
RE[illegible]     27.070 HZ  SHAPE 2 MODIFIED
[illegible]     32.595 HZ  SHAPE 3 MODIFIED
[illegible]     37.980 HZ  SHAPE 4 MODIFIED
REC 10     54.290 HZ  SHAPE 5 MODIFIED

T RECORDS IN USE
REC 1 LC
```

GEOMETRY

LOC	X	Y	Z
1	22	0	0
2	0	0	0
3	0	-18	0
4	-30	0	0
5	0	16	0
6	9	27	0
7	0	36	0
8	0	45	0
9	20	36	0
10	39	36	0
11	36	36	0
12	62	36	0
13	63	36	0
14	99	36	0
15	107	36	0

H RECORDS IN USE

REC	1	9Y+	1Y+	0
REC	2	9Y+	1Z+	0
REC	3	9Y+	2Z+	0
REC	4	9Y+	3Y+	0
REC	5	9Y+	3Z+	0
REC	6	9Y+	4Z+	0
REC	7	9Y+	4Y+	0
REC	8	9Y+	5Z+	0
REC	9	9Y+	6Z+	0
REC	10	9Y+	Z+	0
REC	11	9Y+	8Y+	0
REC	12	9Y+	8Y+	0
REC	13	9Y+	8Z-	0
REC	14	9Y+	9Z-	0
REC	15	9Y+	9Y+	0
REC	16	9Y+	10Z-	0
REC	17	9Y+	10Y+	0
REC	18	9Y+	11Z-	0
REC	19	9Y+	11Y+	0
REC	20	9Y+	12Z-	0
REC	21	9Y+	12Y+	0
REC	22	9Y+	13Z-	0
REC	23	9Y+	13Y+	0
REC	24	9Y+	14Z-	0
REC	25	9Y+	14Y+	0
REC	26	9Y+	15Z-	0
REC	27	9Y+	15Y+	0
REC	28	9Y+	15Y+	0
REC	29	9Y+	3Y-	0
REC	30	9Y+	9Y+	3
REC	31	9Y+	9Y+	2
REC	32	9Y+	9Y+	4
REC	33	9Y+	9Y+	1
REC	34	9Y+	9Y+	15
REC	35	9Y+	9Y+	16

H RECORDS IN USE

REC	1	7Z+	7Z+	16
REC	2	7Z+	7Z+	4
REC	3	7Z+	1Y+	0
REC	4	7Z+	1Z+	0
REC	5	7Z+	2Z+	0
REC	6	7Z+	3Y+	0
REC	7	7Z+	7Z+	15
REC	8	7Z+	3Z+	0
REC	9	7Z+	4Z+	0
REC	10	7Z+	4Y+	0
REC	11	7Z+	5Z+	0
REC	12	7Z+	6Z+	0
REC	13	7Z+	7Z+	0
REC	14	7Z+	8Y+	0
REC	15	7Z+	8Y+	0
REC	16	7Z+	8Z-	0
REC	17	7Z+	9Z-	0
REC	18	7Z+	9Y+	0
REC	19	7Z+	10Z-	0
REC	20	7Z+	10Y+	0
REC	21	7Z+	11Z-	0
REC	22	7Z+	11Y+	0
REC	23	7Z+	12Z-	0
REC	24	7Z+	12Y+	0
REC	25	7Z+	13Z-	0
REC	26	7Z+	13Y+	0
REC	27	7Z+	14Z-	0
REC	28	7Z+	14Y+	0
REC	29	7Z+	15Z-	0
REC	30	7Z+	15Y+	0
REC	31	7Z+	15Y+	0
REC	32	7Z+	3Y-	0

Disk Files For 3" Motor Operated Valve Near V-8 SRV Discharge

```
08-May-81
K3ING .DAT      5 18-Jan-81- Geometry
K3INP .DAT      9 18-Jan-81- Parameter
K3INH1.DAT    194 19-Jan-81- Function  - X
K3INH3.DAT    194 19-Jan-81- Function  - Z
K3INSZ.DAT    121 05-Mar-81- Shape     - Z
K3INZ .DAT     52 08-May-81- Project
K3INT .DAT      7 18-Jan-81- Trace
K3INSX.DAT     61 21-Jan-81- Shape     - X
K3INH2.DAT    194 19-Jan-81- Function  - Y
K3INSY.DAT    121 26-Feb-81- Shape     - Y
K3INP1.DAT      9 10-Mar-81- Parameter - Hi/Lo


 CHECKPOINT 050881-000090
Z K3INZ          050881-000000   0/TAIPOWER 3" VALVE PROJECT
P K3INP          011881-000000   4/TAIPOWER 3" VALVE PARAMETERS
S K3INSZ         030581-000000  20/TAIPOWER 3" VALVE SHAPES 29Z-
G K3ING          011881-000000   1/TAIPOWER 3" VALVE GEOMETRY
H K3INH3         011981-000000  45/TAIPOWER 3" VALVE Z-FUNCTIONS
T K3INT          011881-000000   0/TAIPOWER 3" VALVE TRACES

P RECORDS IN USE
REC 1 5
REC 2 7
REC 3 9
REC 4 11

K3INSZ
S RECORDS IN USE
REC 1      20.550 HZ  Z-AXIS SHAPE 1
REC 2      29.800 HZ  Z-AXIS SHAPE 2
REC 3      44.070 HZ  Z-AXIS SHAPE 3
REC 4      48.220 HZ  Z-AXIS SHAPE 4
REC 5      49.330 HZ  Z-AXIS SHAPE 5
REC 6      72.370 HZ  Z-AXIS SHAPE 6
REC 7      75.780 HZ  Z-AXIS SHAPE 7
REC 8      79.890 HZ  Z-AXIS SHAPE 8
REC 9      29.610 HZ  Z-AXIS SHAPE 9
REC 10      30.190 HZ  Z-AXIS SHAPE 10
REC 11      20.550 HZ  SHAPE 1 MODIFIED
REC 12      29.900 HZ  SHAPE 2 MODIFIED
REC 13      44.070 HZ  SHAPE 3 MODIFIED
REC 14      48.220 HZ  SHAPE 4 MODIFIED
REC 15      49.330 HZ  SHAPE 5 MODIFIED
REC 16      72.370 HZ  SHAPE 6 MODIFIED
REC 17      75.780 HZ  SHAPE 7 MODIFIED
REC 18      79.890 HZ  SHAPE 9 MODIFIED
REC 19      29.610 HZ  SHAPE 9 MODIFIED
REC 20      30.190 HZ  SHAPE 10 MODIFIED
```

```
K3INSY
S RECORDS IN USE
REC 1      21.891 HZ  Y-AXIS 3" VALUE
REC 2      29.650 HZ  Y-AXIS 3" VALUE
REC 3      44.780 HZ  Y-AXIS 3" VALUE
REC 4      48.110 HZ  Y-AXIS 3" VALUE
REC 5      49.540 HZ  Y-AXIS 3" VALUE
REC 6      75.070 HZ  Y-AXIS 3" VALUE
REC 11      21.891 HZ  SHAPE 1 MODIFIED
REC 12      29.650 HZ  SHAPE 2 MODIFIED
REC 13      44.780 HZ  SHAPE 3 MODIFIED
REC 14      48.110 HZ  SHAPE 4 MODIFIED
REC 15      49.540 HZ  SHAPE 5 MODIFIED
REC 16      75.070 HZ  SHAPE 6 MODIFIED

K3INSX
S RECORDS IN USE
REC 1      18.190 HZ  SHAPE # 1
REC 2      21.329 HZ  SHAPE #2
REC 3      30.140 HZ  SHAPE #3
REC 4      33.410 HZ  SHAPE #4
REC 5      74.570 HZ  SHAPE #5
REC 6      74.570 HZ  SHAPE 5 MODIFIED
REC 7      18.190 HZ  SHAPE 1 MODIFIED
REC 8      21.329 HZ  SHAPE 2 MODIFIED
REC 9      30.140 HZ  SHAPE 3 MODIFIED
REC 10      33.410 HZ  SHAPE 4 MODIFIED

T RECORDS IN USE
REC 1 LC
REC 2 LC
REC 3 C

K3INP1 HI-LO FORCE
P RECORDS IN USE
REC 1 11
REC 2 14
REC 3 18
```

H RECORDS IN USE

REC	1	29X+	3X-	0
REC	2	29X+	3X-	0
REC	3	29X+	4X-	0
REC	4	29X+	5X-	0
REC	5	29X+	6X-	0
REC	6	29X+	7X-	0
REC	7	29X+	8X+	0
REC	8	29X+	9X+	0
REC	9	29X+	11X+	0
REC	10	29X+	13X-	0
REC	11	29X+	14X+	0
REC	12	29X+	15X-	0
REC	13	29X+	17X-	0
REC	14	29X+	20X-	0
REC	15	29X+	21X-	0
REC	16	29X+	24X-	0
REC	17	29X+	25X-	0
REC	18	29X+	27X-	0
REC	19	29X+	29X-	4
REC	20	29X+	29X-	16
REC	21	29X+	29X-	3
REC	22	29X+	2.X+	0
REC	23	29X+	30X+	0
REC	24	29X+	31X+	0
REC	25	29X+	16X+	0
REC	26	29X+	18X+	0
REC	27	29X+	29Y-	0
REC	28	29X+	29Z-	3
REC	29	29X+	21Y+	0
REC	30	29X+	21Z-	0
REC	31	29X+	5Z+	0
REC	32	27X+	28X+	10
REC	33	27X+	28X+	11
REC	34	27X+	28X+	12
REC	35	27X+	28X+	13
REC	36	27X+	28X+	6
REC	37	27X+	28X+	7
REC	38	27X+	28X+	8
REC	39	27X+	28X+	9
REC	40	29X+	29X-	15
REC	41	29X+	29X-	2
REC	42	29X+	29X-	0
REC	43	29X+	29X-	1

H TAIPCHER 3" VALVE Y-FUNCTIONS
H RECORDS IN USE

REC	1	25Y+	1Y-	0
REC	2	25Y+	2Y-	0
REC	3	25Y+	5Y-	0
REC	4	25Y+	7Y-	0
REC	5	25Y+	8Y-	0
REC	6	25Y+	10Y+	0
REC	7	25Y+	13Y+	0
REC	8	25Y+	14Y+	0
REC	9	25Y+	15Y+	0
REC	10	25Y+	16Y+	0
REC	11	25Y+	17Y+	0
REC	12	25Y+	18Y+	0
REC	13	25Y+	19Y+	0
REC	14	25Y+	20Y+	0
REC	15	25Y+	21Y+	0
REC	16	25Y+	22Y+	0
REC	17	25Y+	31Y+	0
REC	18	25Y+	32Y+	0
REC	19	25Y+	23Y-	0
REC	20	25Y+	24Y-	0
REC	21	25Y+	25Y-	4
REC	22	25Y+	25Y-	3
REC	23	25Y+	25Y-	2
REC	24	25Y+	25Y-	1
REC	25	25Y+	26Y-	0
REC	26	25Y+	27Y-	0
REC	27	25Y+	28Y-	0
REC	28	25Y+	29Y-	0
REC	29	25Y+	30Y-	0
REC	30	25Y+	3Z+	0
REC	31	25Y+	4Z+	0
REC	32	25Y+	5Z+	0
REC	33	25Y+	6Z+	0
REC	34	25Y+	7Z+	0
REC	35	25Y+	5X-	0
REC	36	25Y+	29X-	0
REC	37	25Y+	29Z-	9
REC	38	30Y+	30Y-	6
REC	39	30Y+	30Y-	7
REC	40	30Y+	30Y-	8
REC	41	30Y+	30Y-	9
REC	42	30Y+	30Y-	10
REC	43	30Y+	30Y-	11
REC	44	30Y+	30Y-	12
REC	45	30Y+	30Y-	13

```
H TAIPOWER 3" VALVE Z-FUNCTIONS
H RECORDS IN USE
REC    1  29Z+    1Z+   0
REC    2  29Z+    2Z+   0
REC    3  29Z+    3Z+   0
REC    4  29Z+    4Z+   0
REC    5  29Z+    5Z+   0
REC    6  29Z+    6Z+   0
REC    7  29Z+    7Z+   0
REC    8  29Z+    8Z+   0
REC    9  29Z+    9Z+   0
REC   10  29Z+   11Z+   0
REC   11  29Z+   15Z+   0
REC   12  29Z+   16Z+   0
REC   13  29Z+   31Z+   0
REC   14  29Z+   19Z+   0
REC   15  29Z+   20Z+   0
REC   16  29Z+   24Z+   0
REC   17  29Z+   23Z+   0
REC   18  29Z+   21Z-   0
REC   19  29Z+   22Z-   0
REC   20  29Z+   25Z-   0
REC   21  29Z+   26Z-   0
REC   22  29Z+   29Z-   4
REC   23  29Z+   29Z-   3
REC   24  29Z+   29Z-   2
REC   25  29Z+   30Z-   0
REC   26  29Z+   27Z+   0
REC   27  29Z+   28Z+   0
REC   28  29Z+   27Y-   0
REC   29  29Z+   27X-   0
REC   30  29Z+    2Y-   0
REC   31  29Z+    3X+   0
REC   32  29Z+   27Z+   6
REC   33  29Z+   27Z+   7
REC   34  29Z+   27Z+   8
REC   35  29Z+   27Z+   9
REC   36  29Z+   27Z+  10
REC   37  29Z+   27Z+  11
REC   38  29Z+   27Z+  12
REC   39  29Z+   27Z+  13
REC   40  29Z+   29Z-   1
REC   41  29Z+   29Z-   0
```

GEOMETRY

LOC	X	Y	Z
1	25	18	0
2	6	16	0
3	0	12	0
4	0	6	0
5	0	0	0
6	0	-6	0
7	0	-17	0
8	0	-22	0
9	4	0	7
10	0	-4	7
11	-4	0	7
12	0	4	7
13	2	0	14
14	-2	0	14
15	3	-3	21
16	-3	-3	21
17	3	-3	25
18	-3	-3	25
19	6	-1	21
20	13	-1	21
21	13	-1	25
22	6	-1	25
23	6	4	21
24	13	4	21
25	13	4	25
26	6	4	25
27	4	16	18
28	-3	16	18
29	4	16	24
30	-3	16	24
31	-4	3	21
32	-7	3	21

Disk Files For 480V Motor Control Center 1C1D (Located in Auxiliary Building)

```
KMCCG .DAT     5 26-Jan-81 - Geometry
KMCCP .DAT     9 26-Jan-81 - Parameter
KMCCH2.DAT   215 26-Jan-81 - Function-Front
KMCCS .DAT    73 03-Feb-81 - Shape
KMCCZ .DAT    52 08-May-81 - Project
KMCCT .DAT    11 26-Jan-81 - Trace
KMCCH1.DAT   215 26-Jan-81 - Function-Rear
KMCCH3.DAT   215 26-Jan-81 - Function-Front
```

```
 CHECKPOINT 050881-000000
Z KMCCZ        050881-000000   0/TPC KMCC-1C1D CONTROL PANEL
P KMCCP        012681-000000   4/TPC KMCC-1C1D PARAMETERS
S KMCCS        020381-000000  12/TPC KMCC-1C1D MODE SHAPES
G KMCCG        012681-000000   1/TPC MCC-1C1D GEOMETRY
H KMCCH3       012681-000000  50/TPC KMCC-1C1D FUNCTIONS FRONT #2
T KMCCT        012681 000000  10/TPC KMCC-1C1D TRACES

P RECORDS IN USE
REC 1 10
REC 2 7

KMCCS
S RECORDS IN USE
REC 1       7.405 HZ  MCC-1C1D SHAPE 1
REC 2      29.200 HZ  MCC-1C1D SHAPE 2
REC 3      33.930 HZ  MCC-1C1D SHAPE 3
REC 4      39.720 HZ  MCC-1C1D SHAPE 4
REC 5      47.420 HZ  MCC-1C1D SHAPE 5
REC 6      62.980 HZ  MCC-1C-1D SHAPE 6
REC 7       7.405 HZ  SHAPE 1 MODIFIED
REC 8      29.200 HZ  SHAPE 2 MODIFIED
REC 9      33.930 HZ  SHAPE 3 MODIFIED
REC 10      39.720 HZ  SHAPE 4 MODIFIED
REC 11      47.420 HZ  SHAPE 5 MODIFIED
REC 12      62.980 HZ  SHAPE 6 MODIFIED

T RECORDS IN USE
REC 1 LC
REC 2 LC
REC 3 LC
REC 4 C
REC 5 C
REC 6 C
REC 7 C
REC 8 C
REC 9 C
REC 10 C
```

GEOMETRY

LOC	X	Y	Z
1	0	0	0
2	0	40	0
3	0	80	0
4	0	100	0
5	40	0	0
6	40	40	0
7	40	80	0
8	40	100	0
9	80	0	0
10	80	40	0
11	80	80	0
12	80	100	0
13	120	0	0
14	120	40	0
15	120	80	0
16	120	100	0
17	160	0	0
18	160	40	0
19	160	80	0
20	160	100	0
21	180	0	0
22	180	40	0
23	180	80	0
24	180	100	0
25	200	0	0
26	200	40	0
27	200	80	0
28	200	100	0
29	220	0	0
30	220	40	0
31	220	80	0
32	220	100	0
33	0	0	20
34	0	20	20
35	0	40	20
36	0	60	20
37	0	80	20
38	0	100	20
39	20	0	20
40	20	20	20
41	20	40	20
42	20	60	20
43	20	80	20
44	20	100	20
45	40	0	20
46	40	20	20
47	40	40	20
48	40	60	20
49	40	80	20
50	40	100	20
61	80	80	20
51	60	0	20
52	60	20	20
53	60	40	20
54	60	60	20
55	60	80	20
56	60	100	20
57	80	0	20
58	80	20	20
62	80	100	20
63	100	0	20
64	100	20	20
65	100	40	20
66	100	60	20
67	100	80	20
68	100	100	20
69	120	0	20
70	120	20	20
71	120	40	20
72	120	60	20
73	120	80	20
74	120	100	20
75	140	0	20
76	140	20	20
77	140	40	20
78	140	60	20
79	140	80	20
80	140	100	20
81	160	0	20
82	160	20	20
83	160	40	20
84	160	60	20
85	160	80	20
86	160	100	20
87	180	0	20
88	180	20	20
89	180	40	20
90	180	60	20
91	180	80	20
92	180	100	20
93	200	0	20
94	200	20	20
95	200	40	20
96	200	60	20
97	200	80	20
98	200	100	20
99	220	0	20
100	220	20	20
101	220	40	20
102	220	60	20
103	220	80	20
104	220	100	20

H RECORDS IN USE

REC	1	92Z+	92Z+	1
REC	2	92Z+	92Z+	2
REC	3	92Z+	92Z+	3
REC	4	92Z+	92Z+	4
REC	5	92Z+	1Z-	0
REC	6	92Z+	2Z-	0
REC	7	92Z+	3Z-	0
REC	8	92Z+	4Z-	0
REC	9	92Z+	4X-	0
REC	10	92Z+	4Y+	0
REC	11	92Z+	5Z-	0
REC	12	92Z+	6Z-	0
REC	13	92Z+	7Z-	0
REC	14	92Z+	8Z-	0
REC	15	92Z+	8Y+	0
REC	16	92Z+	9Z-	0
REC	17	92Z+	10Z-	0
REC	18	92Z+	11Z-	0
REC	19	92Z+	12Z-	0
REC	20	92Z+	12Y+	0
REC	21	92Z+	13Z-	0
REC	22	92Z+	14Z-	0
REC	23	92Z+	15Z-	0
REC	24	92Z+	16Z-	0
REC	25	92Z+	16Y+	0
REC	26	92Z+	17Z-	0
REC	27	92Z+	18Z-	0
REC	28	92Z+	19Z-	0
REC	29	92Z+	20Z-	0
REC	30	92Z+	20Y+	0
REC	31	92Z+	21Z-	0
REC	32	92Z+	22Z-	0
REC	33	92Z+	23Z-	0
REC	34	92Z+	24Z-	0
REC	35	92Z+	24Y+	0
REC	36	92Z+	25Z-	0
REC	37	92Z+	26Z-	0
REC	38	92Z+	27Z-	0
REC	39	92Z+	28Z-	0
REC	40	92Z+	28Y+	0
REC	41	92Z+	29Z-	0
REC	42	92Z+	30Z-	0
REC	43	92Z+	31Z-	0
REC	44	92Z+	31X+	0
REC	45	92Z+	32Z-	0
REC	46	92Z+	32X+	0
REC	47	92Z+	32Y+	0
REC	48	92Z+	33Z+	0
REC	49	92Z+	34Z+	0
REC	50	92Z+	35Z+	0

H RECORDS IN USE

REC	1	92Z+	69Z+	0
REC	2	92Z+	70Z+	0
REC	3	92Z+	71Z+	0
REC	4	92Z+	72Z+	0
REC	5	92Z+	73Z+	0
REC	6	92Z+	74Z+	0
REC	7	92Z+	74Y+	0
REC	8	92Z+	75Z+	0
REC	9	92Z+	76Z+	0
REC	10	92Z+	77Z+	0
REC	11	92Z+	78Z+	0
REC	12	92Z+	79Z+	0
REC	13	92Z+	80Z+	0
REC	14	92Z+	80Y+	0
REC	15	92Z+	81Z+	0
REC	16	92Z+	82Z+	0
REC	17	92Z+	83Z+	0
REC	18	92Z+	84Z+	0
REC	19	92Z+	85Z+	0
REC	20	92Z+	86Z+	0
REC	21	92Z+	86Y+	0
REC	22	92Z+	87Z+	0
REC	23	92Z+	88Z+	0
REC	24	92Z+	89Z+	0
REC	25	92Z+	90Z+	0
REC	26	92Z+	91Z+	0
REC	27	92Z+	92Z+	0
REC	28	92Z+	92Z+	2
REC	29	92Z+	92Z+	3
REC	30	92Z+	92Z+	4
REC	31	92Z+	92Y+	0
REC	32	92Z+	93Z+	0
REC	33	92Z+	94Z+	0
REC	34	92Z+	95Z+	0
REC	35	92Z+	96Z+	0
REC	36	92Z+	97Z+	0
REC	37	92Z+	98Z+	0
REC	38	92Z+	99Z+	0
REC	39	92Z+	100Z+	0
REC	40	92Z+	101Z+	0
REC	41	92Z+	101X+	0
REC	42	92Z+	102Z+	0
REC	43	92Z+	102X+	0
REC	44	92Z+	103Z+	0
REC	45	92Z+	103X+	0
REC	46	92Z+	104Z+	0
REC	47	92Z+	104X+	0
REC	48	92Z+	104Y+	0
REC	49	92Z+	92Z+	1

H RECORDS IN USE

REC	1	92Z+	37Z+	0
REC	2	92Z+	38Z+	0
REC	3	92Z+	36Z+	0
REC	4	92Z+	37Z+	0
REC	5	92Z+	38Z+	0
REC	6	92Z+	38Y+	0
REC	7	92Z+	38X-	0
REC	8	92Z+	39Z+	0
REC	9	92Z+	40Z+	0
REC	10	92Z+	41Z+	0
REC	11	92Z+	42Z+	0
REC	12	92Z+	43Z+	0
REC	13	92Z+	44Z+	[illegible]
REC	14	92Z+	44Y+	
REC	15	92Z+	45Z+	0
REC	16	92Z+	46Z+	0
REC	17	92Z+	47Z+	0
REC	18	92Z+	48Z+	0
REC	19	92Z+	49Z+	0
REC	20	92Z+	50Z+	0
REC	21	92Z+	50Y+	0
REC	22	92Z+	51Z+	0
REC	23	92Z+	52Z+	0
REC	24	92Z+	53Z+	0
REC	25	92Z+	54Z+	0
REC	26	92Z+	55Z+	0
REC	27	92Z+	56Z+	0
REC	28	92Z+	56Y+	0
REC	29	92Z+	57Z+	0
REC	30	92Z+	58Z+	0
REC	31	92Z+	59Z+	0
REC	32	92Z+	60Z+	0
REC	33	92Z+	61Z+	0
REC	34	92Z+	62Z+	0
REC	35	92Z+	62Y+	0
REC	36	92Z+	63Z+	0
REC	37	92Z+	64Z+	0
REC	38	92Z+	65Z+	0
REC	39	92Z+	66Z+	0
REC	40	92Z+	67Z+	0
REC	41	92Z+	68Z+	0
REC	42	92Z+	68Y+	0

APPENDIX D

MODE SHAPE DATA

The microfiche in this appendix lists 63 files of mode shape data. The files are in the following order:

1-6	480V Motor Control Center
7-25	Jet Pump Instrumentation Panel
26-36	3-Inch Motor Operated Valve
37-40	RHR Pump
41-53	Recirculation Control Valve
54-63	3-Inch Motor Operated Valve